Studies on perispawning mortalities in brown trout (Salmo trutta L.) from Loch Leven, Kinross, Scotland.

by

Randolph H. Richards

A thesis submitted to the University of Stirling for the degree of Doctor of Philosophy.

June 1979

Fig. 1. Map of Loch Leven, Kinross.

Trapping sites arrowed.

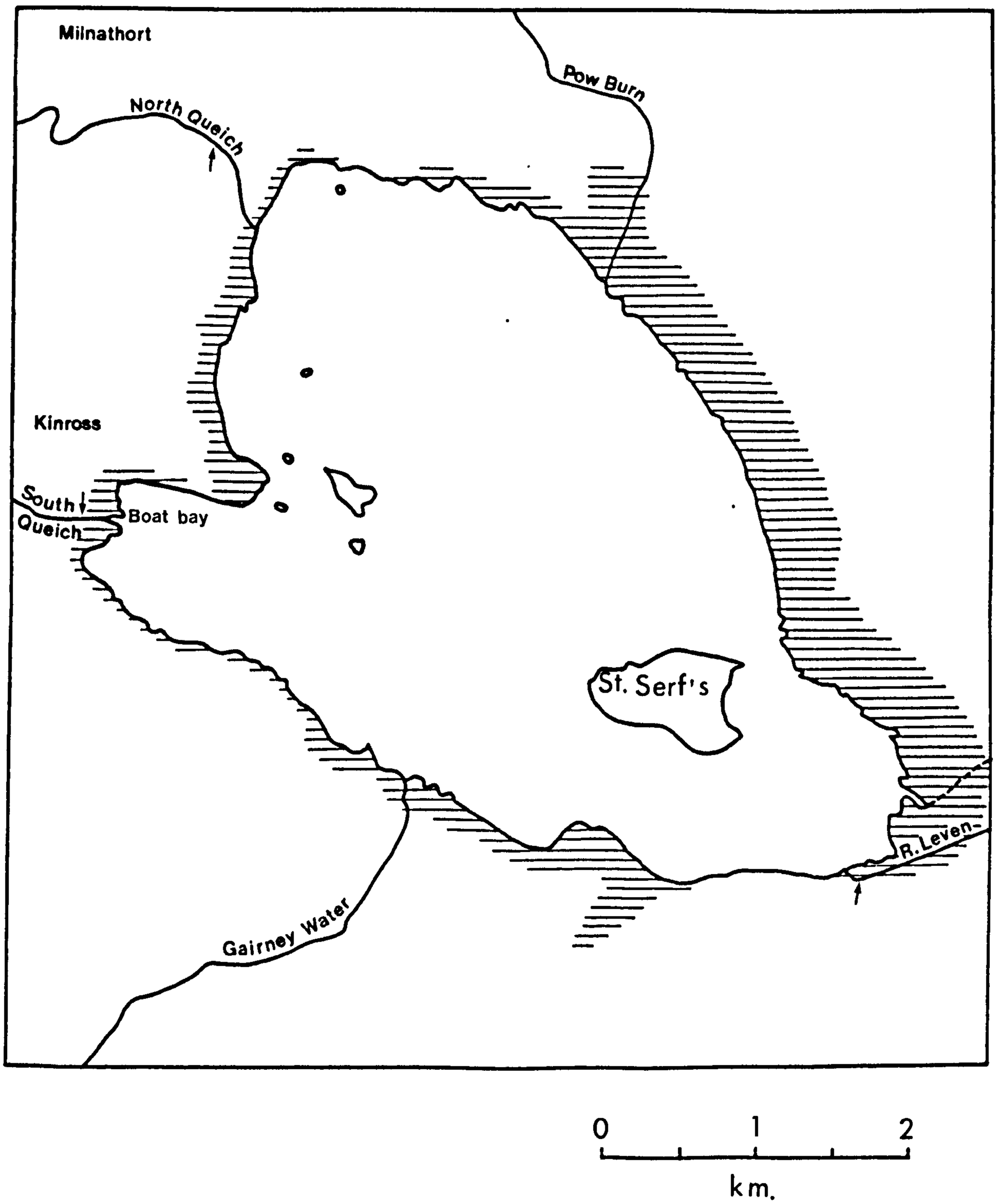
Milnathort
Pow Burn
North Queich
Kinross
South Queich
Boat bay
St. Serf's
R. Leven-
Gairney Water
0
1
2
km.

Fig. 2. Skin of sexually immature fish.

Epidermis consists of basal layer (b) above which are mucous cells (m) and malpighian cells.

Note prominent scales (S) in dermis.

H & E x 320

Fig. 3. Mucous cells apparently opening at the surface through a pore.

P.A.S. x 500

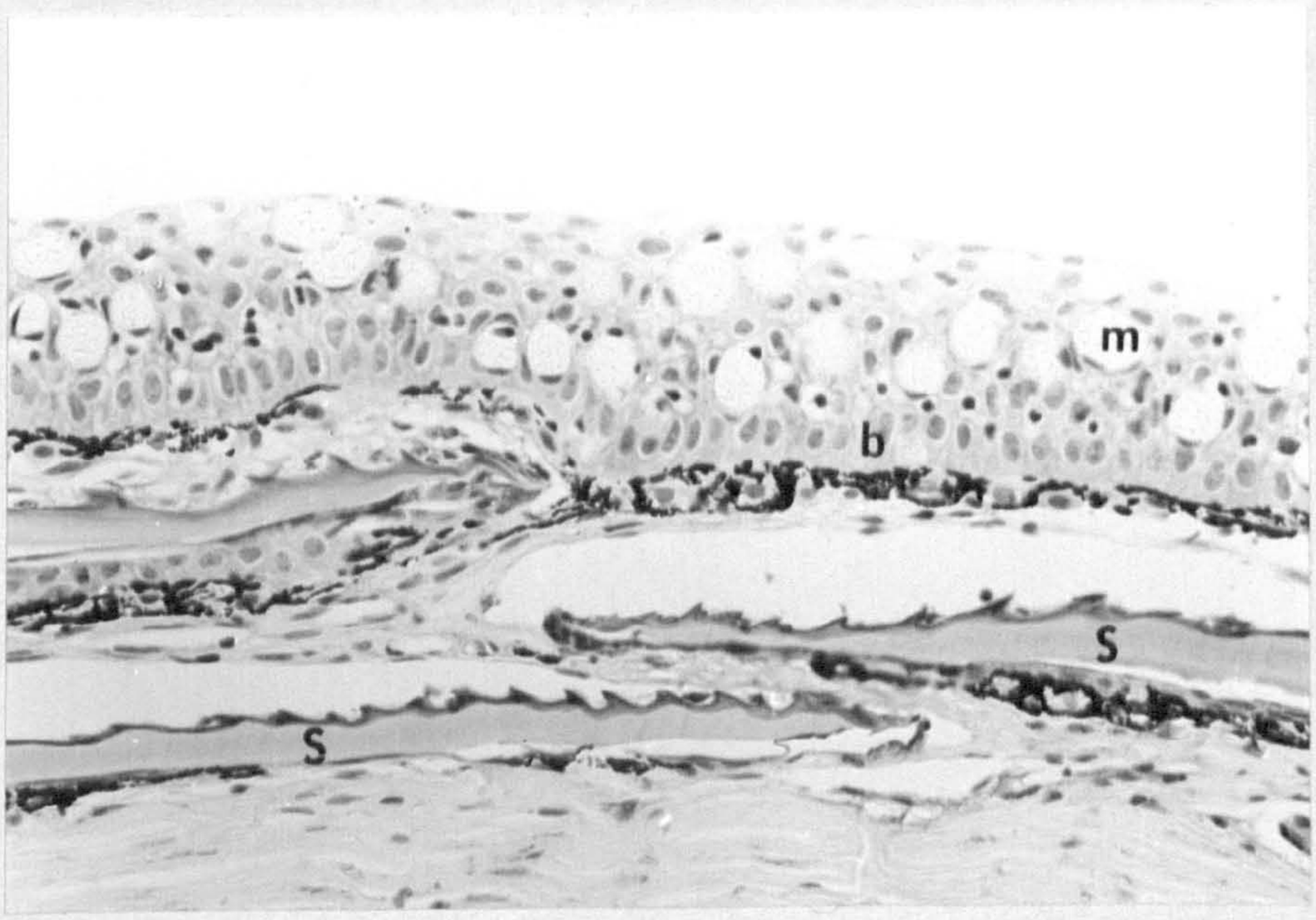
m
b
S
S

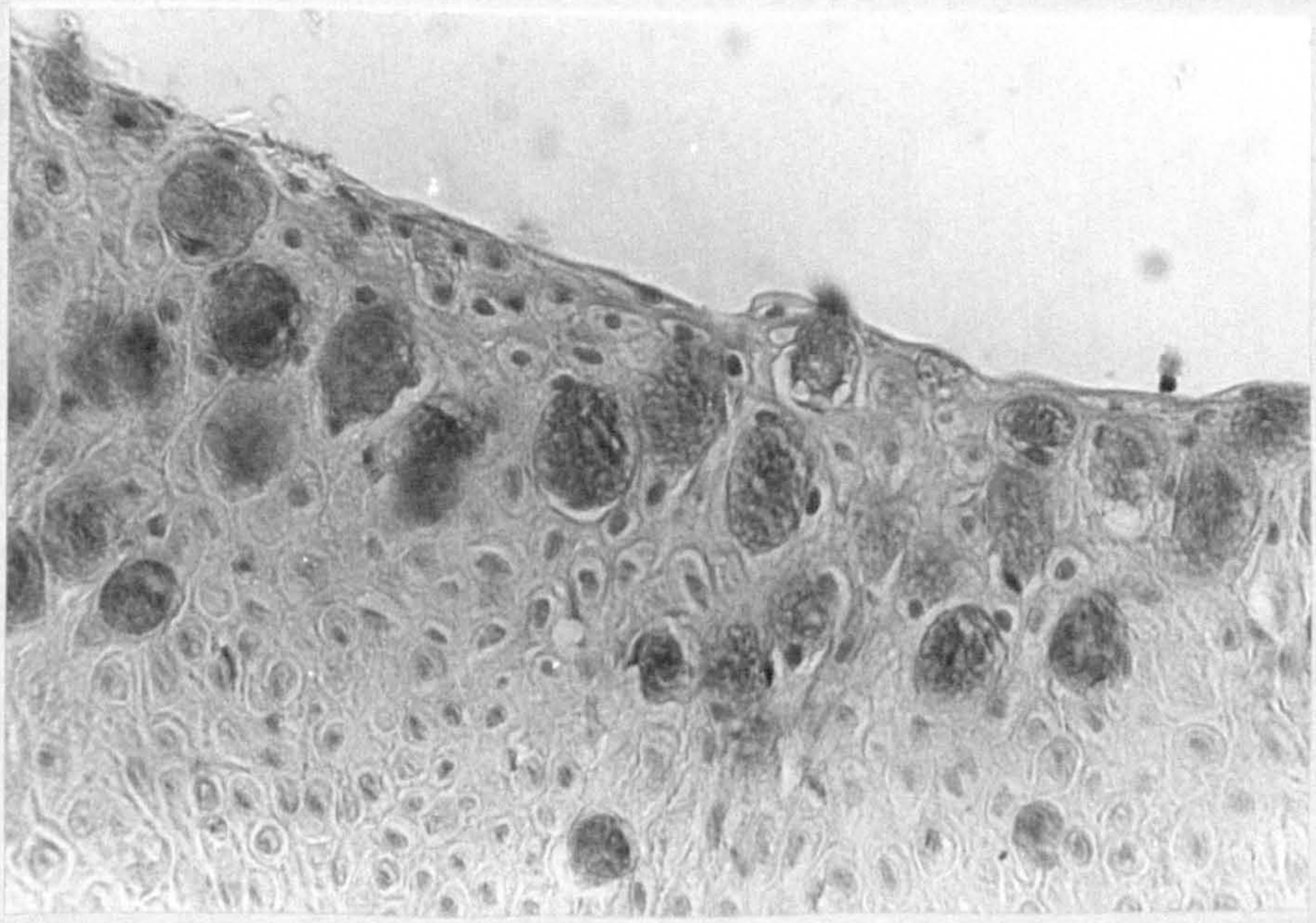

Fig. 4. "Albumen" cells (a). Note also mucous cells (m).

H & E x 1250

Fig. 5. Stratum spongiosum of dermis with prominent melanocyte (m).

H & E x 500

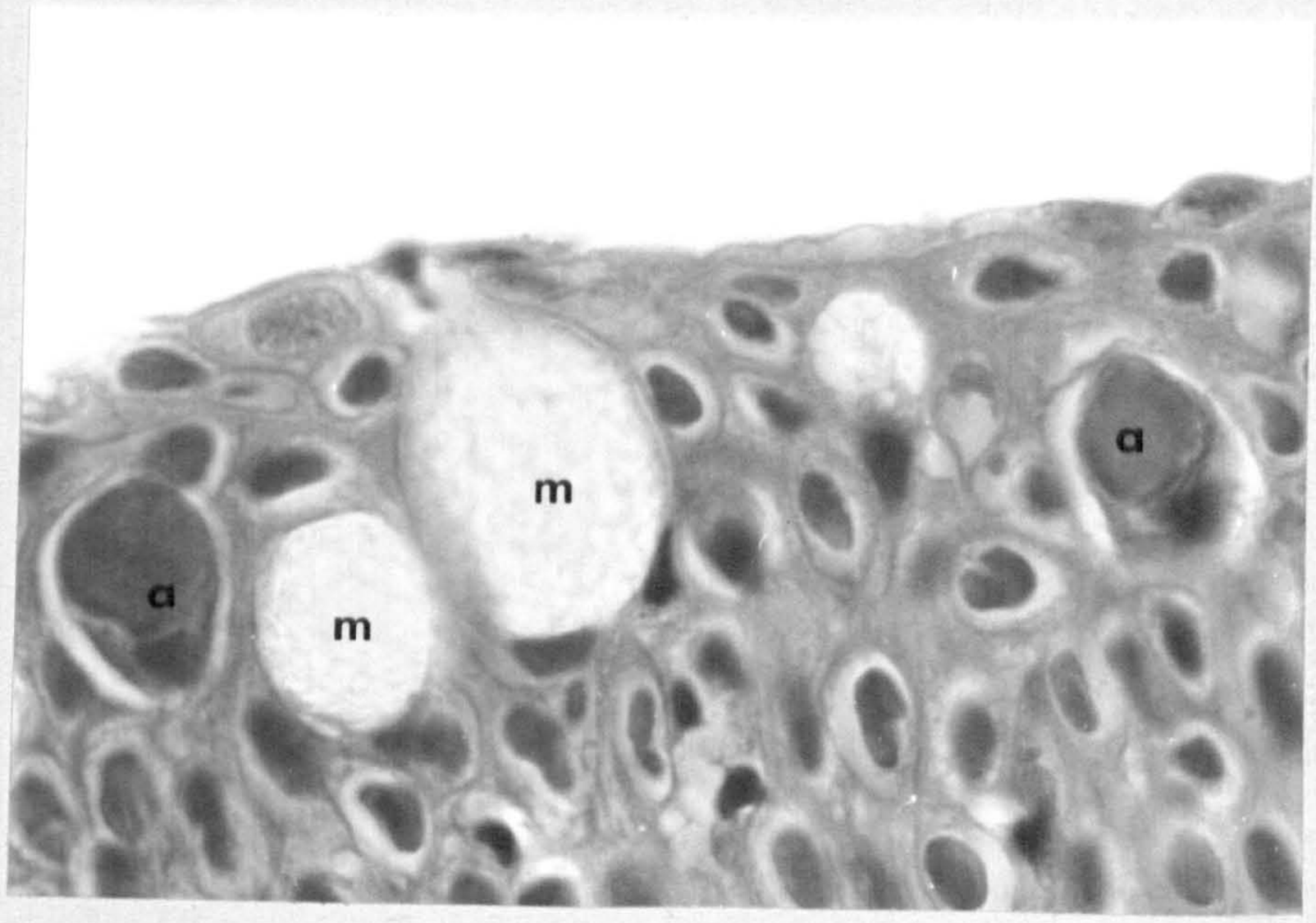
a
m
m
a

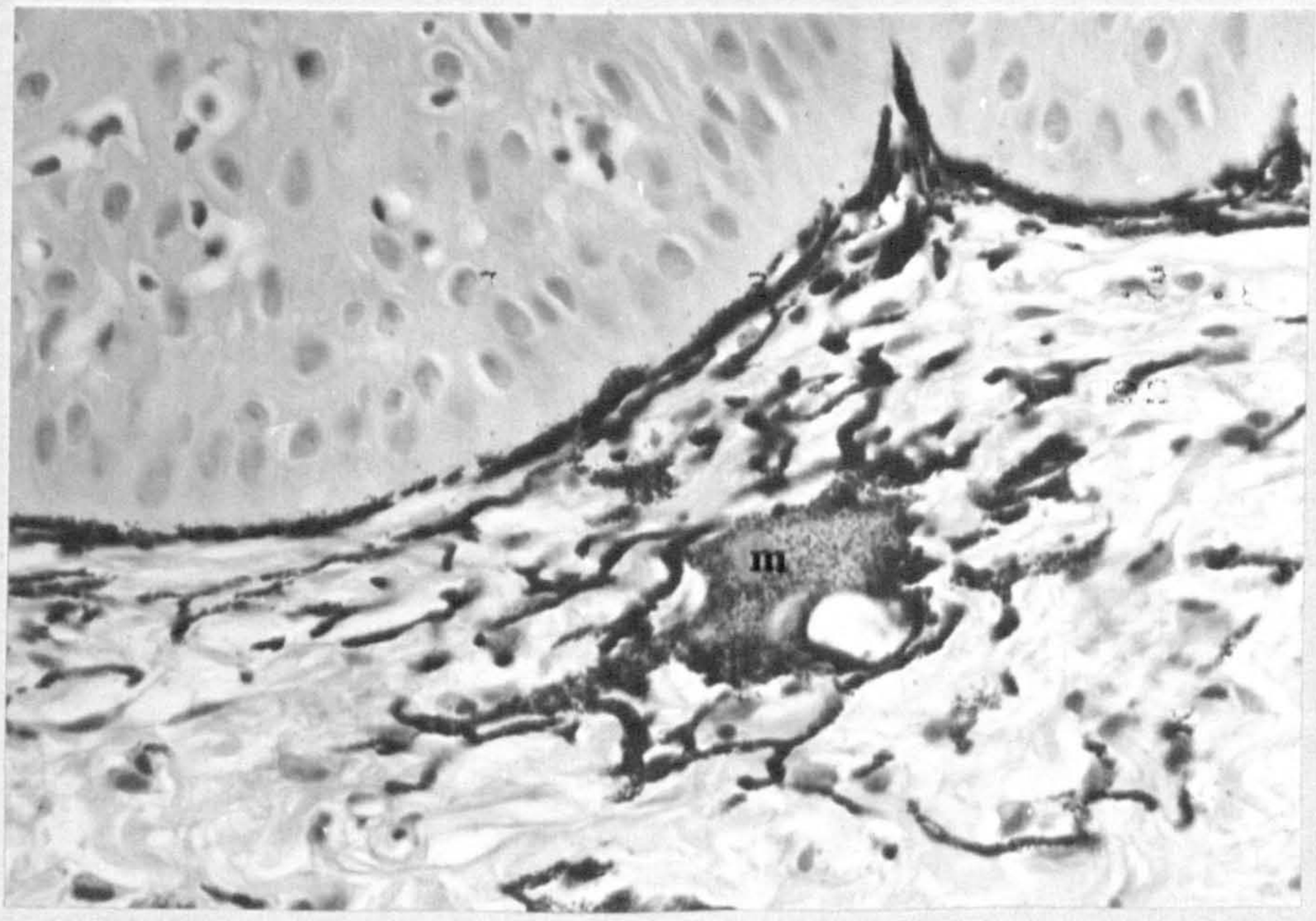
m

Fig. 6. Stratum compactum of dermis, consisting of collagen bundles and occasional fibroblasts.

H & E x 320

Fig. 7. Ridges at epidermis/dermis junction in sexually mature male fish.

H & E x 125

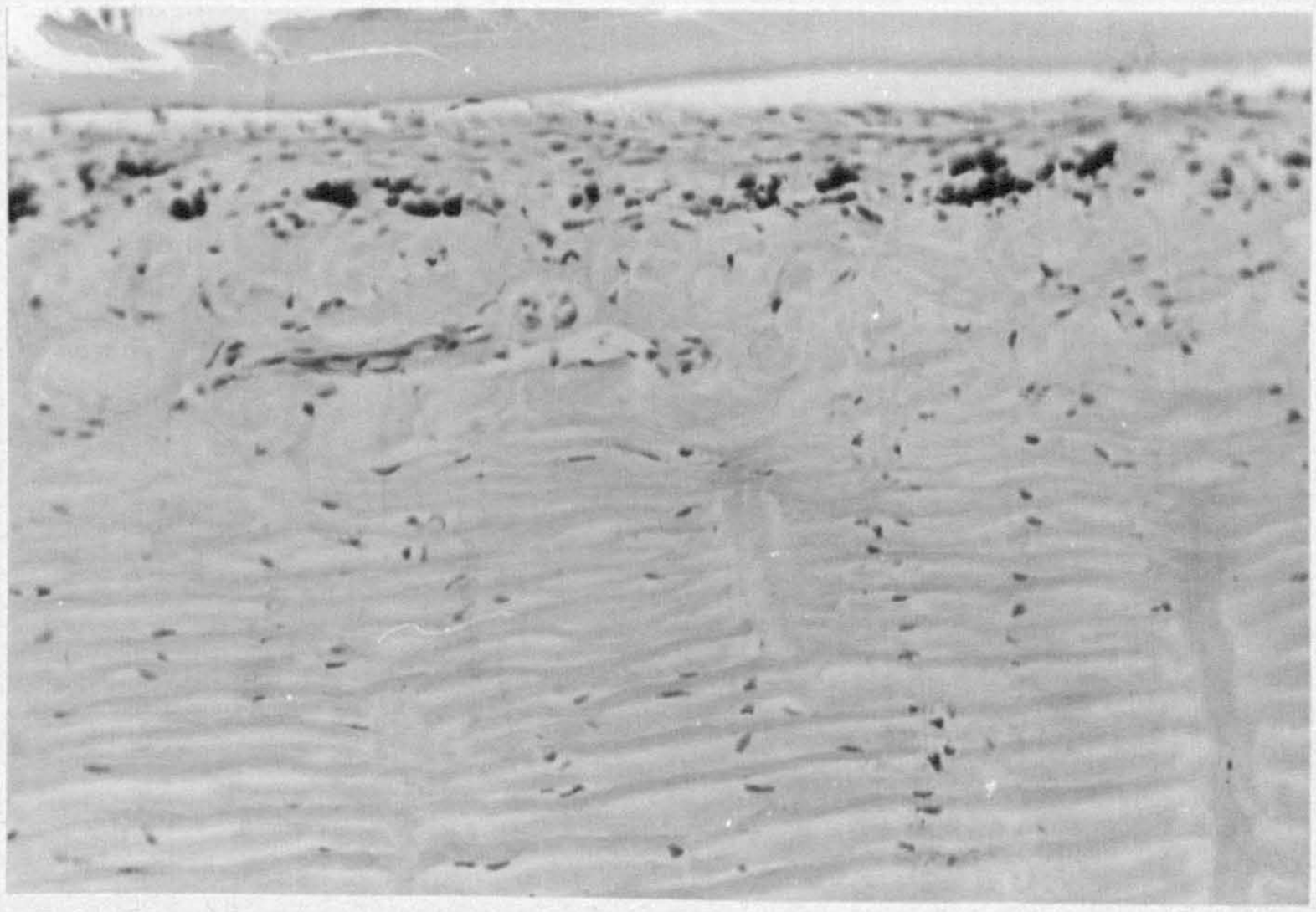

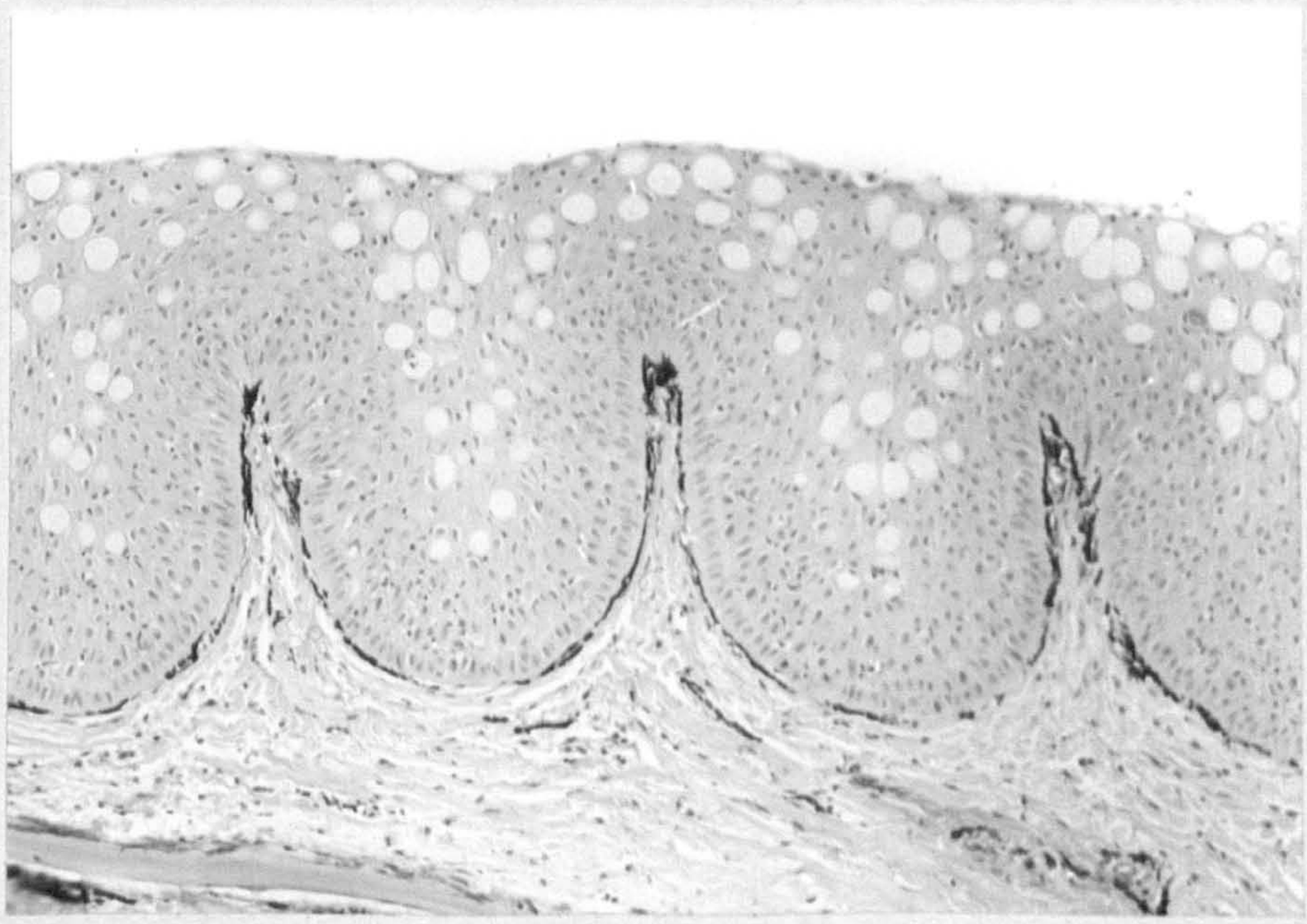

Fig. 8. Mucous cells absent in epidermis of sexually mature male fish.

H & E x 125

Fig. 9. Sloughing of surface malpighian cells in sexually mature male fish.

H & E x 320

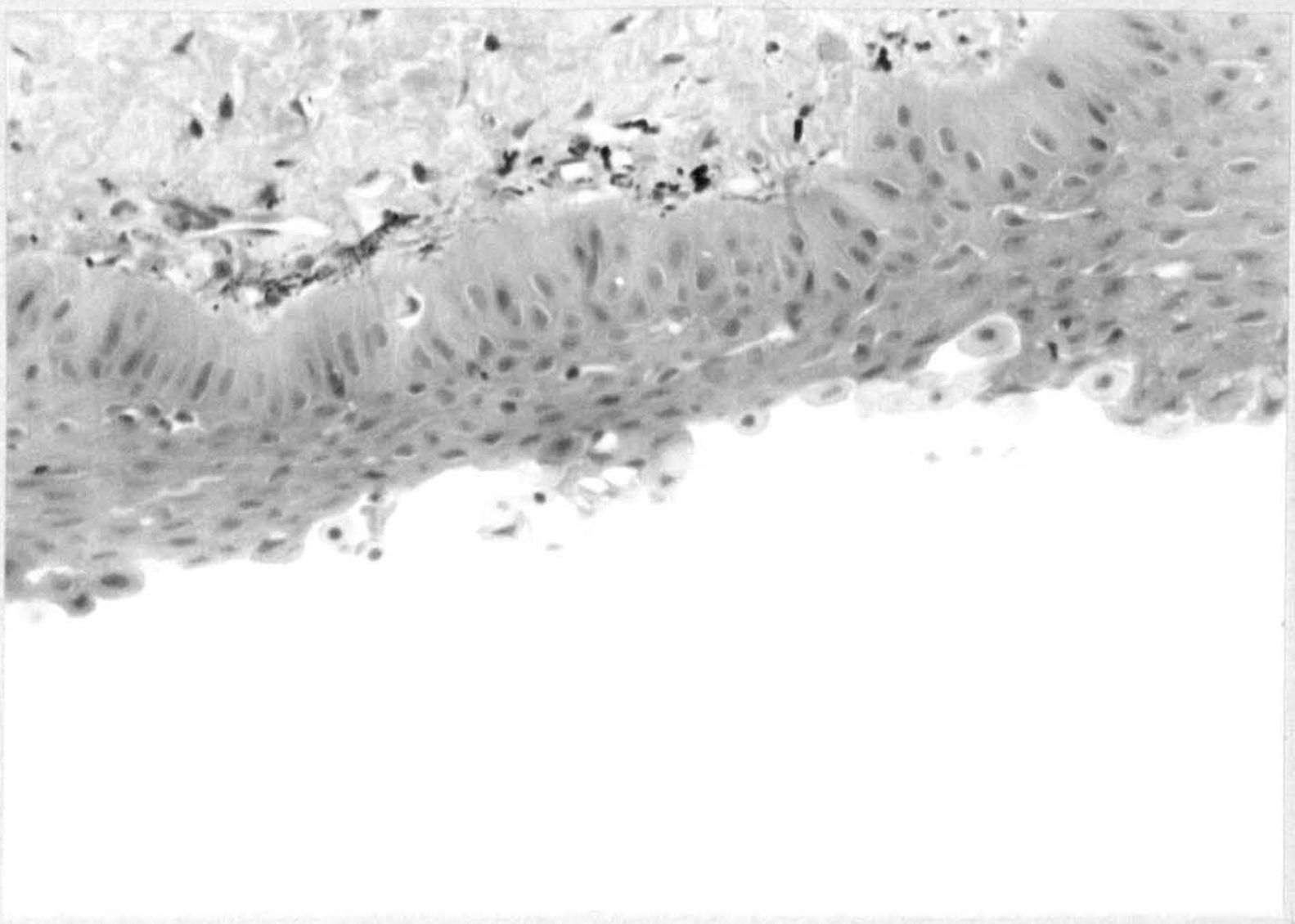

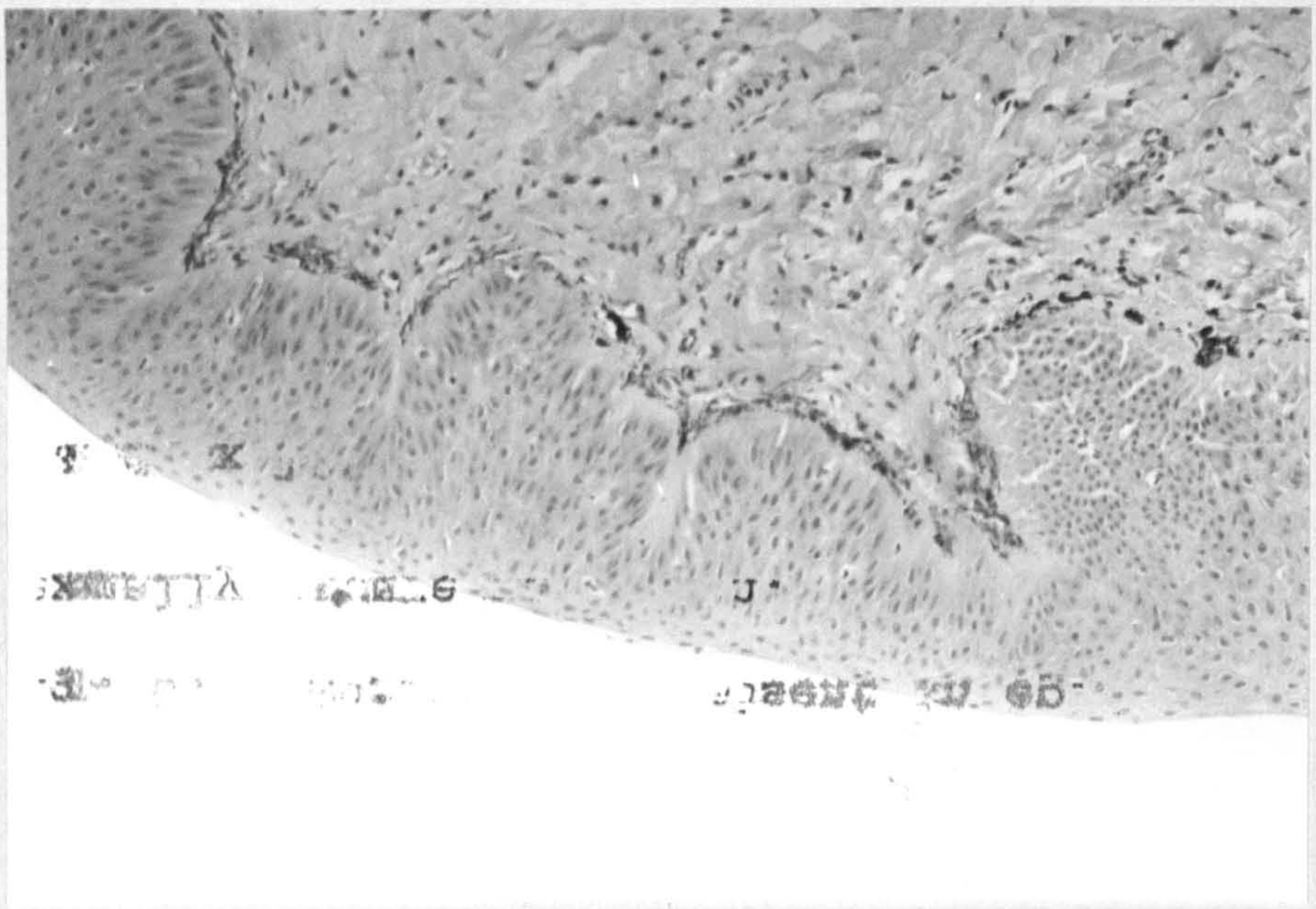

Fig. 10. Scales embedded in depths of dermis in sexually mature fish.

H & E x 50

Fig. 11. Scale near epidermis/dermis junction in sexually mature fish. Note invagination of dermis along lower surface of scale.

H & E x 125

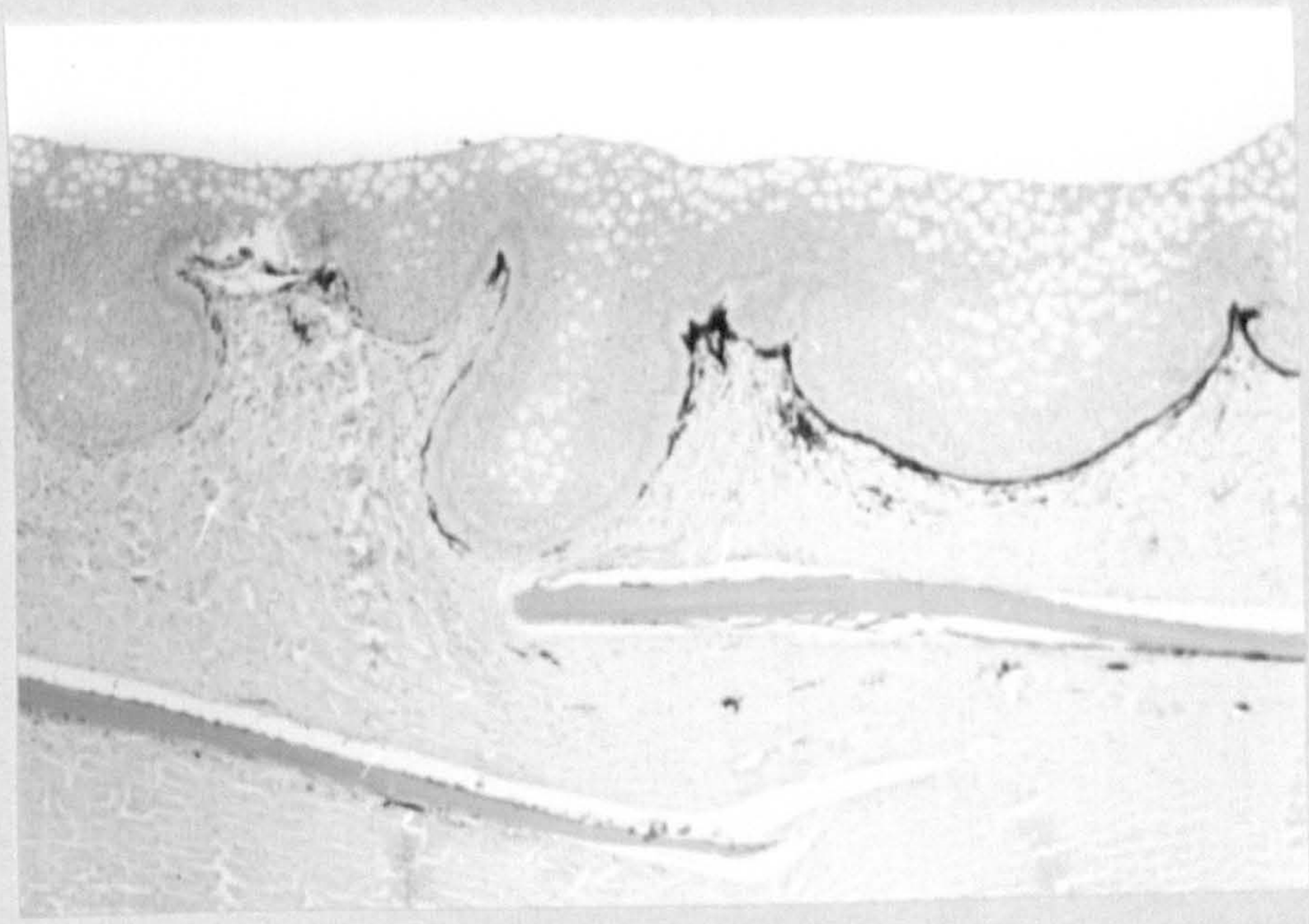

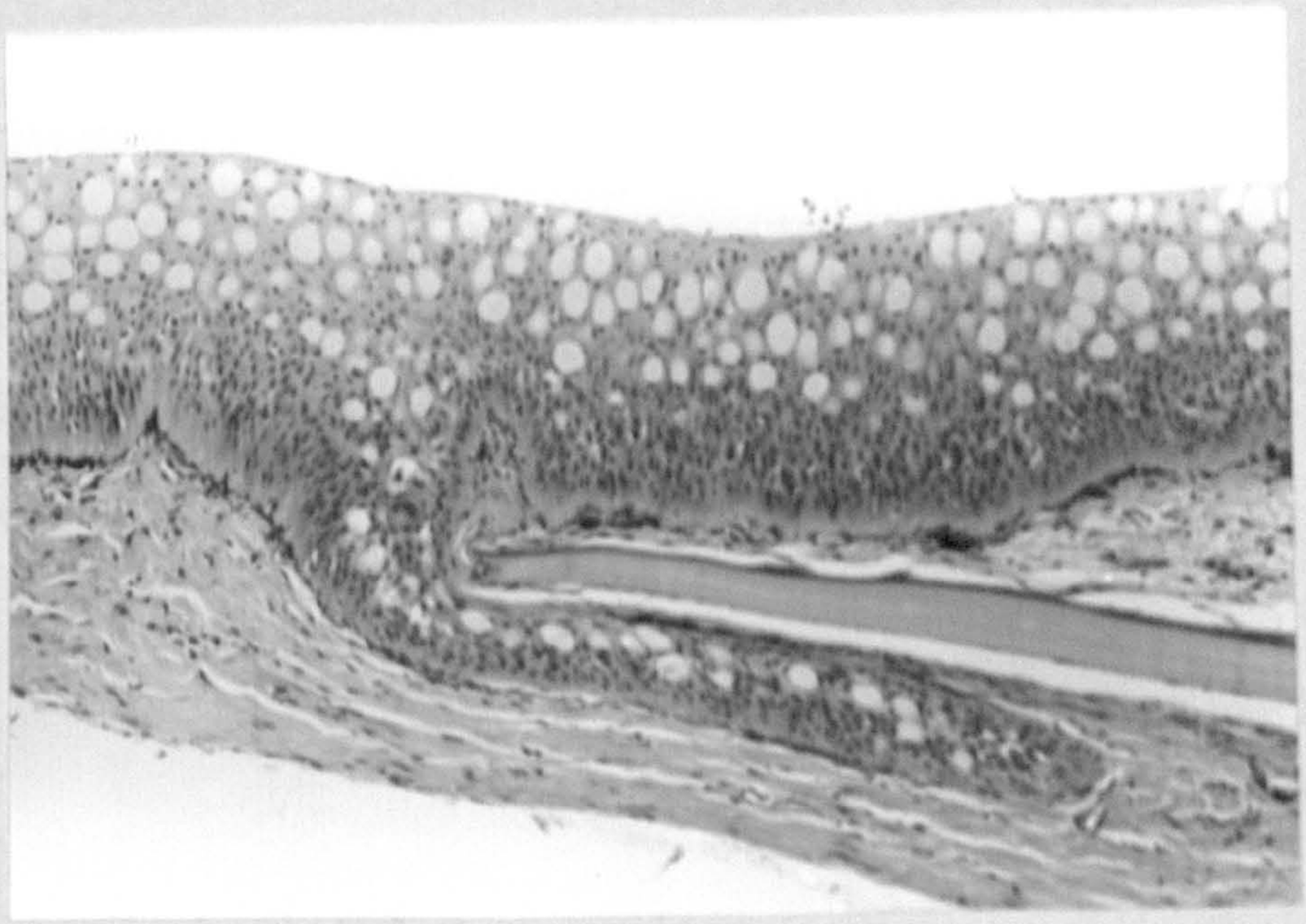

Fig. 12. Necrotic cells present in basal and suprabasal cells of epidermis in spent fish.

H & E x 320

Fig. 13. Melanin (arrowed) in epidermis of sexually mature male fish.

H & E x 320

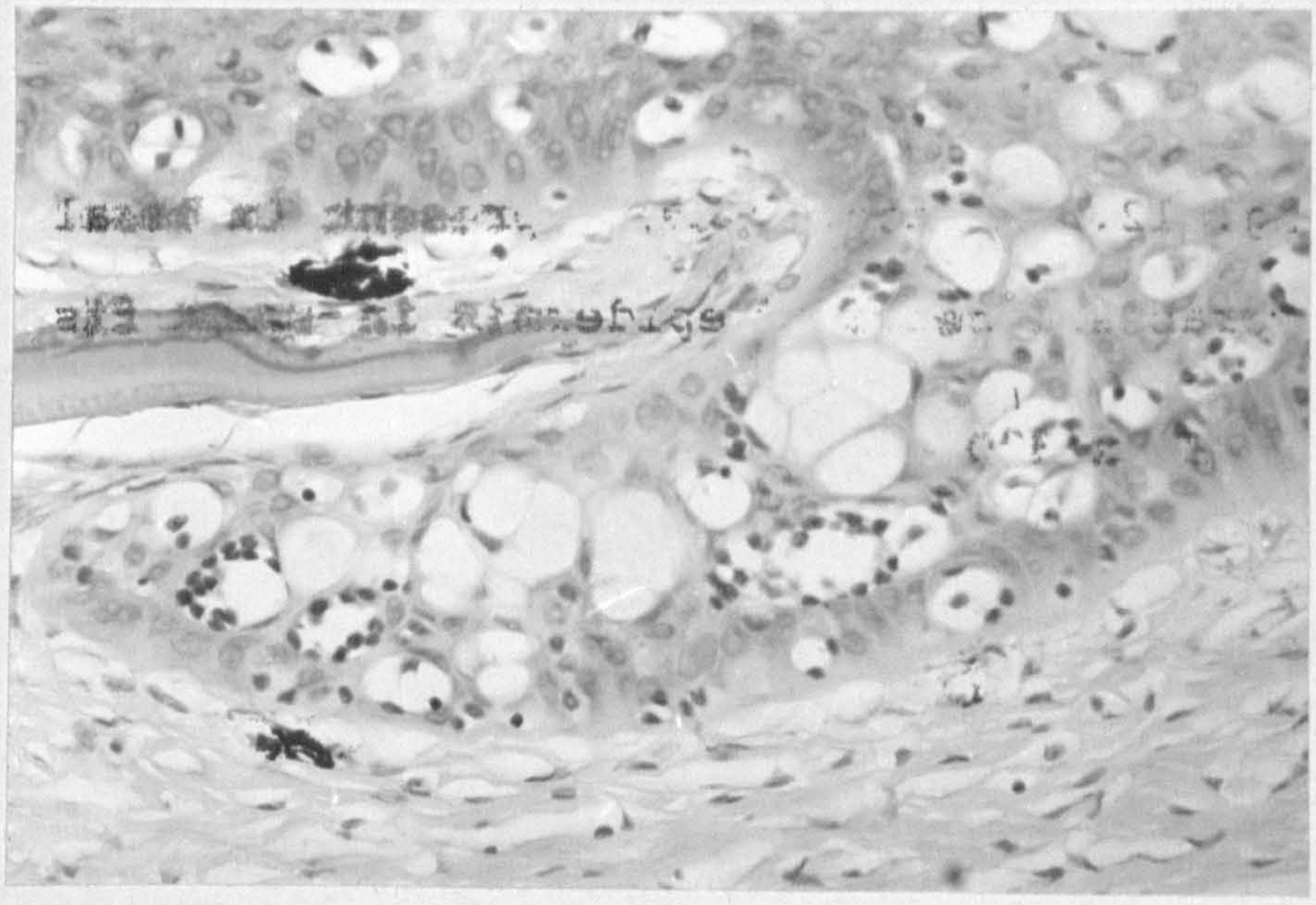

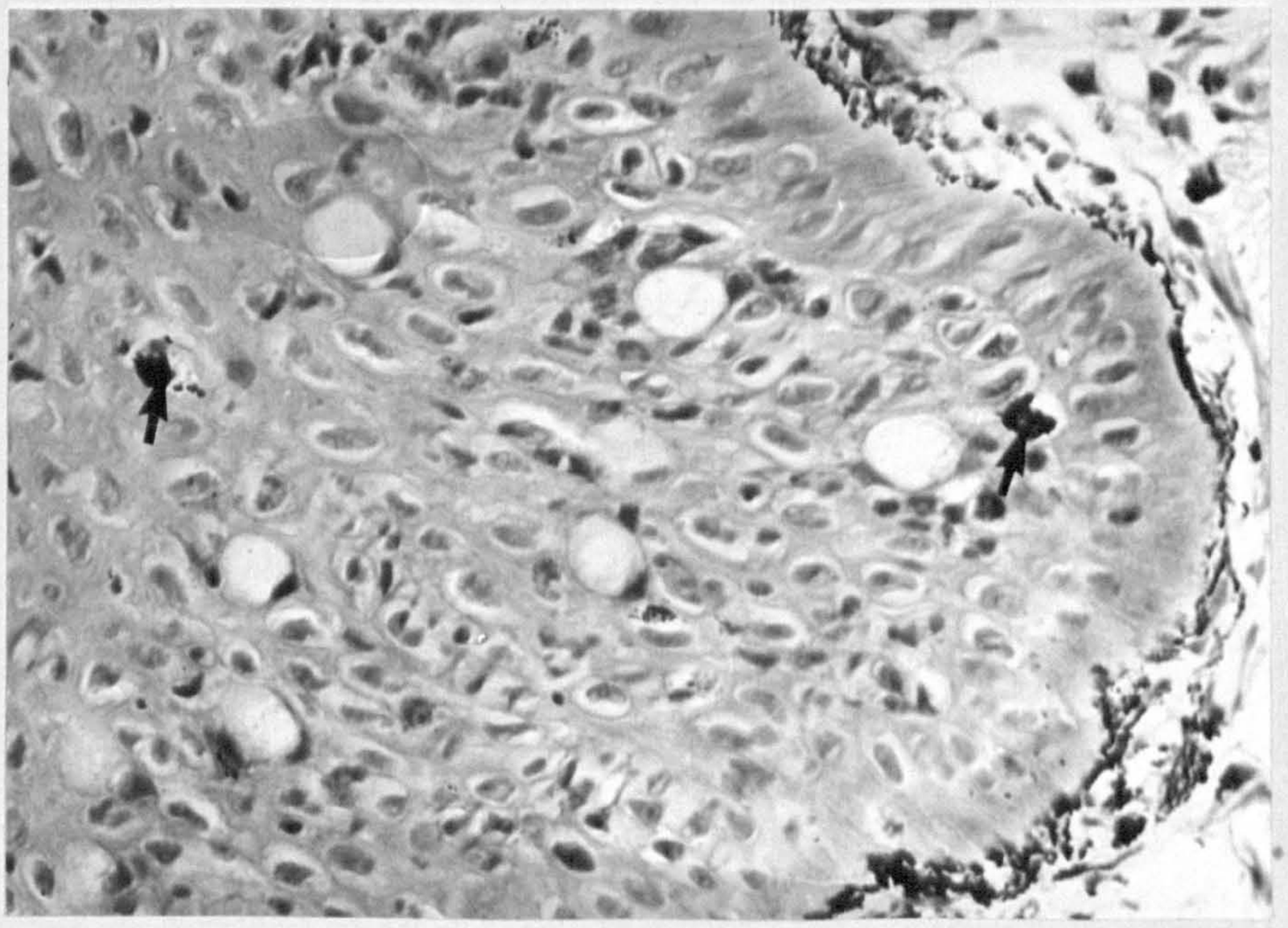

Fig. 14. Skin of sexually mature male fish.
Note the thick, cellular stratum spongiosum (S).

H & E x 125

Fig. 15. Epidermis of sexually mature female fish. Note columnar basal layer (b).

H & E x 320

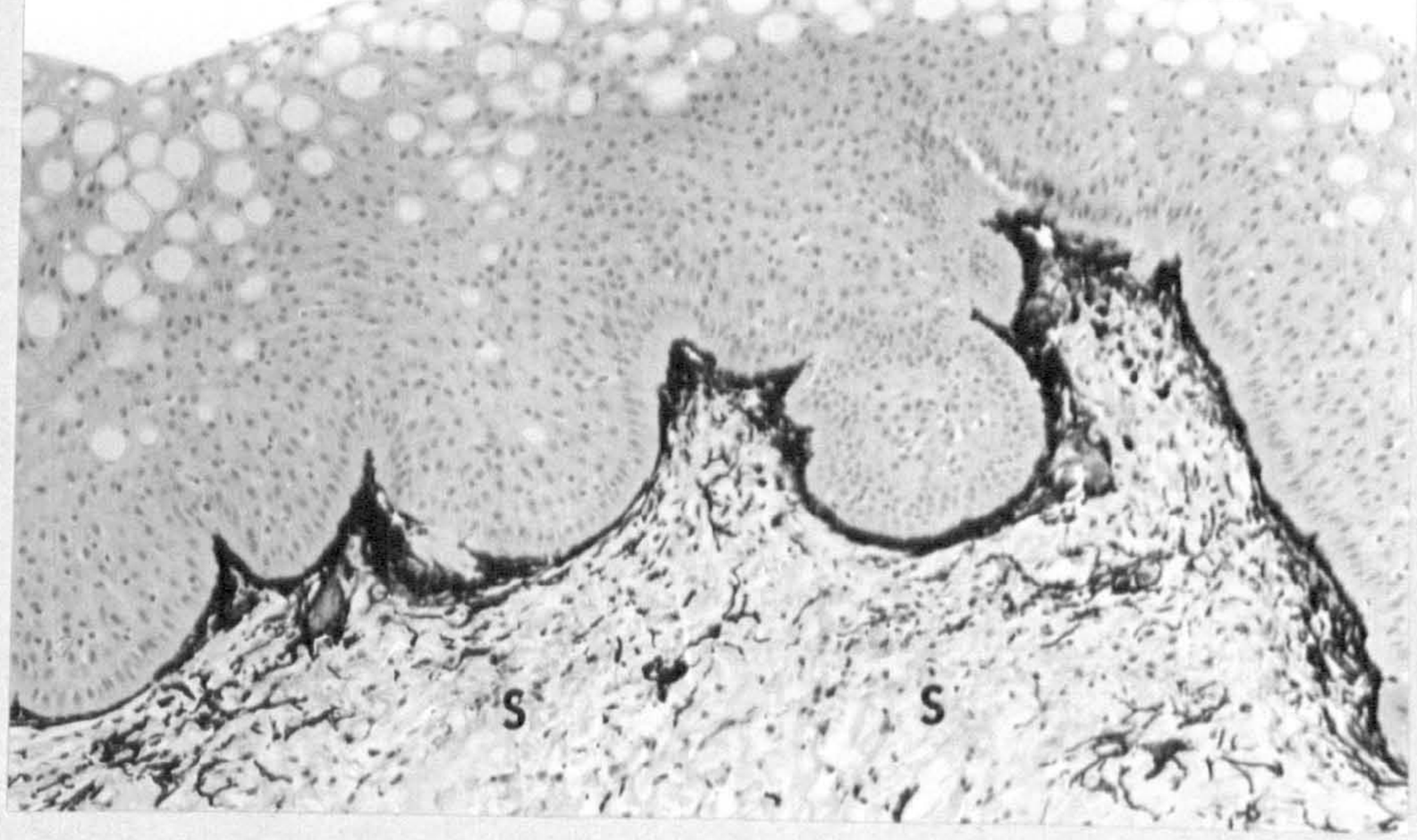
S
S

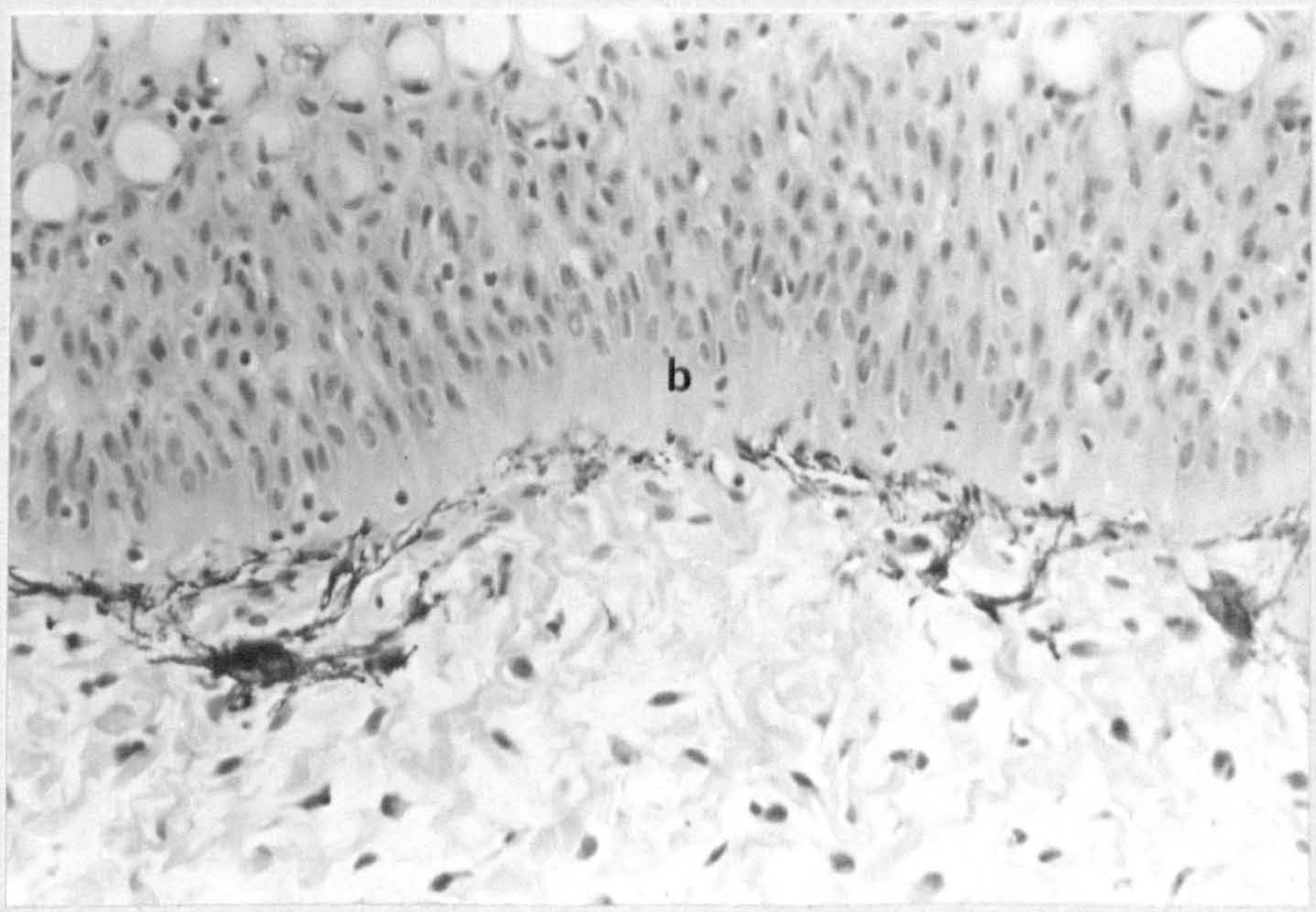
b

Fig. 16. Skin of sexually mature female fish with prominent band of melanin at epidermis/ dermis junction.

H & E x 320

Fig. 17. Heart with Cotylurus spp. infection. Note marked inflammatory response at junction of bulbus and ventricle.

H & E x 125

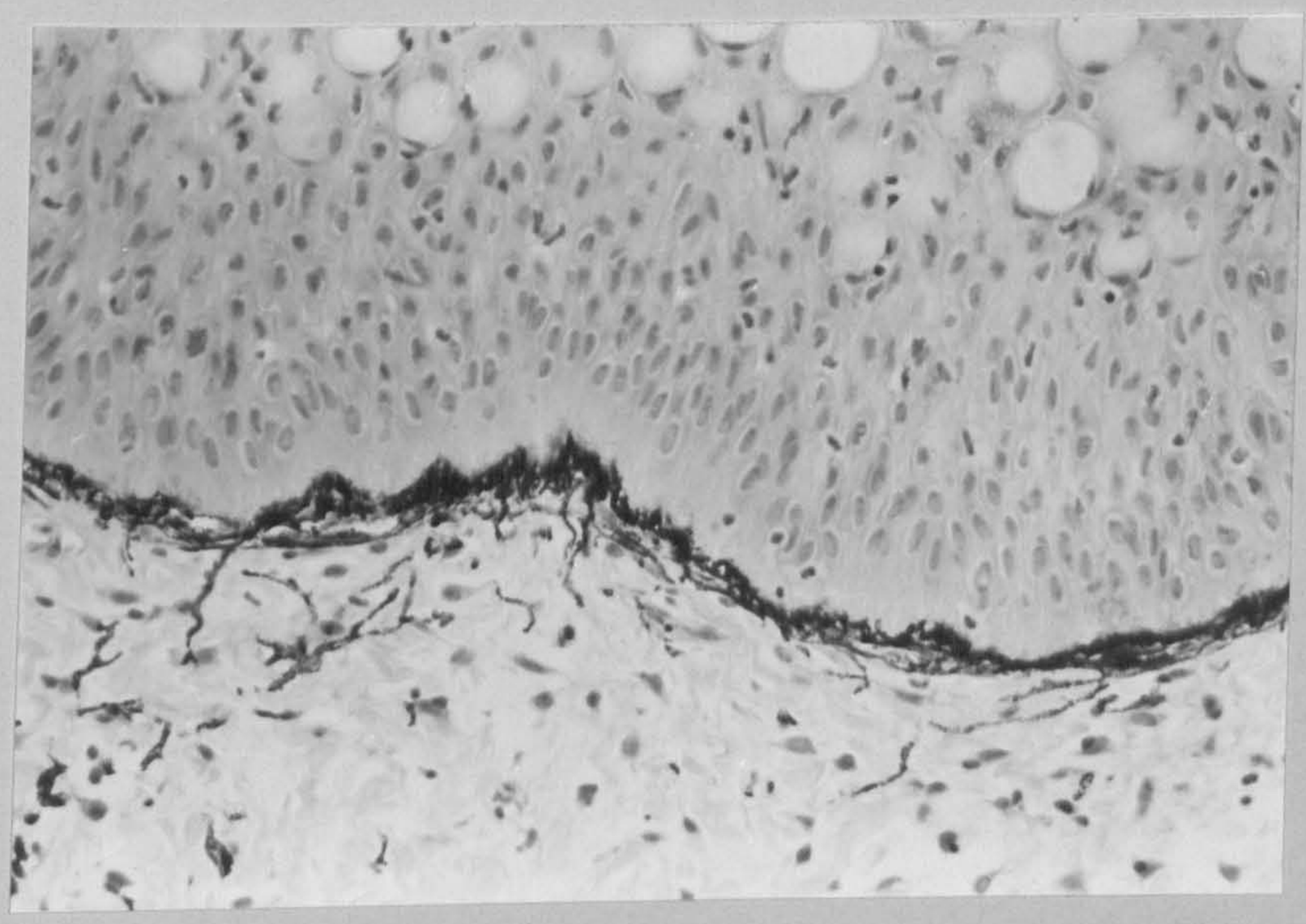

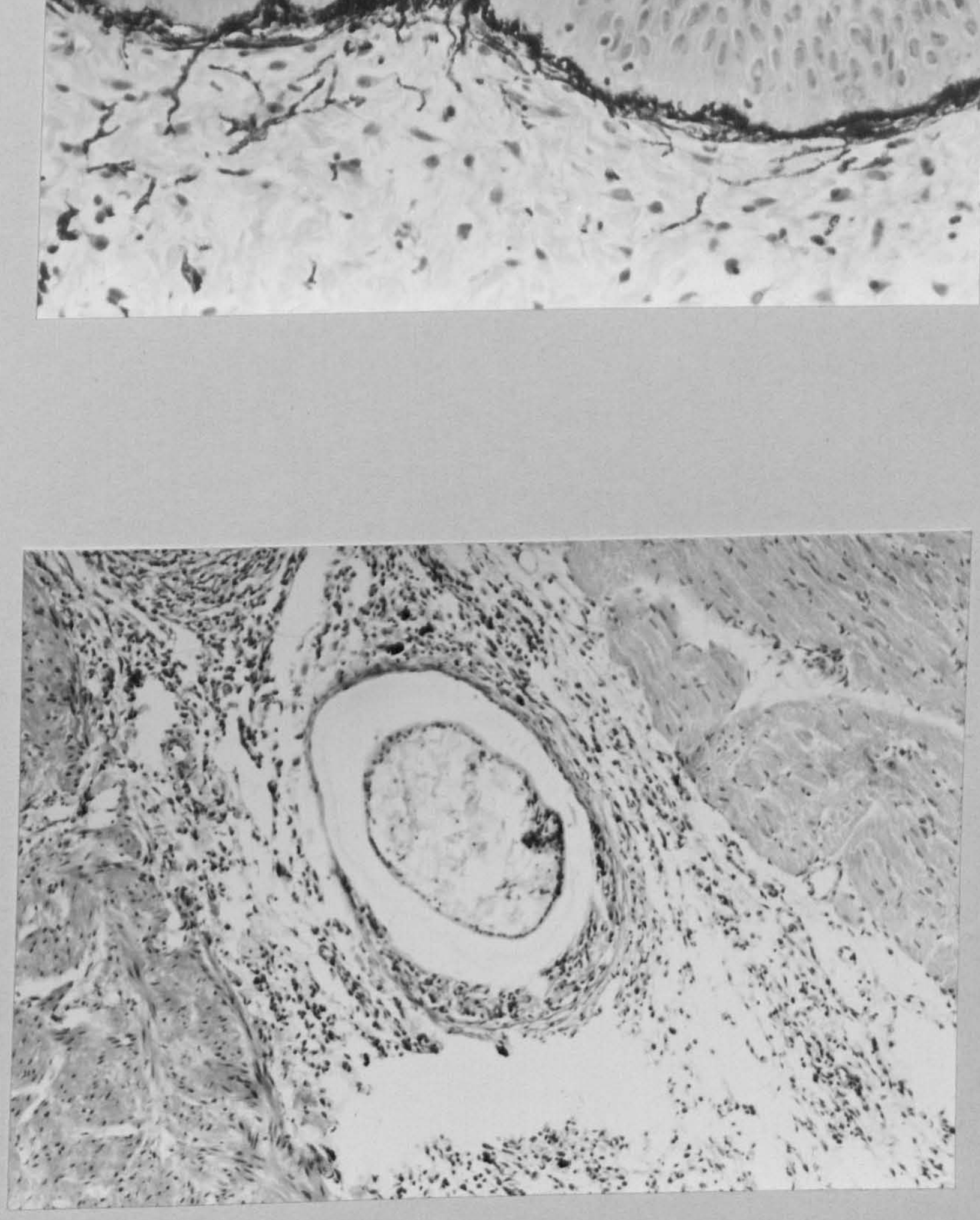

Fig. 18. Heart with Cotylurus spp. infection. Inflammatory response involving only superficial epicardium. Note the presence of numerous eosinophilic granule cells.

H & E x 320

Fig. 19. Heart with Cotylurus spp. infection. Extensive inflammatory response.

H & E x 320

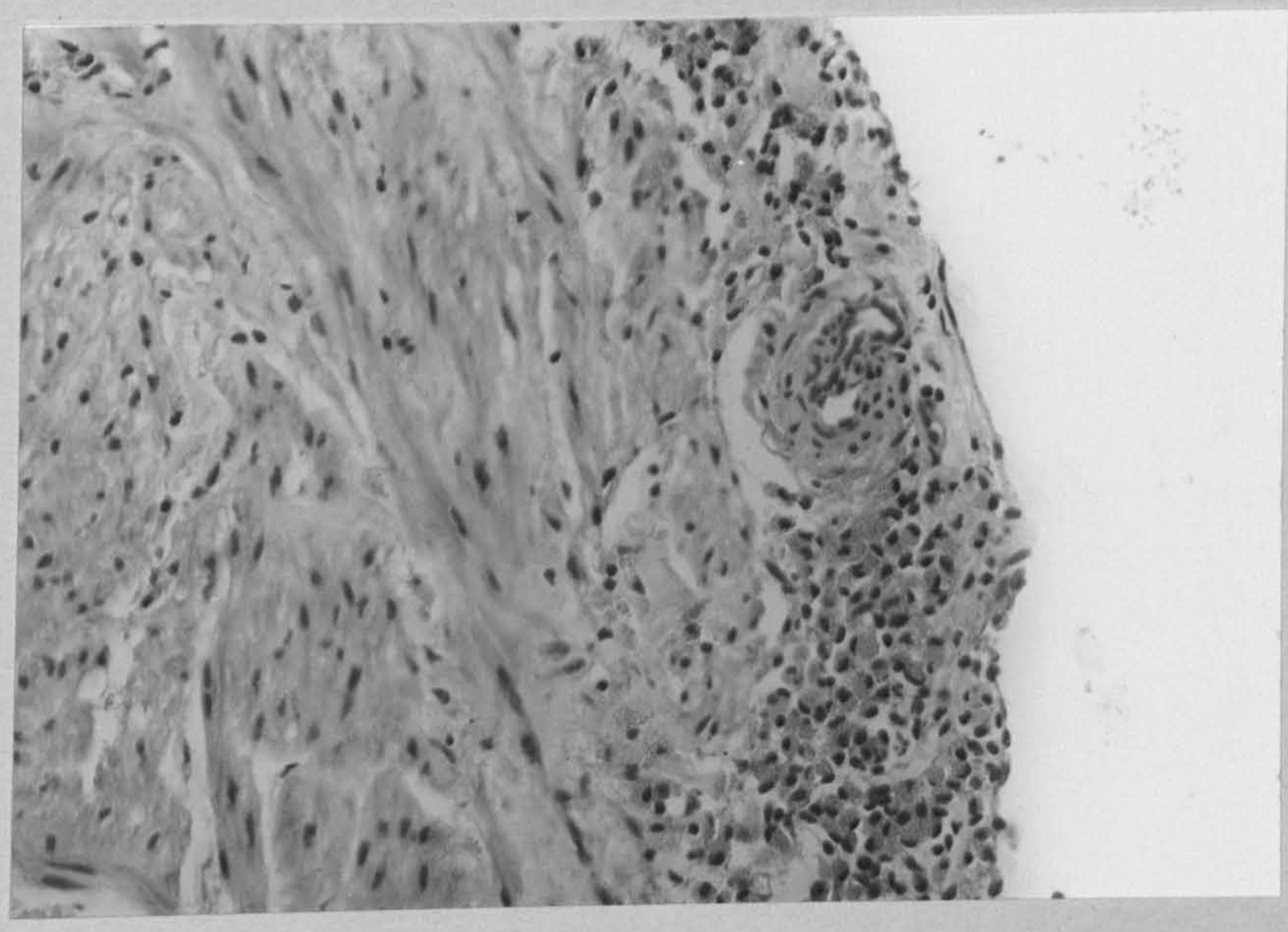

Fig. 20. Heart with Cotylurus spp. infection.
Note areas of local myofibrillar necrosis.

H & E x 320

Fig. 21. Heart with Cotylurus spp. infection.
Note areas of myofibrillar necrosis associated
with EGC infiltration.

H & E x 320

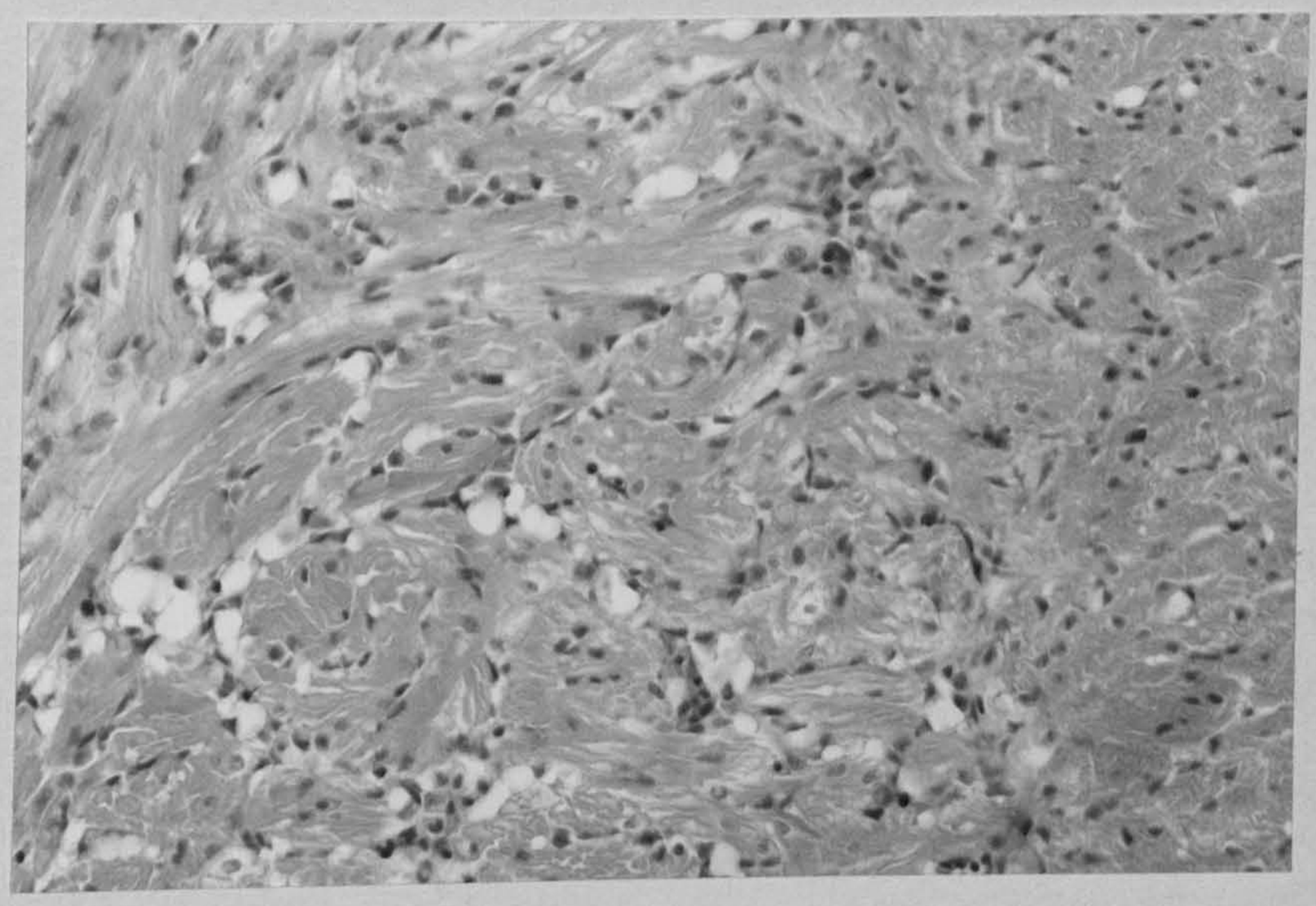

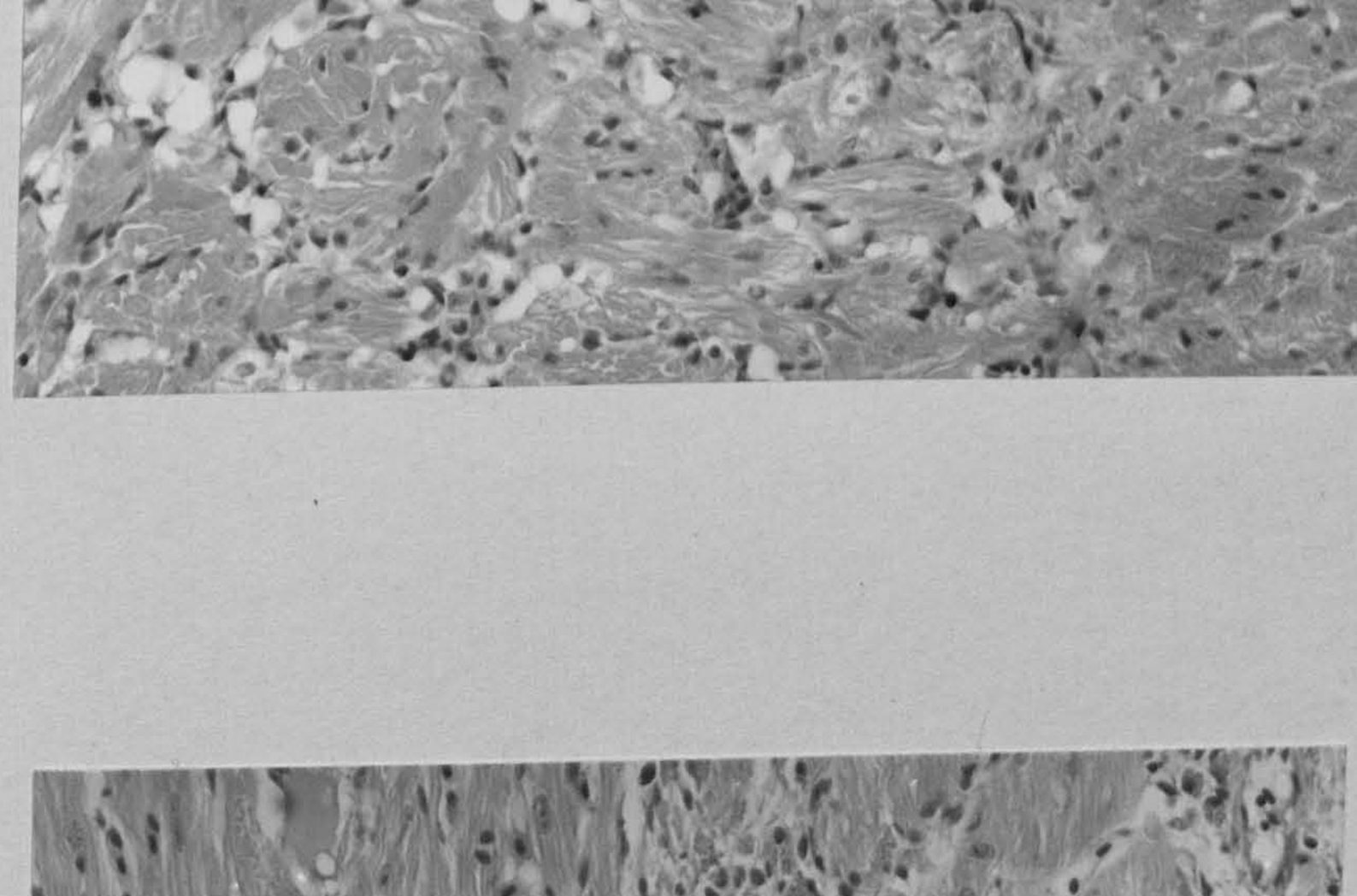

Fig. 22. Heart with extensive Cotylurus spp. infection. Note cyst walls and limited inflammatory response.

H & E x 125

Fig. 23. Outgrowths (arrowed) from blood vessel walls at vessel junctions.

Weigert's Elastic Stain x 320

Fig. 24. Liver of sexually mature fish. Note lack of glycogen or fat vacuolation.

H & E x 320

Fig. 25. Liver of sexually mature fish. Note haemorrhage and focal cytoplasmic vacuolation.

H & E x 320

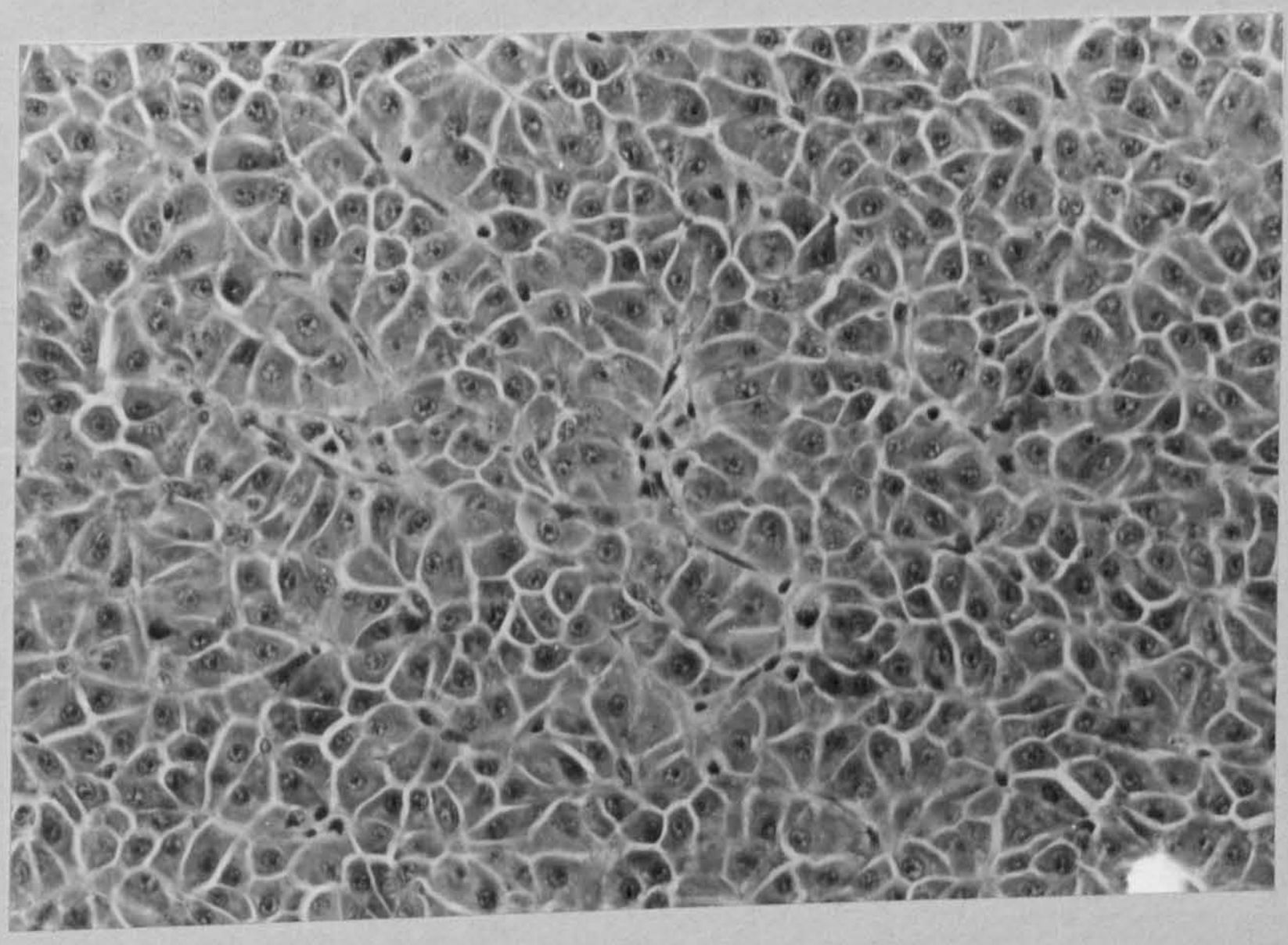

Fig. 26. Hepatoma. Note marked EGC response (E).

H & E x 320

Fig. 27. Liver of spawning fish. Note cells of Ito (arrowed).

H & E x 320

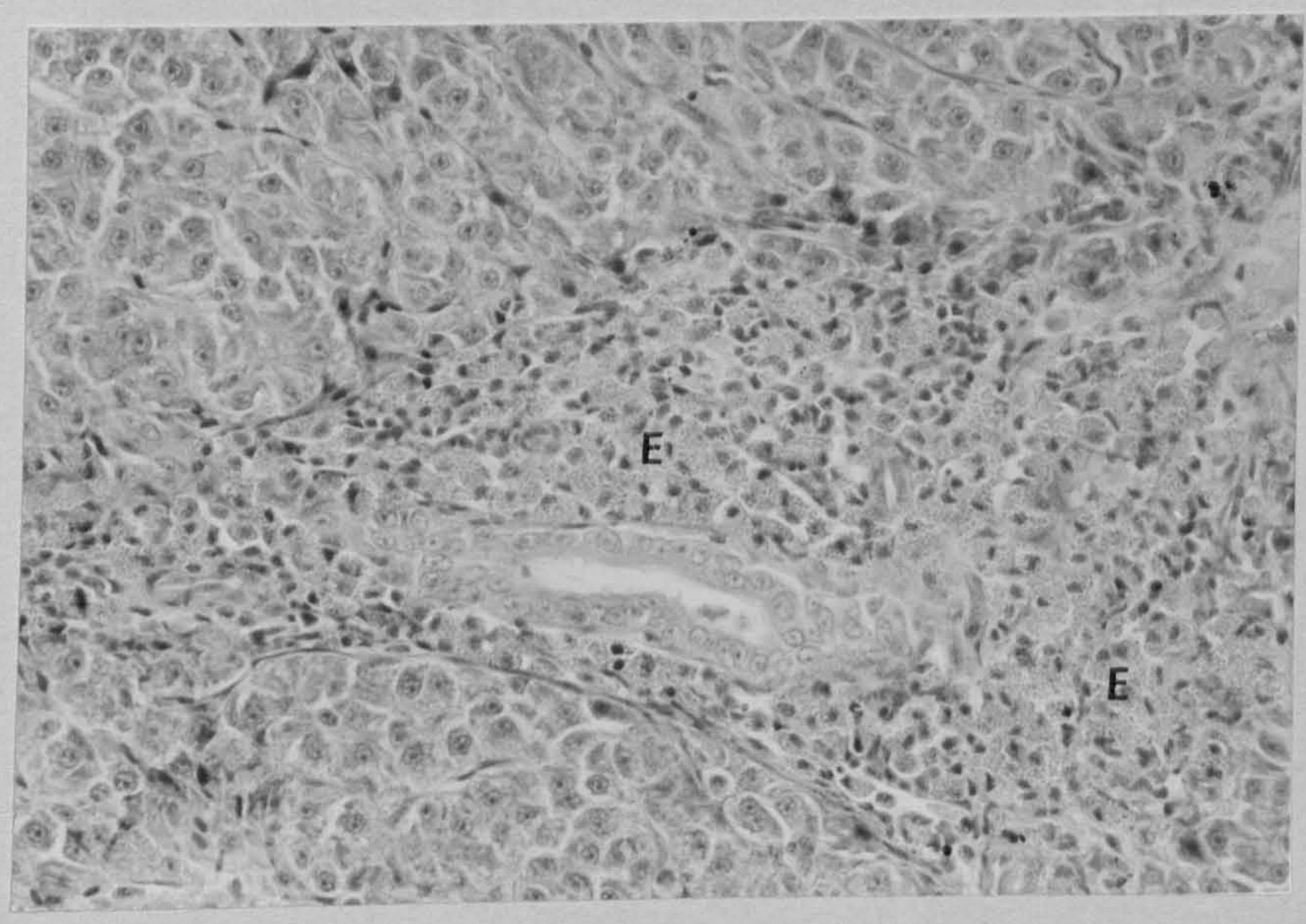
E
E

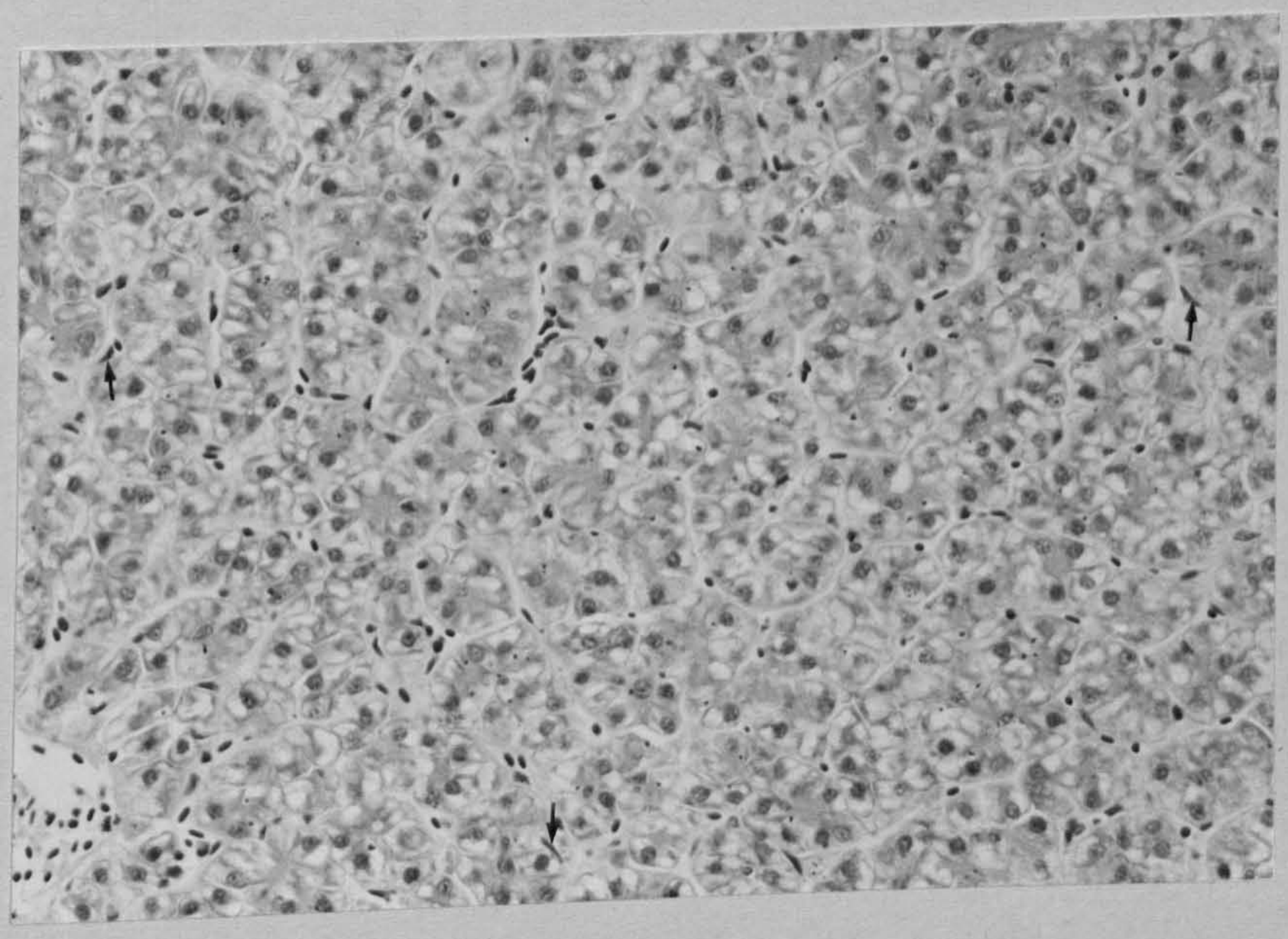

Fig. 28. Telangiectasis of gill (arrowed).

H & E x 125

Fig. 29. Gill. Note fusion and overgrowth of epithelium of secondary lamellae (arrowed).

H & E x 125

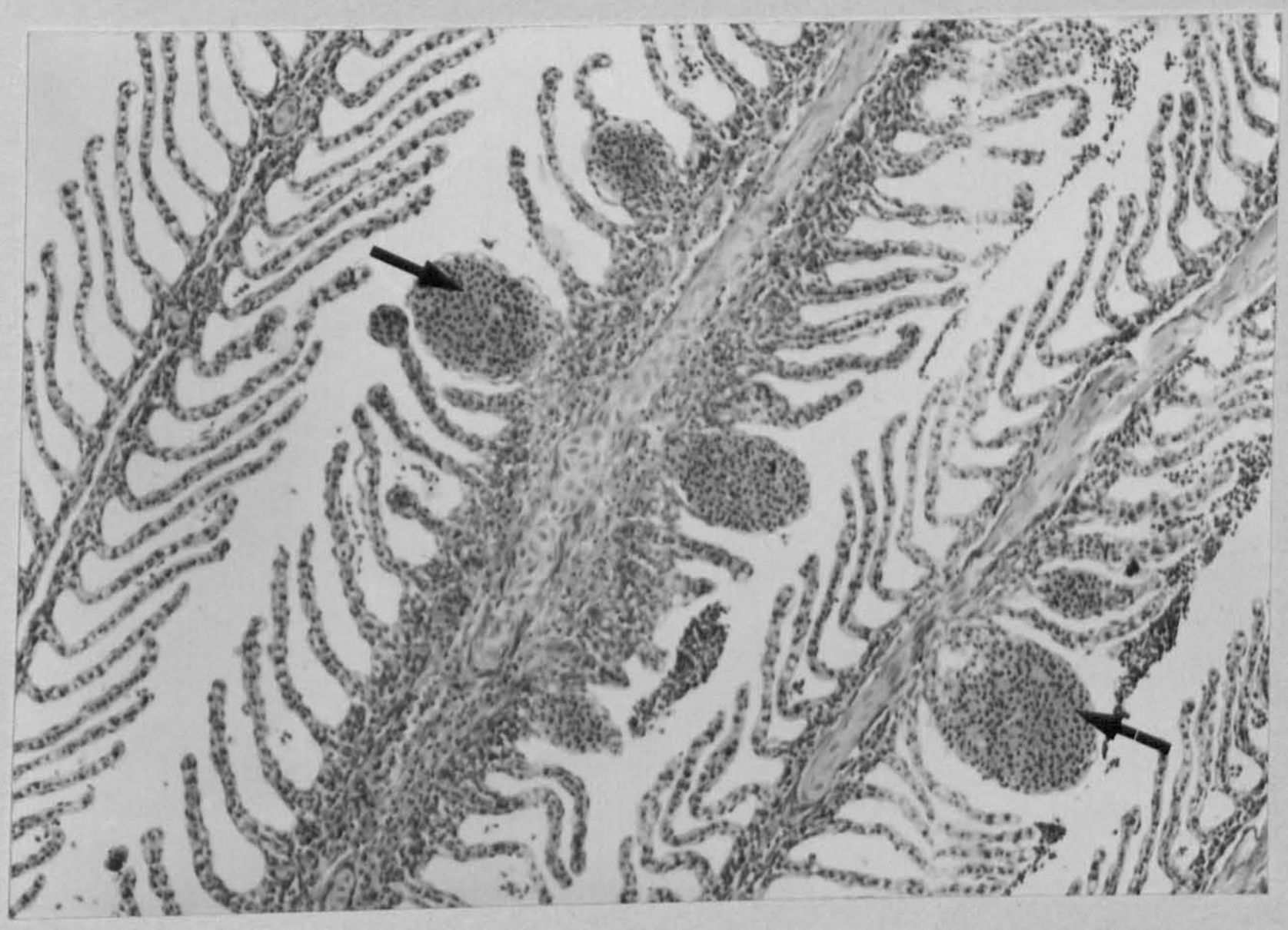

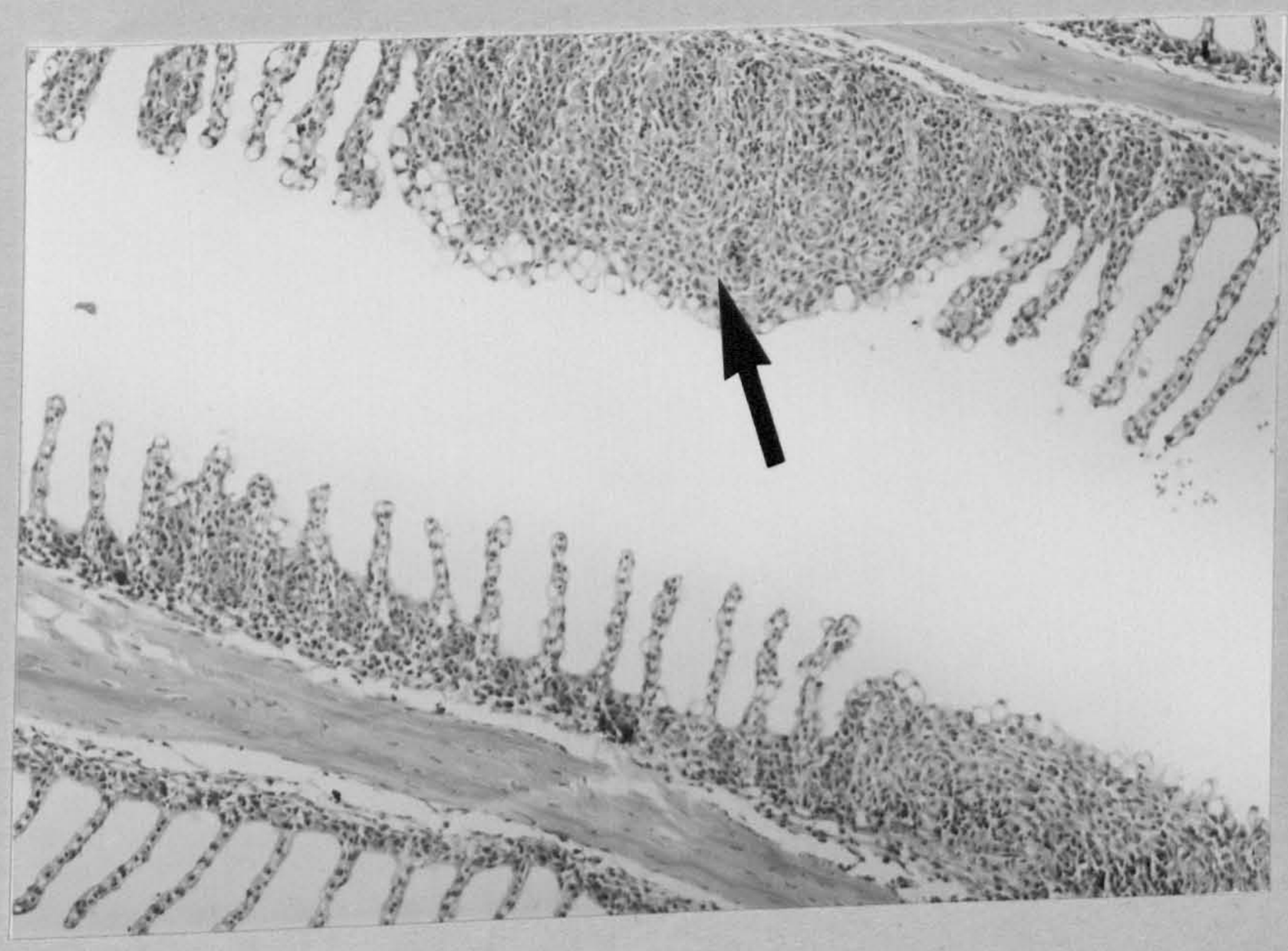

Fig. 30. Immature testis. Note primordial germ cells (p), sertoli cells (white arrows) and lobule boundary cells (black arrows).

H & E x 500

Fig. 31. Developing testis. Note secondary spermatogonia (S), primary spermatocytes (p) and secondary spermatocytes (b).

H & E x 320

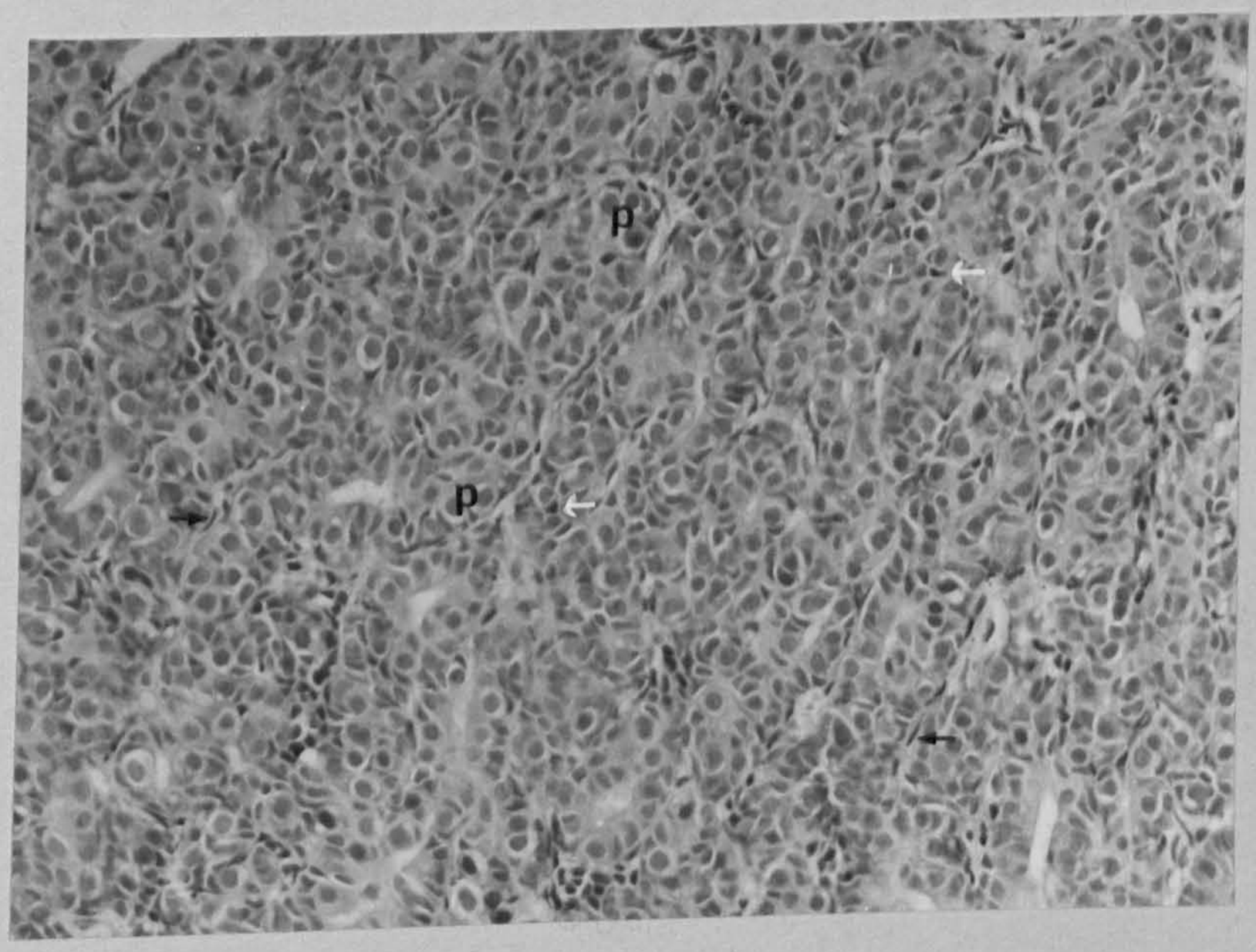
p
p

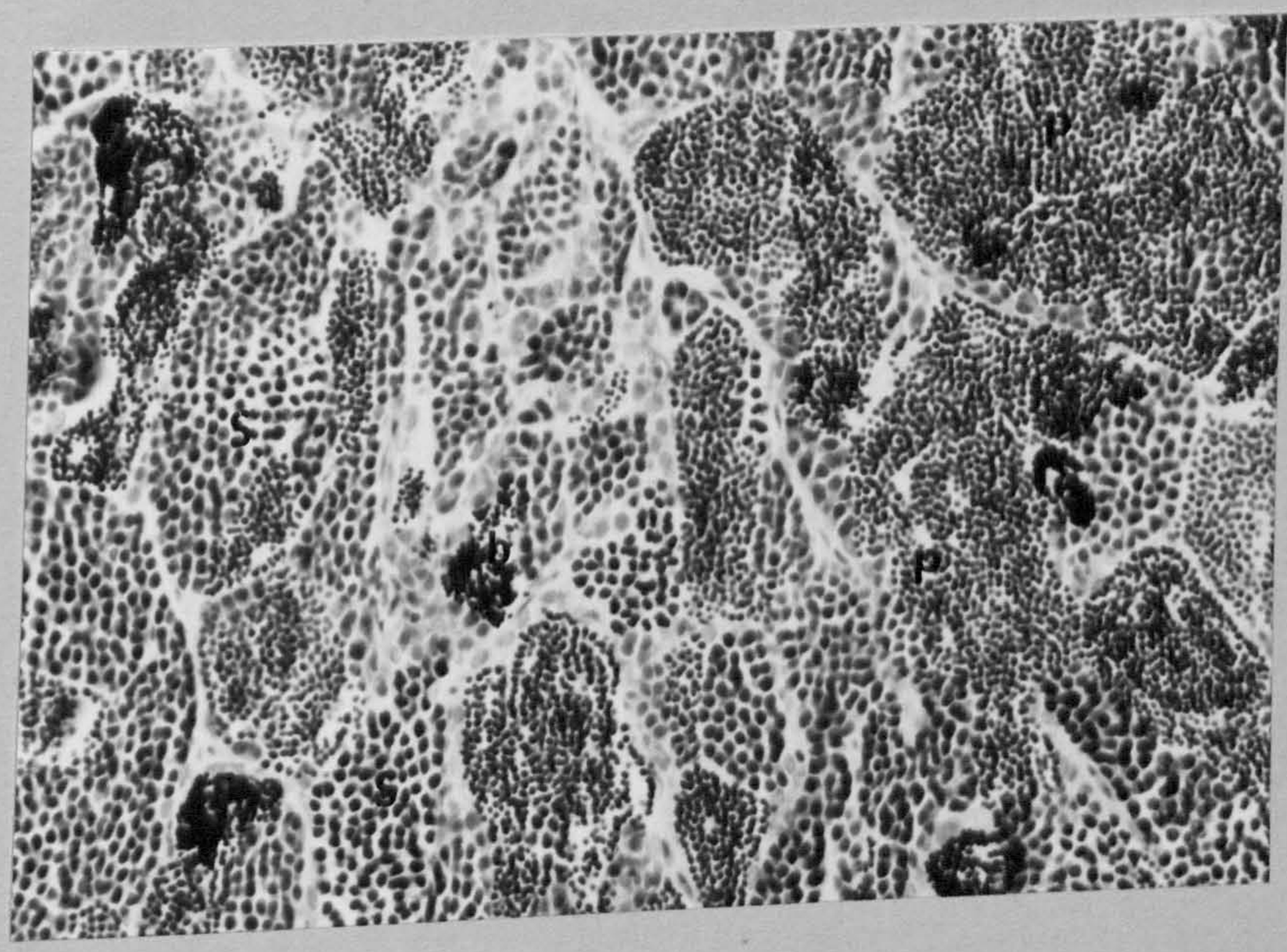

Fig. 32. Developing testis. Note secondary spermatogonia (s), primary spermatocytes (p) and secondary spermatocytes (b).

H & E x 320

Fig. 33. Mature testis with spermatids predominant.

H & E x 320

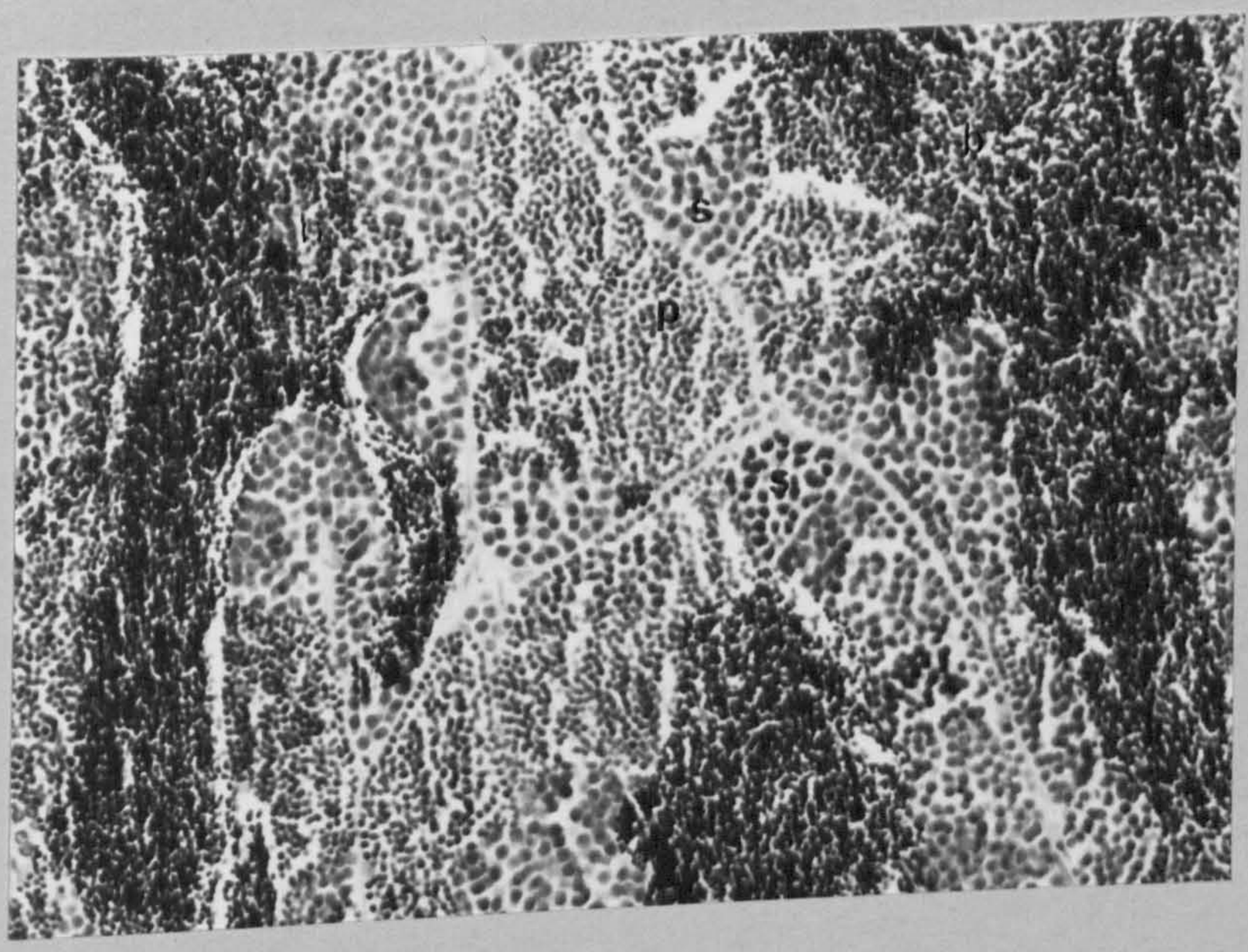
S
P
S

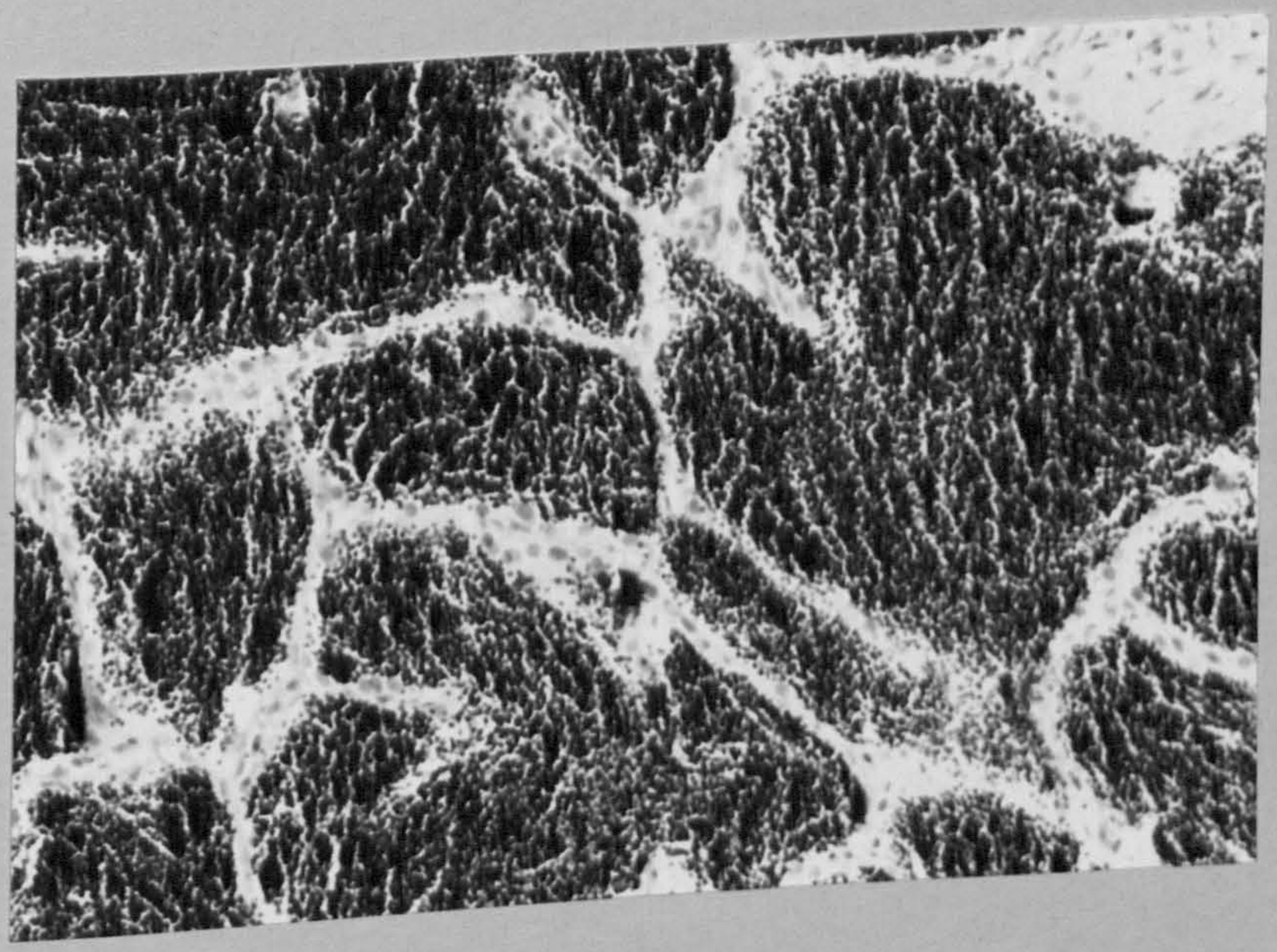

Fig. 34. Spent fish. Note thickened septa.

H & E x 320

Fig. 35. Immature ovary. Note stage II (a) and stage IV (c) oocytes.

H & E x 125

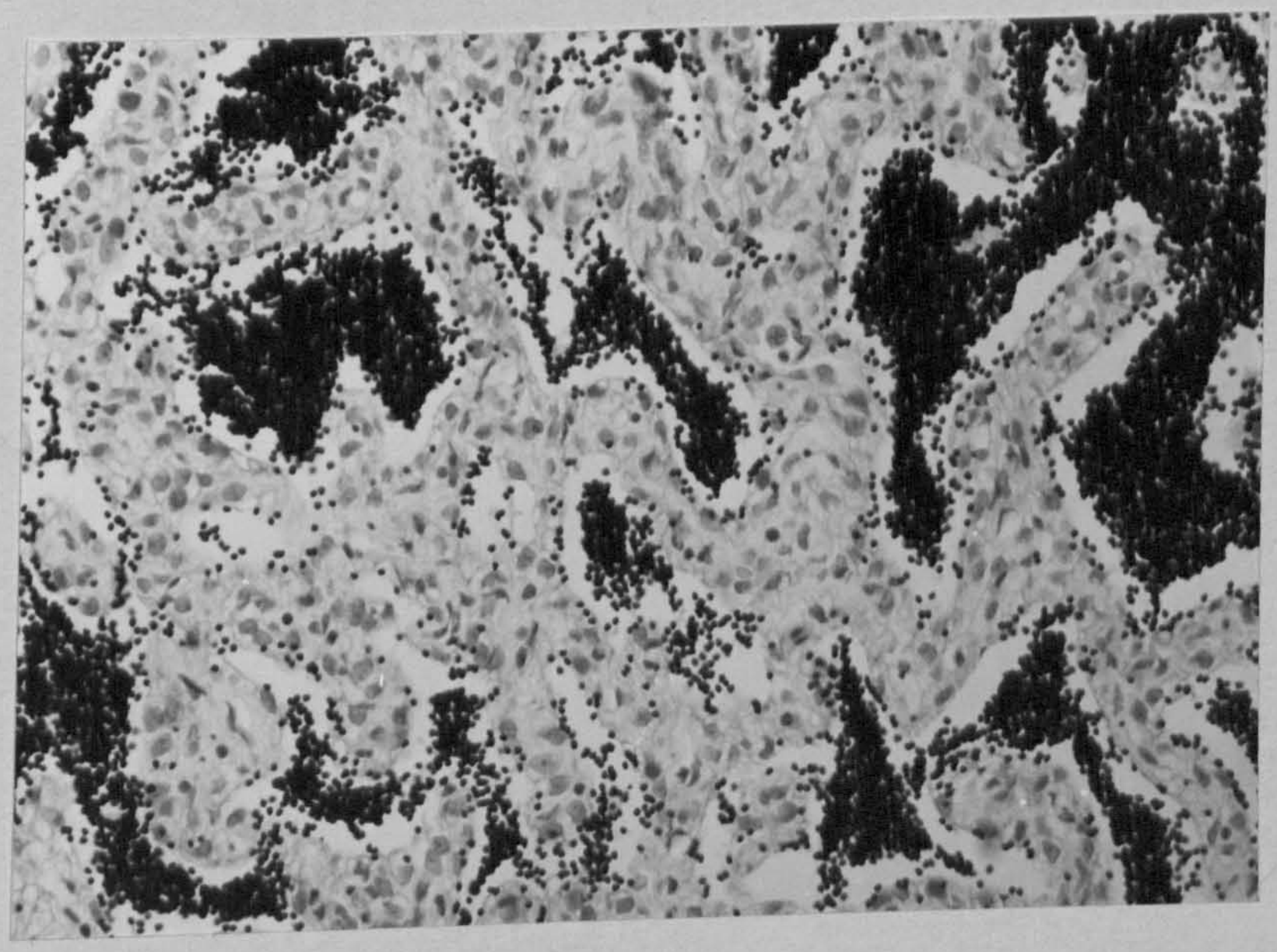

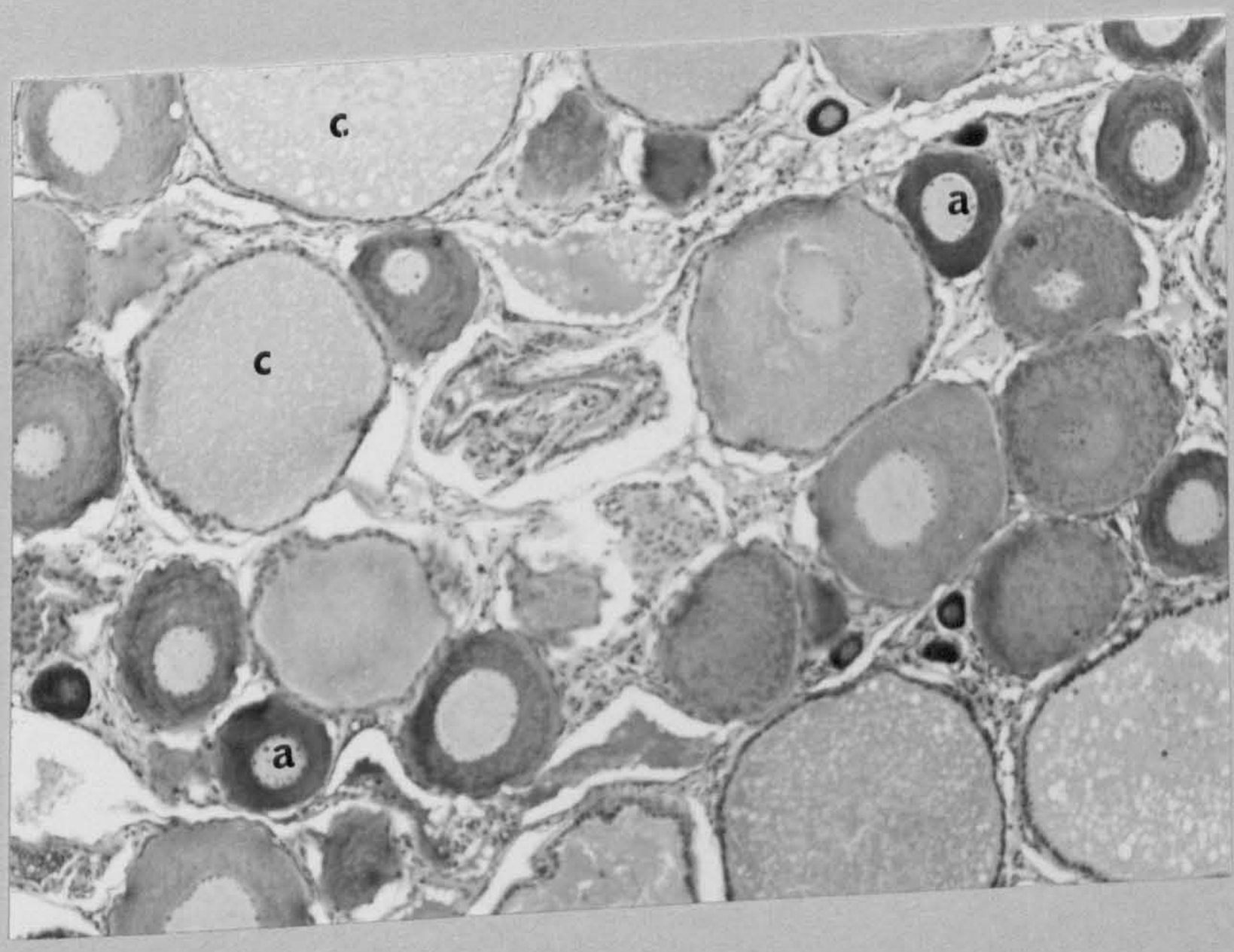
c
c
a
a

Fig. 36. Ovary of maturing fish. Stage III oocytes (b).

H & E x 320

Fig. 37. Ovary at vitellogenic stage. Note stage IV oocytes (c).

H & E x 50

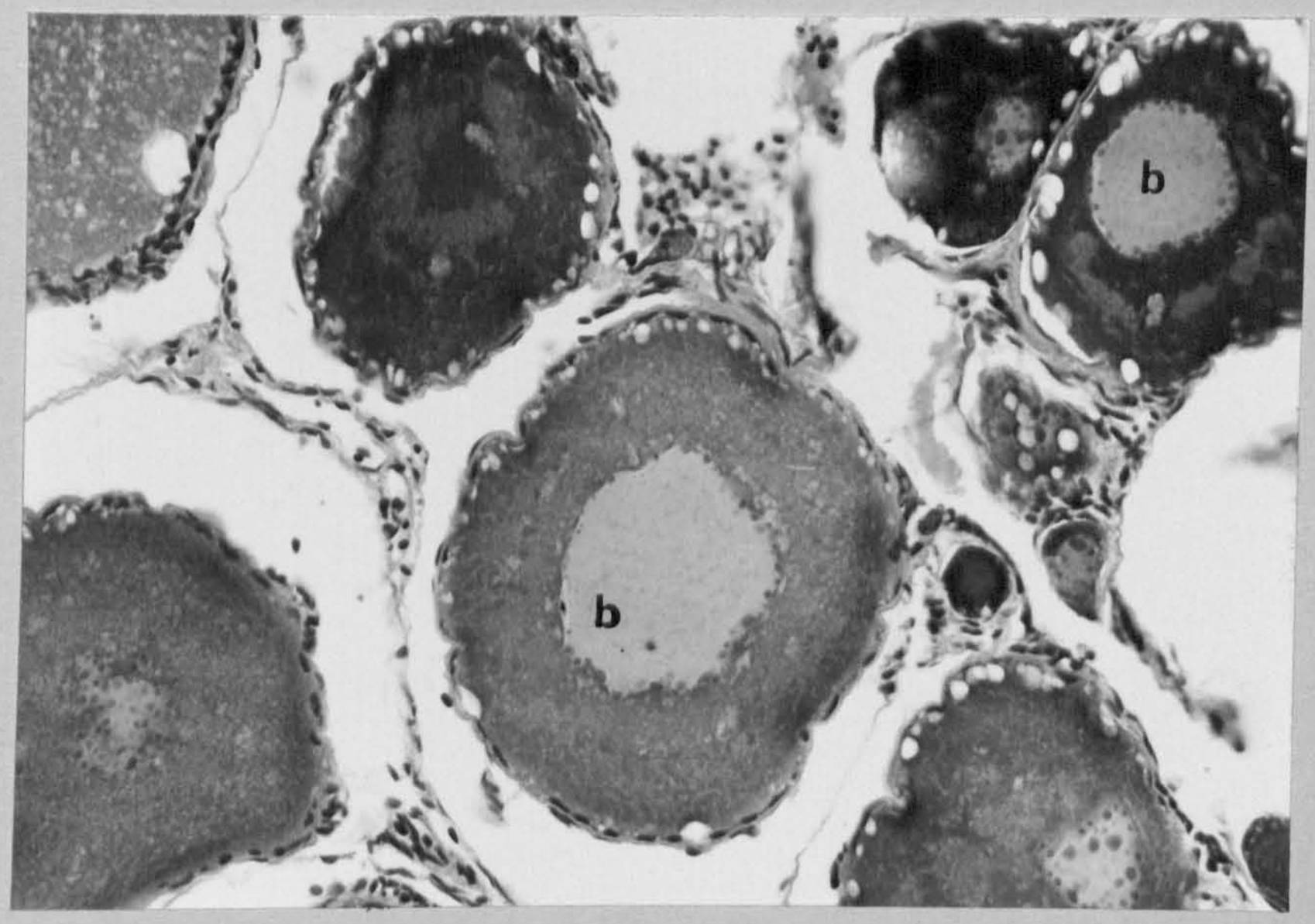
b
b

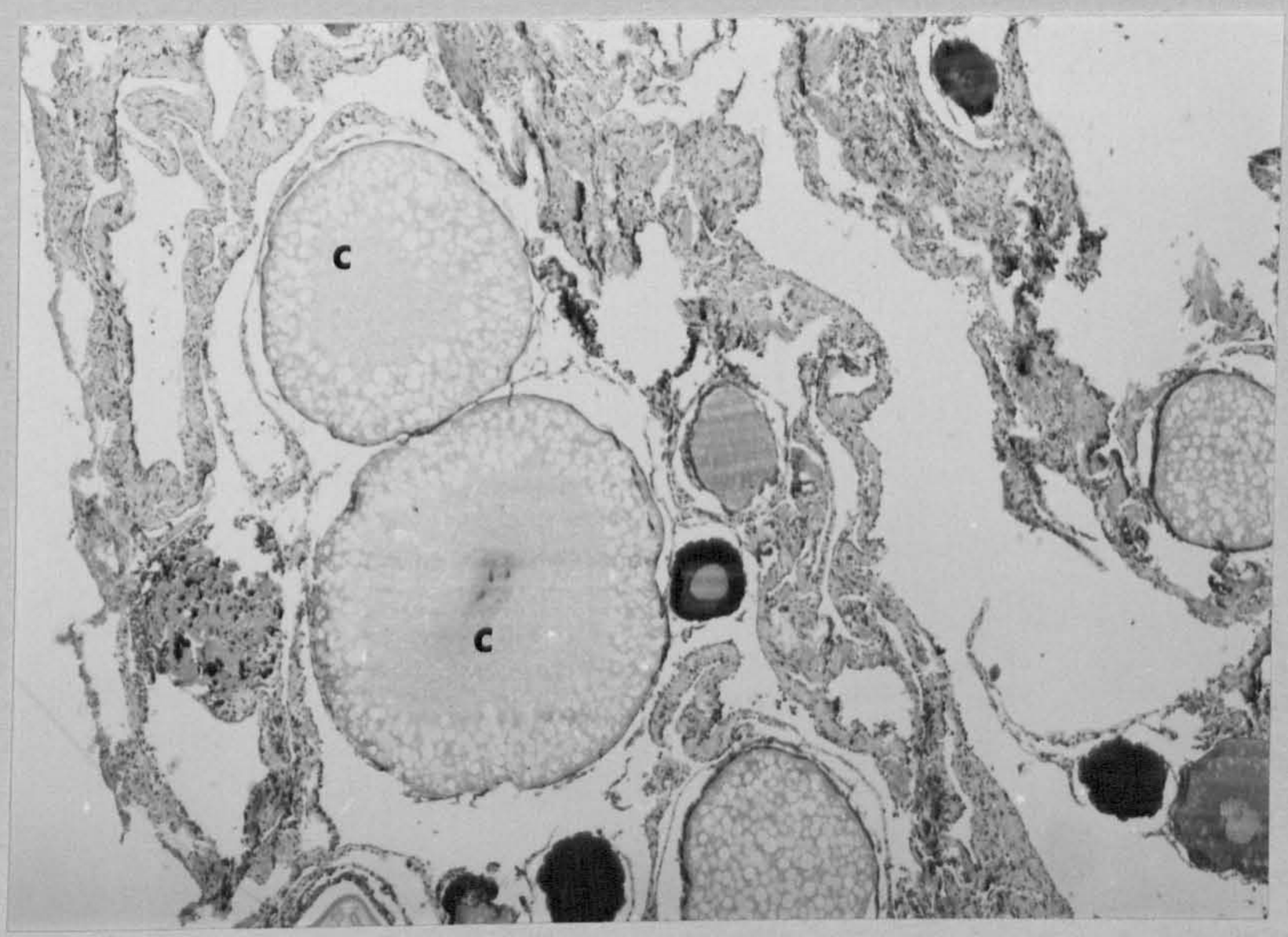
c
c

Fig. 38. Ovary of spent fish. Note corpora atretica (d).

H & E x 50

Fig. 39. Kidney of sexually mature fish. Note degenerative cytoplasmic changes in tubules.

H & E x 320

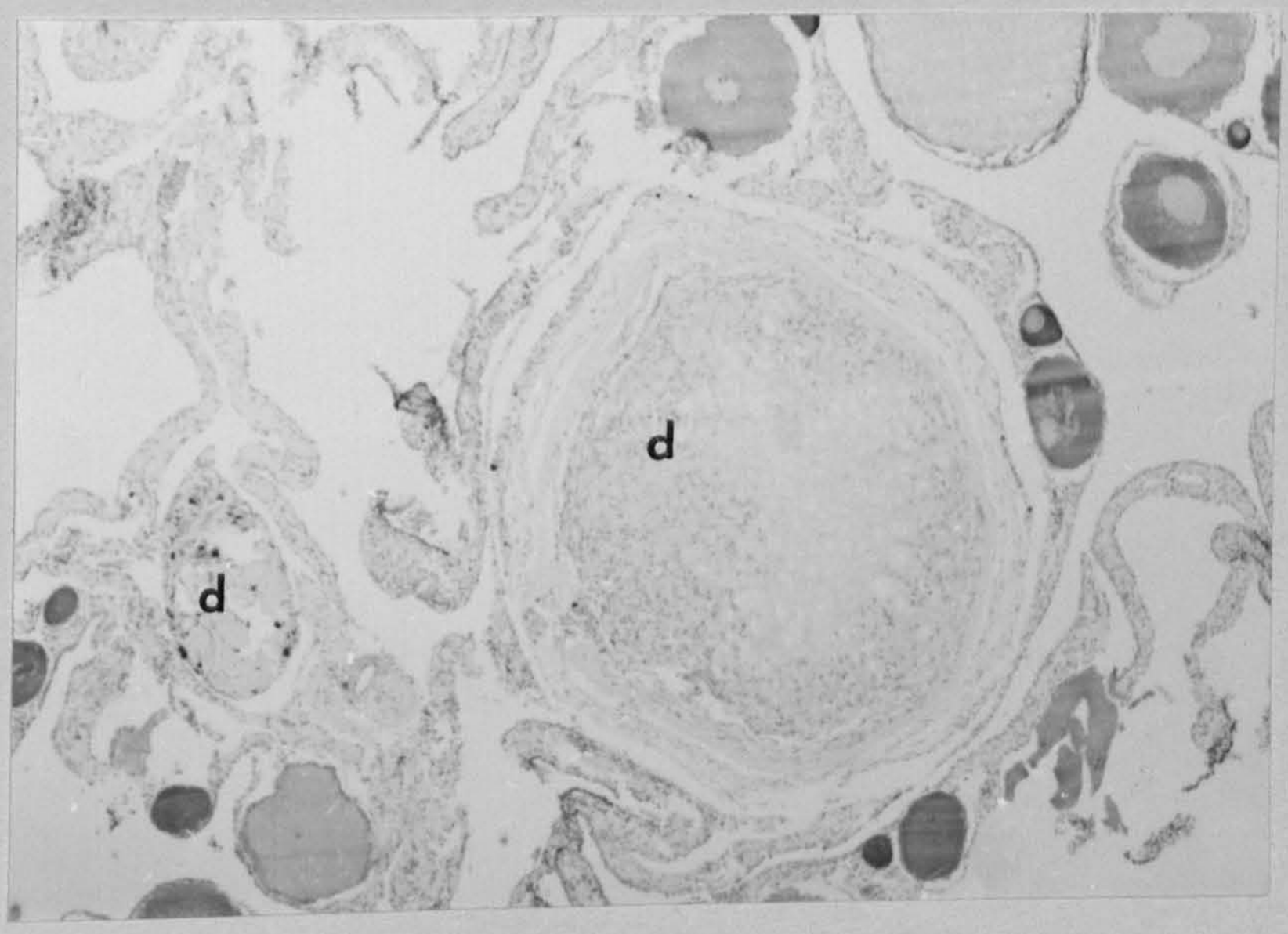
d
d

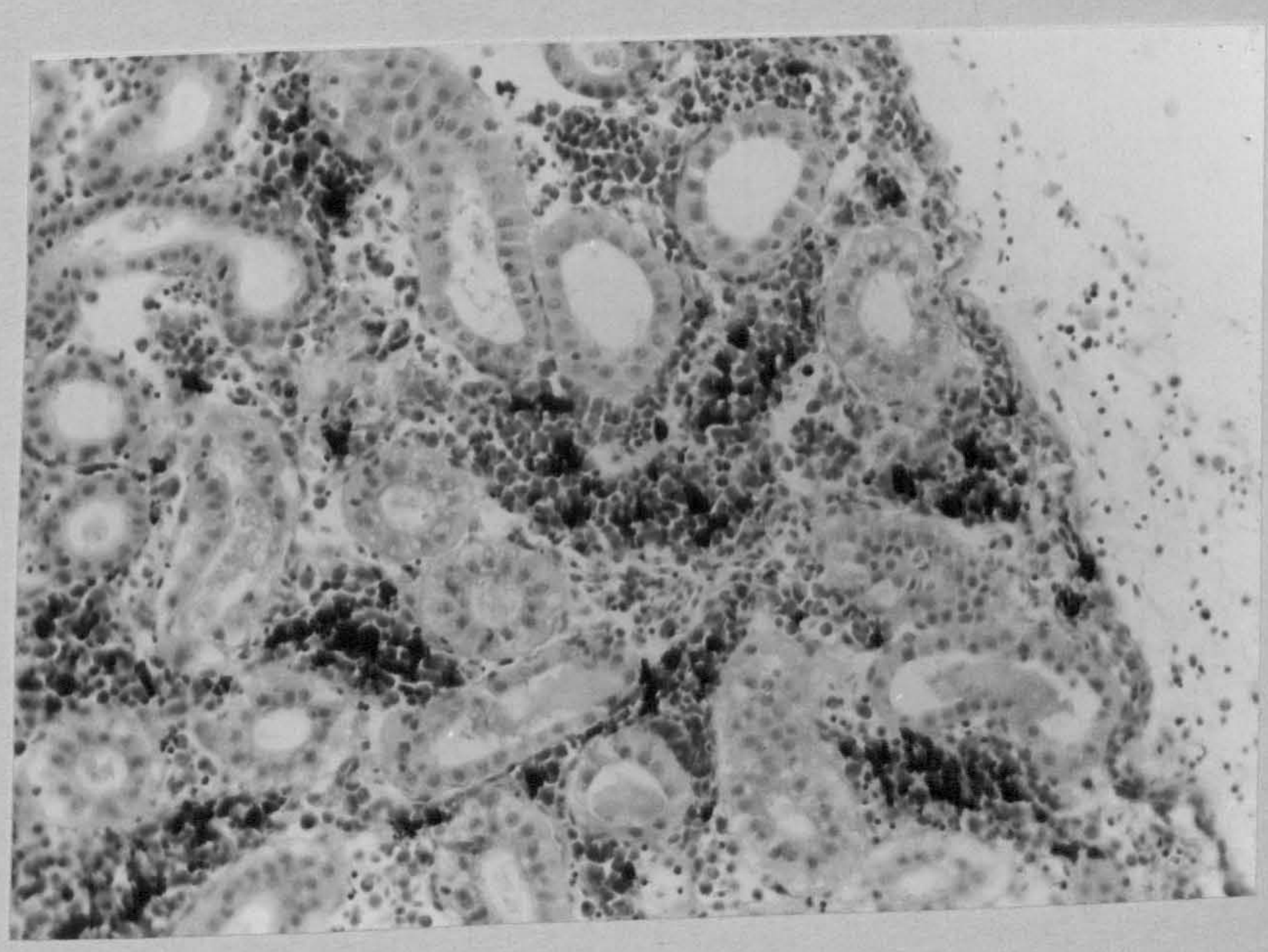

Fig. 40. Kidney of sexually mature fish.
Note hyaline eosinophilic droplet formation
(arrowed) in tubules.

H & E x 320

Fig. 41. Kidney of sexually mature fish.
Note thickening of Bowman's capsule and
periglomerular fibrosis.

H & E x 320

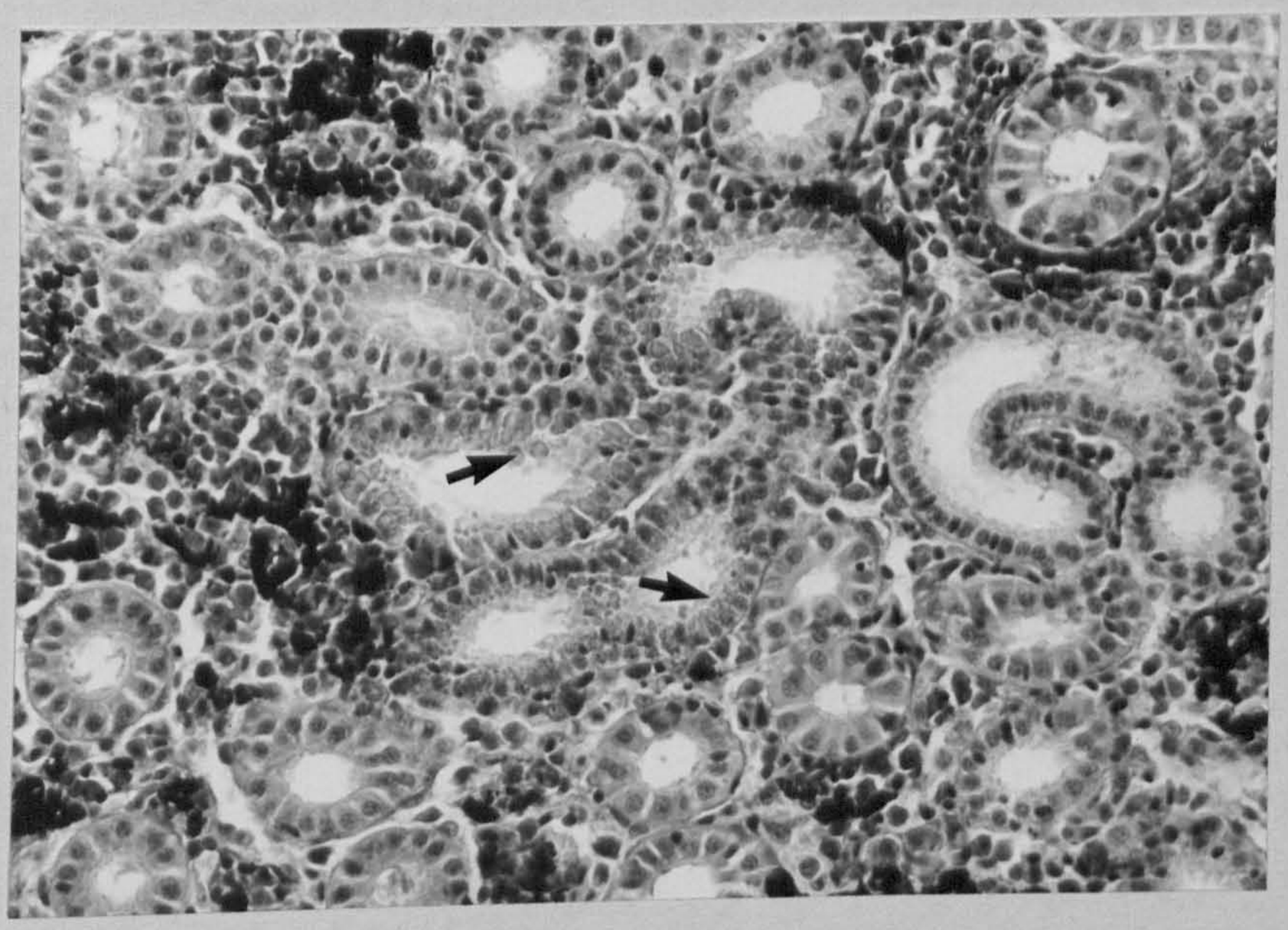

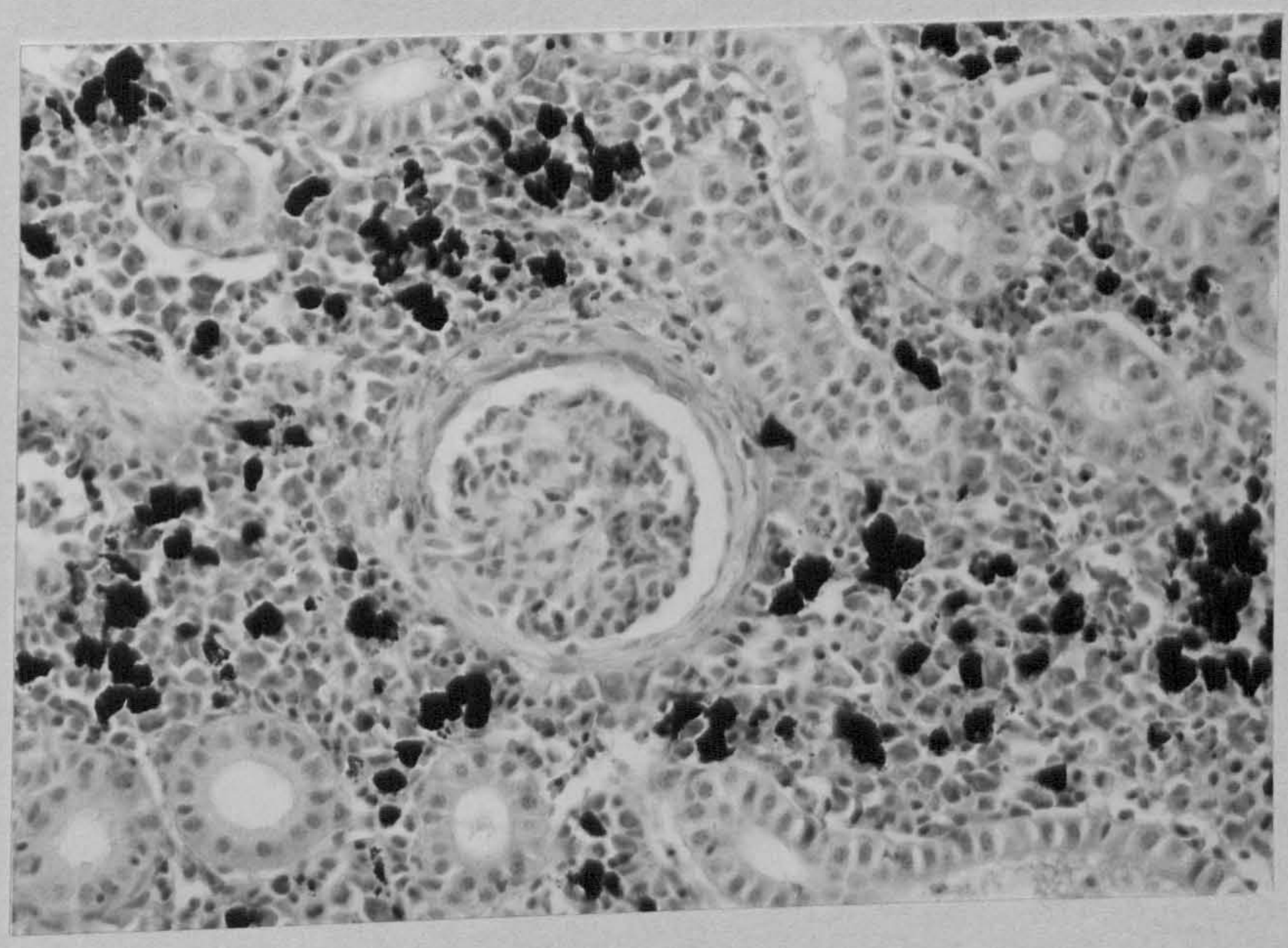

Fig. 42. Kidney of sexually immature fish.

Note large cells (arrowed) amongst haemopoietic tissue.

H & E x 500

Fig. 43. Dissection of brown trout to show cruciform head kidney.

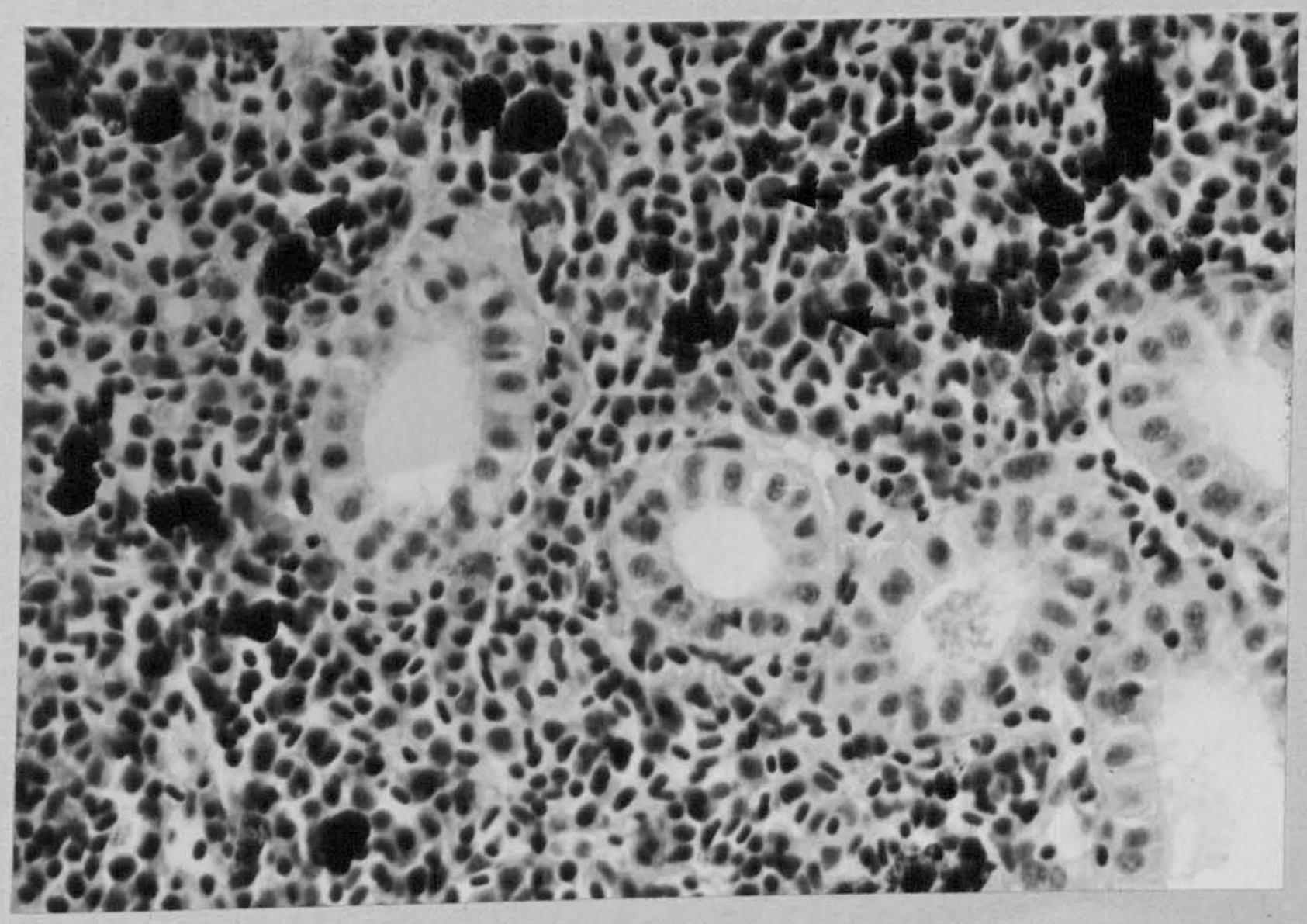

Fig. 44. Interrenal tissue in sexually immature fish. Note duct formation (d).

H & E x 320

Fig. 45. Anterior kidney of sexually immature fish.

H & E x 50

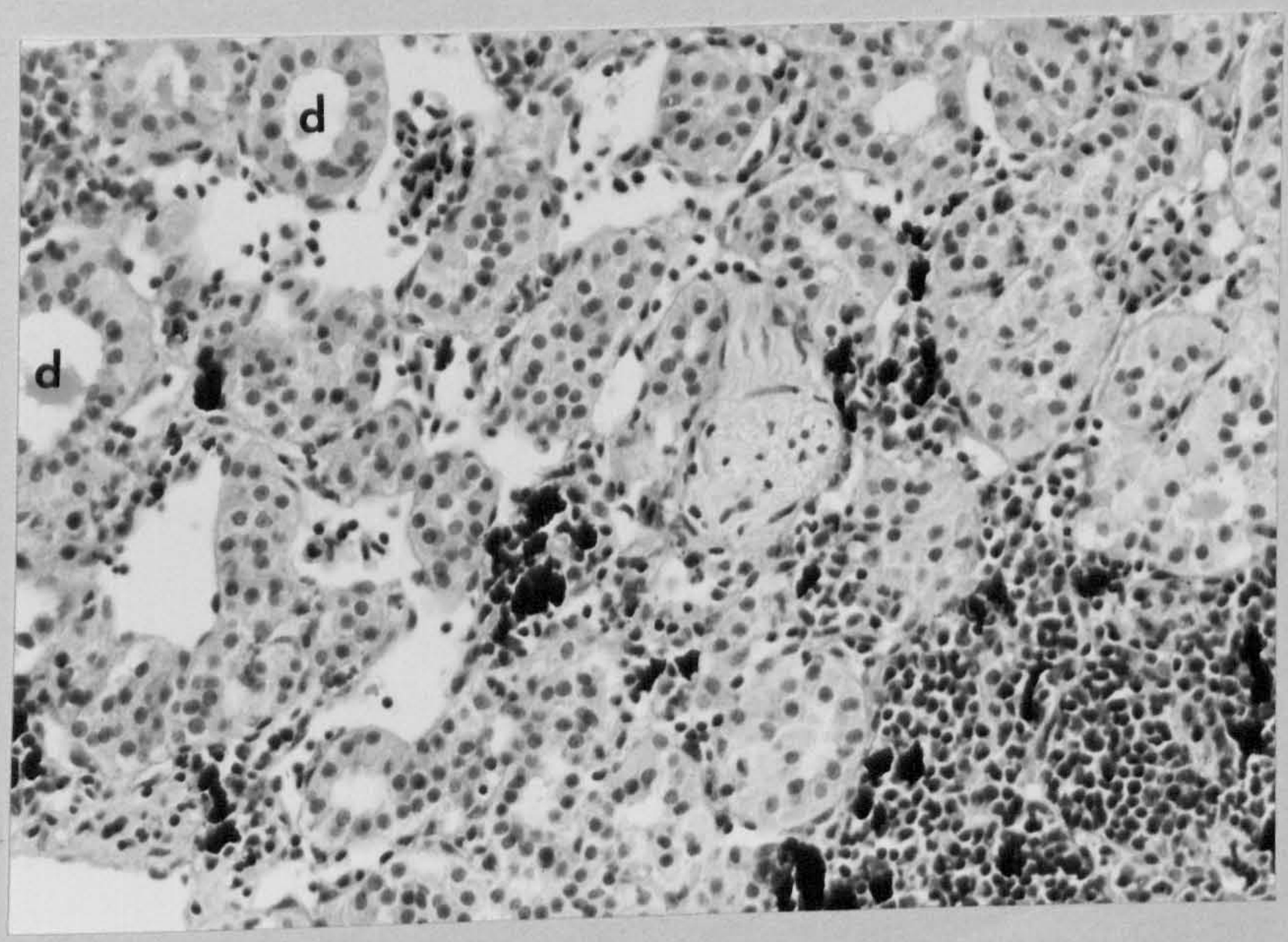
d
d

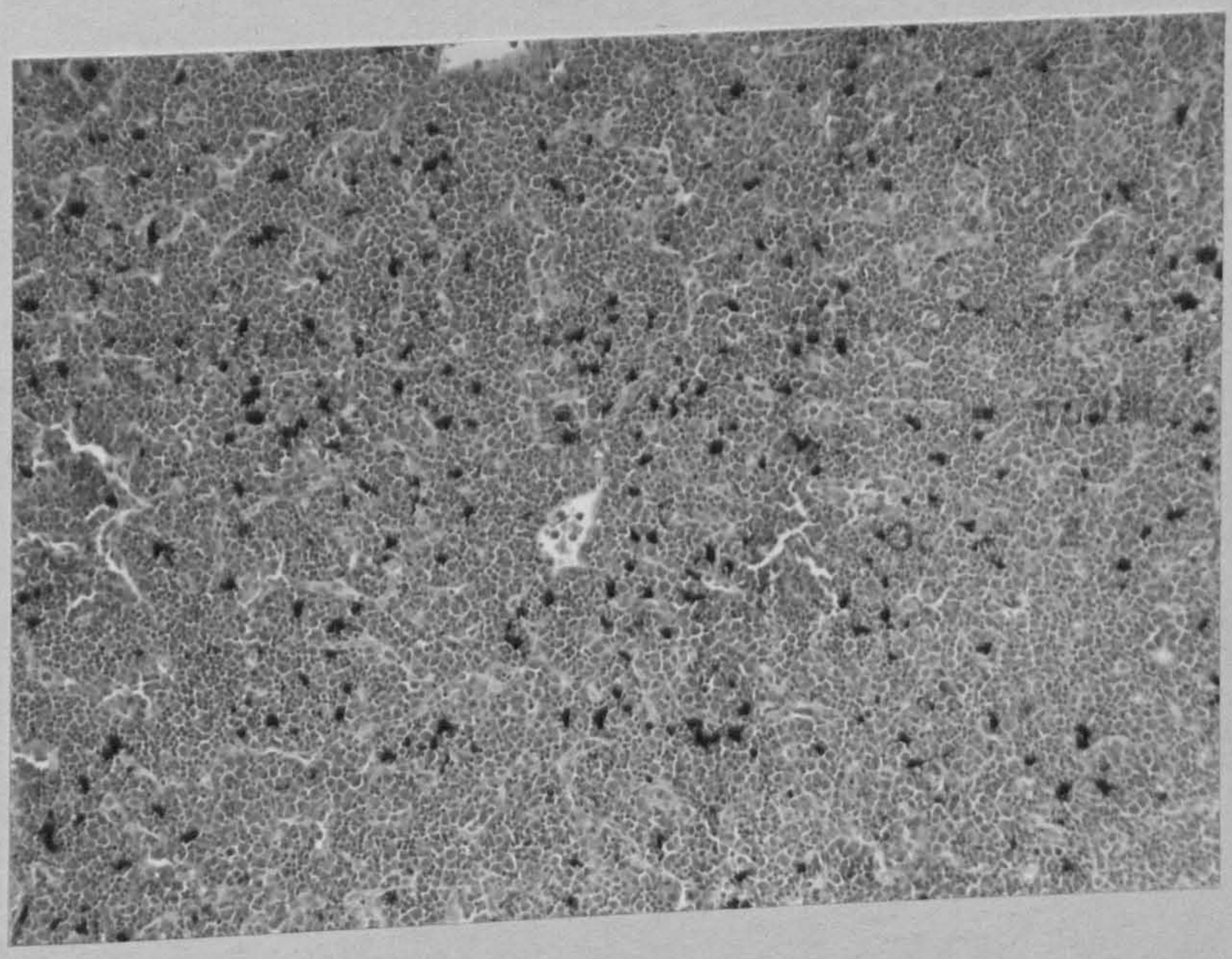

Fig. 46. Anterior kidney of sexually immature fish. Note "nests" of small cells with densely-staining nuclei and little cytoplasm.

H & E x 125

Fig. 47. Interrenal tissue of sexually immature fish. Note well-developed blood sinusoids (arrowed).

H & E x 320

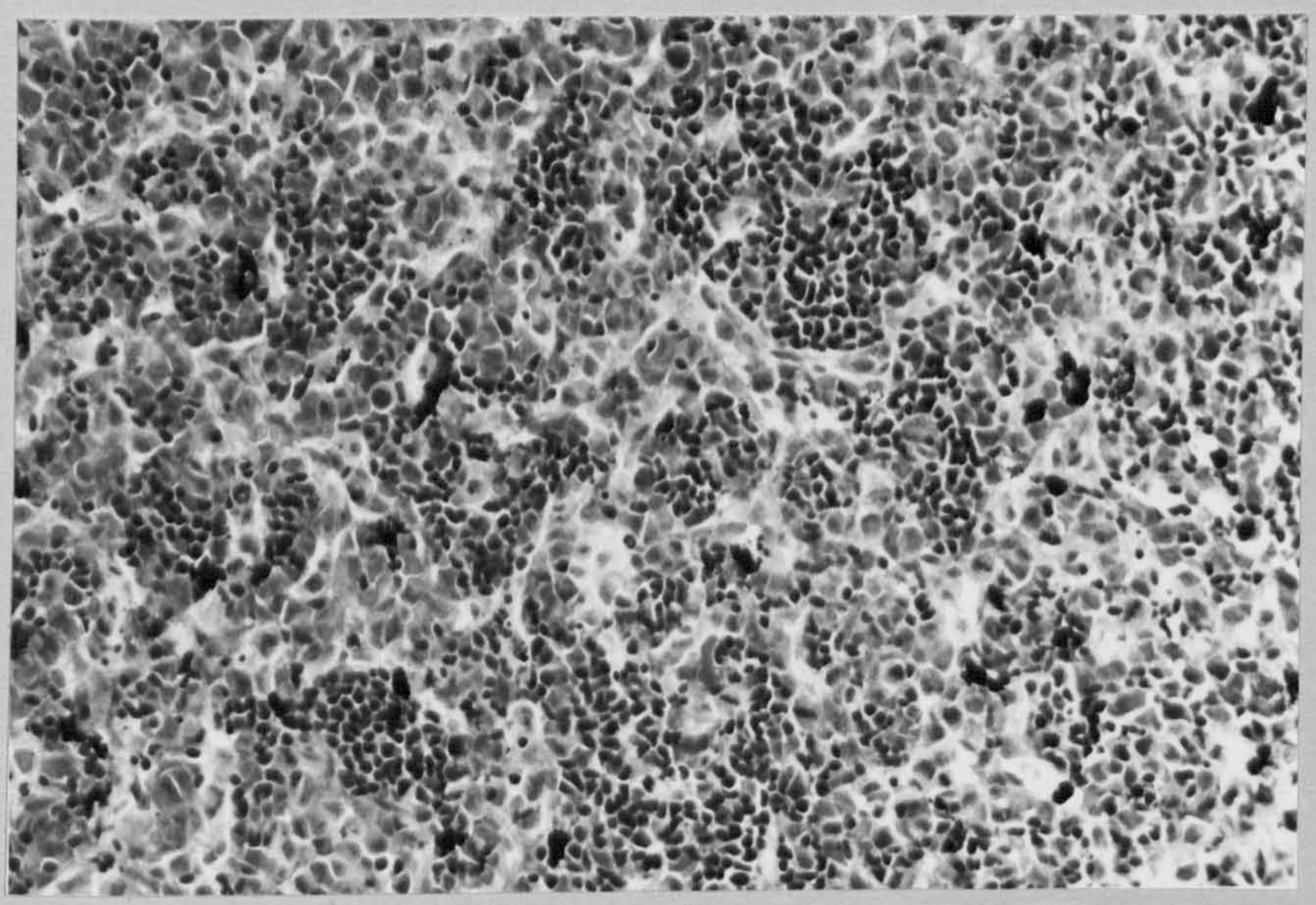

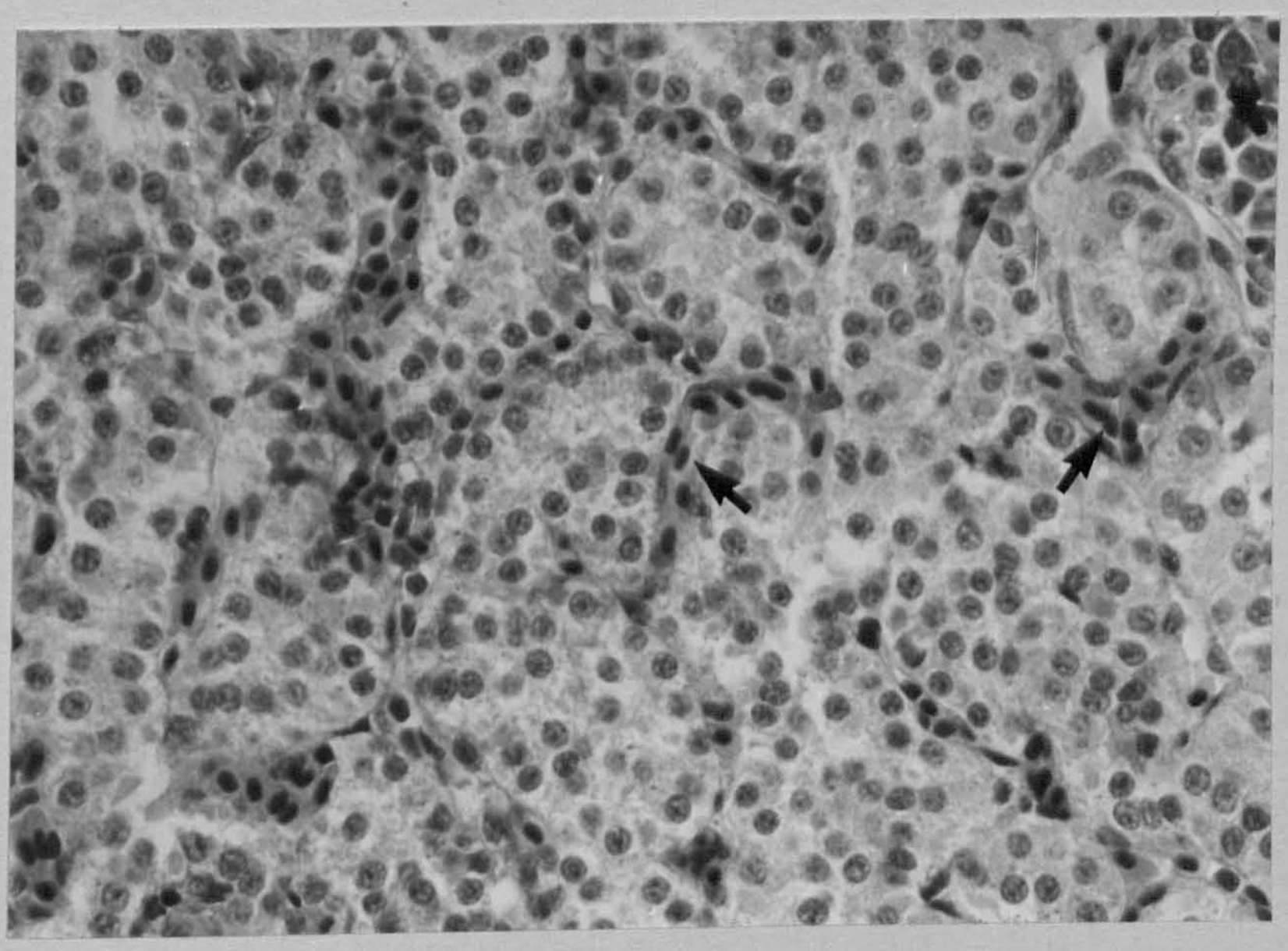

Fig. 48. Interrenal tissue of sexually mature fish. Note distinctly granular cytoplasm.

H & E x 500

Fig. 49. Interrenal tissue of sexually mature fish. Note early degenerative change consisting of loss of cell outline and cytoplasmic breakdown.

H & E x 320

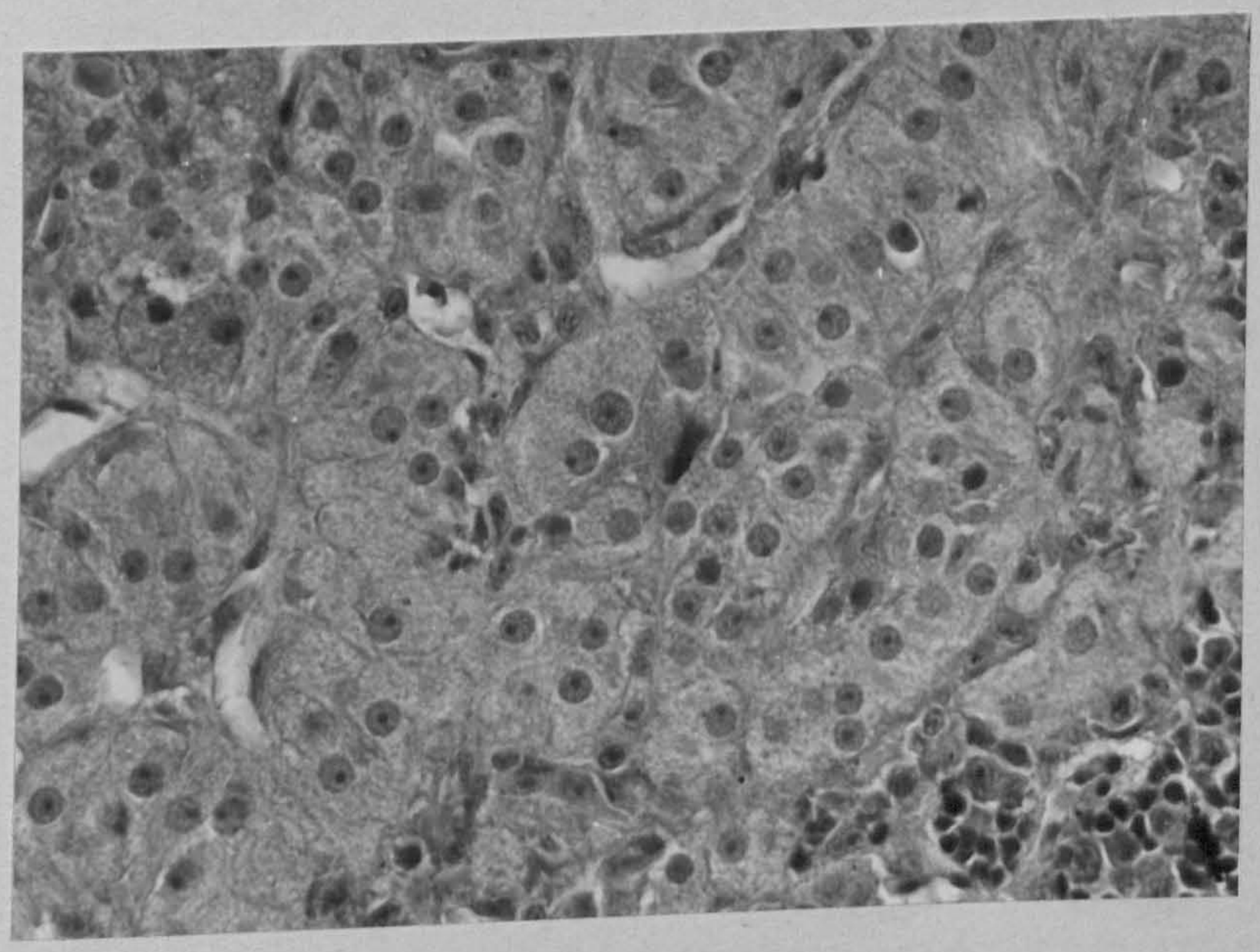

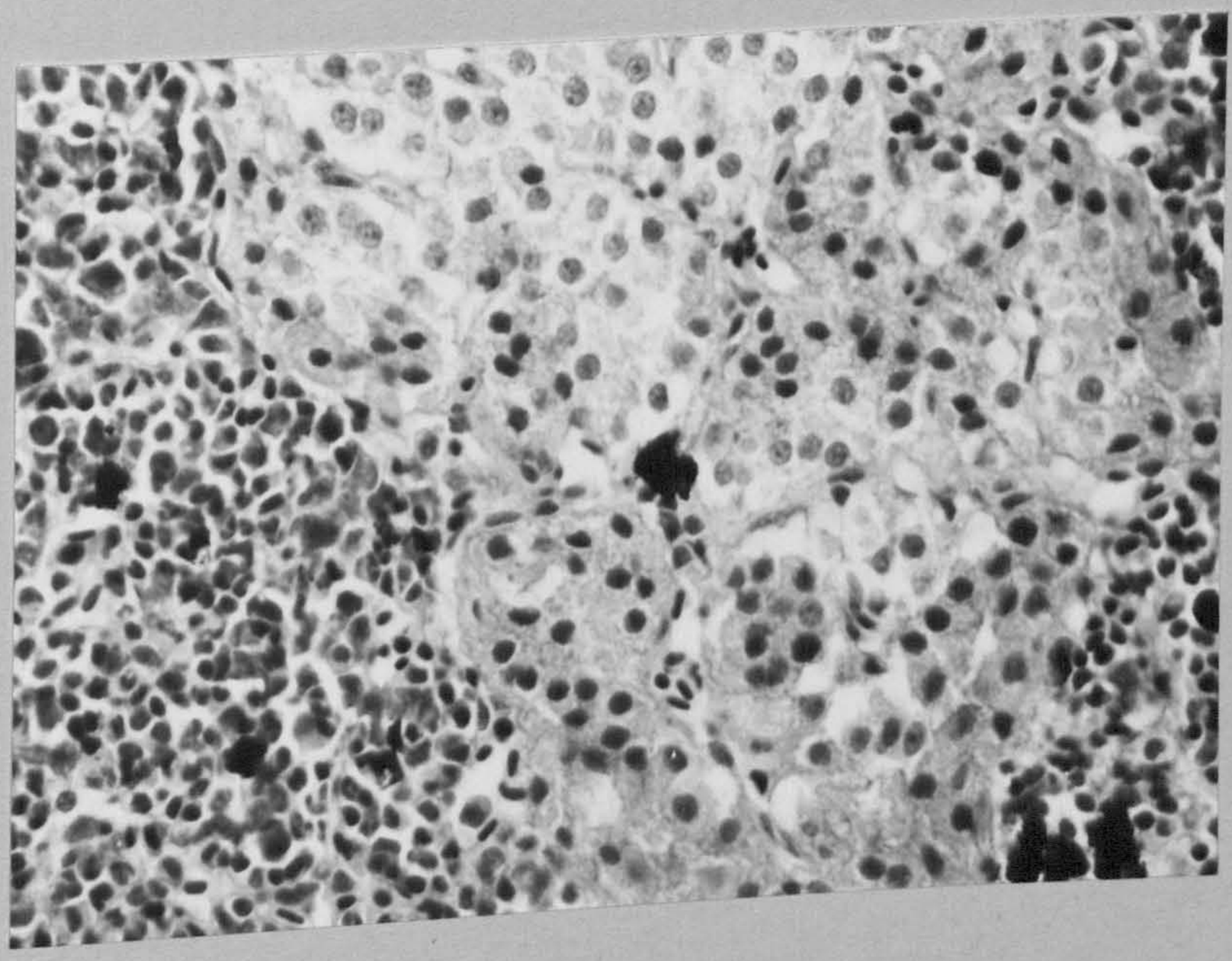

Fig. 50. Interrenal tissue of sexually mature fish. Note marked degenerative changes and early bulla formation.

H & E x 320

Fig. 51. Pancreas of sexually immature fish. Note the large quantities of fat cells.

H & E x 50

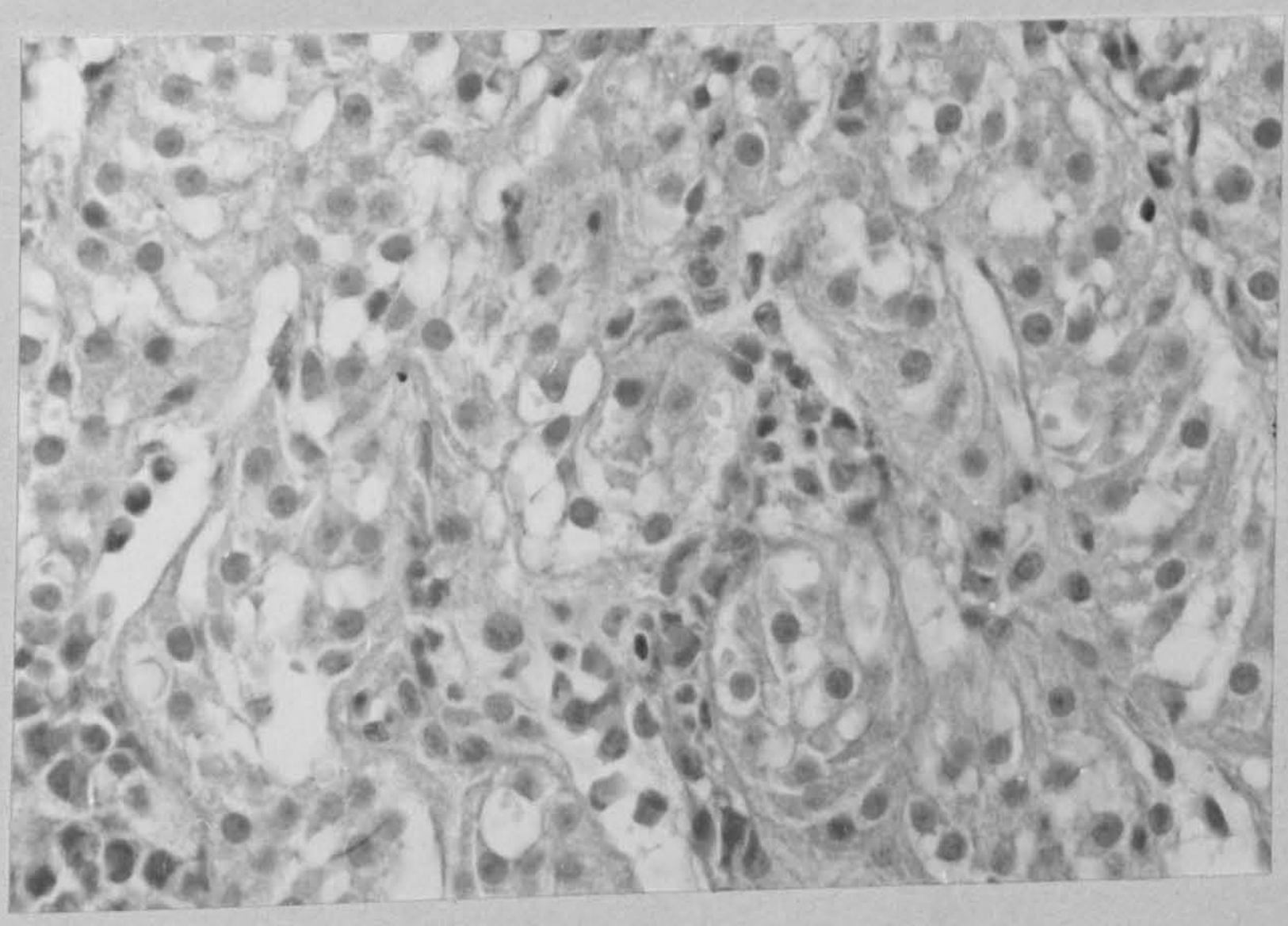

Fig. 52. Pancreas of sexually mature fish.
Note the increase in connective tissue amongst the reduced quantities of fat tissue.

H & E x 500

Fig. 53. Islet of Langerhans in sexually mature fish. Note the extensive cellular degeneration leaving only cell "ghosts".

H & E x 500

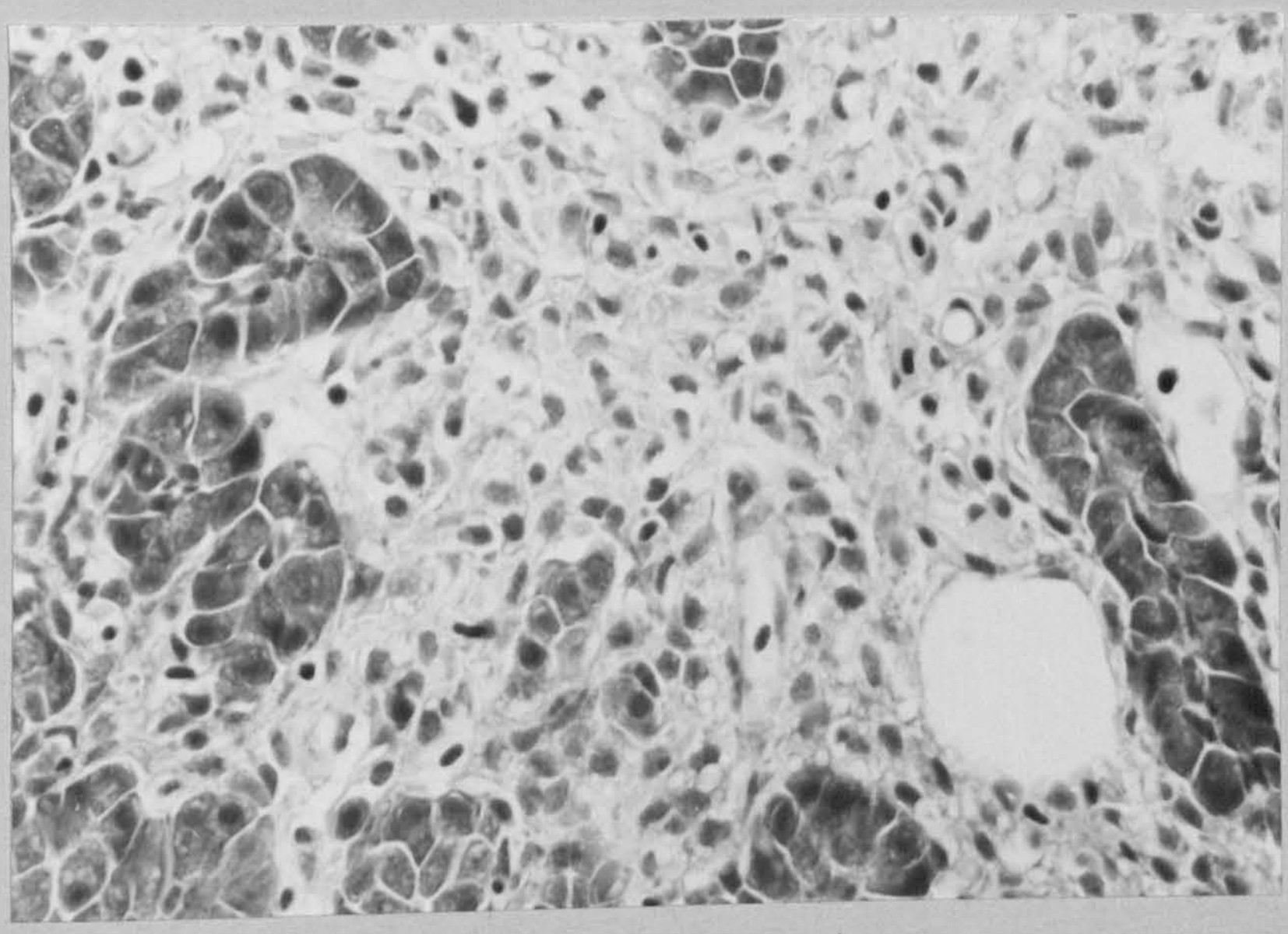

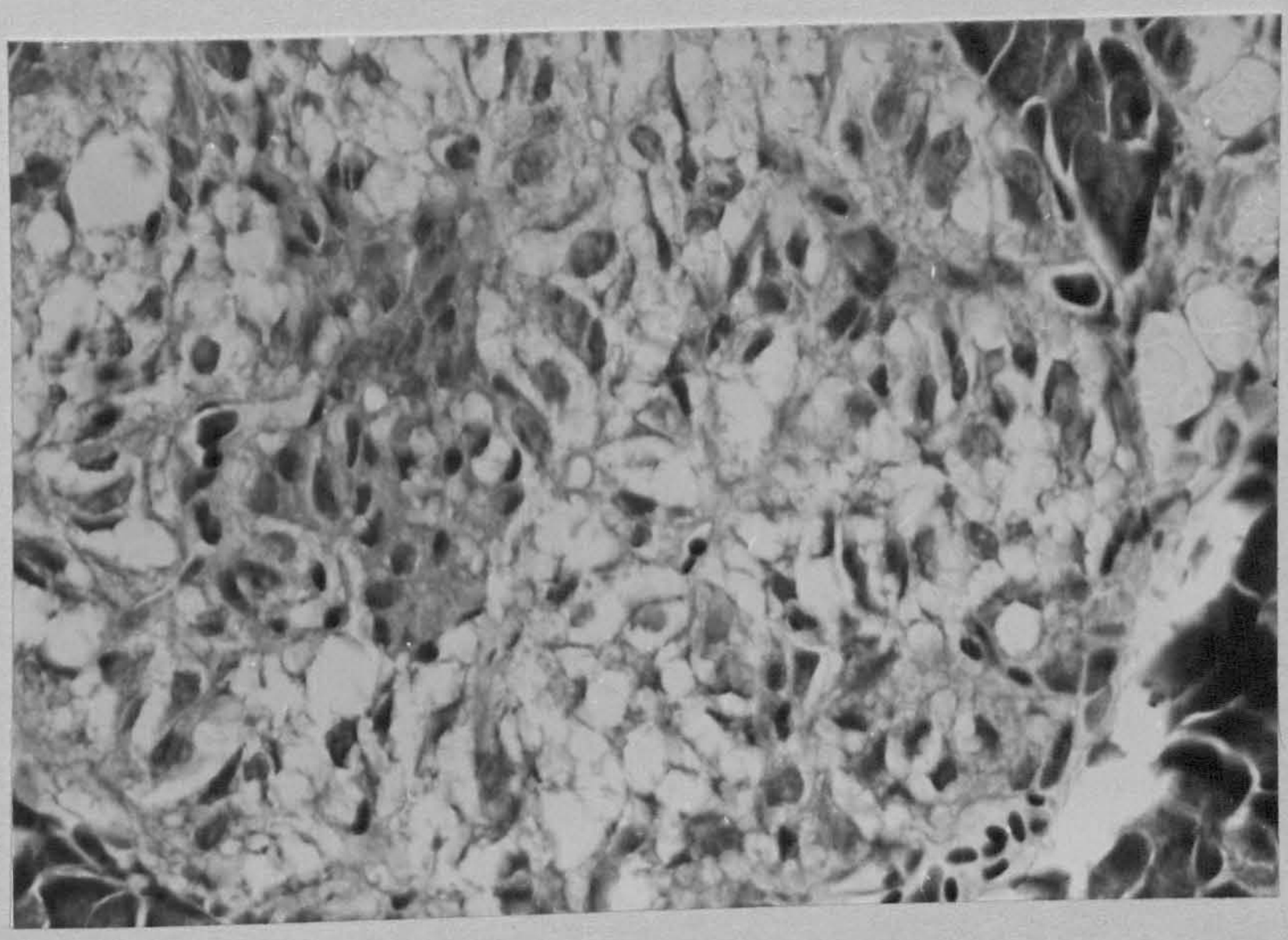

Fig. 54. Pyloric caecum of sexually mature fish. Note the marked cellularity of the submucosa.

H & E x 320

Fig. 55. Stomach of sexually mature fish. Note oedema (o) at junction of stratum compactum and circular muscle layer.

H & E x 50

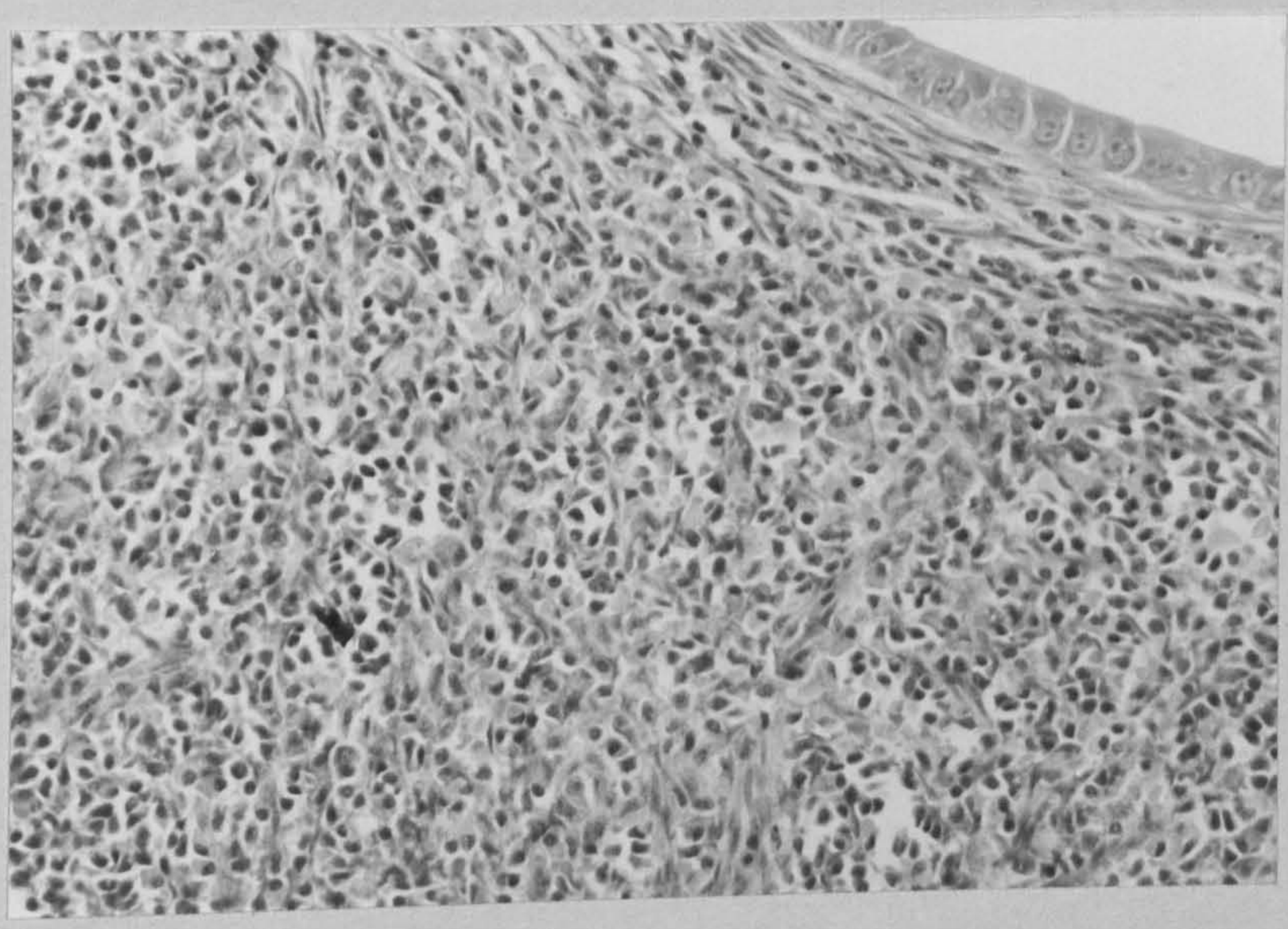

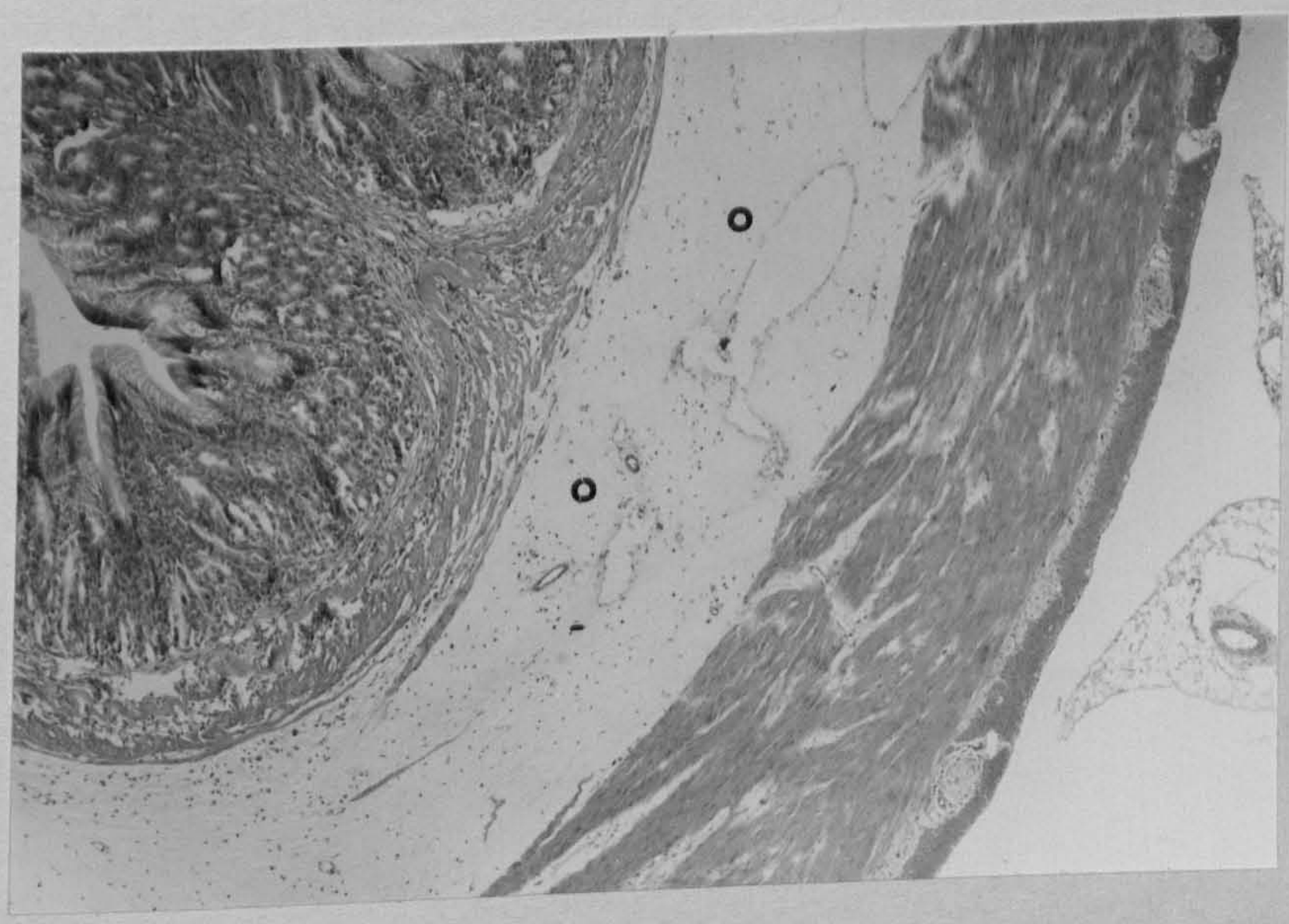

Fig. 56. Stomach of sexually mature fish.
Note large areas of muscle necrosis (n).

H & E x 125

Fig. 57. Mesenteric artery in sexually mature fish. Note early intimal hyperplasia (arrowed).

H & E x 500

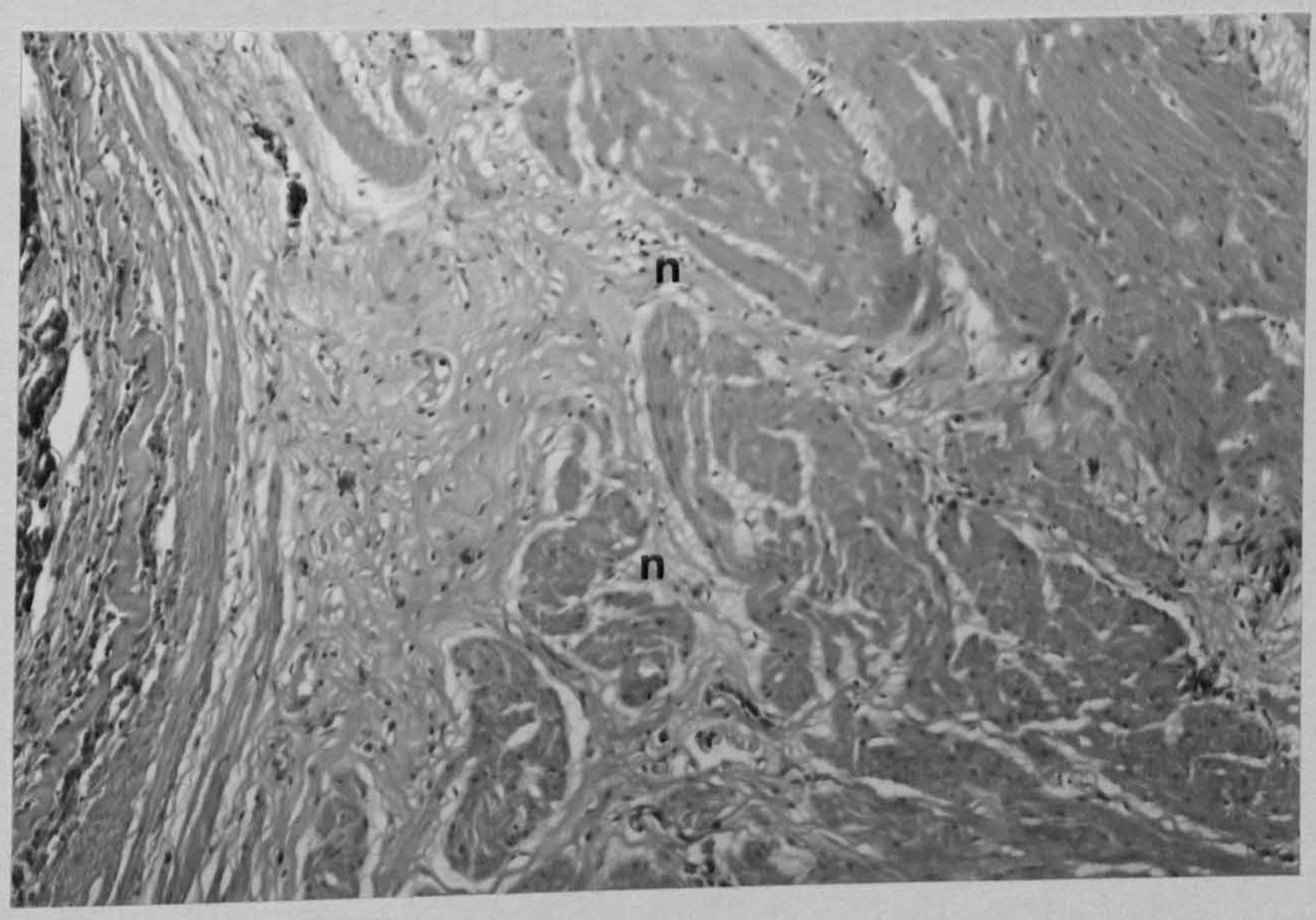
n
n

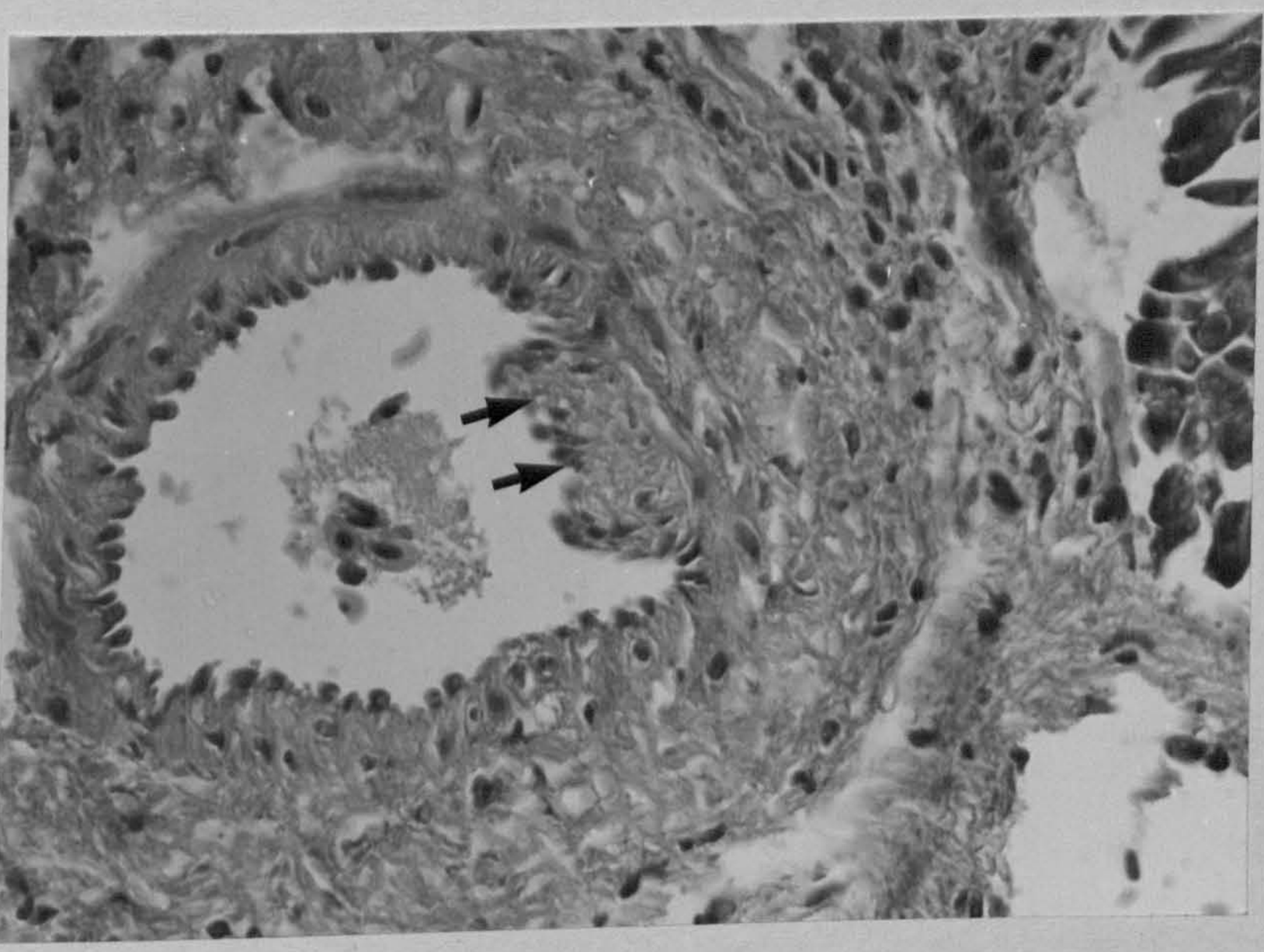

Fig. 58. Gut of sexually immature fish.

Note cestode (c) with no associated degenerative

gut changes.

H & E x 50

Fig. 59. Encysted larval cestode in abdominal

fat. Note marked inflammatory response (R)

walling off the parasite.

H & E x 50

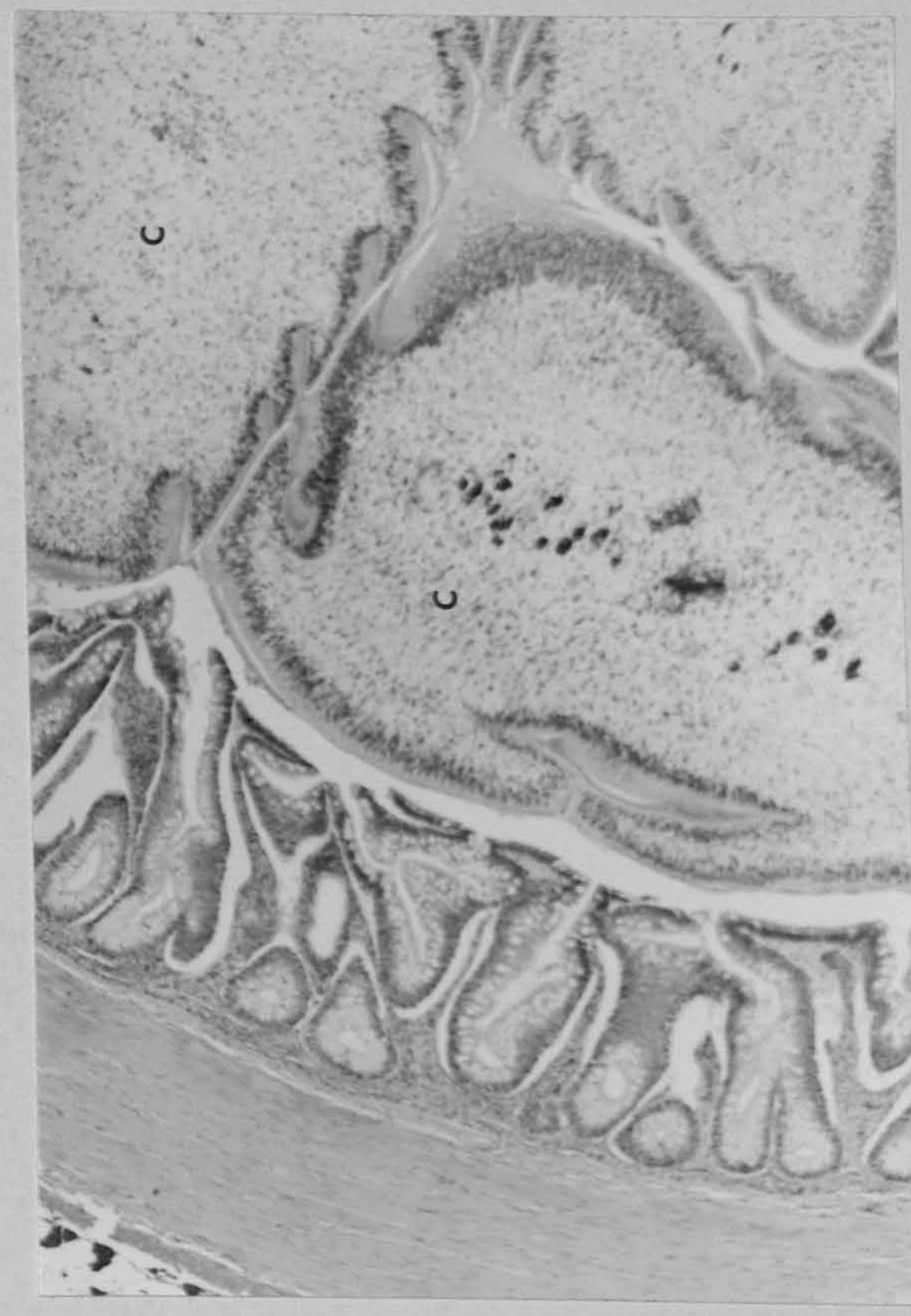
C
C

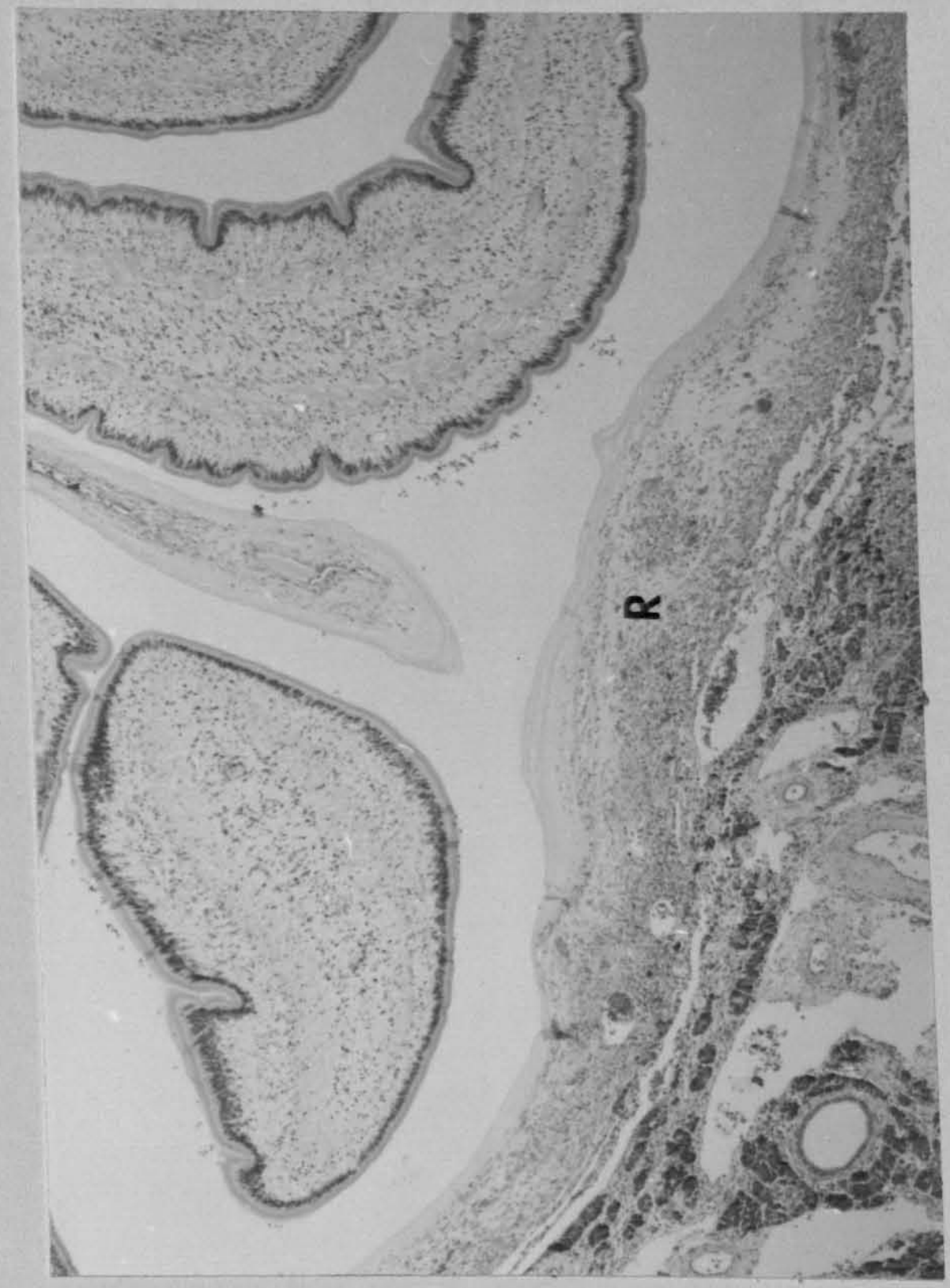
R

Fig. 60. Spleen of sexually immature fish.
Note indistinct ellipsoid (e) surrounded by
blast cells.

H & E x 320

Fig. 61. Spleen of sexually mature fish.
Note large numbers of melanomacrophages (arrowed)
in lumen of splenic blood vessel.

H & E x 500

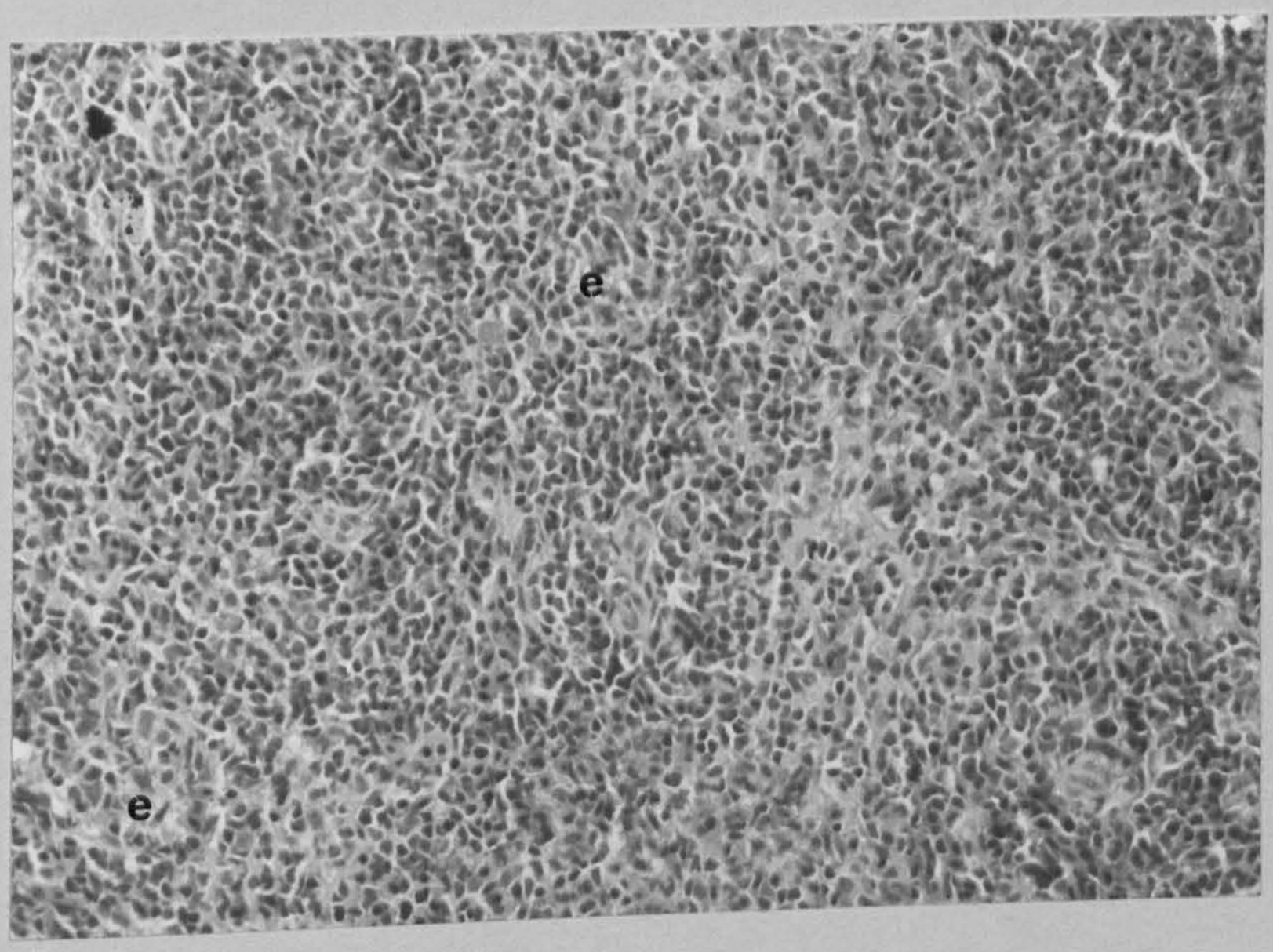
e
e

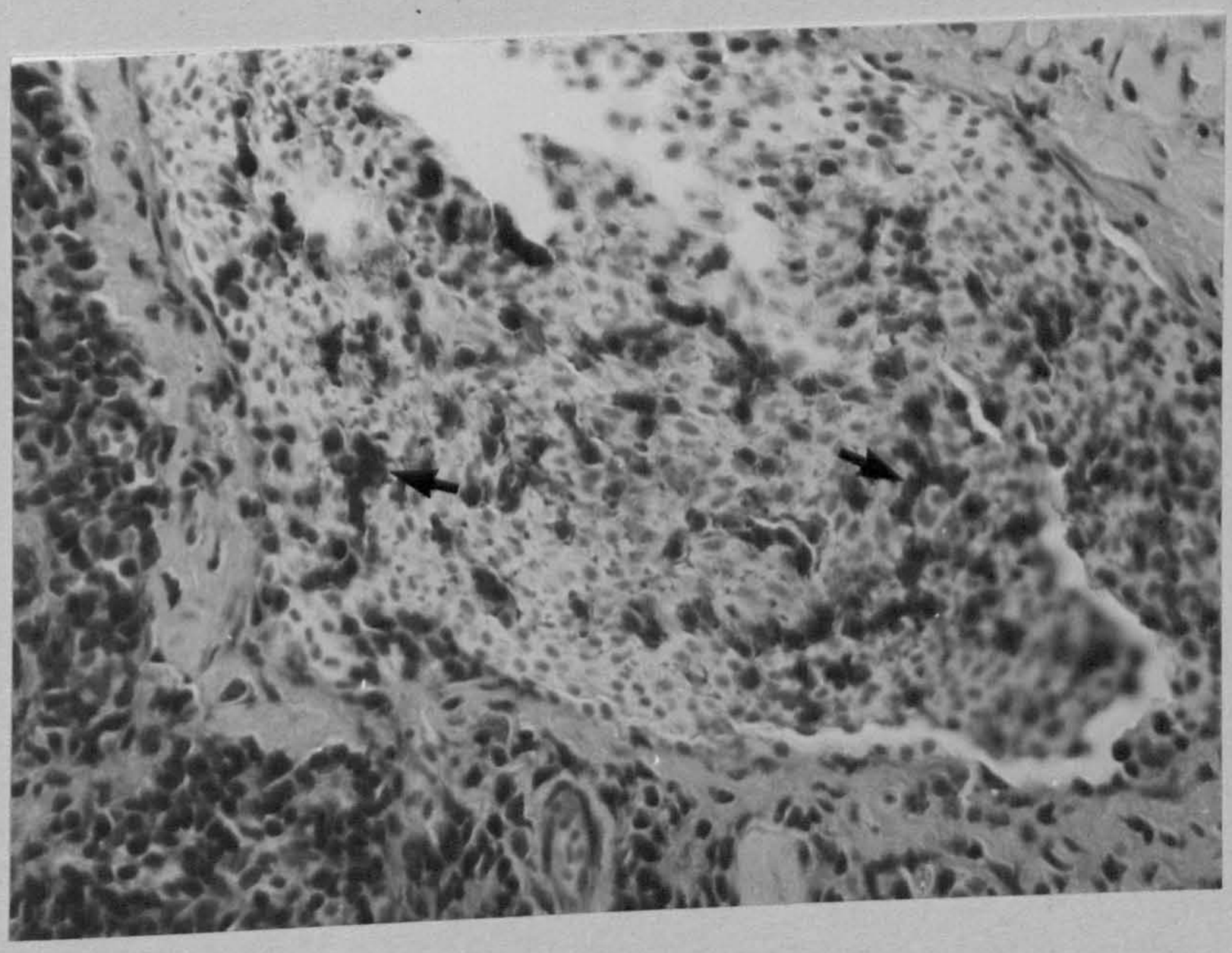

Fig. 62. Spleen of 6-year old sexually mature fish. Note prominent dark melanin deposited.

H & E x 320

Fig. 63. Spleen of sexually immature fish. Note large numbers of cells containing light-staining melanin precursors (arrowed).

H & E x 500

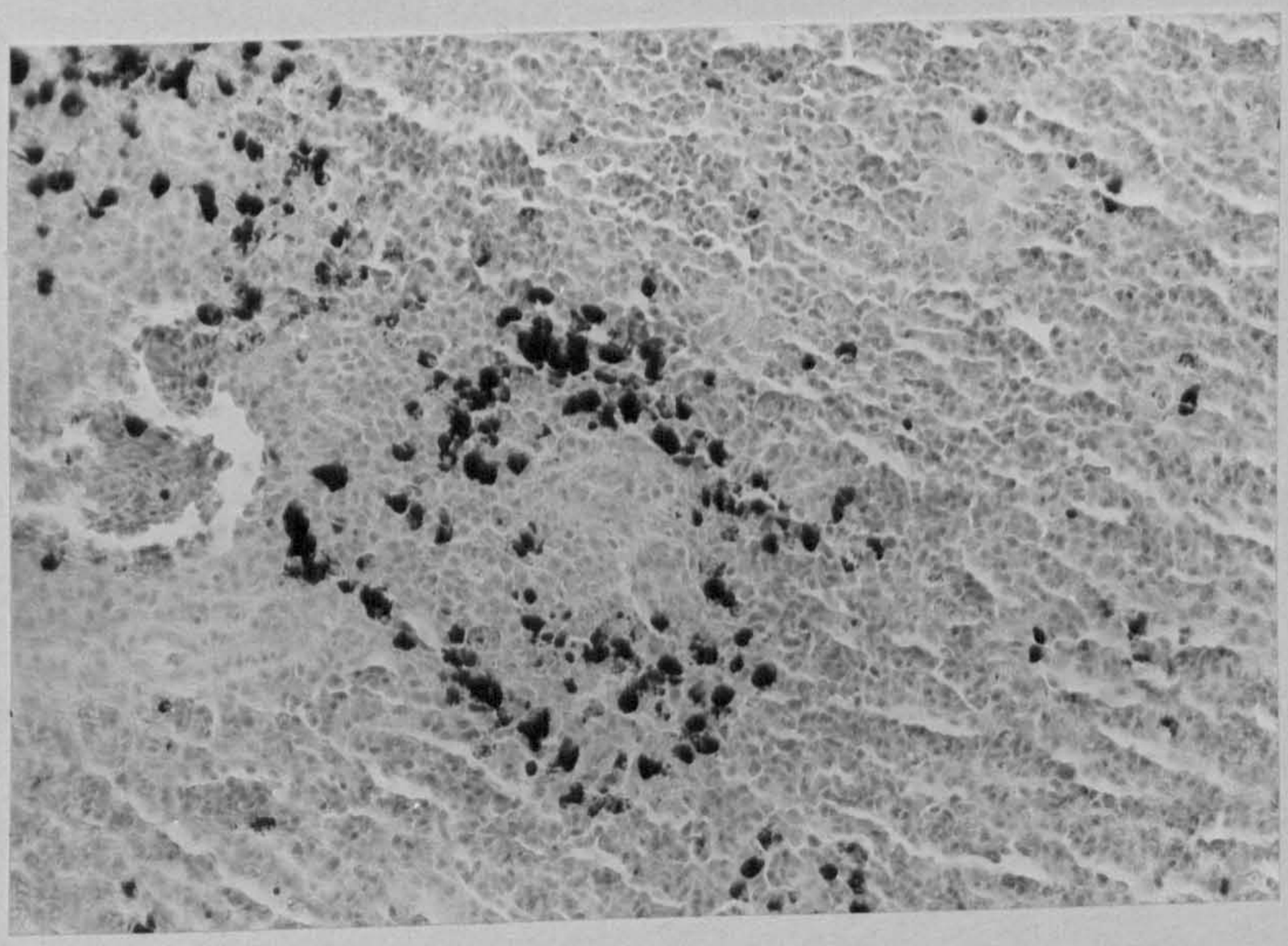

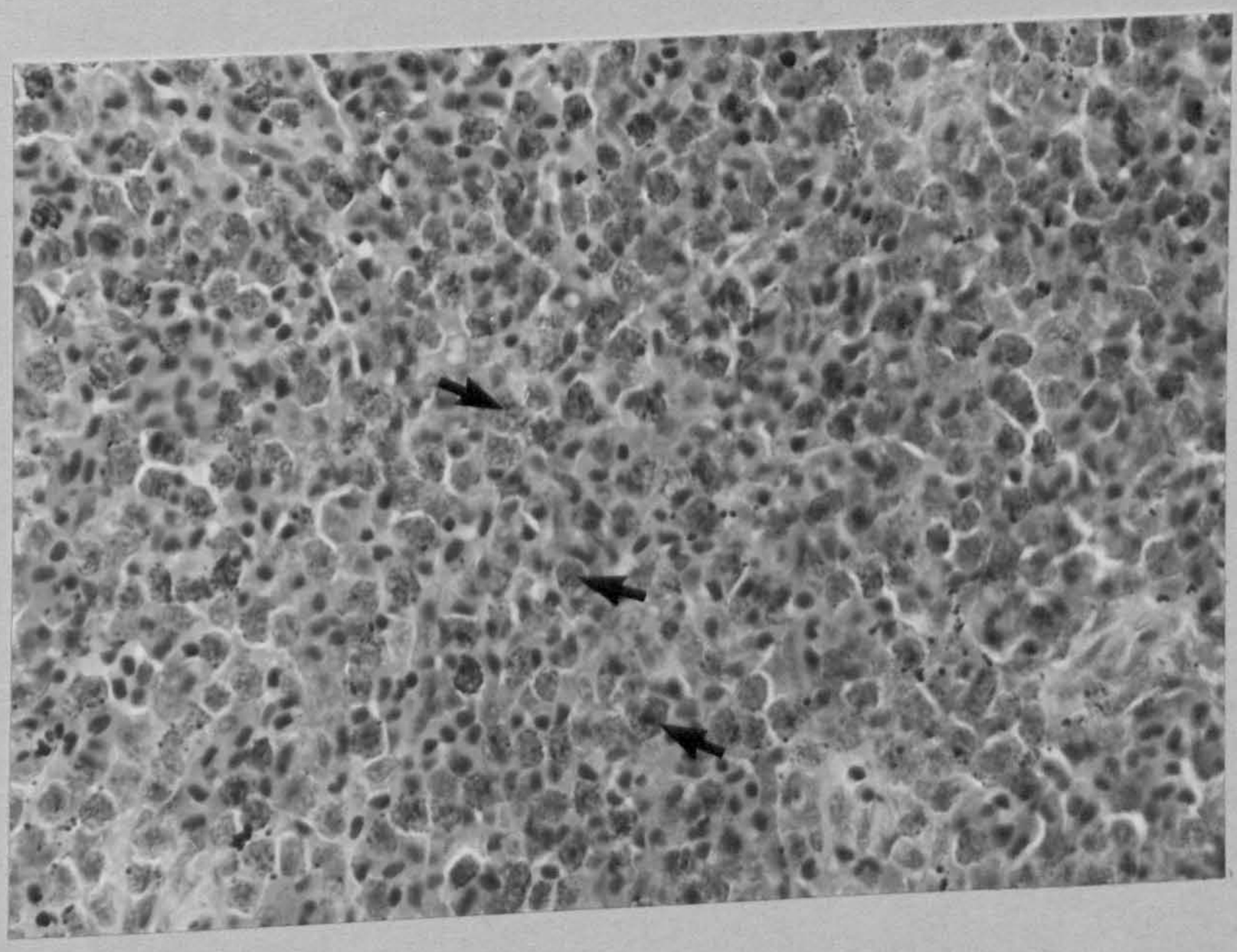

Fig. 64. Dorsal lobe of pituitary gland of sexually immature fish. Acidophil cells (a) predominate.

Barrett's stain x 500

Fig. 65. Anterior lobe of pituitary gland of maturing fish. Note folliculoid appearance.

Slidders stain x 500

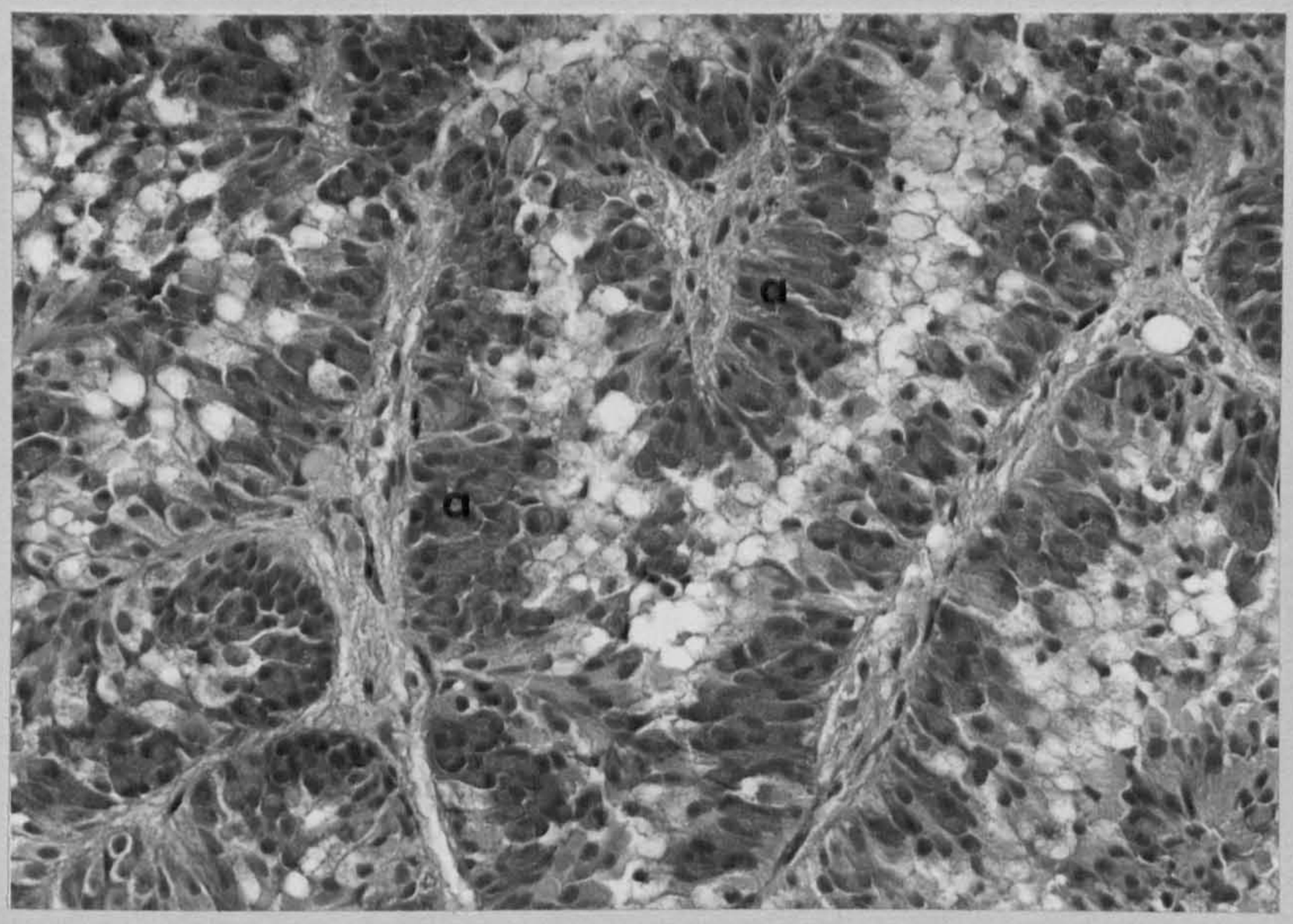
a

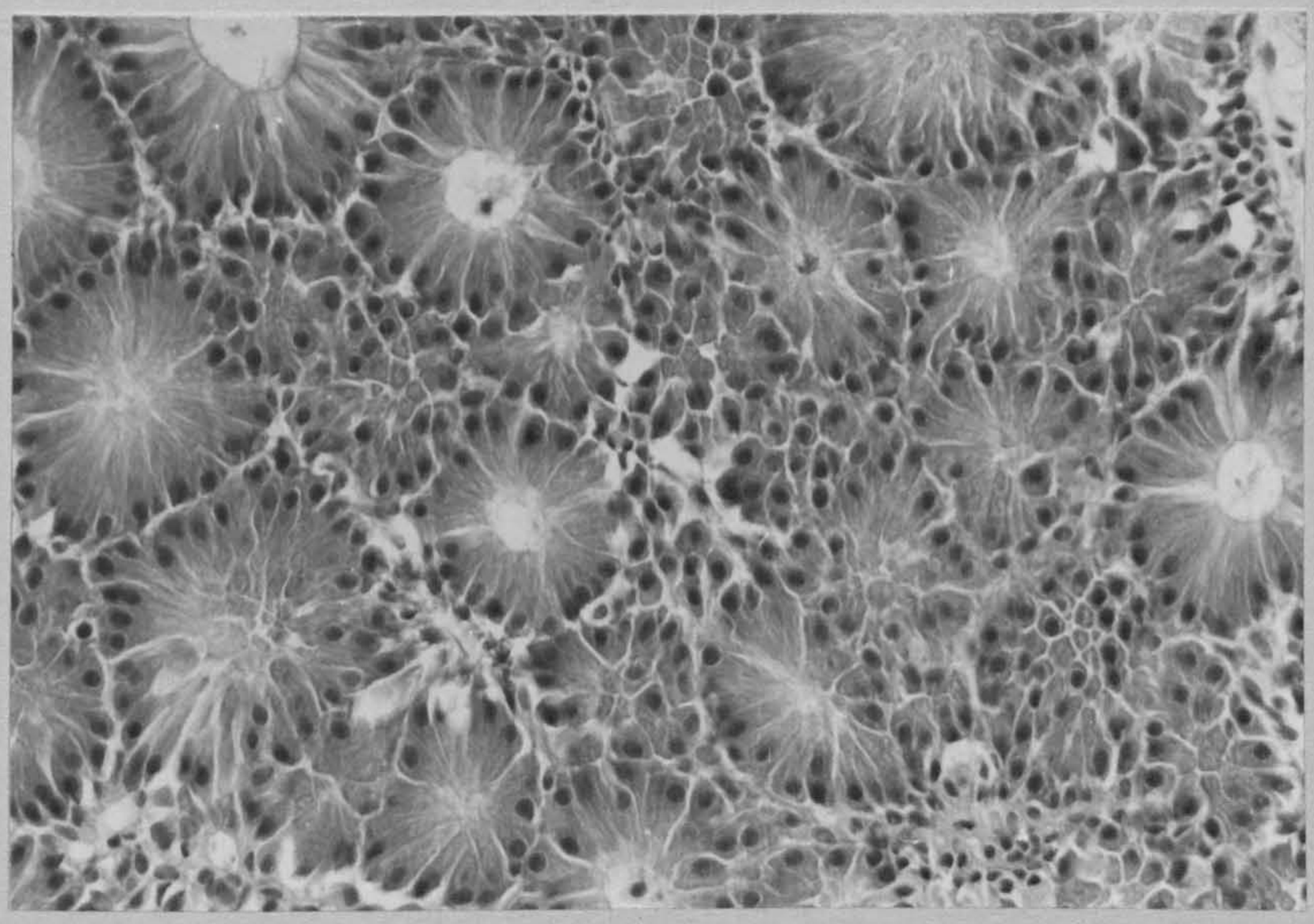

Fig. 66. Dorsal lobe of sexually mature fish.

Note prominent chromophobe cells (arrowed).

Slidders stain x 1250

Fig. 67. Kidney of sexually mature fish suffering Aeromonas infection. Early changes consist of tubule damage resulting in increased quantities of cellular debris in tubular lumina.

H & E x 320

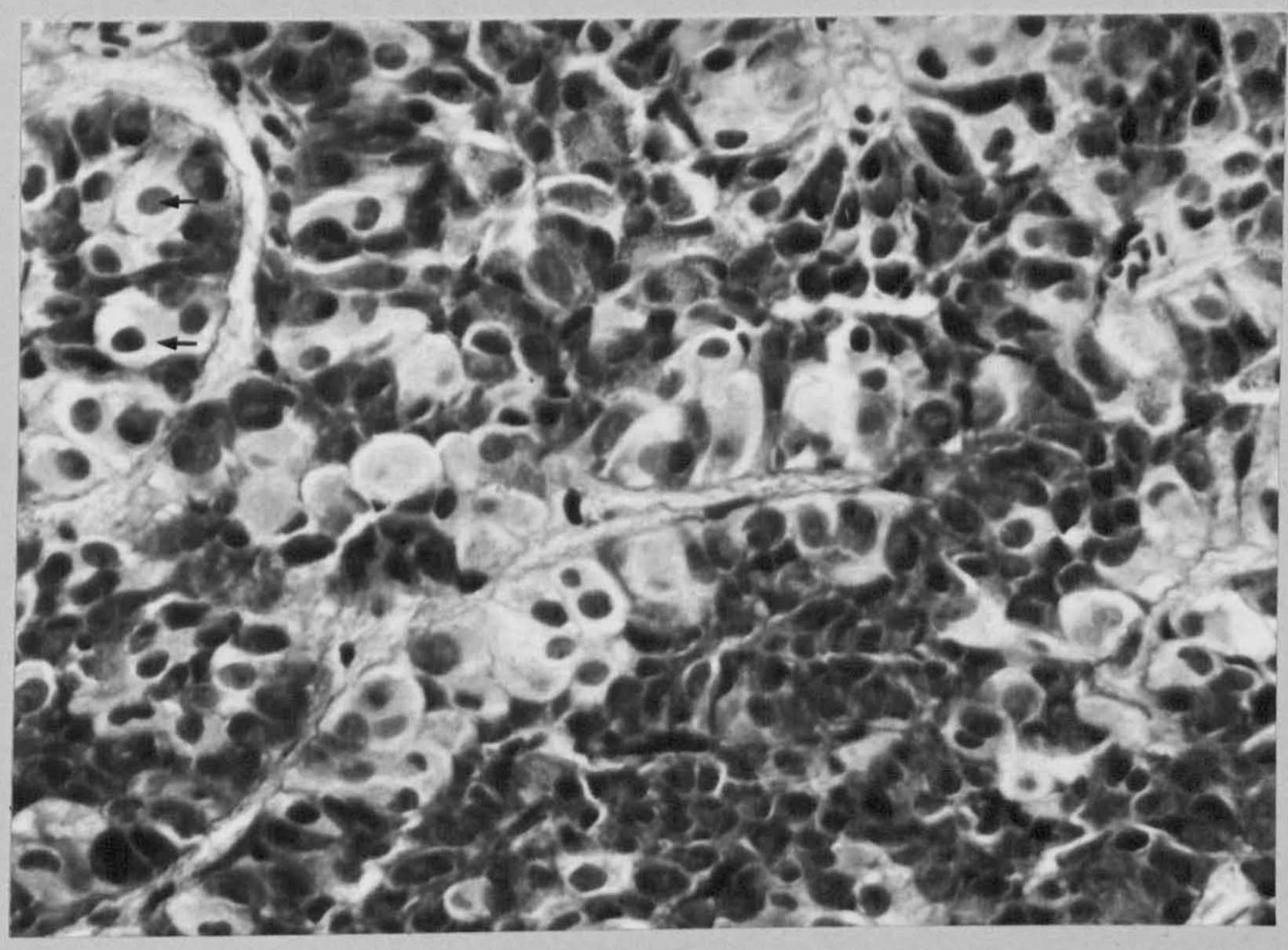

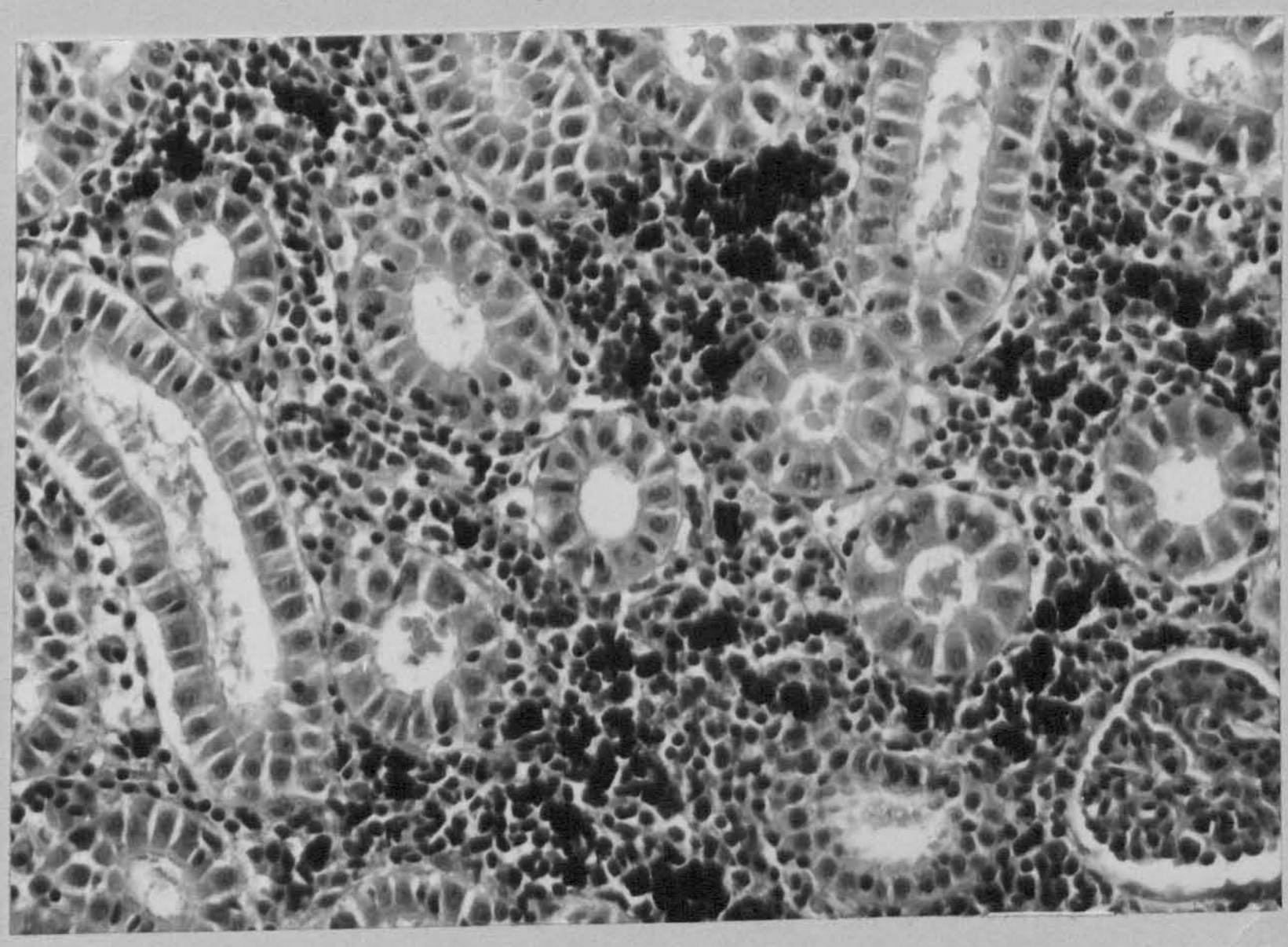

Fig. 68. Anterior kidney of sexually mature fish suffering massive bacterial infection. Note bacterial colonies (arrowed) amongst pyknotic haemopoietic cells.

Gram Humberstone x 320

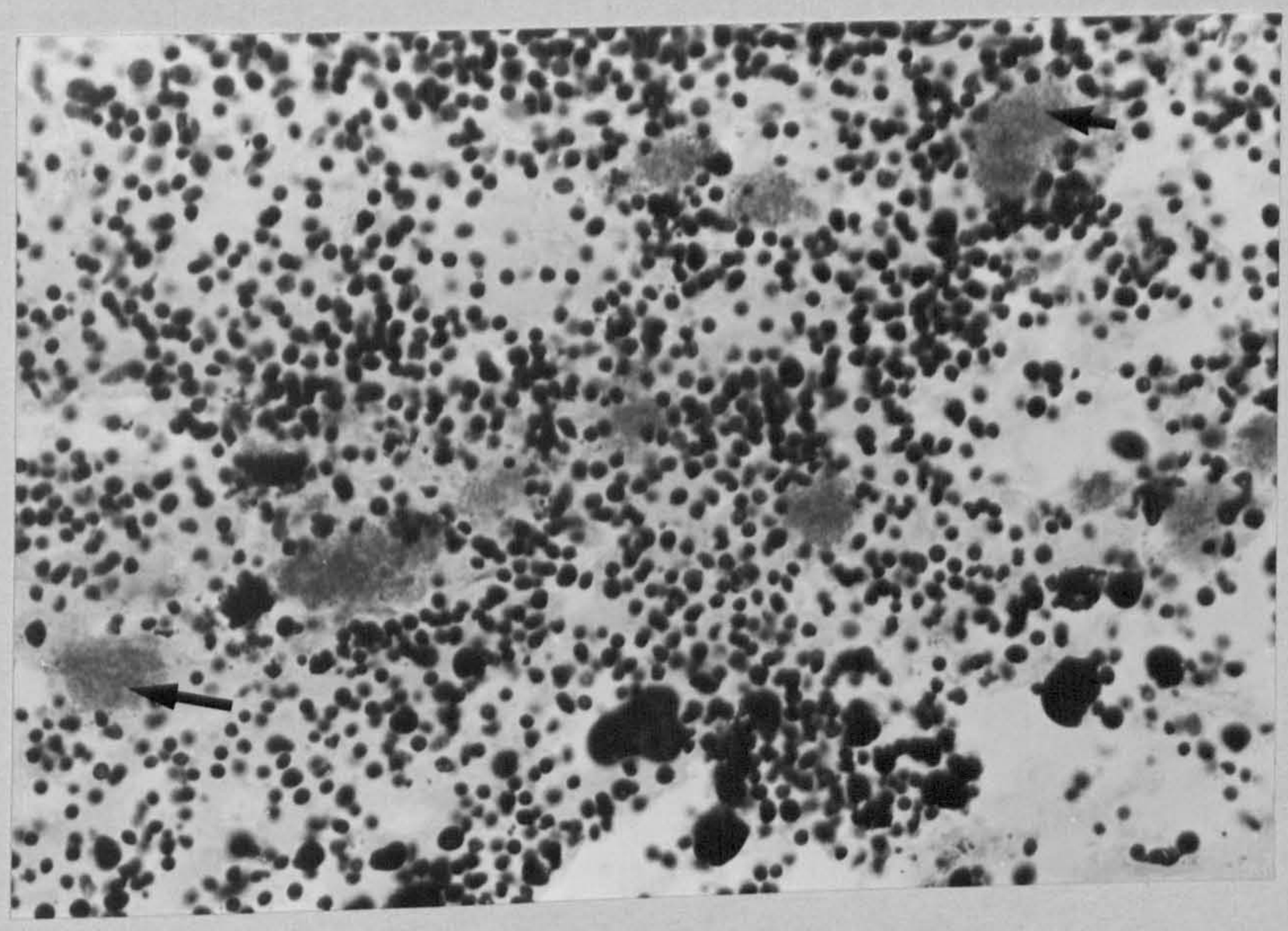

Fig. 69. Standard chart used to map areas of fungal infection. Fish surface (one side) divided into 391 areas.

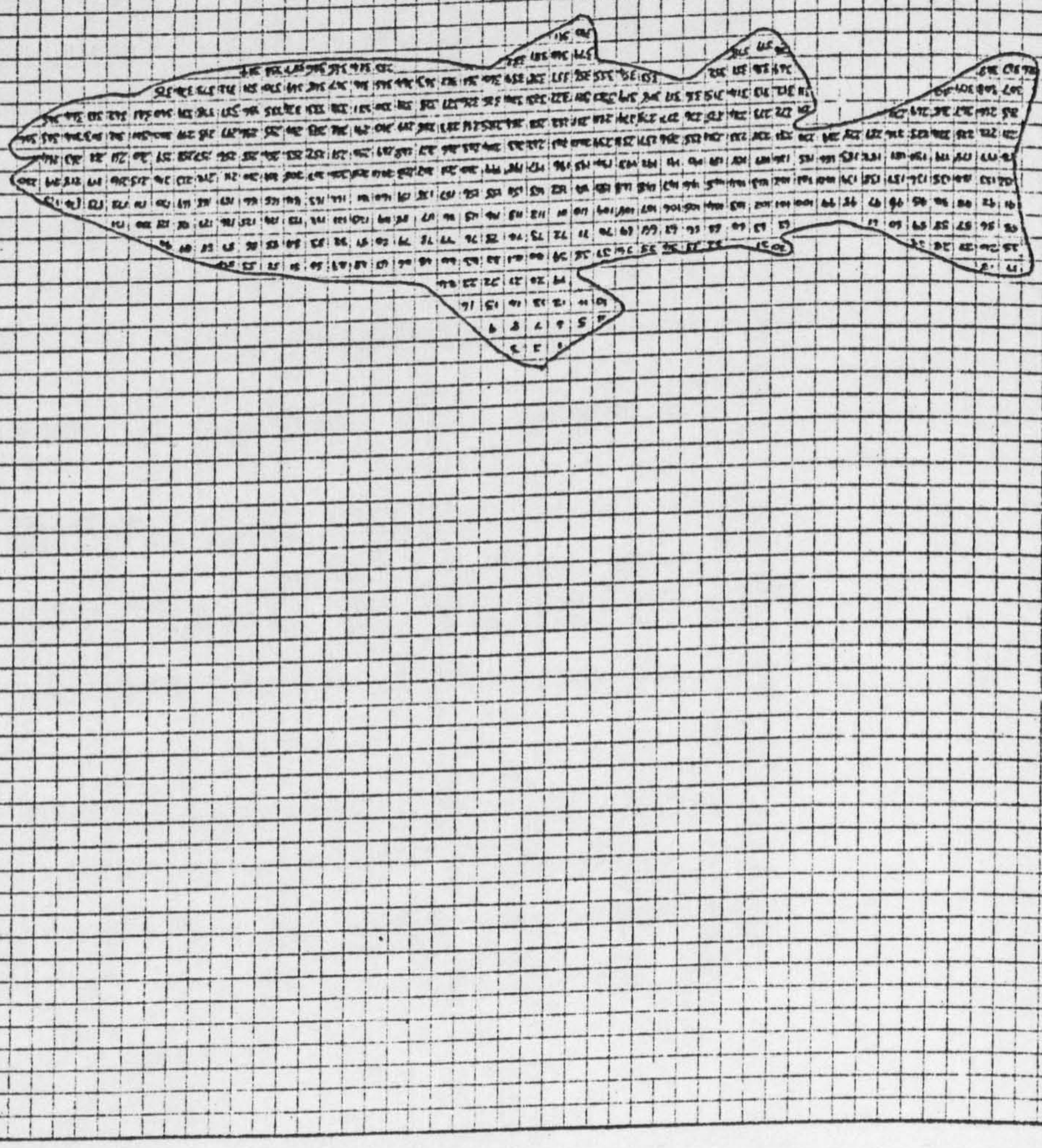

Fig. 70. Correction curve to allow for multiple inoculation of the agar sectors used in Saprolegniales estimations.

Vertical axis = Observed mean number of positive sectors

Horizontal axis = True mean number of propagules per sector

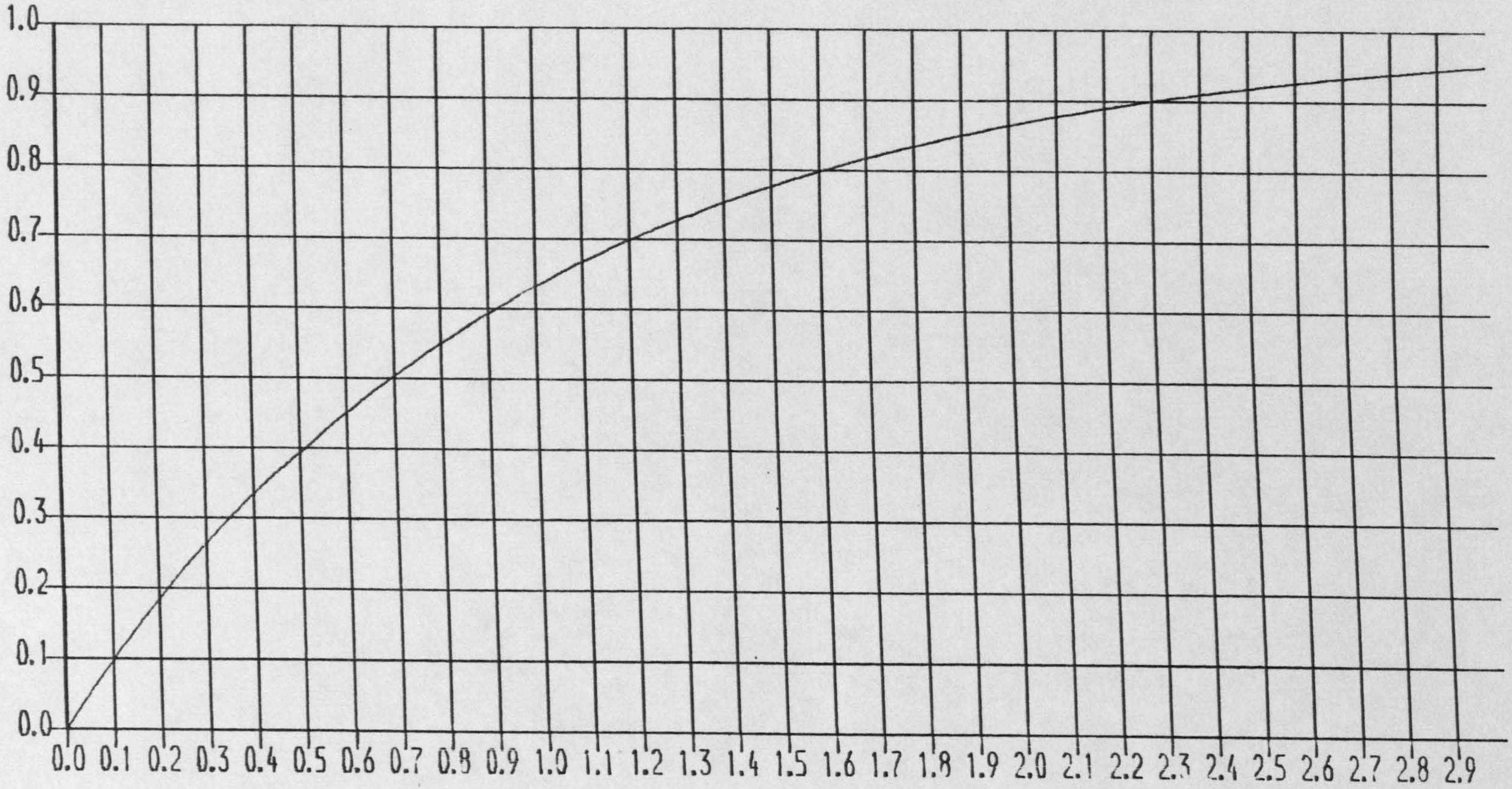
1.0
0.9
0.8
0.7
0.6
0.5
0.4
0.3
0.2
0.1
0.0
0.0 0.1 0.2 0.3 0.4 0.5 0.6 0.7 0.8 0.9 1.0 1.1 1.2 1.3 1.4 1.5 1.6 1.7 1.8 1.9 2.0 2.1 2.2 2.3 2.4 2.5 2.6 2.7 2.8 2.9

Fig. 71. Saprolegnia diclina Humphrey type 1.

Zoosporangium(arrowed) liberating zoospores.

Phase contrast x 500

Fig. 72. Aplanoid zoospore discharge in old cultures.

Phase contrast x 600

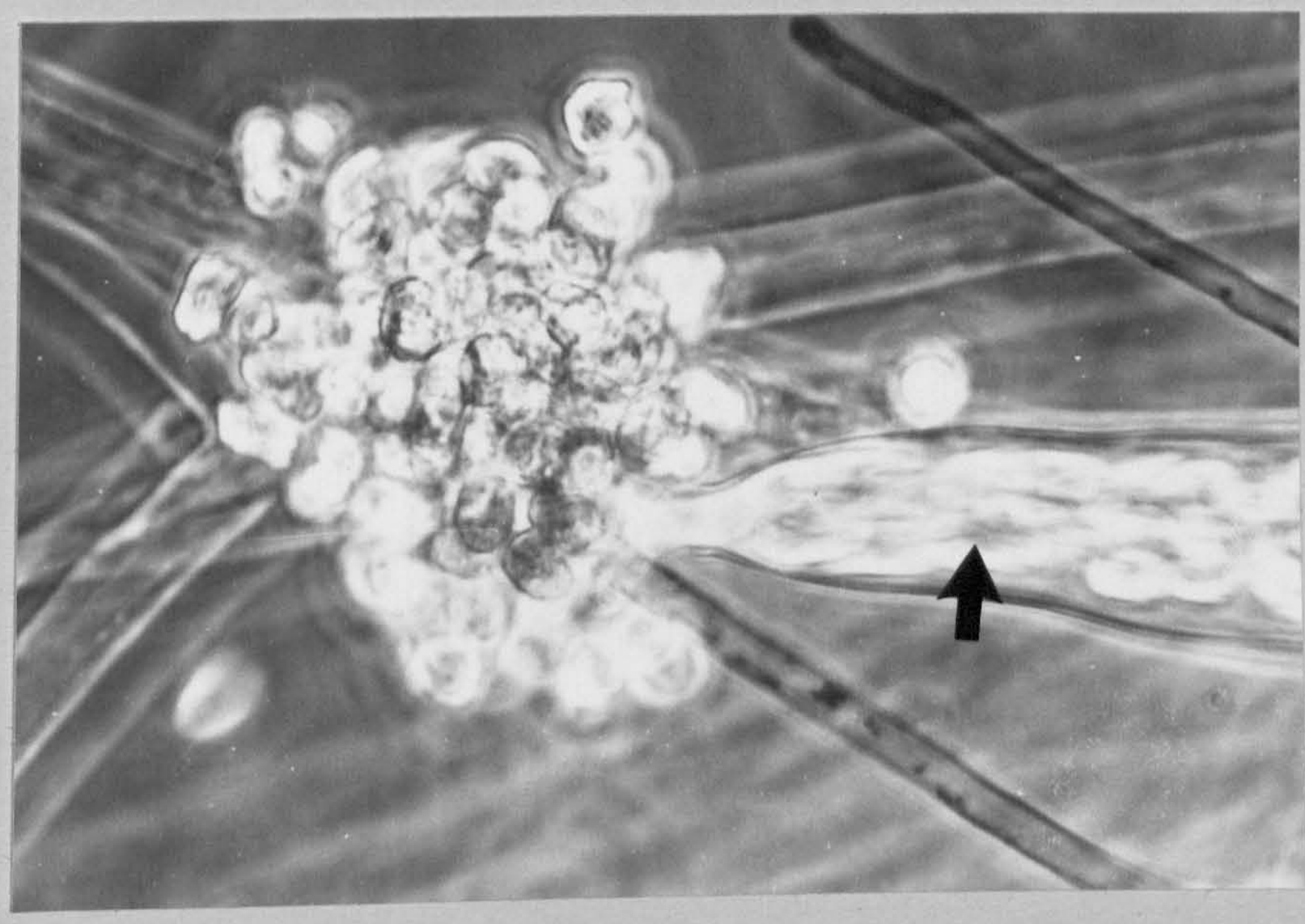

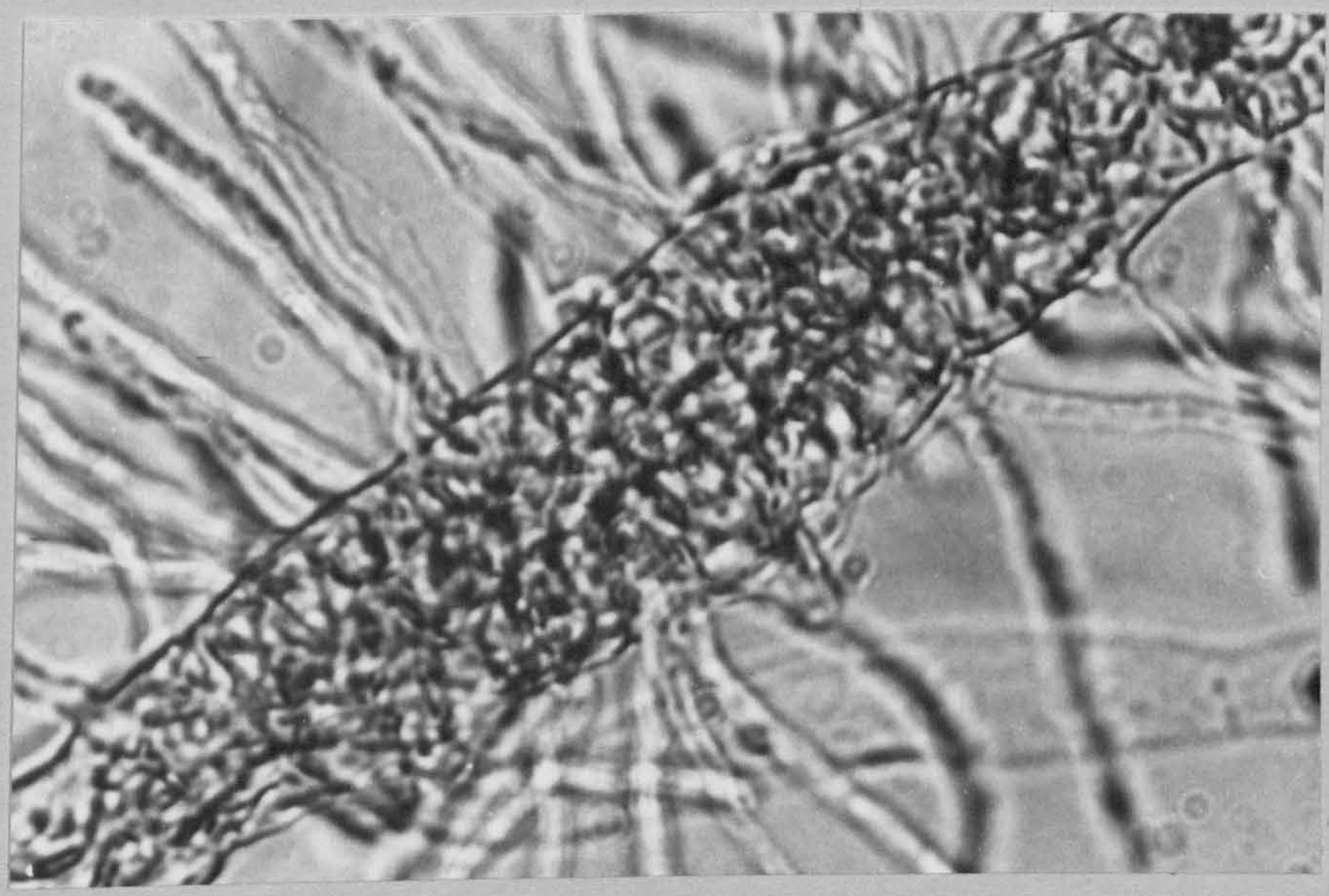

Fig. 73. Oogonia of Saprolegnia diclina

Type 1.

Phase contrast x 750

Fig. 74. "Birdnest" type investment of oogonia by antheridia.

Phase contrast x 600

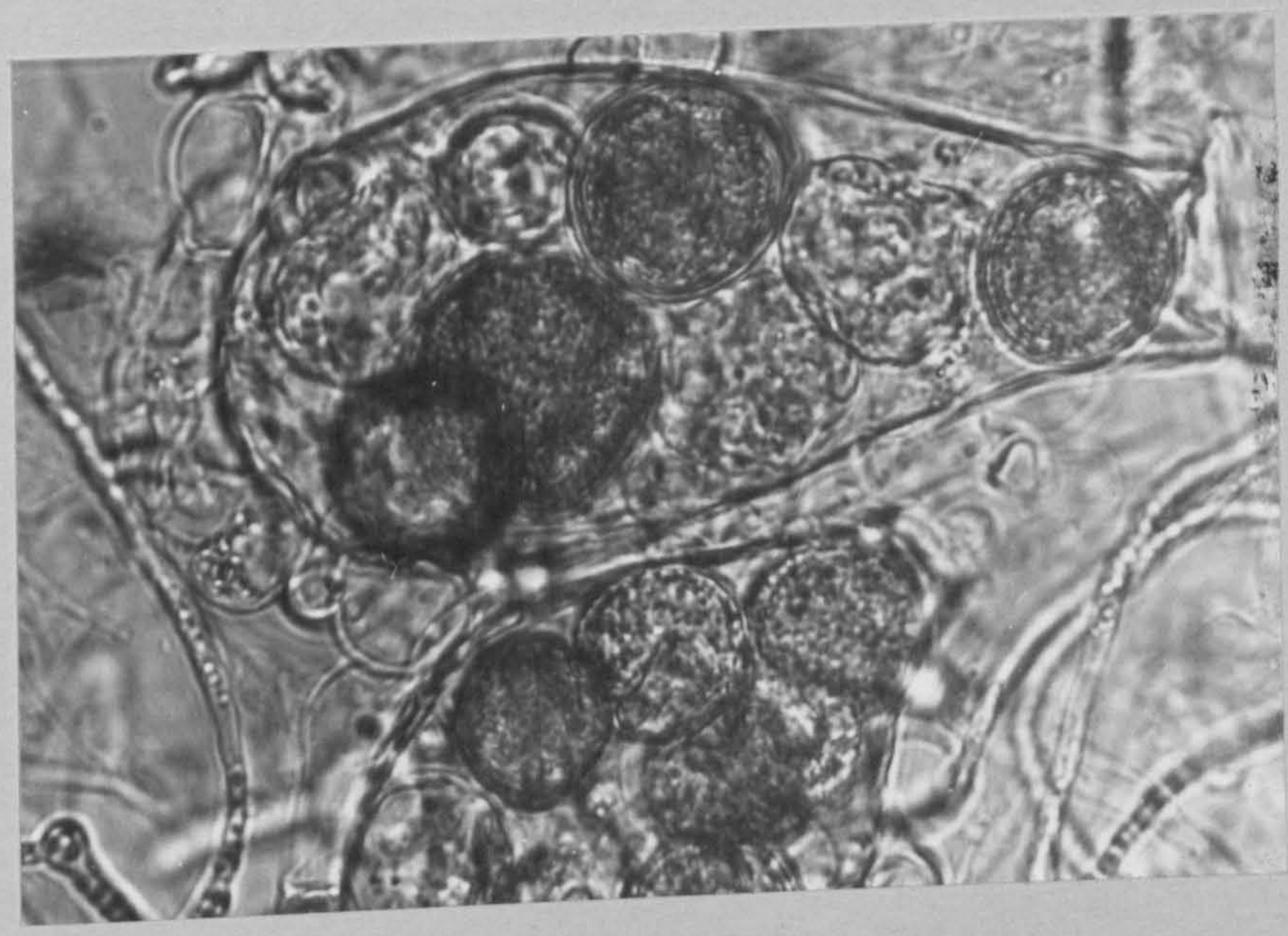

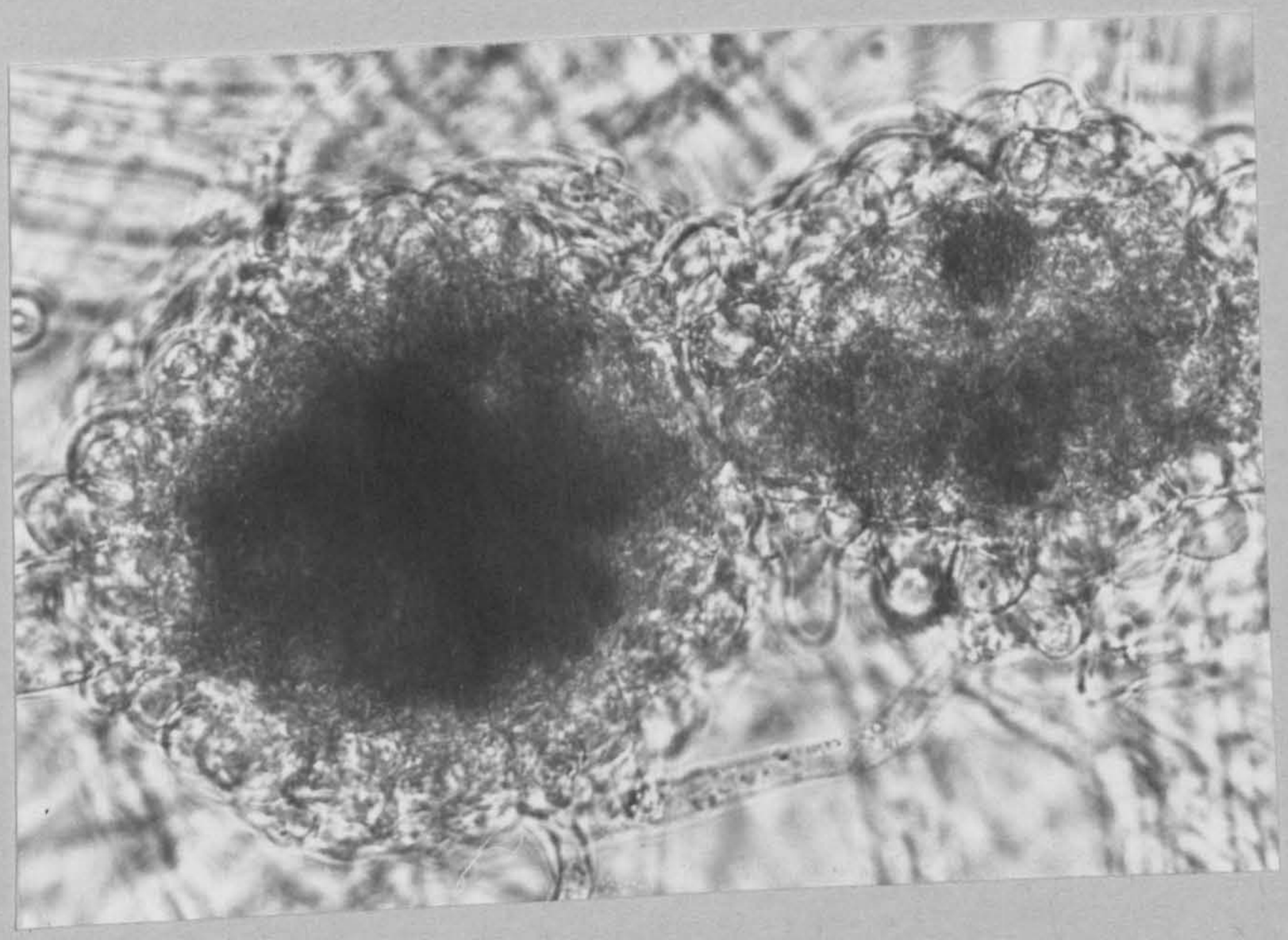

Fig. 75a. Fungal distribution in Loch Leven brown trout.

Shaded areas are significantly less frequently infected than the rest of the body.

Black : $p < 0.001$

Stippled : $p < 0.05$

Upper figure: male fish

Lower figure: female fish

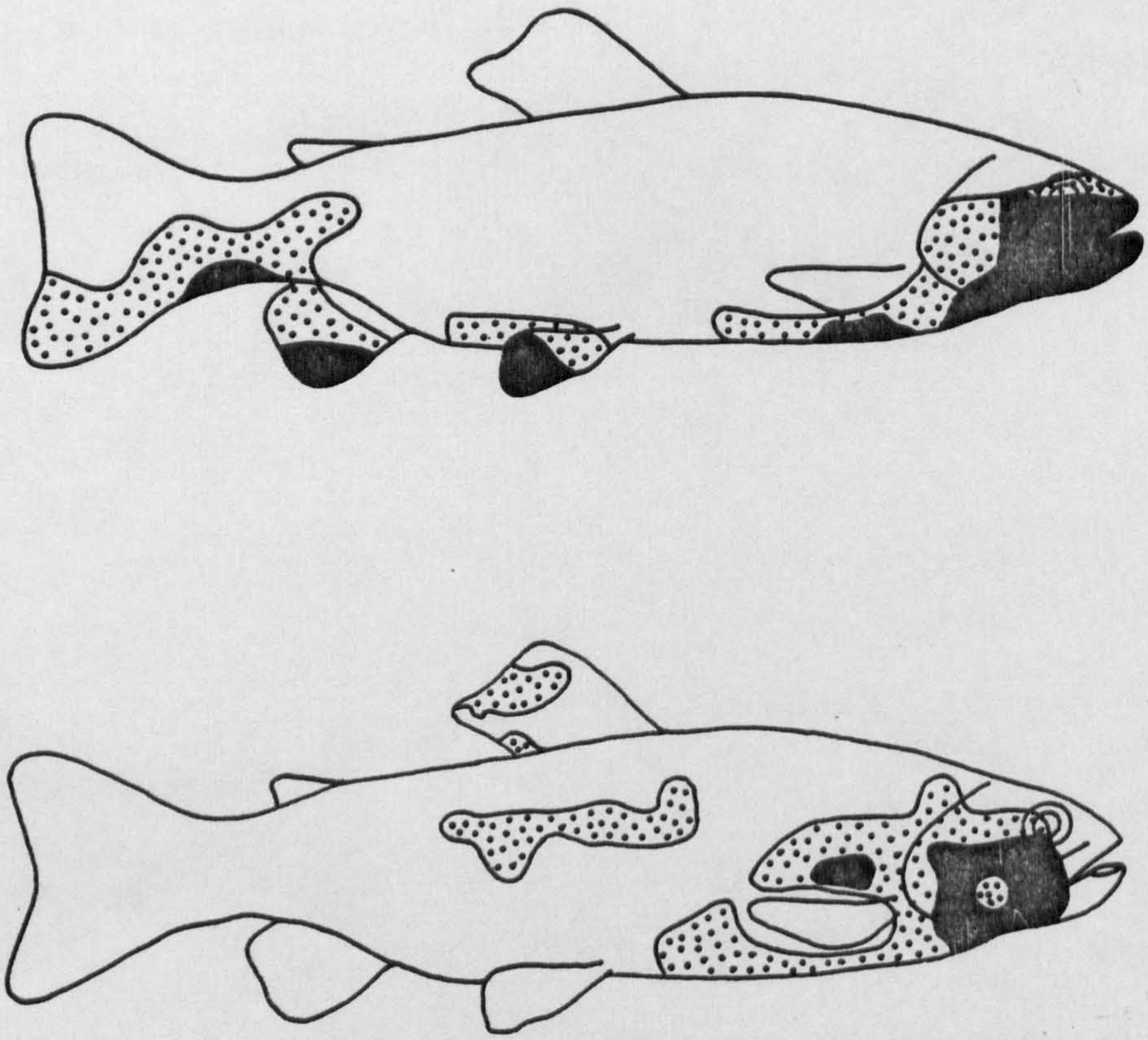

Fig. 75b. Fungal distribution in Loch Leven brown trout.

Shaded areas are significantly more frequently infected than the rest of the body.

Black : $p < 0.001$

Stippled : $p < 0.05$

Upper figure: male fish

Lower figure: female fish

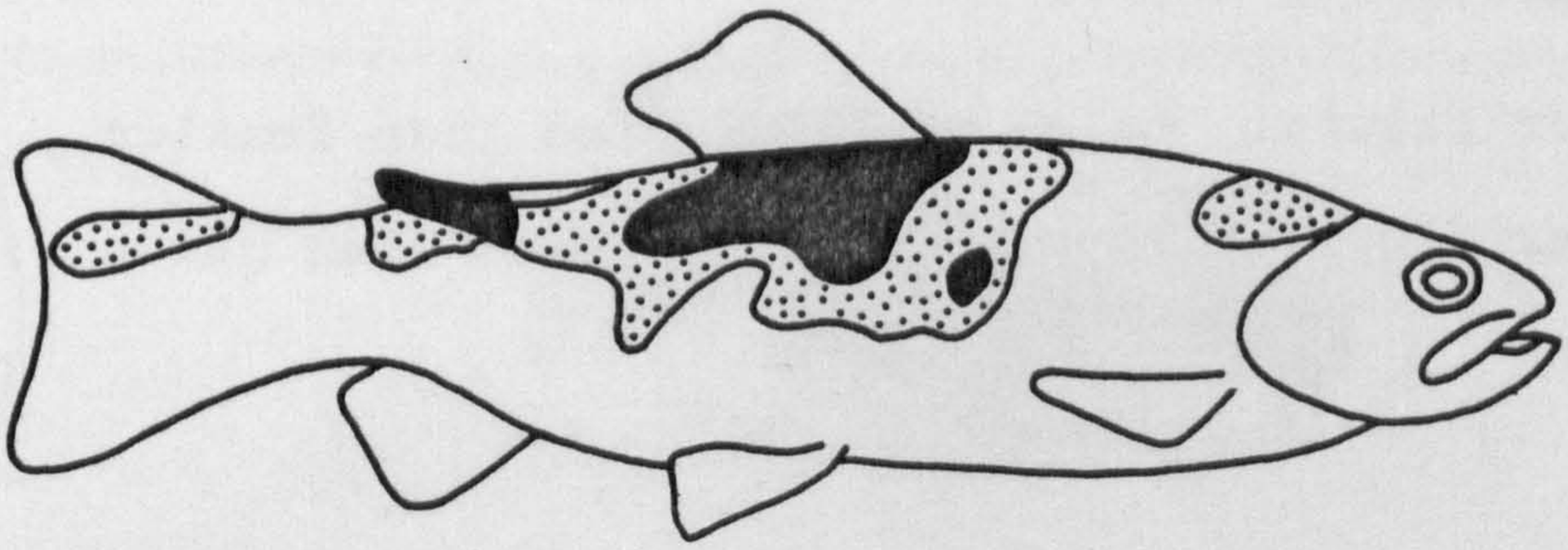

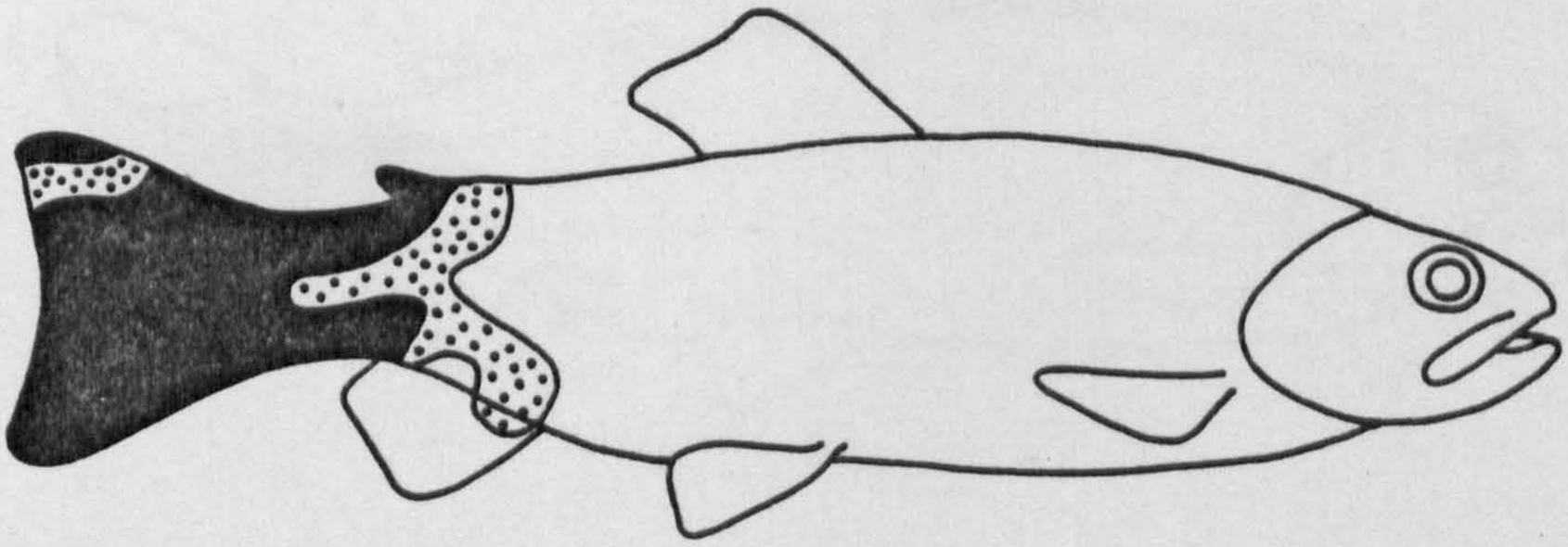

Fig. 76. Statistical comparison of the patterns of infection between male and female brown trout from Loch Leven.

Black : $p < 0.001$

Stippled : $p < 0.05$

Upper figure: males more infected than females

Lower figure: females more infected than males

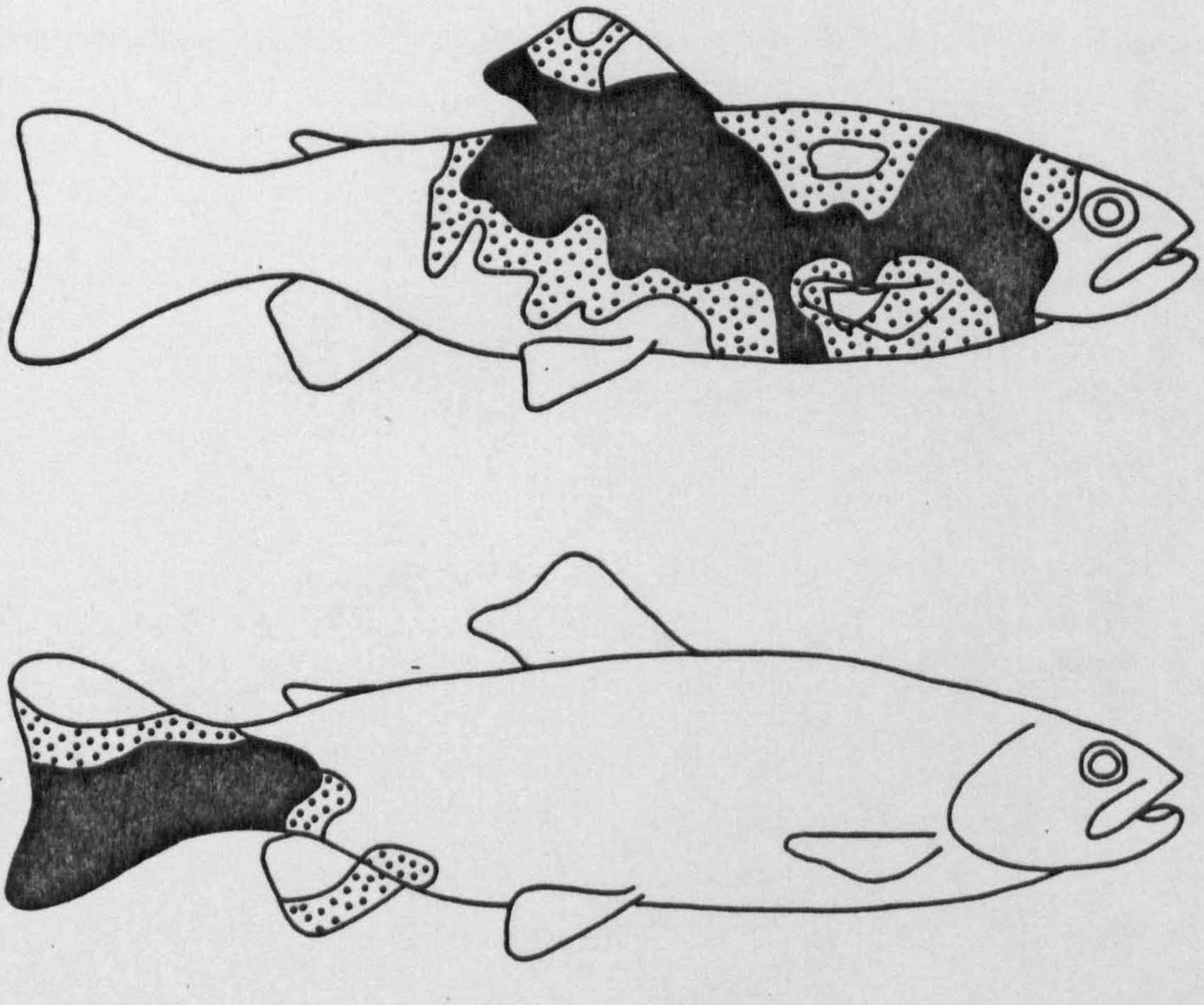

Fig. 77. Saprolegnia infection of brown trout. Note radial extension of the fungus (arrowed) which remains superficial so that pigmented areas of the skin are still visible.

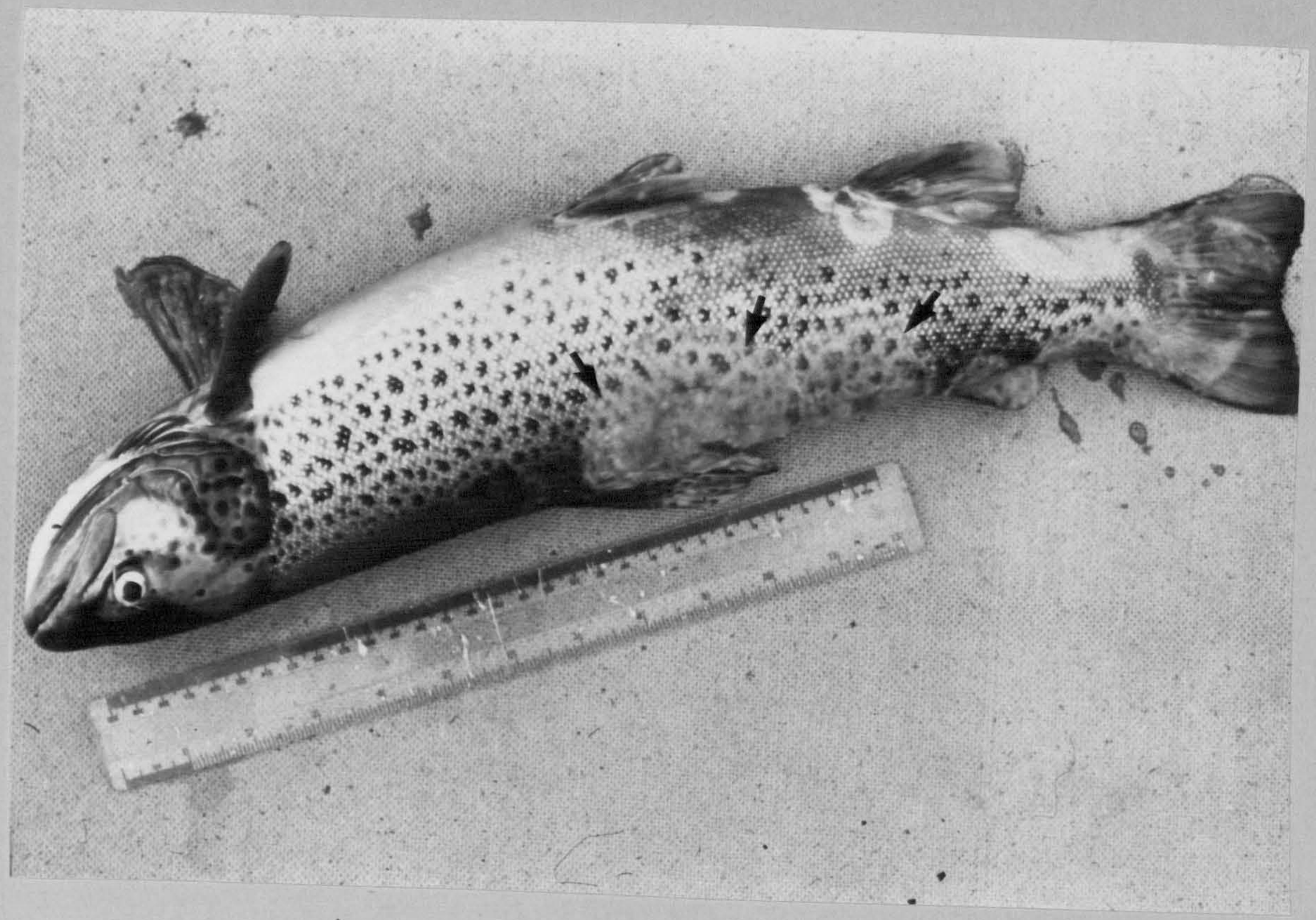

Fig. 78. Saprolegnia infection of brown trout. Radial extension of the fungus is obvious. In this fish, bacterial infection was also present leading to haemorrhages and deeper infection at the centre of the lesions (L).

Fig. 79. Early "type 1" lesion consisting of swelling and degeneration of isolated nuclei (arrowed) throughout the epidermis.

H & E x 500

Fig. 80. Early "type 1" lesion. Cell damage in the suprabasal areas (arrowed).

H & E x 320

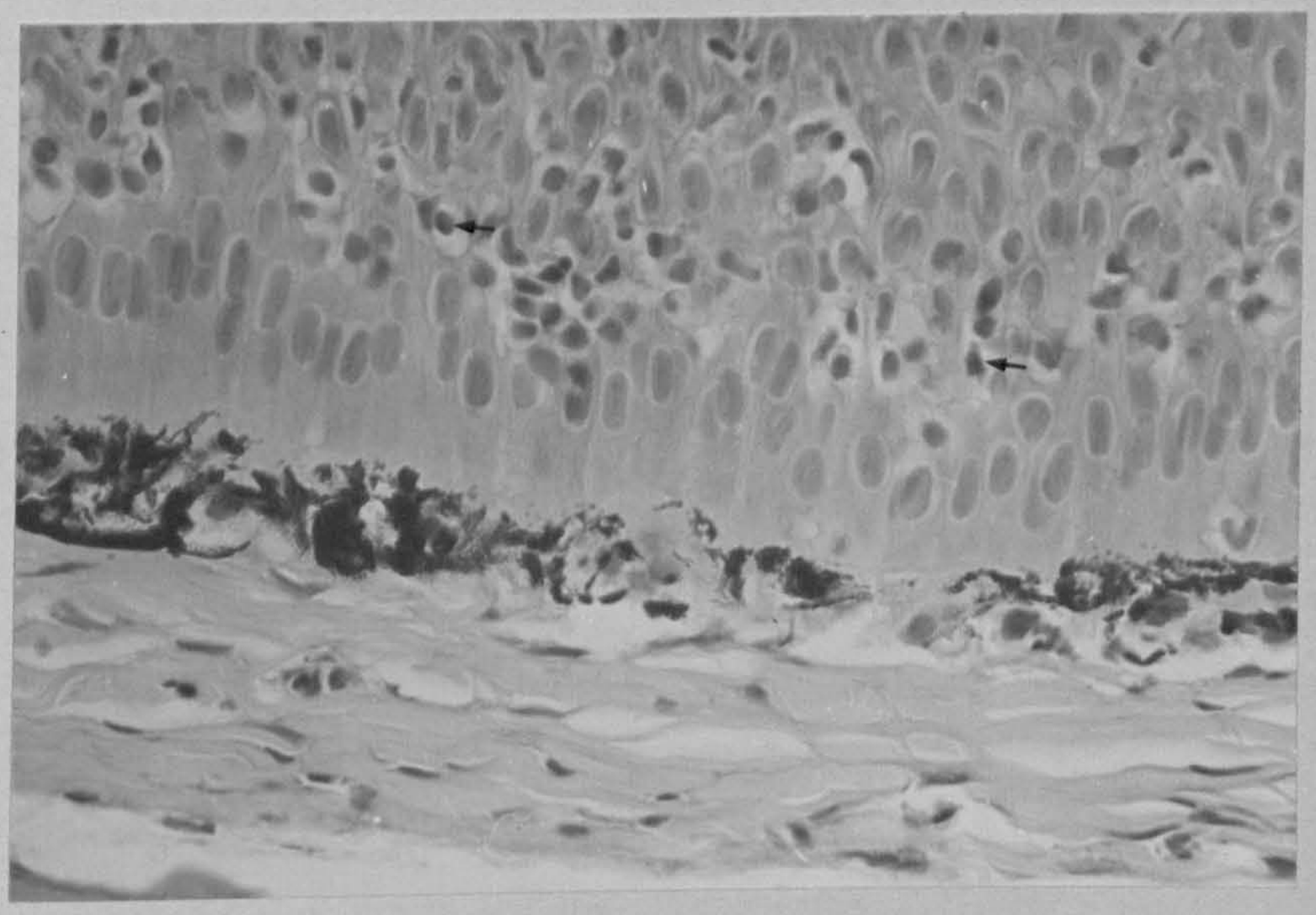

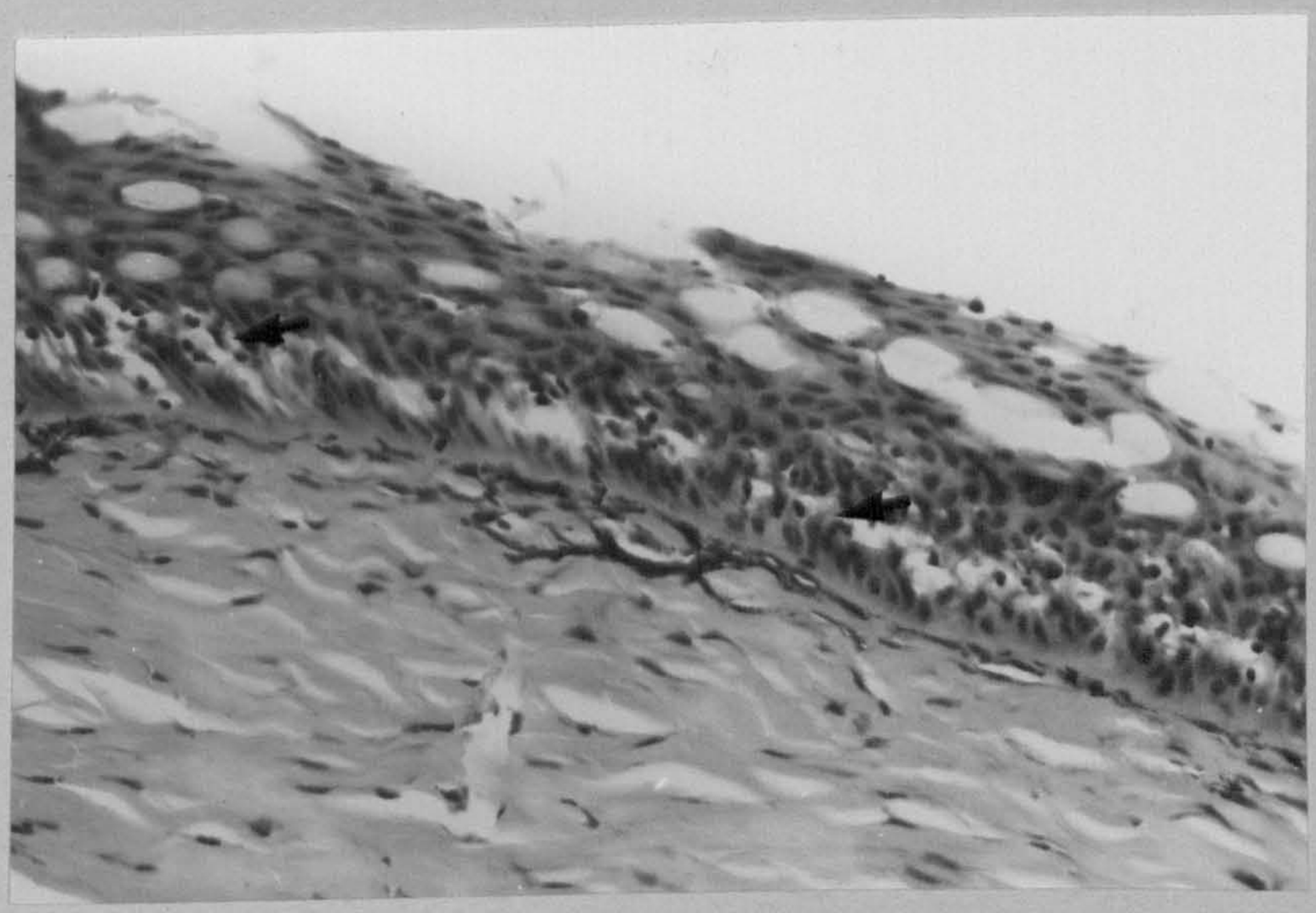

Fig. 81. "Type 1" change. Widespread cellular degeneration in epidermis.

H & E x 320

Fig. 82. "Type 1" change. Bulla formation (b).

H & E x 320

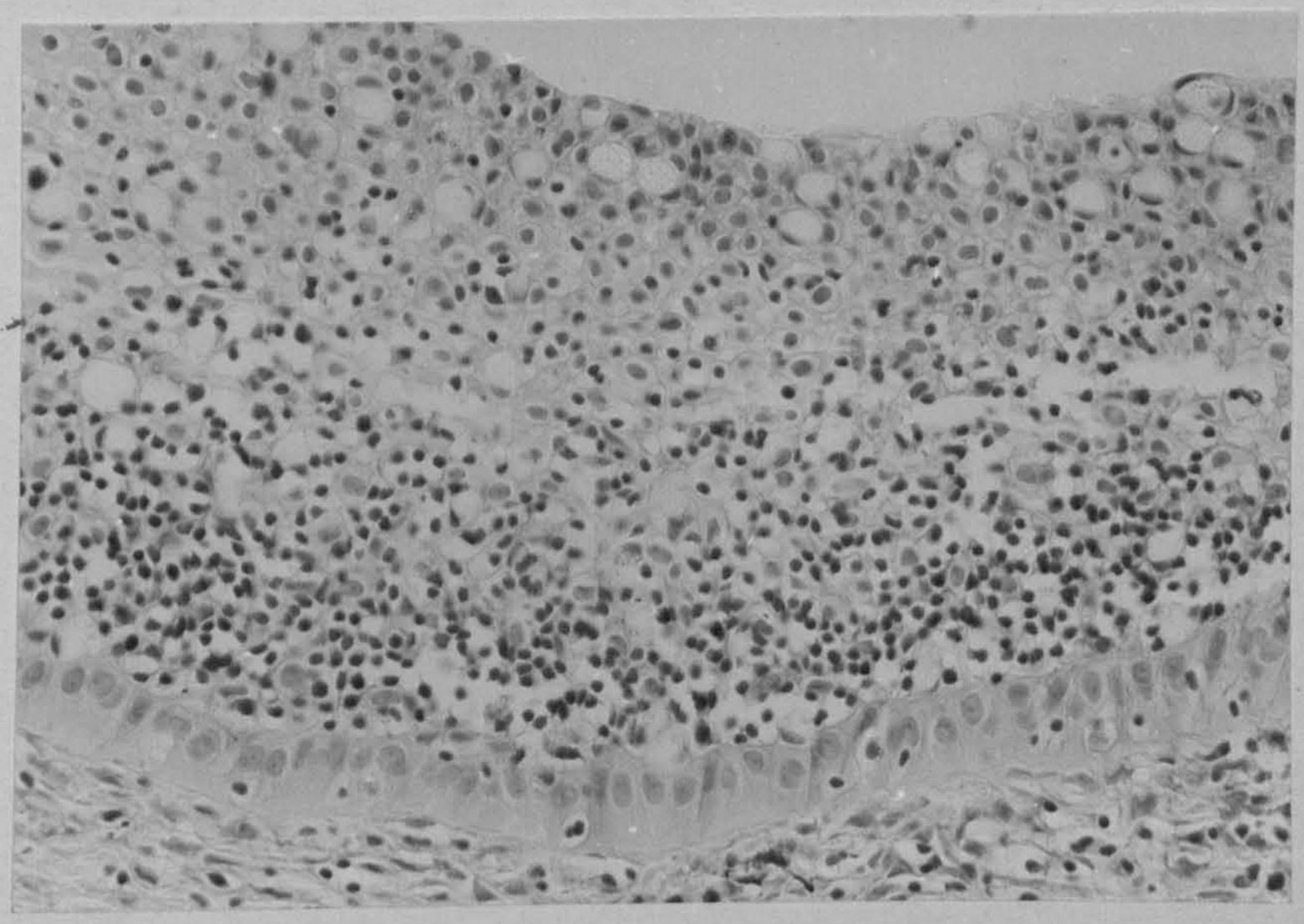

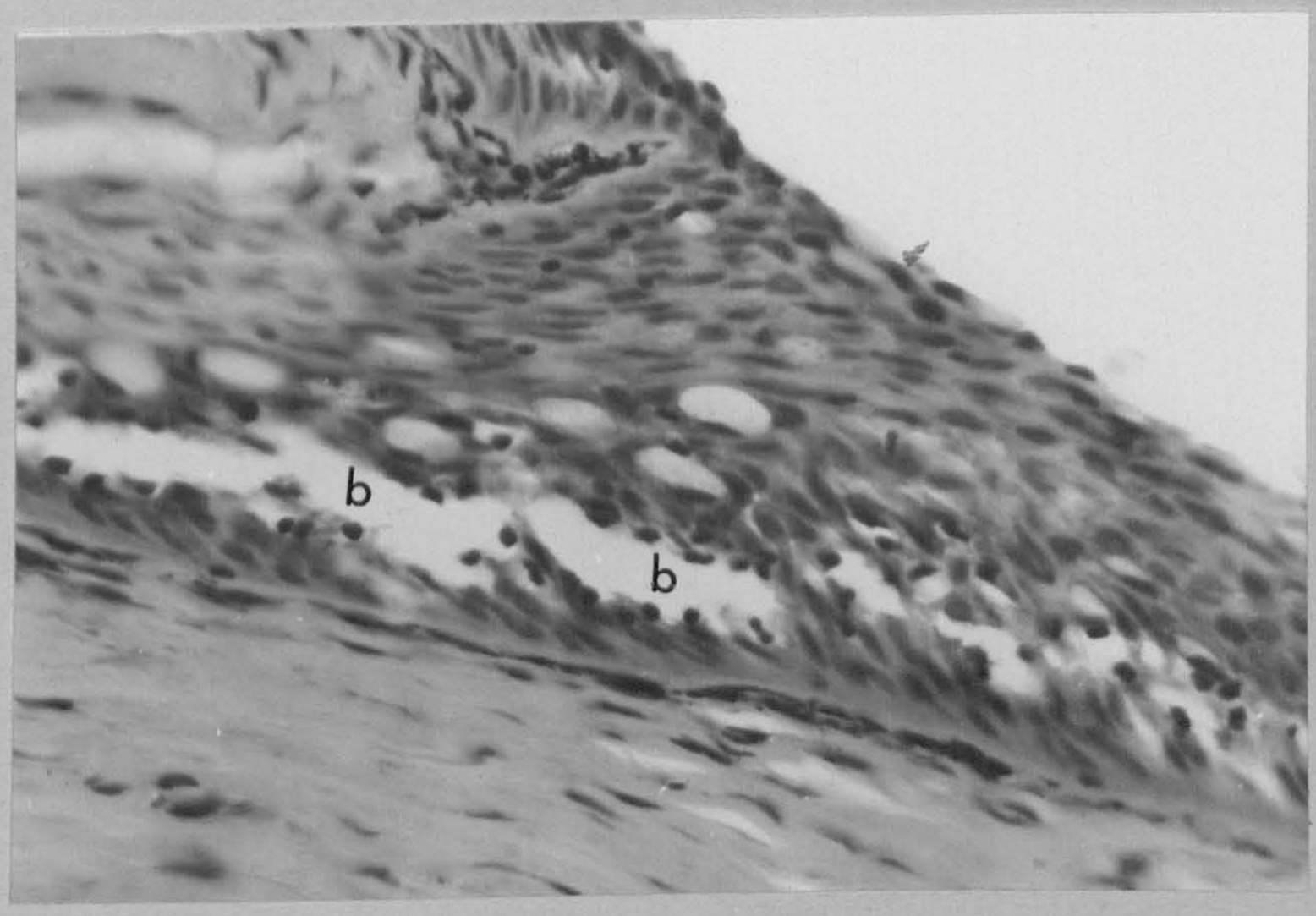
b
b

Fig. 83. Mitotic figures (arrowed) in epidermis.

H & E x 320

Fig. 84. "Type 2" lesion. Note sloughing of surface cells and nuclear pyknosis.

H & E x 320

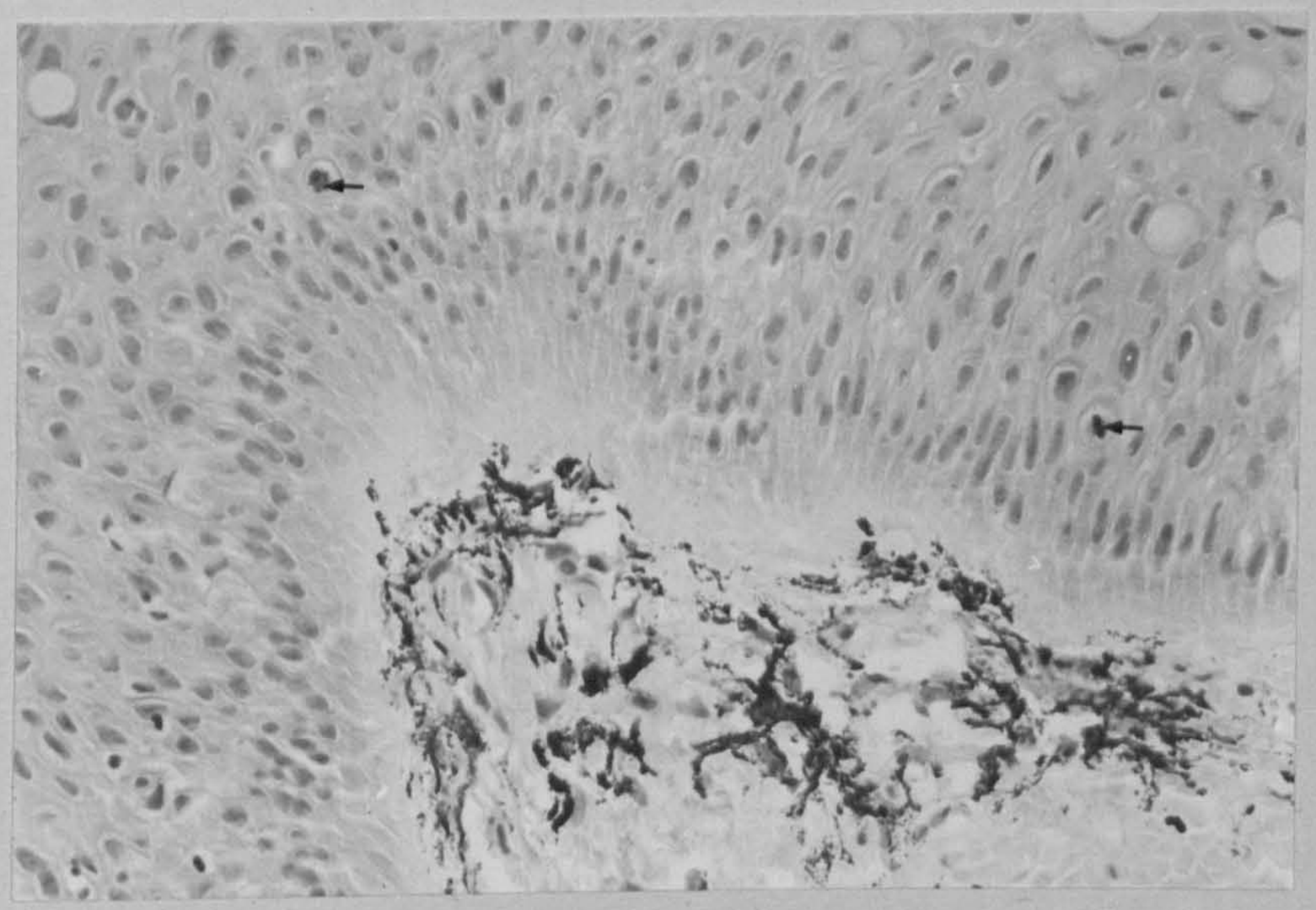

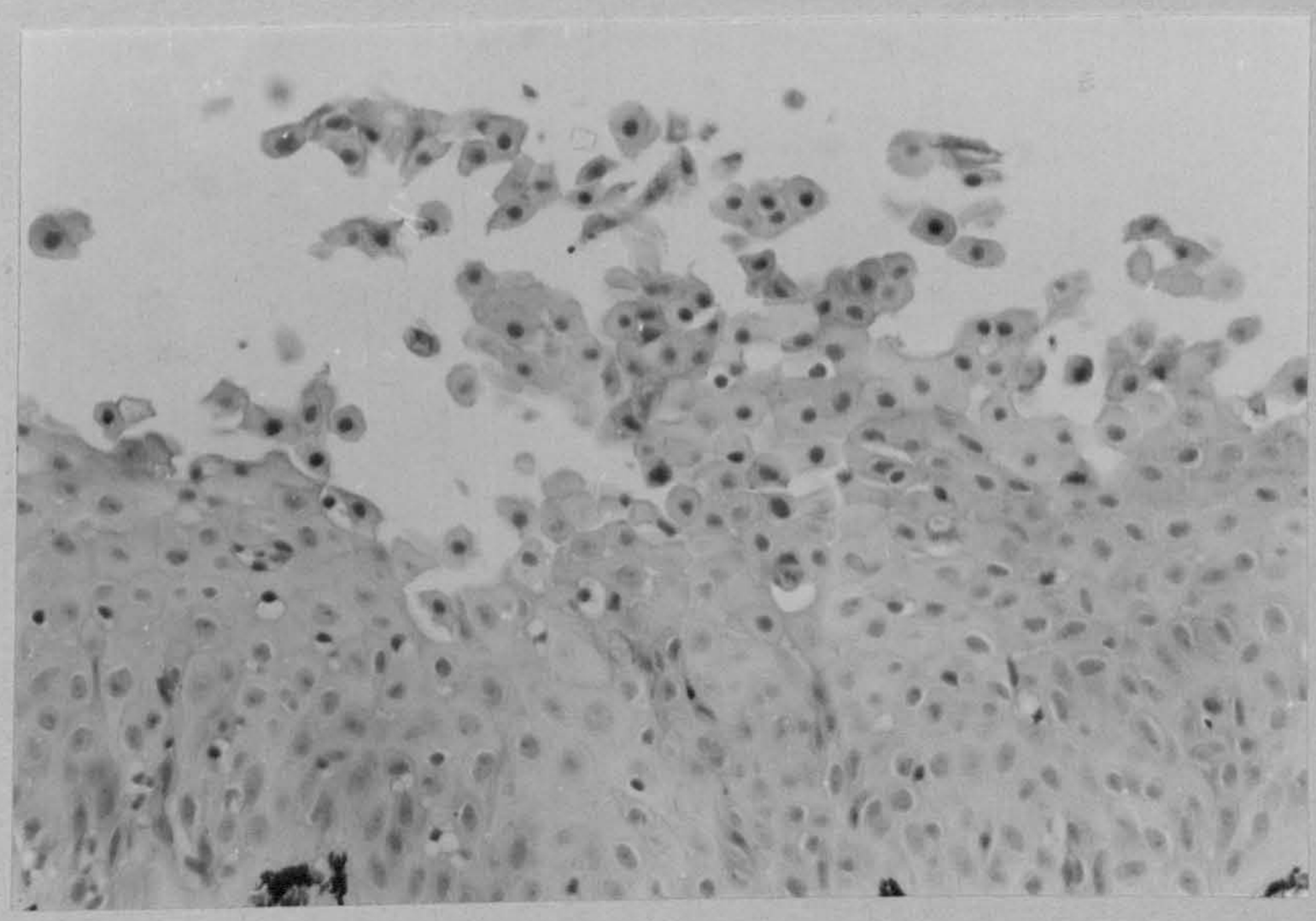

Fig. 85. "Type 2" change with fungal hyphae (arrowed) present. Note localised necrosis adjacent to hyphae.

H & E x 320

Fig. 86. "Type 2" change with fungal hyphae (arrowed) present. Note localised necrosis adjacent to hyphae.

H & E x 320

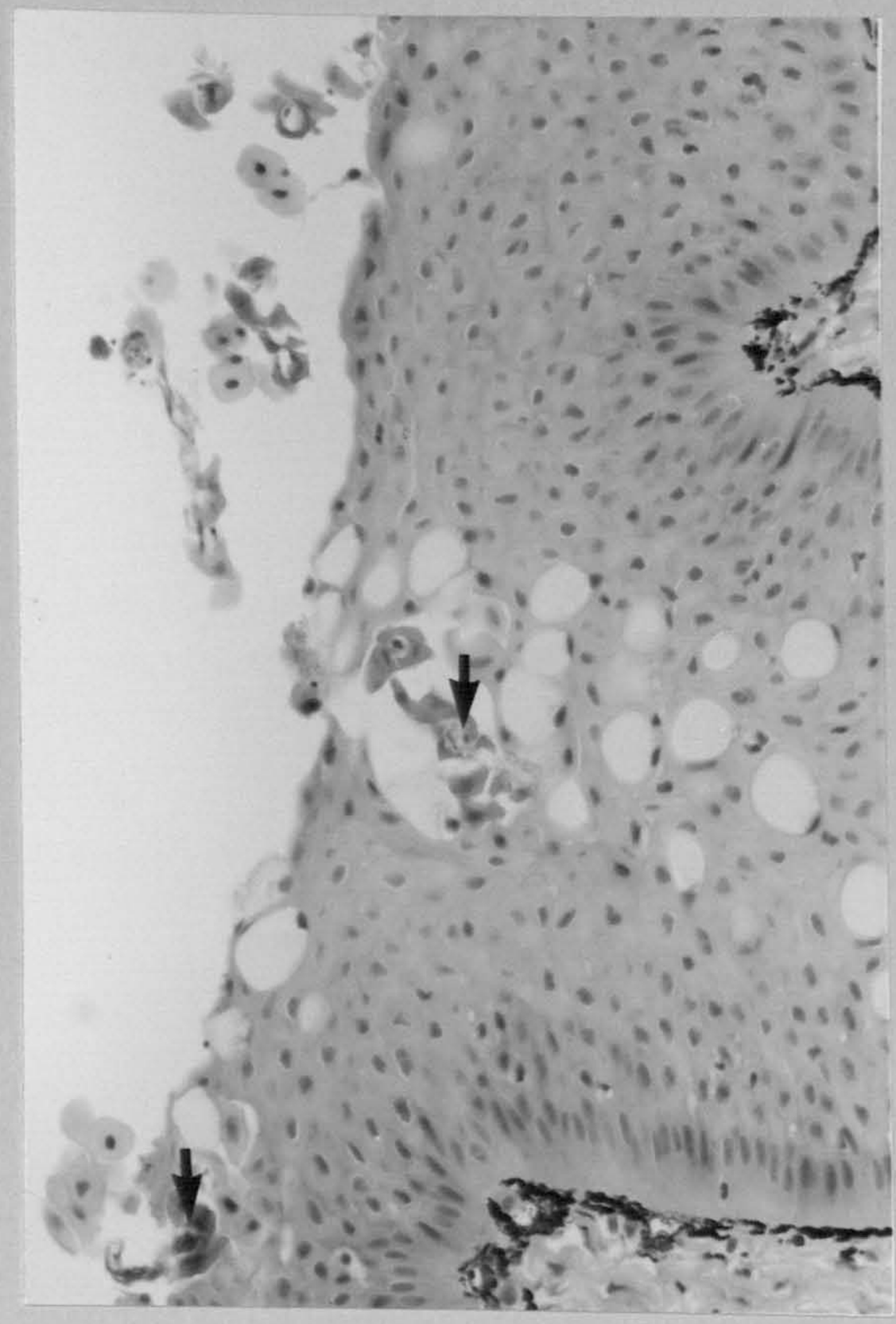

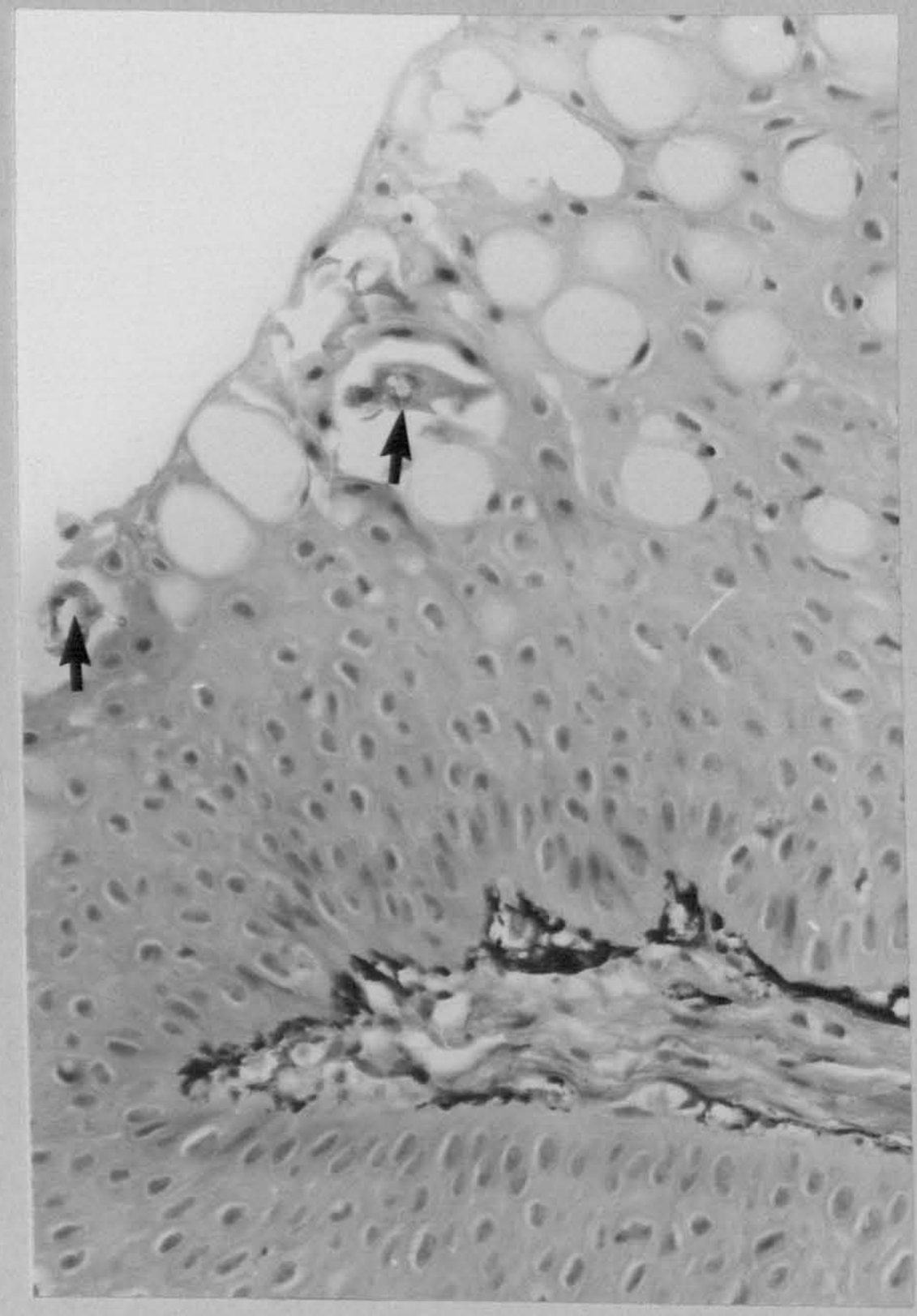

Fig. 87. "Type 2" change. Note fungal hyphae.

P.A.S. x 320

Fig. 88. "Type 3" lesion. Note spongiosis and epidermal sloughing.

H & E x 320

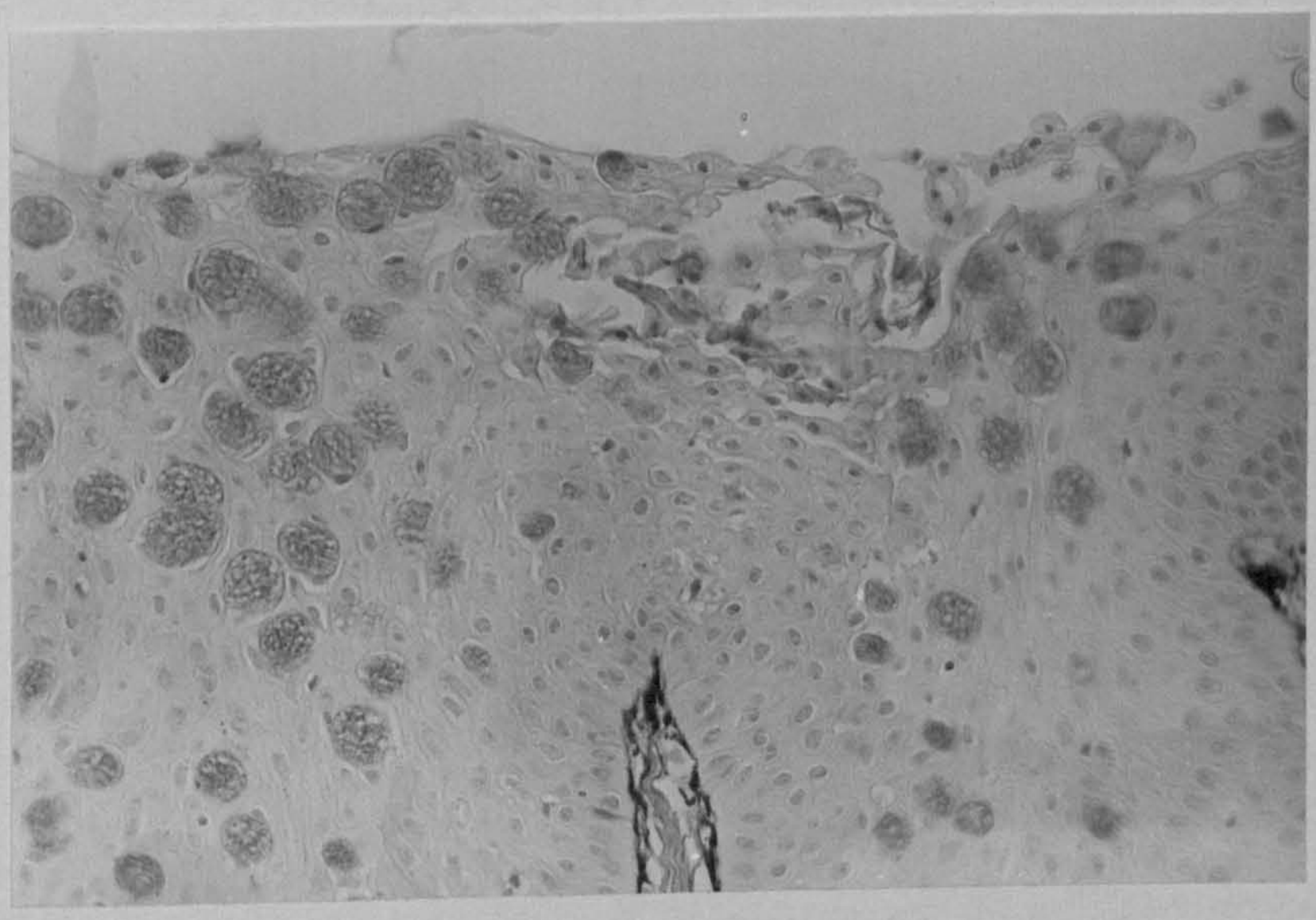

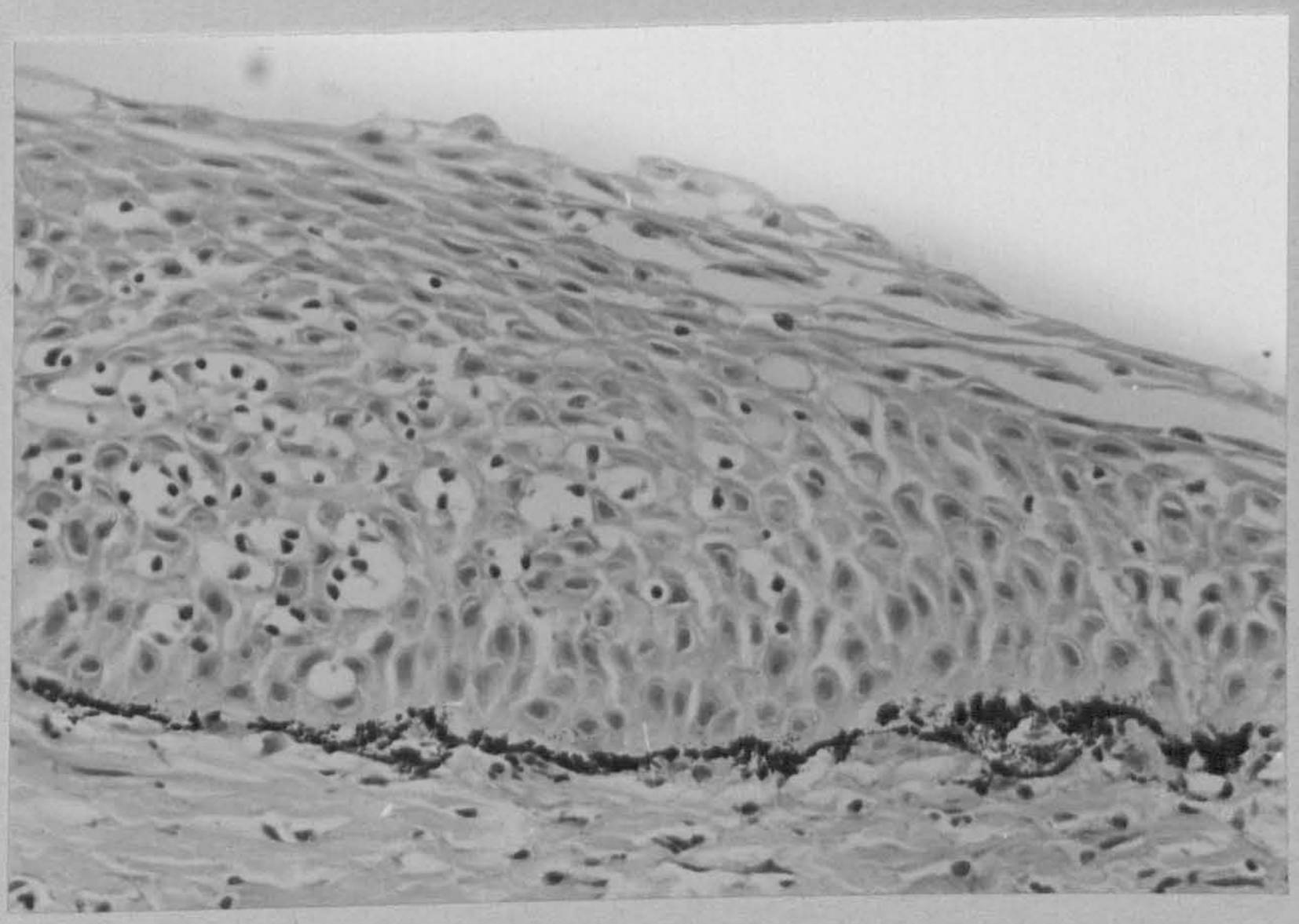

Fig. 89. "Type 3" change. Note epidermal spongiosis (S) associated with fungal infection and clumping of dermal melanin (M).

H & E x 320

Fig. 90. "Type 3" change. Note extensive dermal oedema.

H & E x 125

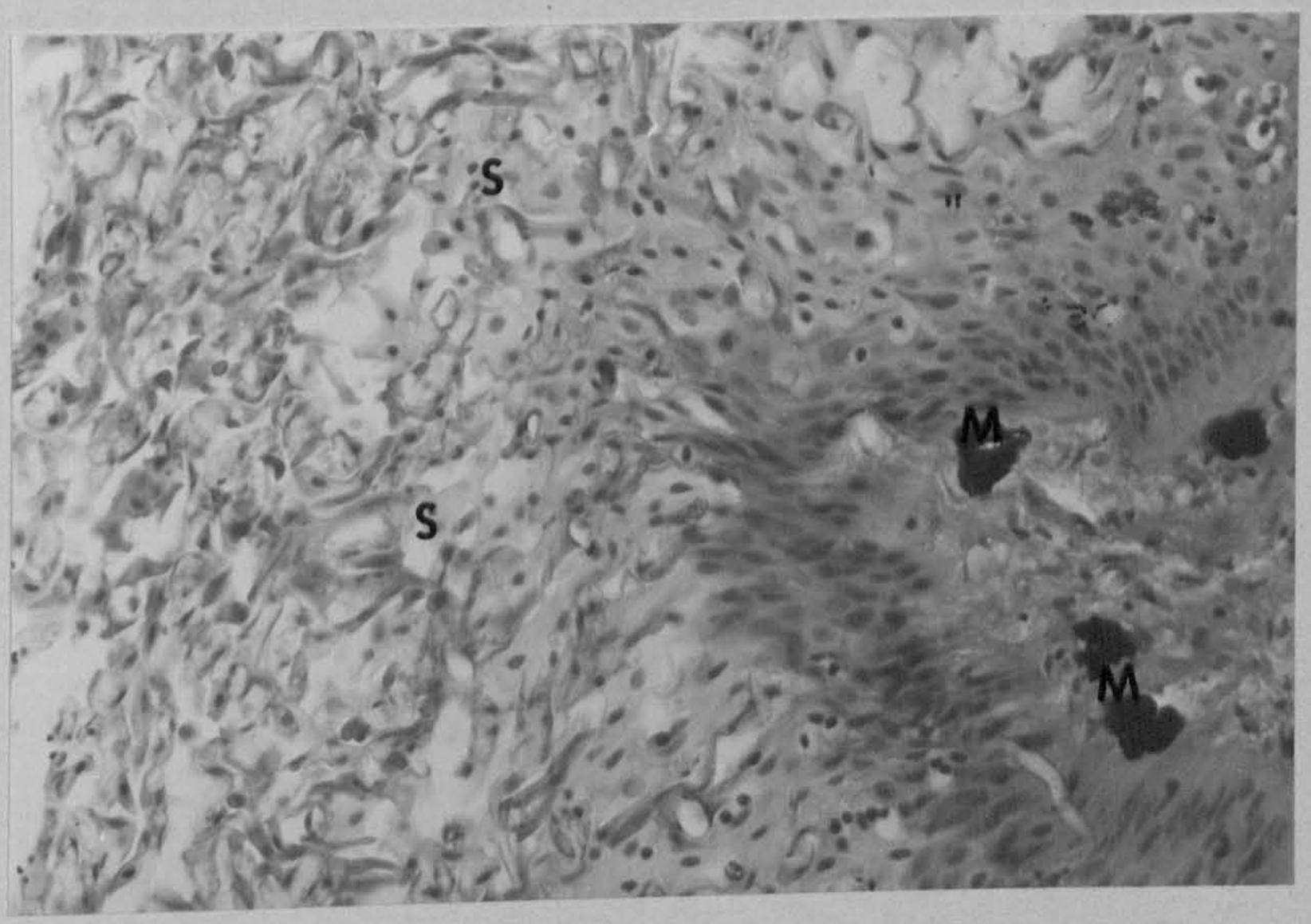
S
S
M
M

Fig. 91. "Type 3" lesion. Note haemorrhage (arrowed) into dermis and muscle and muscle degeneration.

H & E x 125

Fig. 92. "Type 4" lesion. Bacterial dermal infection (arrowed) leading to widespread dermal necrosis.

H & E x 320

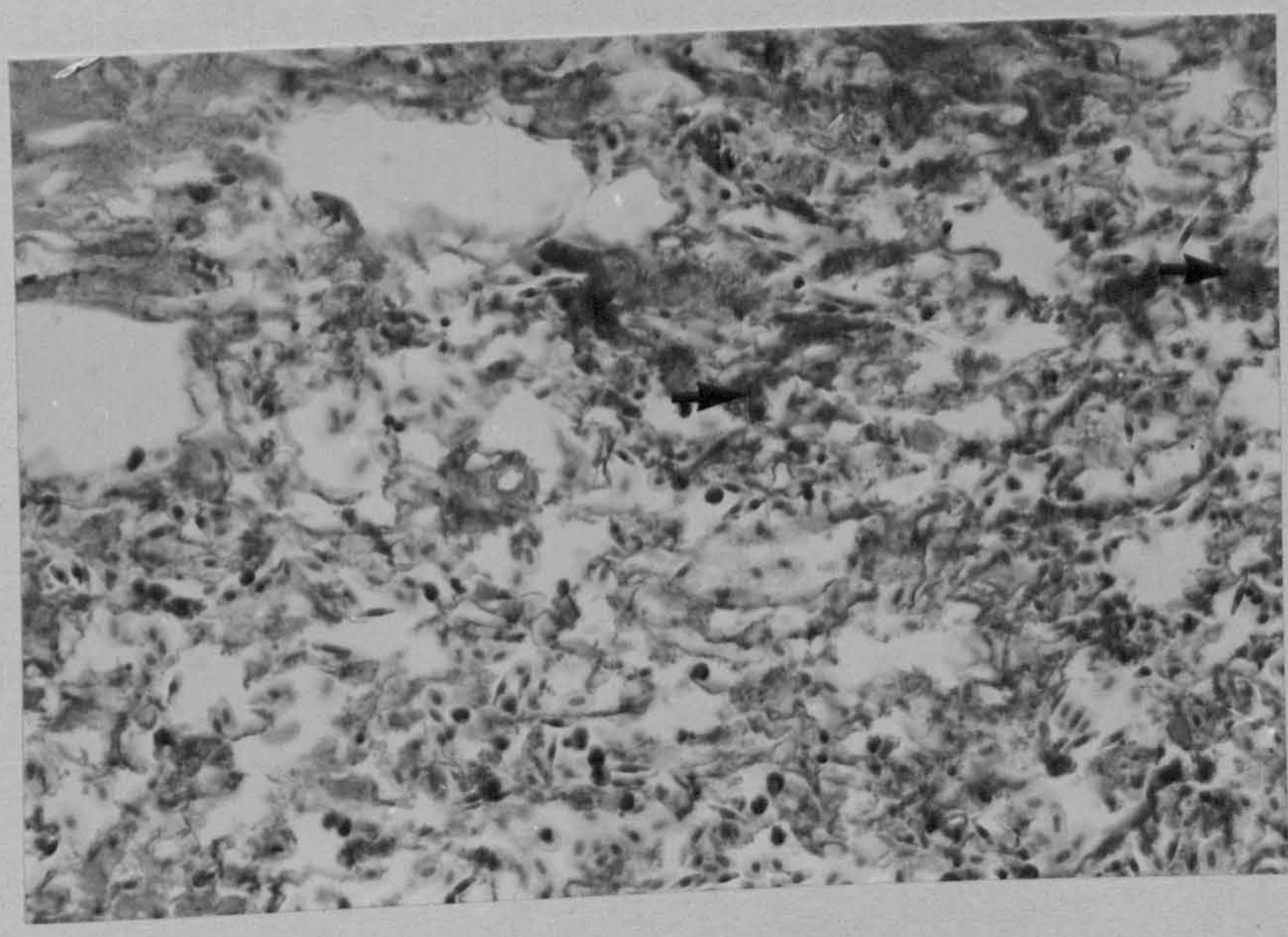

Fig. 93. "Type 5" lesion. Note myophagia (arrowed) and muscle necrosis associated with spread of bacteria (b) and fungi along fascial planes.

H & E x 320

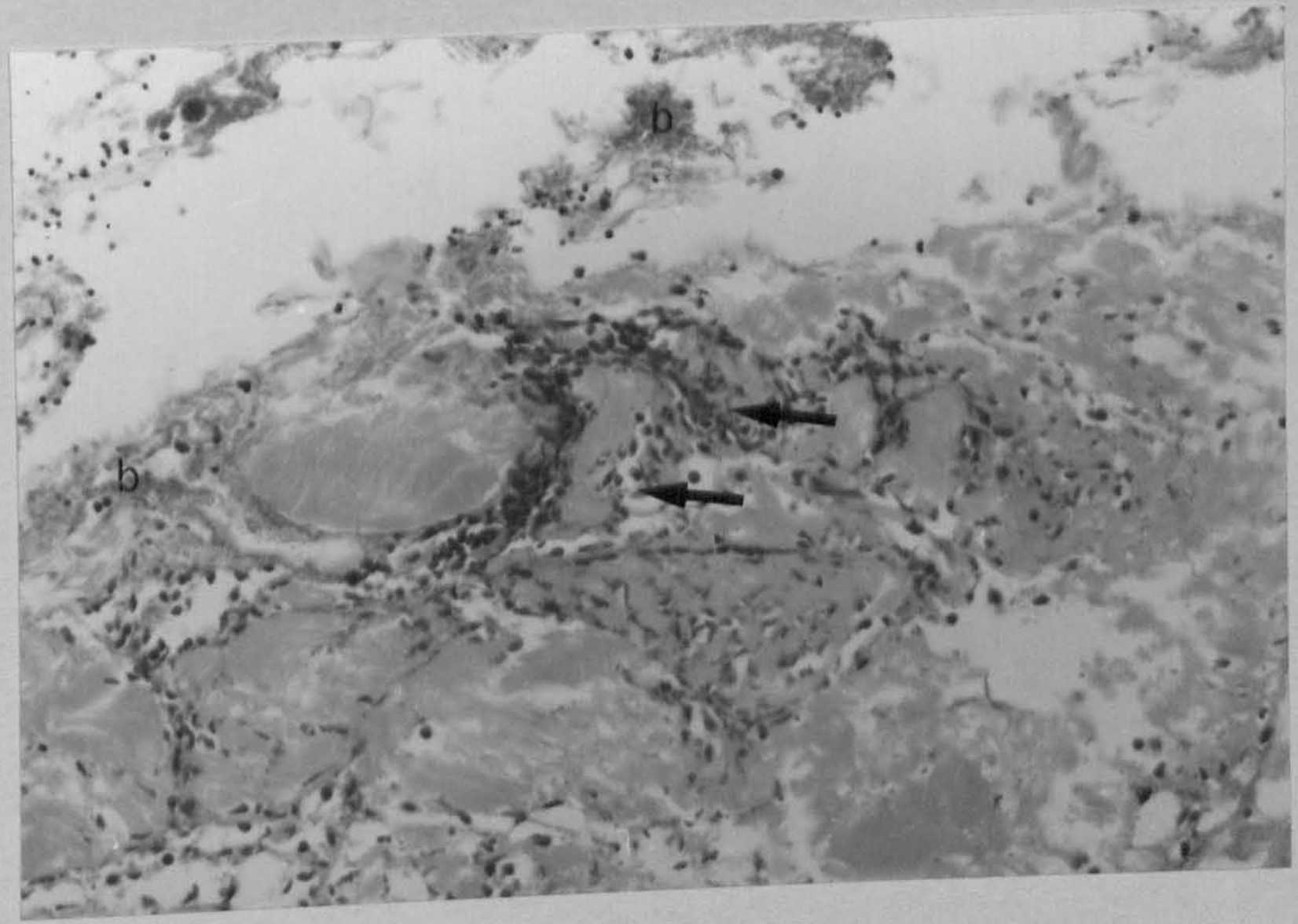
b
b

Fig. 94. Electron-micrograph of secondary cyst case of Saprolegnia diclina Humphrey type 1 isolate. Note typical long hooked hairs in bundles.

x 8,500

Fig. 95. Electron micrograph of secondary cyst case of Saprolegnia diclina Humphrey type 2 isolate. Note single short hooked hairs.

x 5,000

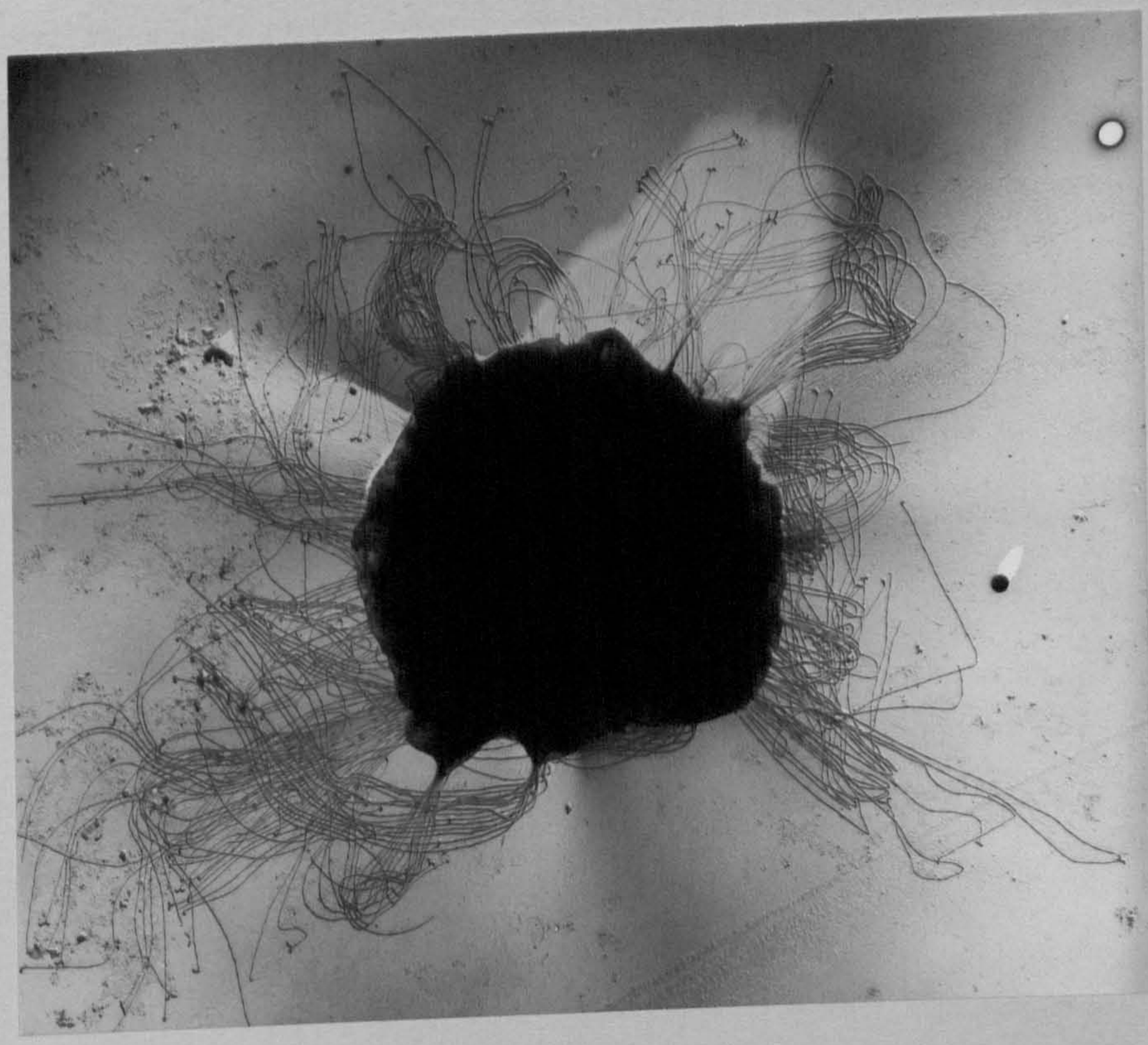

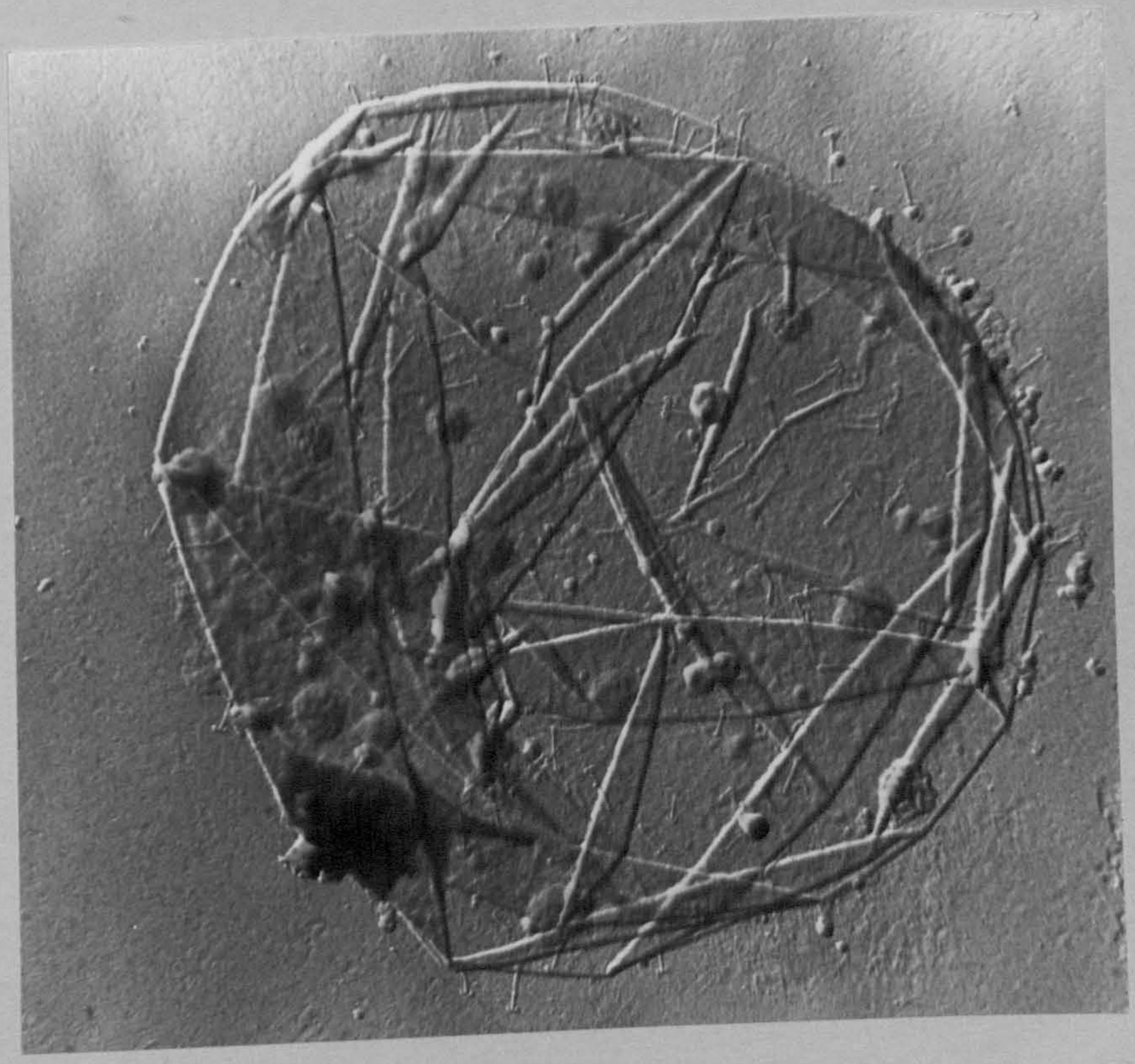

Fig. 96. Correlation between the concentration of sodium in the blood serum of Saprolegnia-infected brown trout from the spawning streams of Loch Leven and the degree of infection expressed as the percentage body surface area of the fish covered by fungus. Regression analysis $y = -0.94x + 161.7$. Correlation coefficient $r = 0.884$ ($p < 0.001$). Significance of the regression $p < 0.001$.

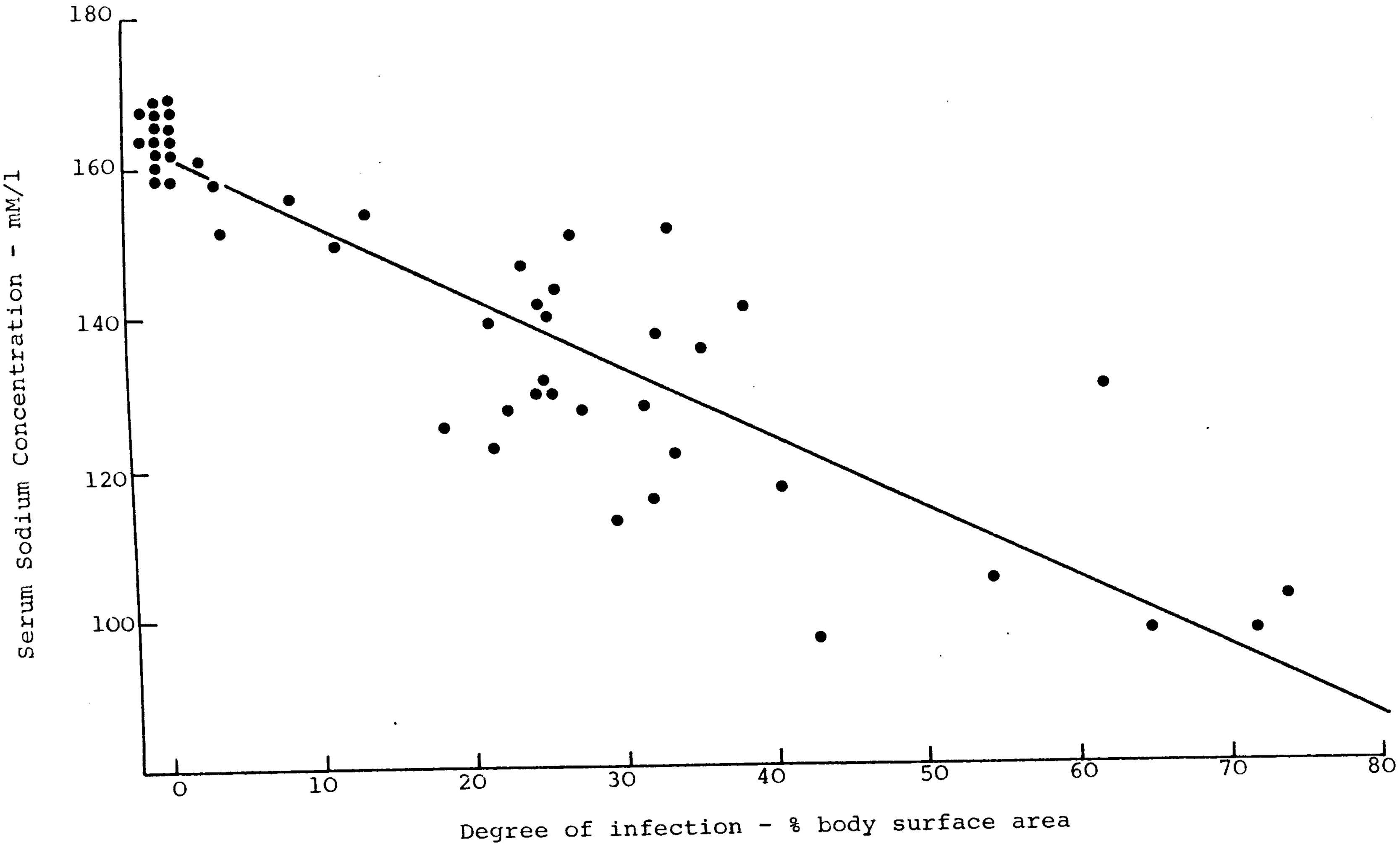
Serum Sodium Concentration - mM/l
180
160
140
120
100
0
10
20
30
40
50
60
70
80
Degree of infection - % body surface area

Fig. 97. Diagrammatic representation of the serum electrophoretograms for uninfected and Saprolegnia-infected brown trout from the spawning streams of Loch Leven. The diagrams are based upon the mean dimensions of each peak for all the fish examined. Peaks were identified by their mobilities relative to bromophenol blue. Major peaks (occurring in over 50% of the fish) are represented by solid shading and minor peaks (occurring in less than 50% of the fish) are represented by stippled shading.

UNINFECTED

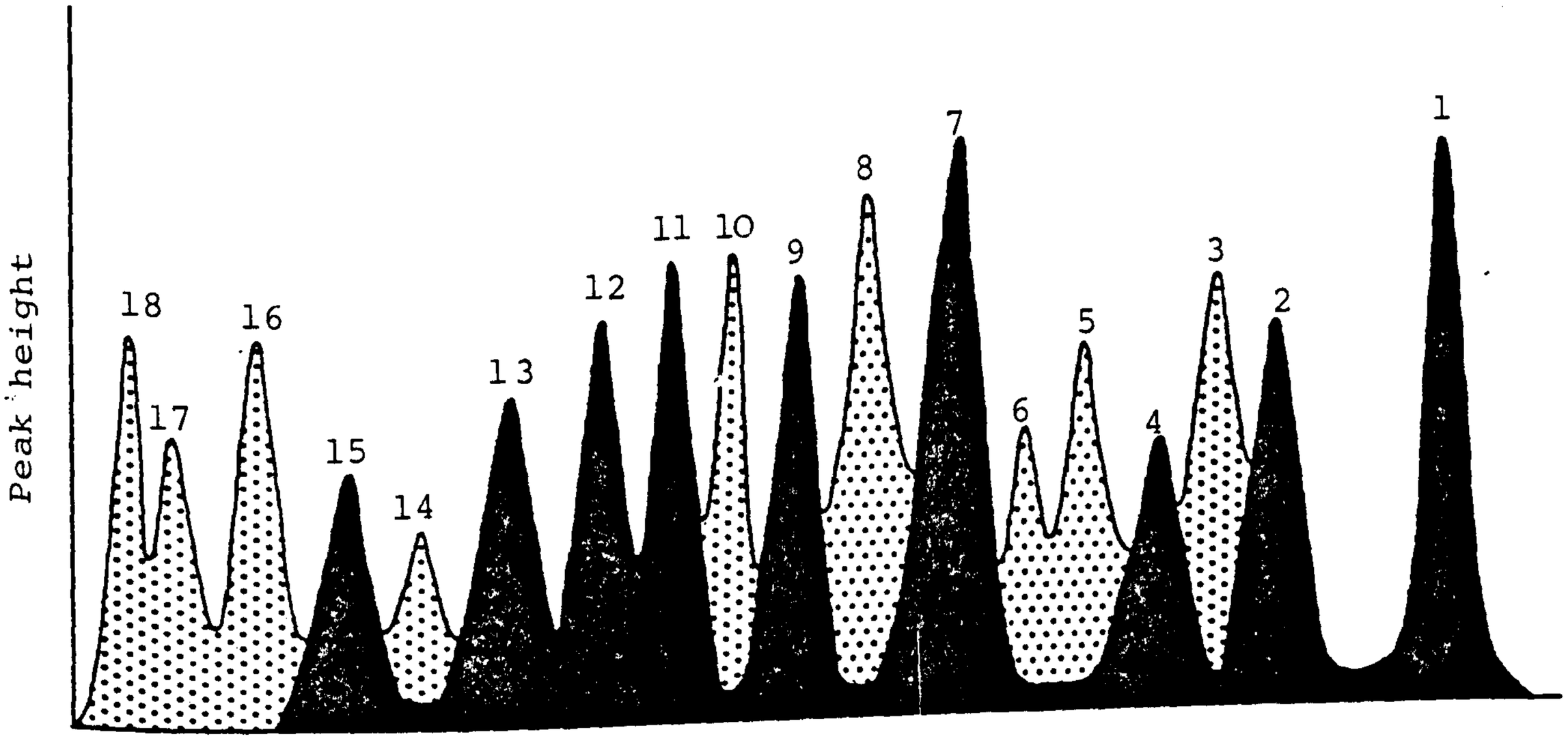

Increasing electrophoretic mobility

SAPROLEGNIA - INFECTED

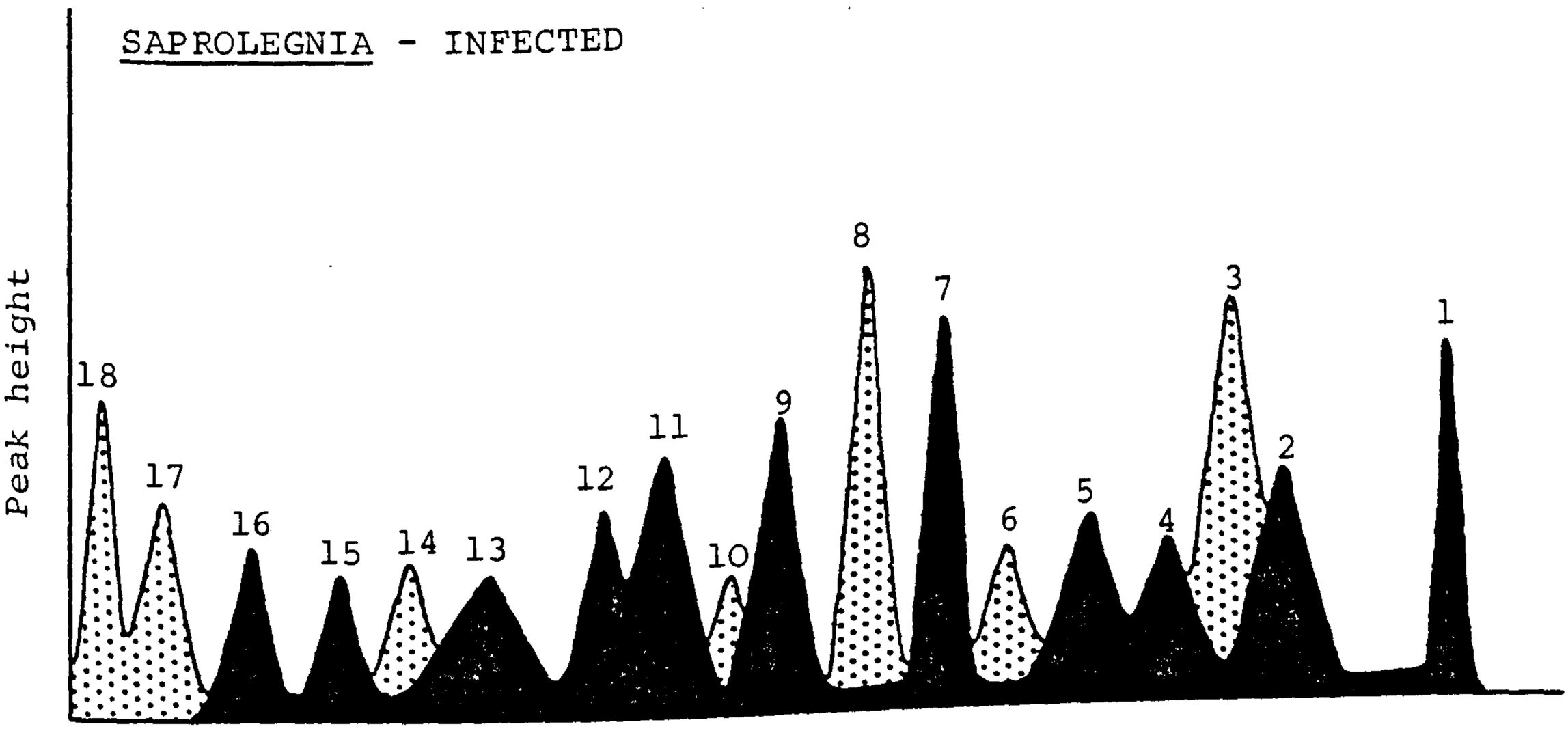

Increasing electrophoretic mobility

Fig. 98. Diagrammatic representation of blood flow through salmonid heart.

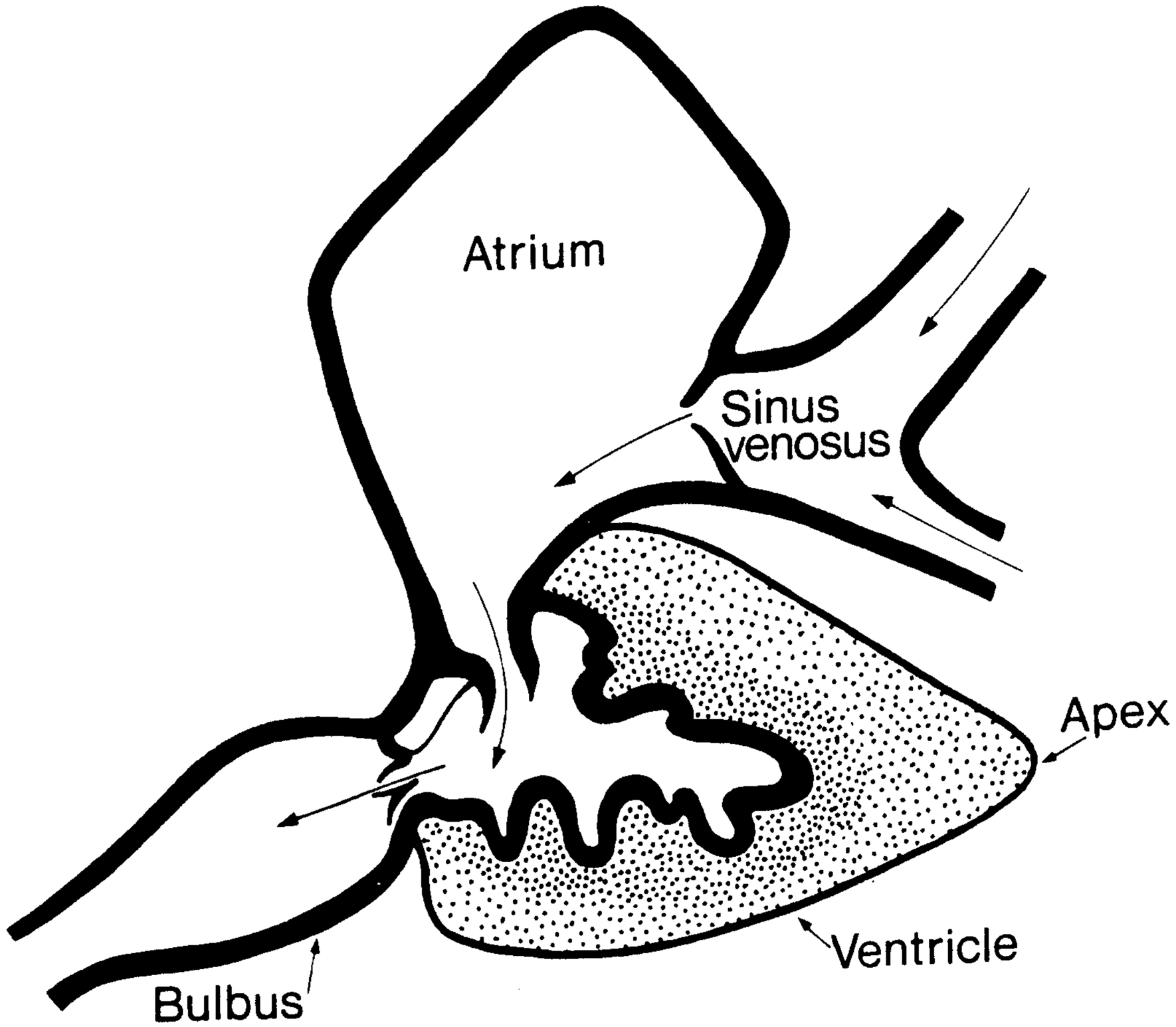

TROUT

Fig. 99. Anaesthetic system used in studies on electrocardiogram parameters.

Anaesthetic solution is contained in the upper reservoir and is gravity fed to the fish through a rotameter which monitors flow-rate. Spent anaesthetic is collected in the sump below the fish and then drained to the lower reservoir, from which it is periodically returned to the upper reservoir in the pipe (a). It is stirred by a propeller stirrer (b), aerated with an airstone (c), cooled by the cooling coil (e) and thermostatically heated by the contact thermometer (d).

Fish may be revived by alternative perfusion with fresh water, which is run to waste.

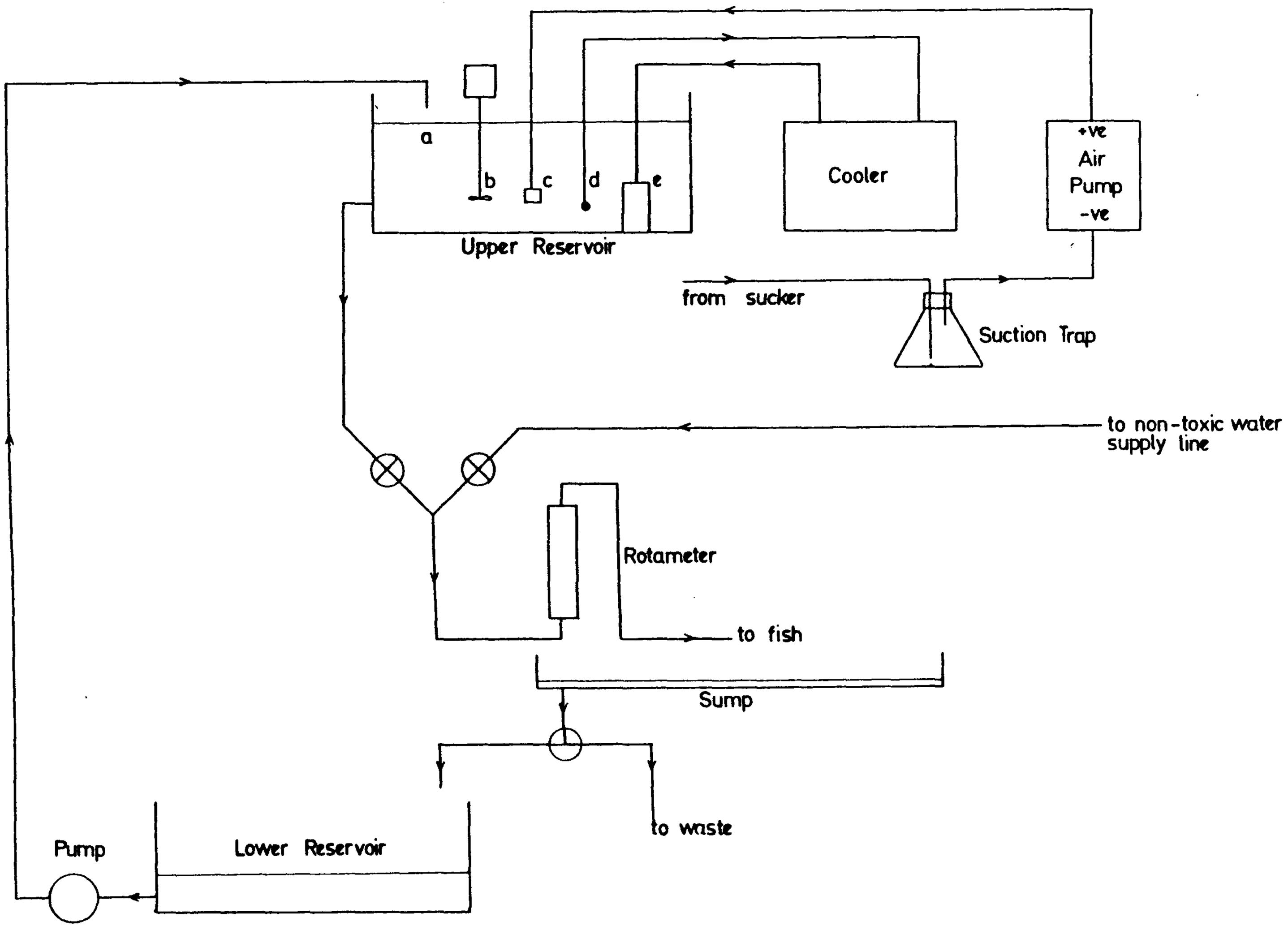
a
b
c
d
e
Upper Reservoir
Cooler
+ve
Air
Pump
-ve
from sucker
Suction Trap
to non-toxic water
supply line
Rotameter
to fish
Sump
to waste
Pump
Lower Reservoir

Figure 100. Oscilloscope photograph of normal brown trout ECG to show the conventions employed in measurement in this investigation.

Vertical calibration : 250μV

Horizontal calibration : 1s

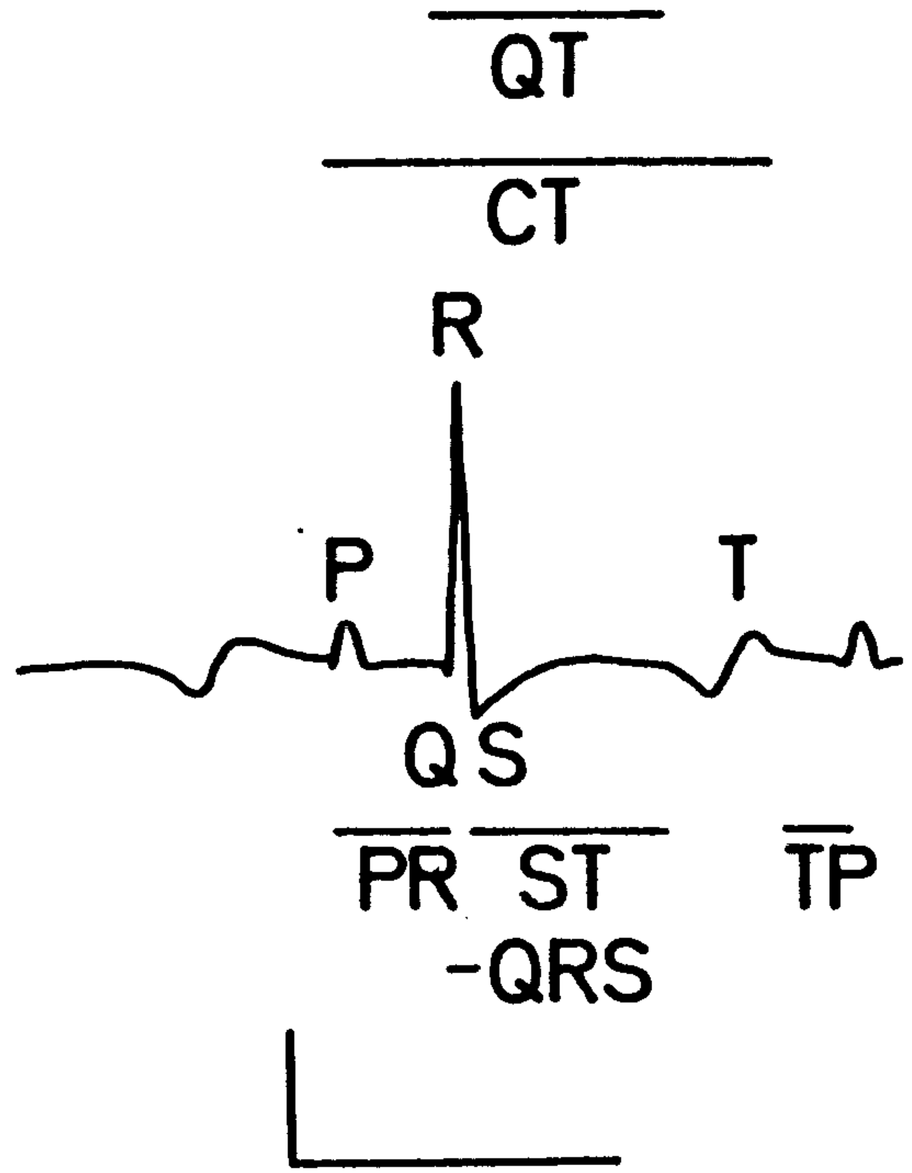
QT
CT
R
P
T
Q
S
PR
ST
TP
-QRS

Fig. 101. Electrocardiograms recorded from uninfected fish. (a, b, c) Brown trout (Salmo trutta), (d) Perch (Perca fluviatilis), (e) Mora mora (Gadidae), (f) Rainbow trout (Salmo gairdneri), (g) Centroscymnus crepidater (Squalidae).

Vertical calibration : 250 μV

Horizontal calibration : 1s

a

(a,b)

b

c

(c,d,e,f,g

d

e

f

g

Fig. 102. Electrocardiograms recorded from Brown trout exhibiting varying degrees of Saprolegnia infection.

Vertical calibration : 250μV

Horizontal calibration : 1s

a

b

c

(a,b,c)

d

e

f

(d,e,f)

Fig. 103. Home Office facility at Howietown and Northern Fisheries, Bannockburn.

Fig. 104. Healed scar on ventral abdominal surface, four weeks post gonadectomy.

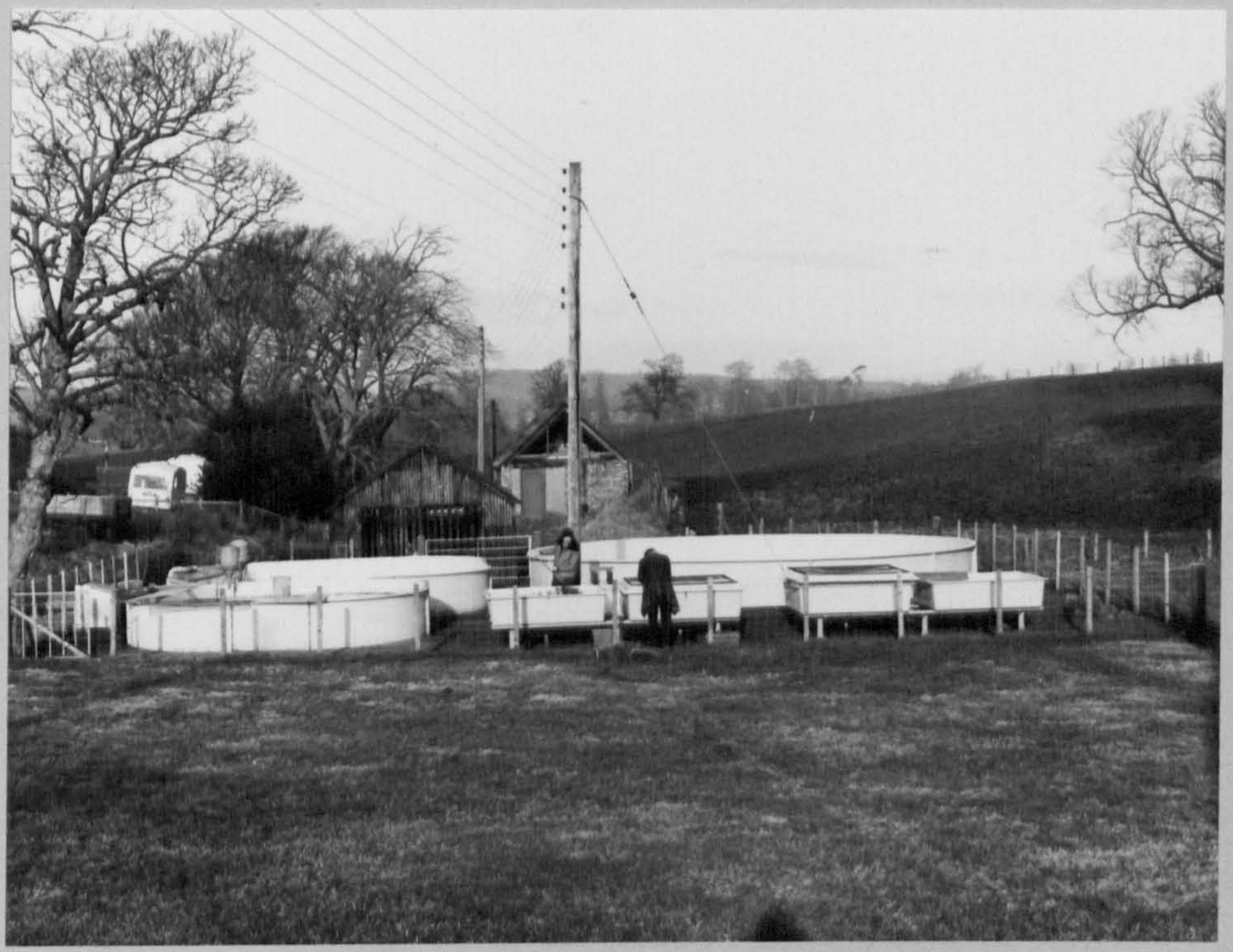

Fig. 105. Freeze-brand on experimental gonadectomised fish.

Fig. 106. Freeze-branding equipment.

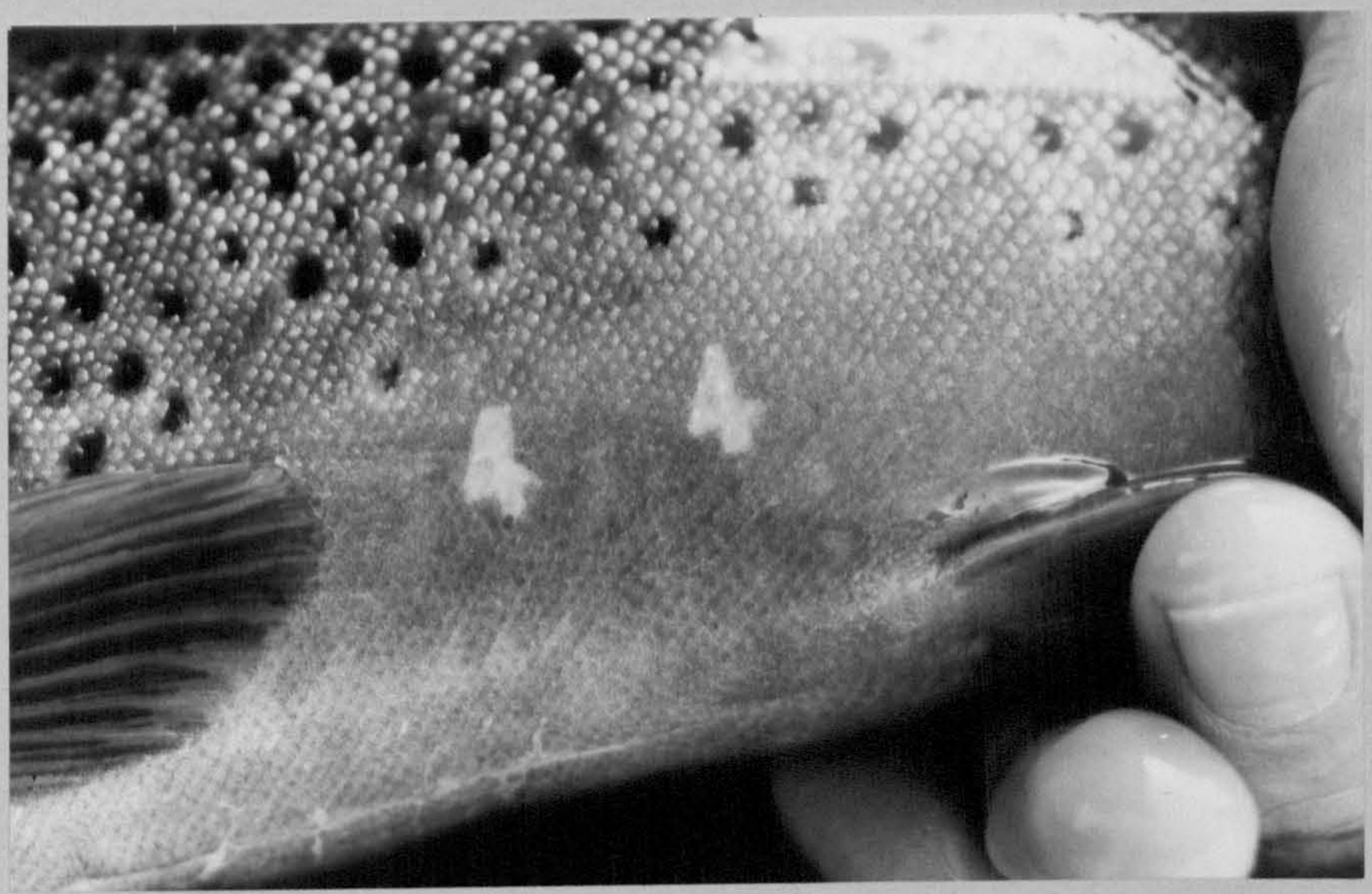

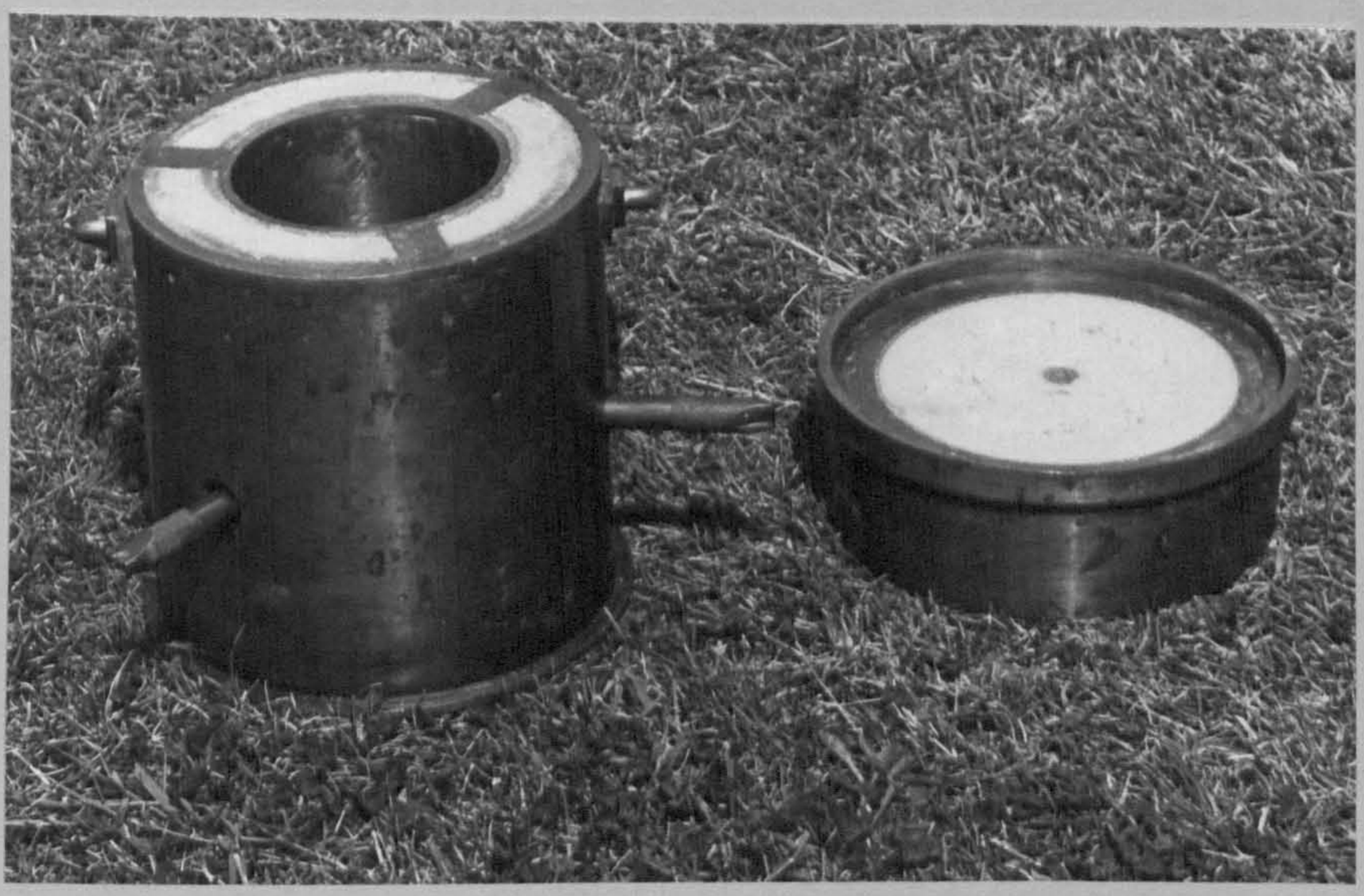

Fig. 107. Interrenal tissue of control fish. An isolated group of cells surrounding a small vein.

H & E x 320

Fig. 108. Interrenal hyperplasia following androgen administration. Note the increased vacularity.

H & E x 500

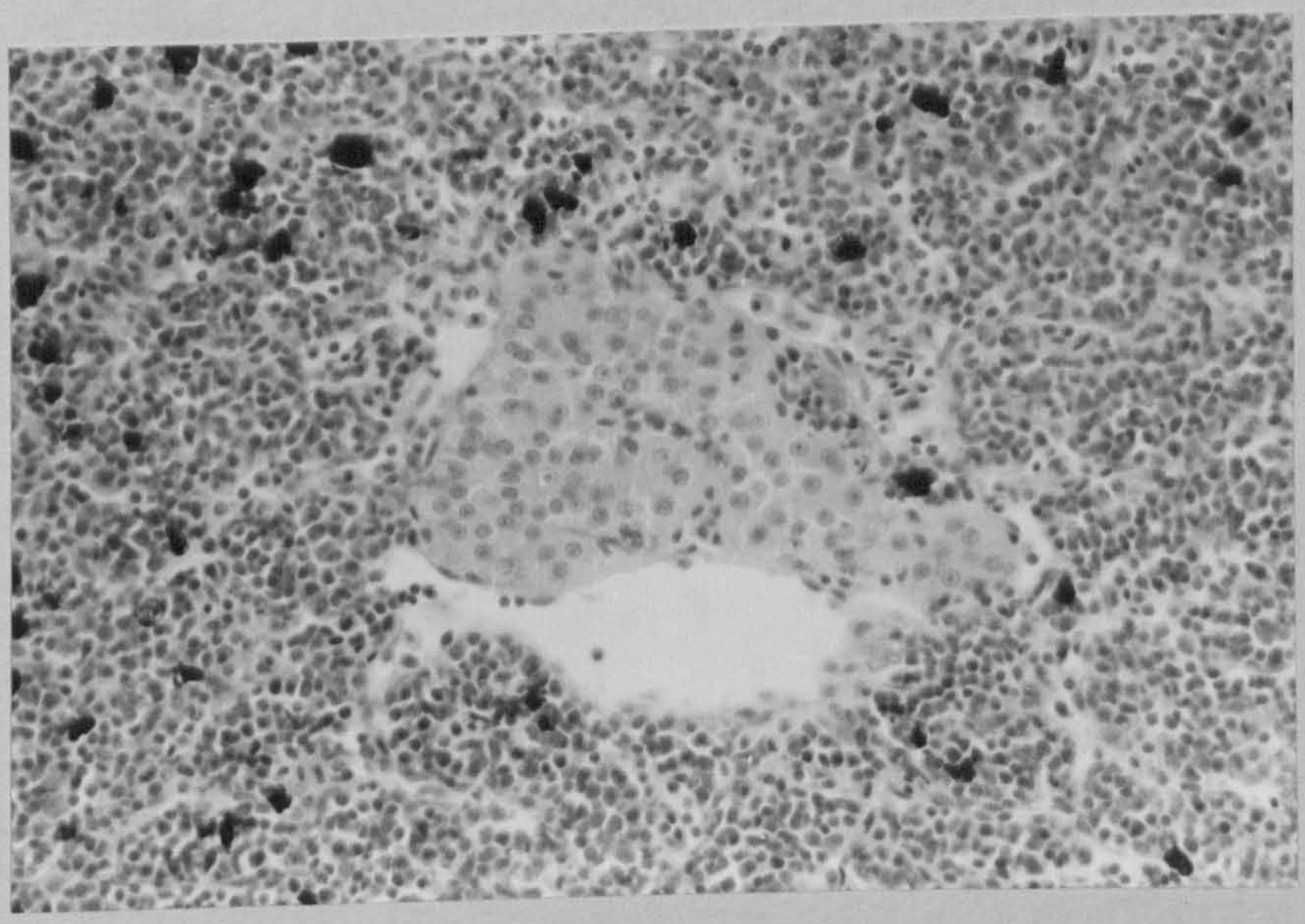

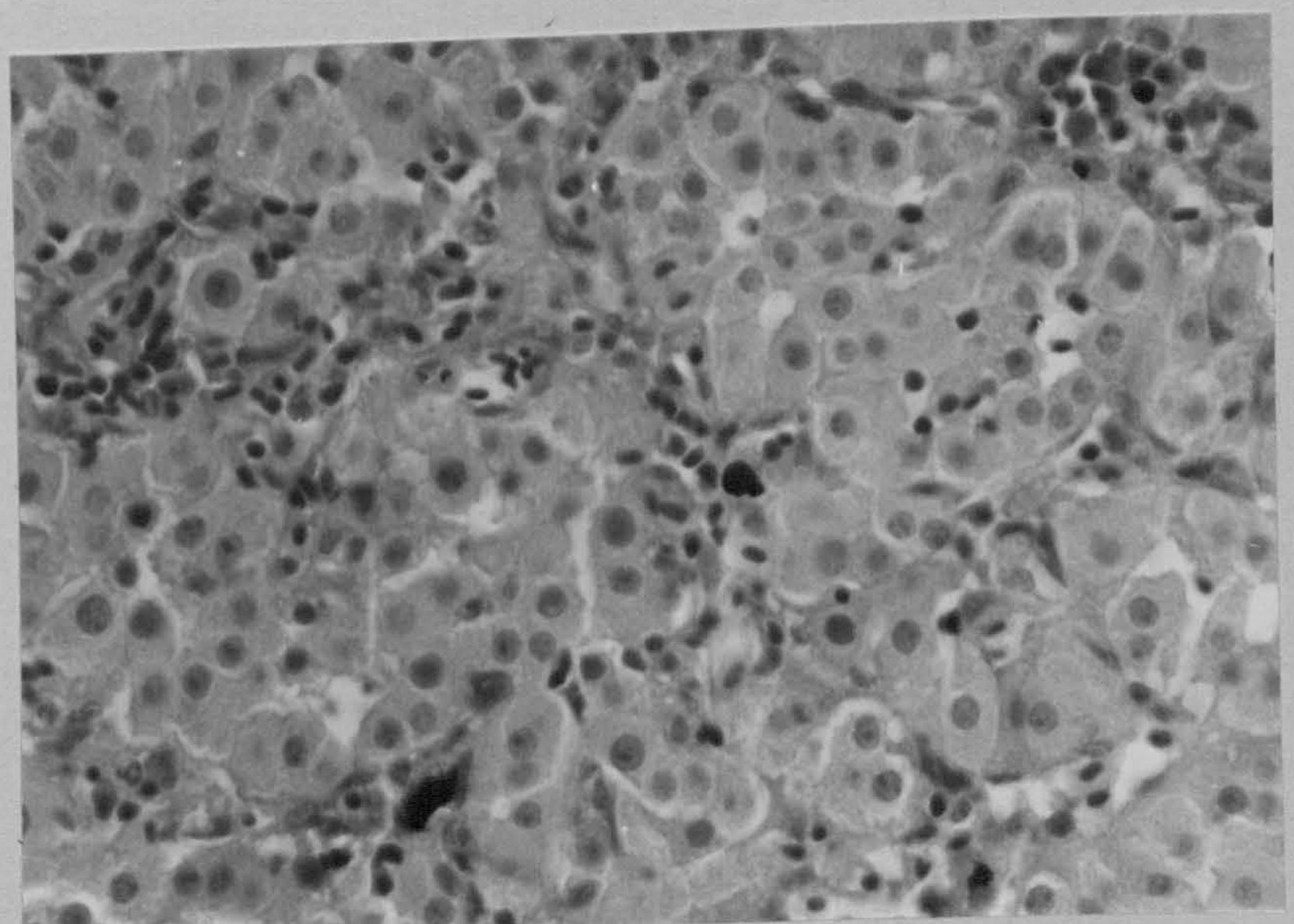

Fig. 109. Interrenal tissue of androgen-injected fish. Note prominent nucleoli and mitotic figures.

H & E x 320

Fig. 110. Interrenal tissue of androgen-injected fish. Note duct-like appearance.

H & E x 320

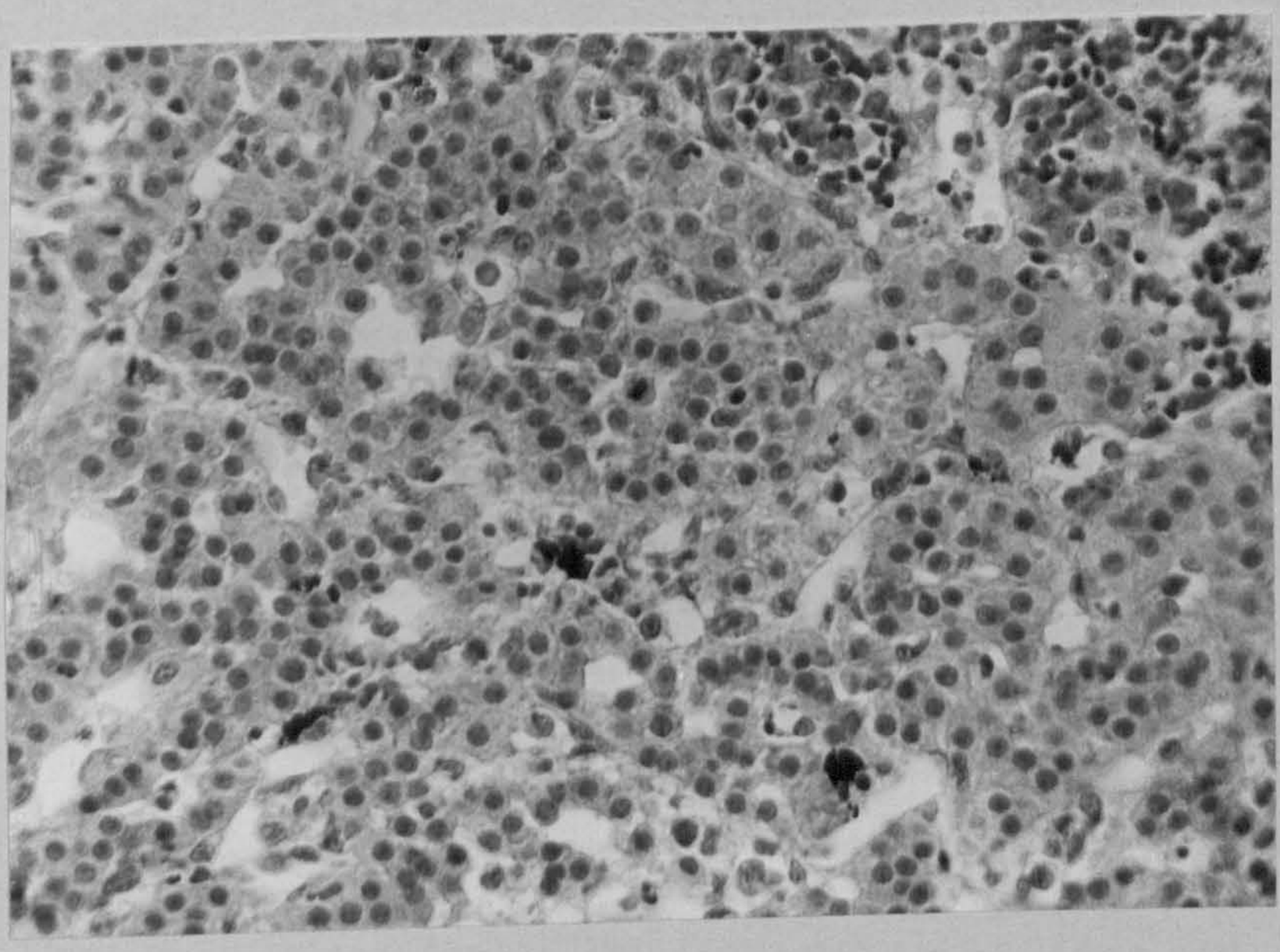

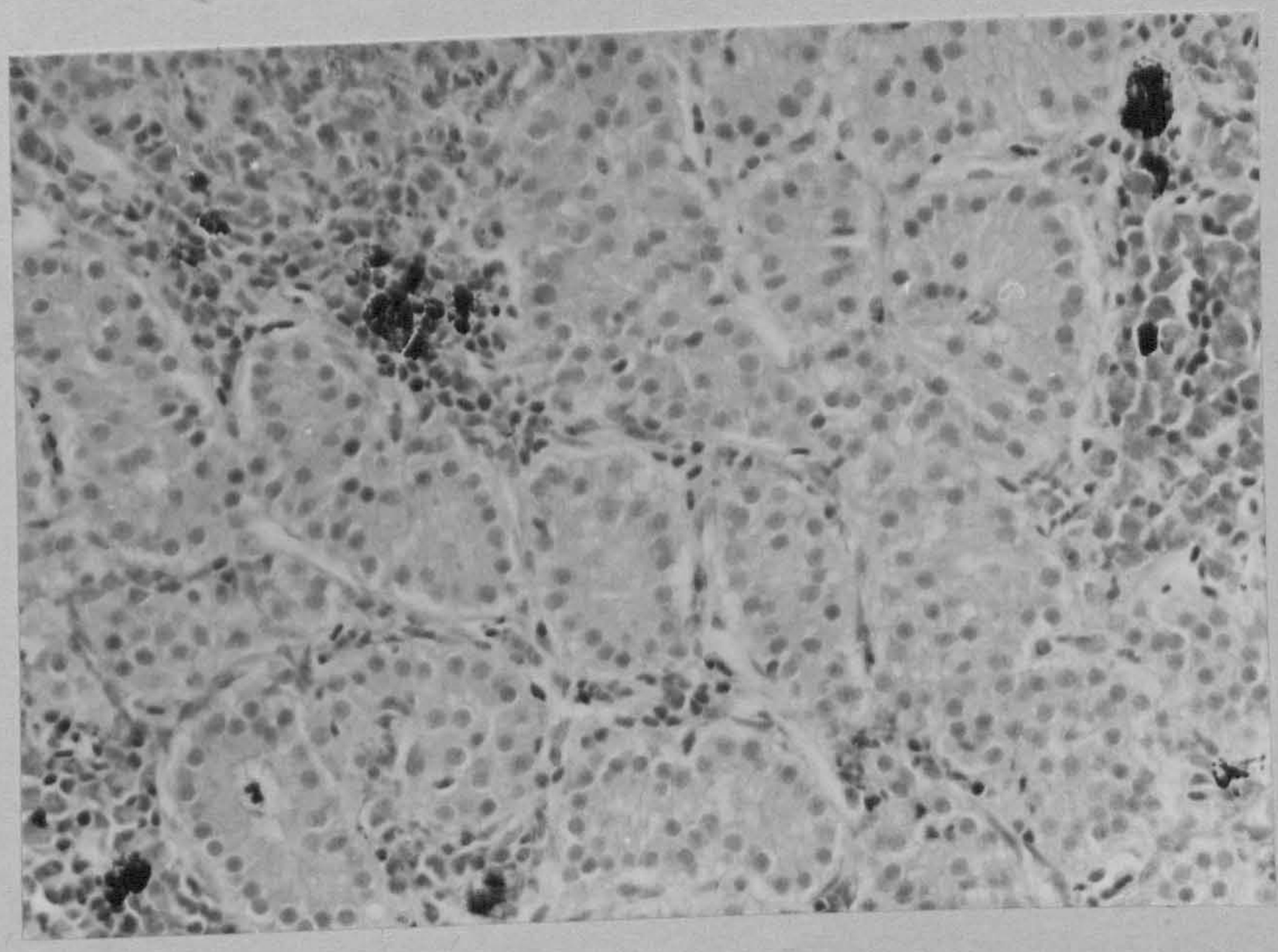

Fig. 111. Degenerative change in interrenal tissue of fish receiving 11 ketotestosterone. Note loss of cell outline and cytoplasmic degeneration.

H & E x 320

Fig. 112. Bile-ducts of fish receiving 11 ketotestosterone. Note thickened bile-duct walls.

H & E x 500

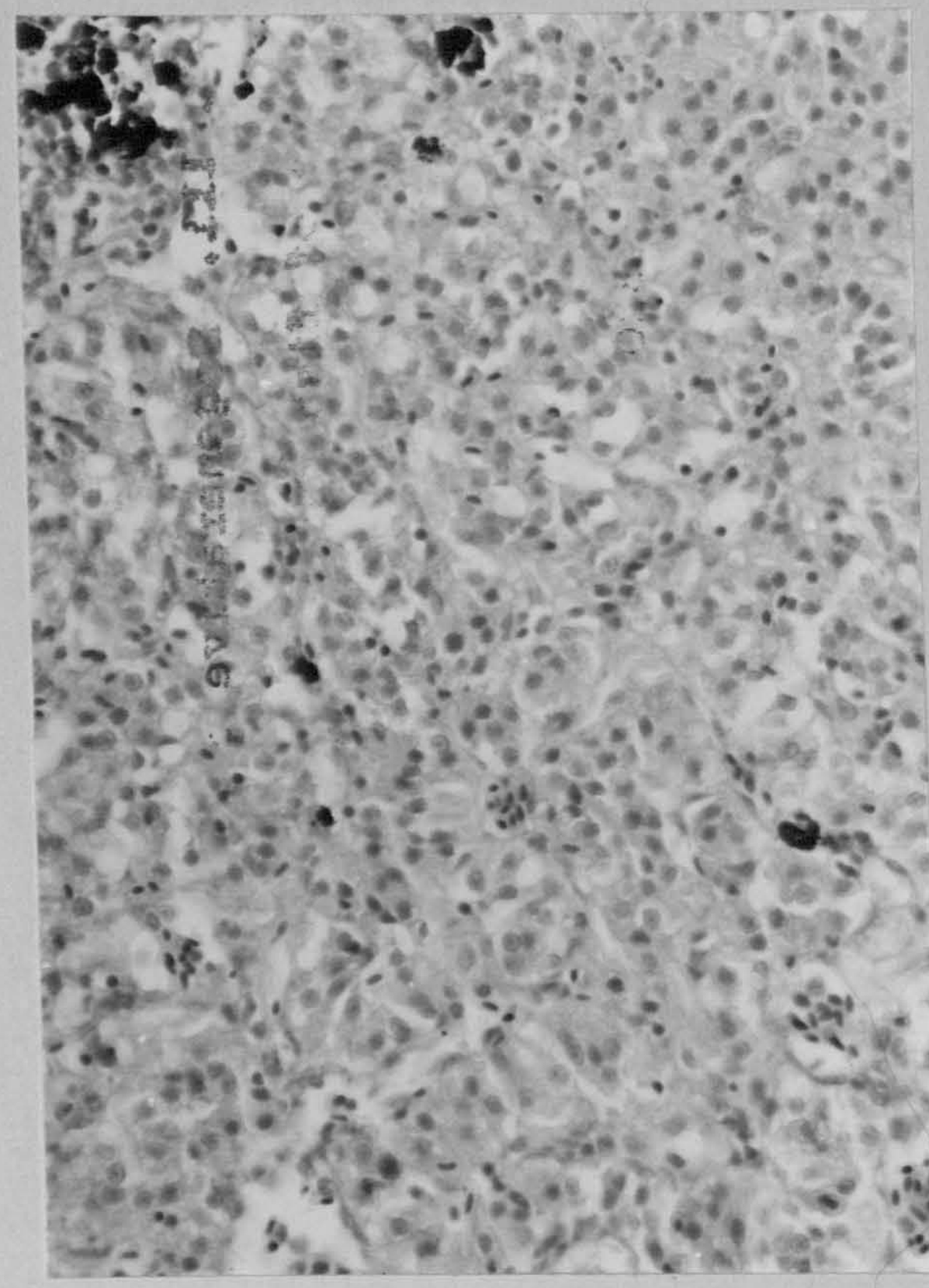

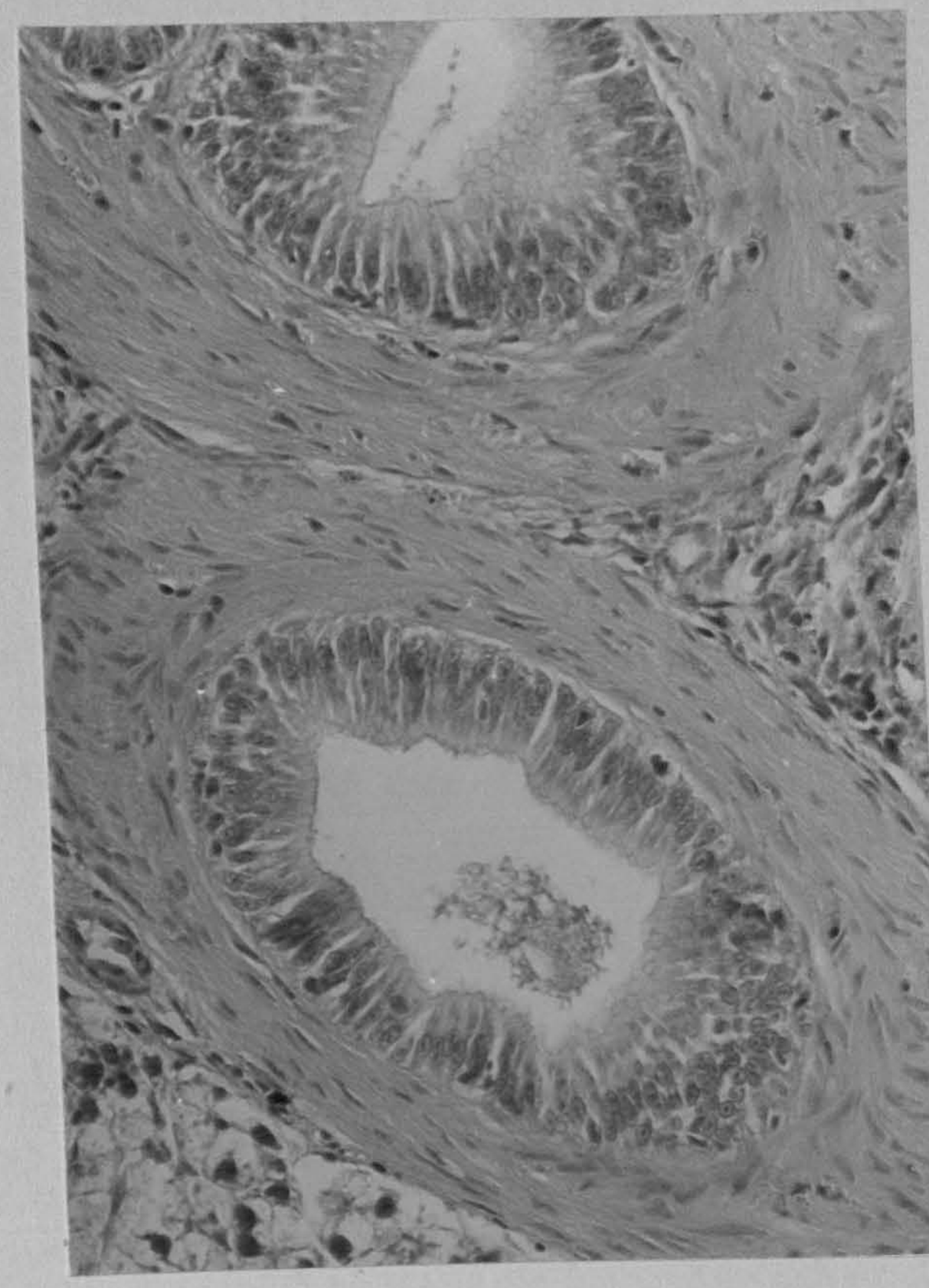

Fig. 113. Focal liver necrosis in fish receiving 11 ketotestosterone. Note extensive karyolysis (arrowed).

H & E x 320

Fig. 114. Islet of Langerhans in androgen-injected fish. B cells are grouped around an apparent vascular channel.

H & E x 320

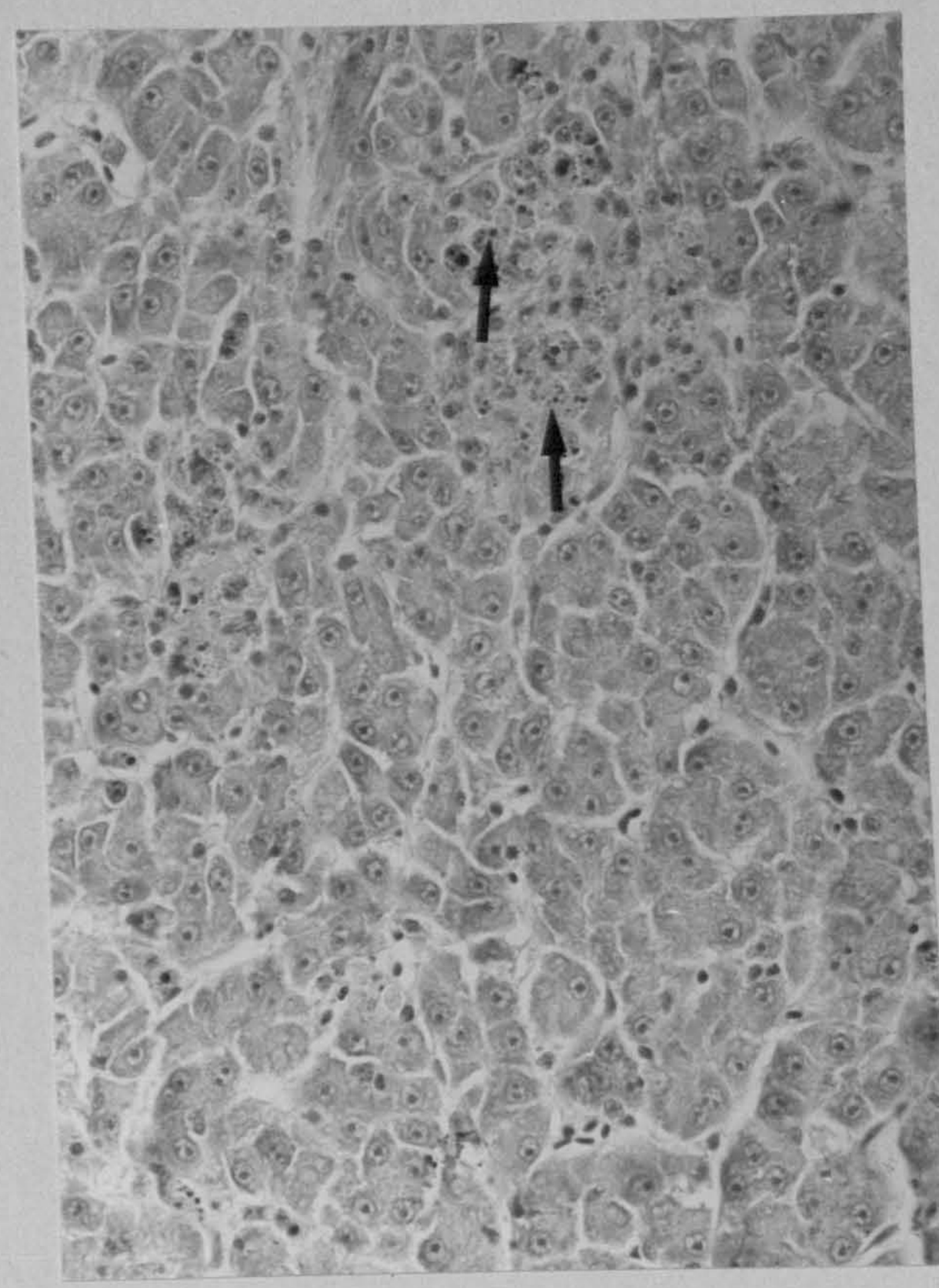

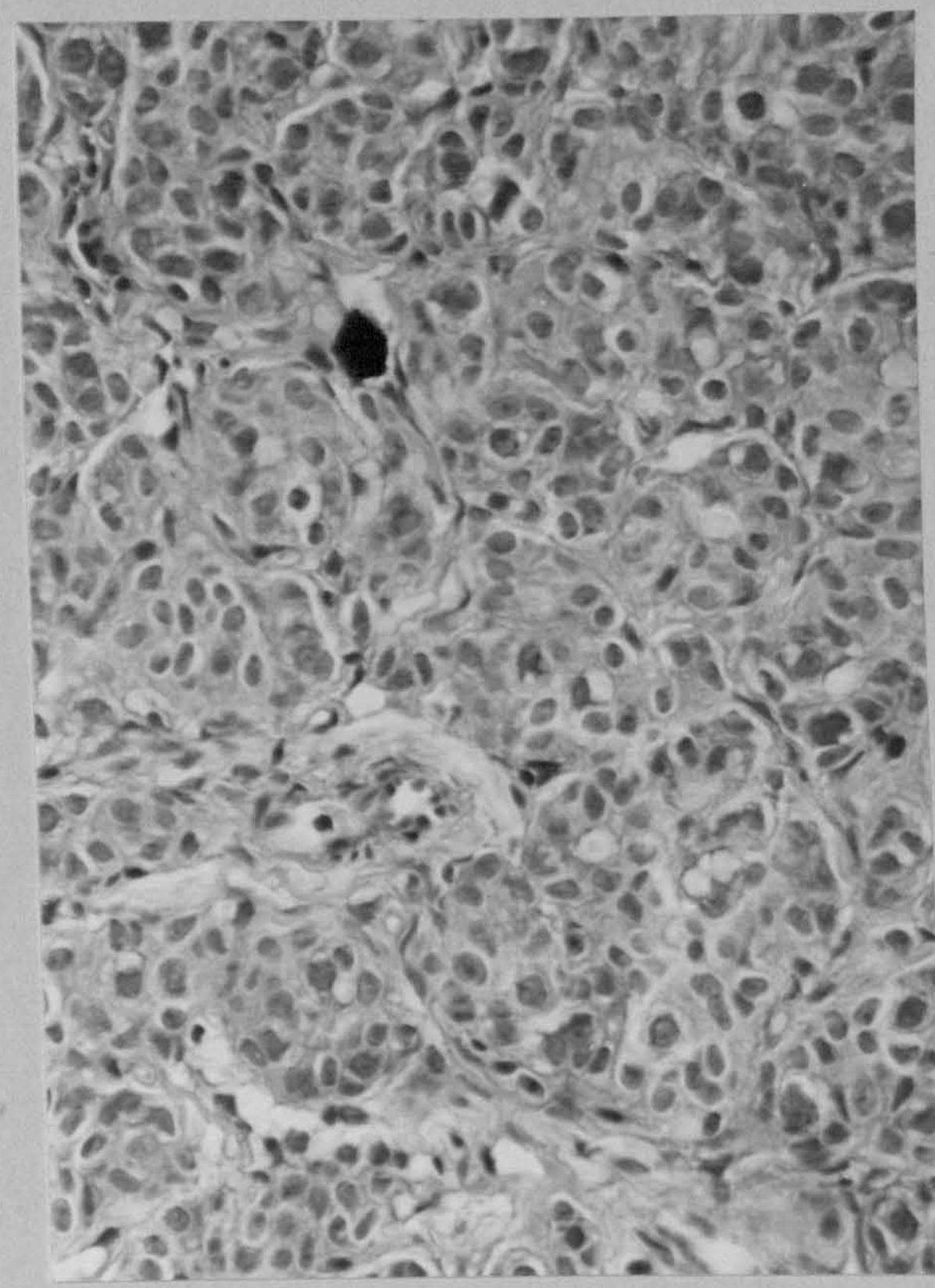

Fig. 115. Cytoplasmic vacuolation of pancreatic acinar cells in fish receiving arachis oil.

H & E x 320

Fig. 116. Arteriosclerotic change in androgen-injected fish. Note intimal proliferation and splitting and reduplication of internal elastic lamina.

Weigert's Elastic stain x 500

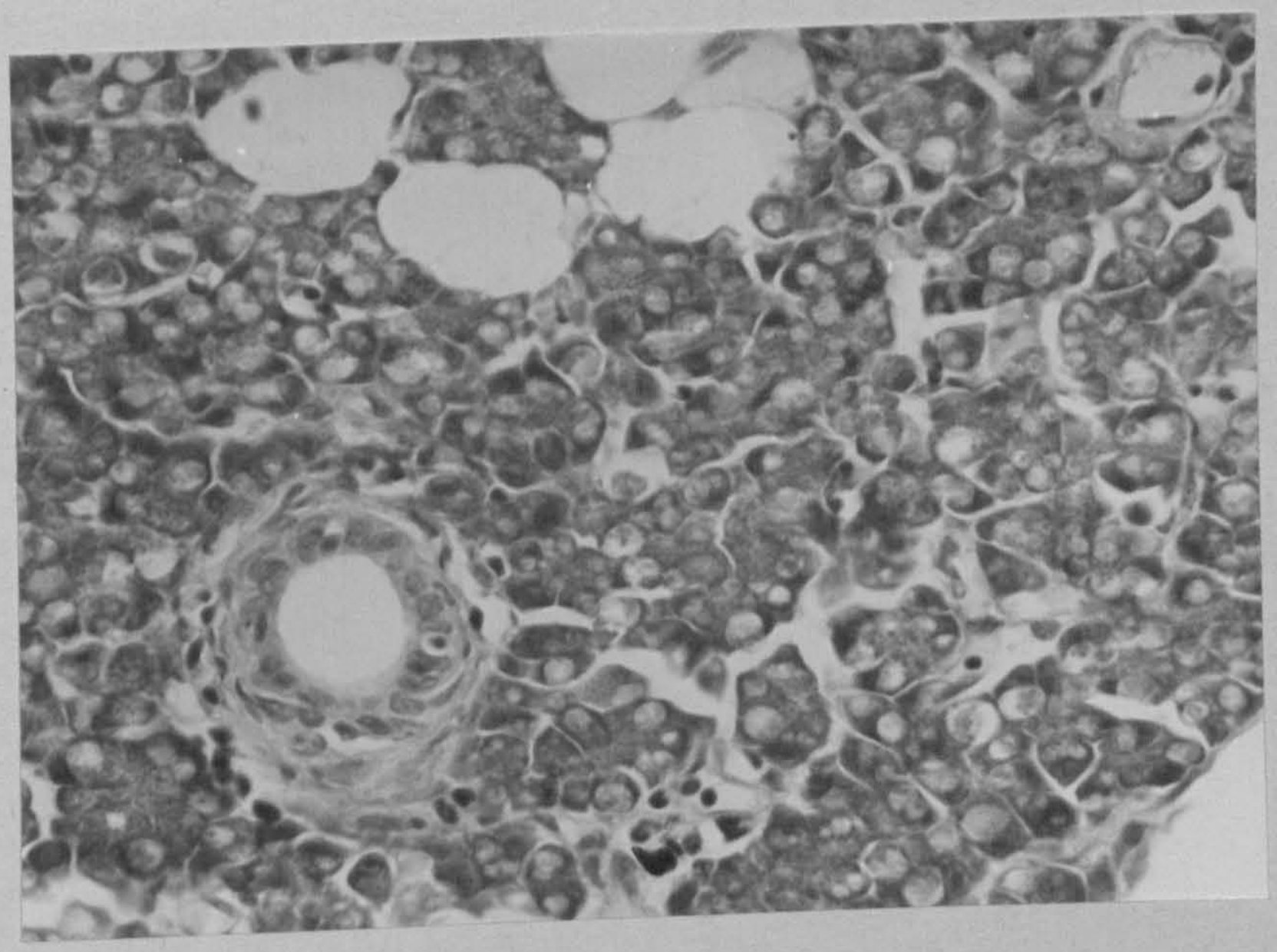

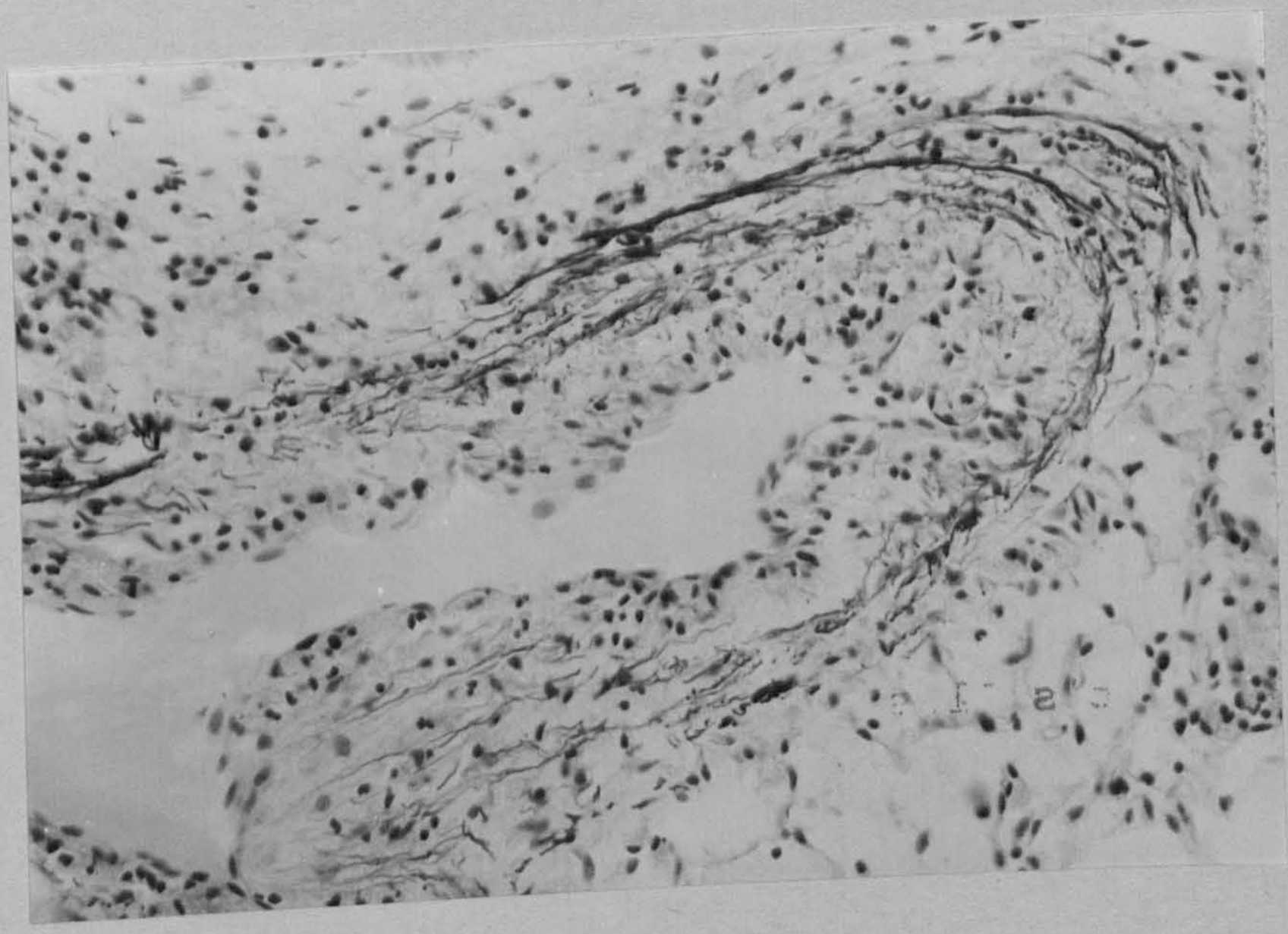

Fig. 117. Early intimal hyperplasia (arrowed) in control fish.

H & E x 320

Fig. 118. Large asteroid-shaped islet in androgen-injected fish.

H & E x 125

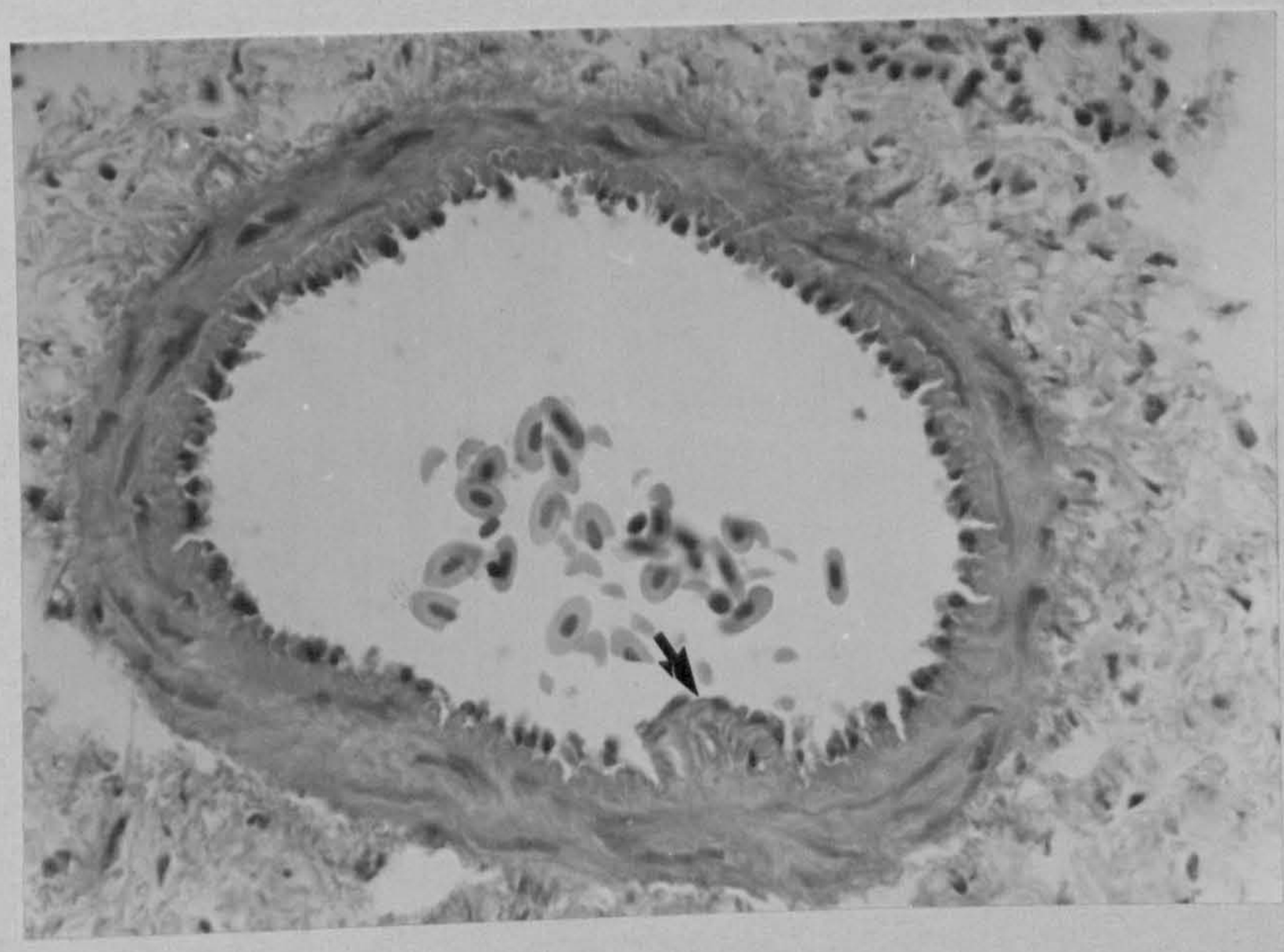

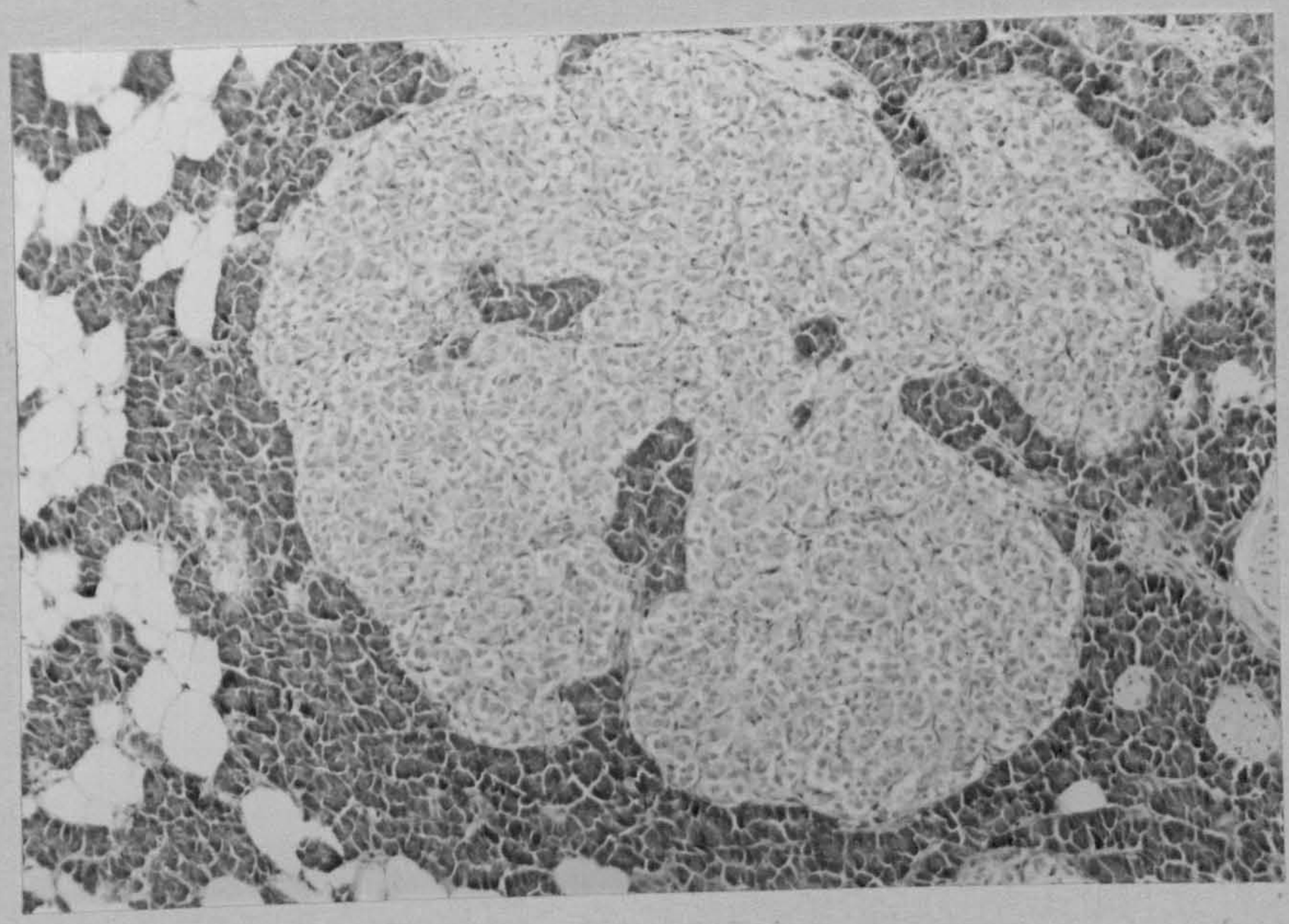

Fig. 119. Focal round-cell infiltration in pancreas of control fish.

H & E x 320

Fig. 120. Islet degeneration in androgen-injected fish.

H & E x 320

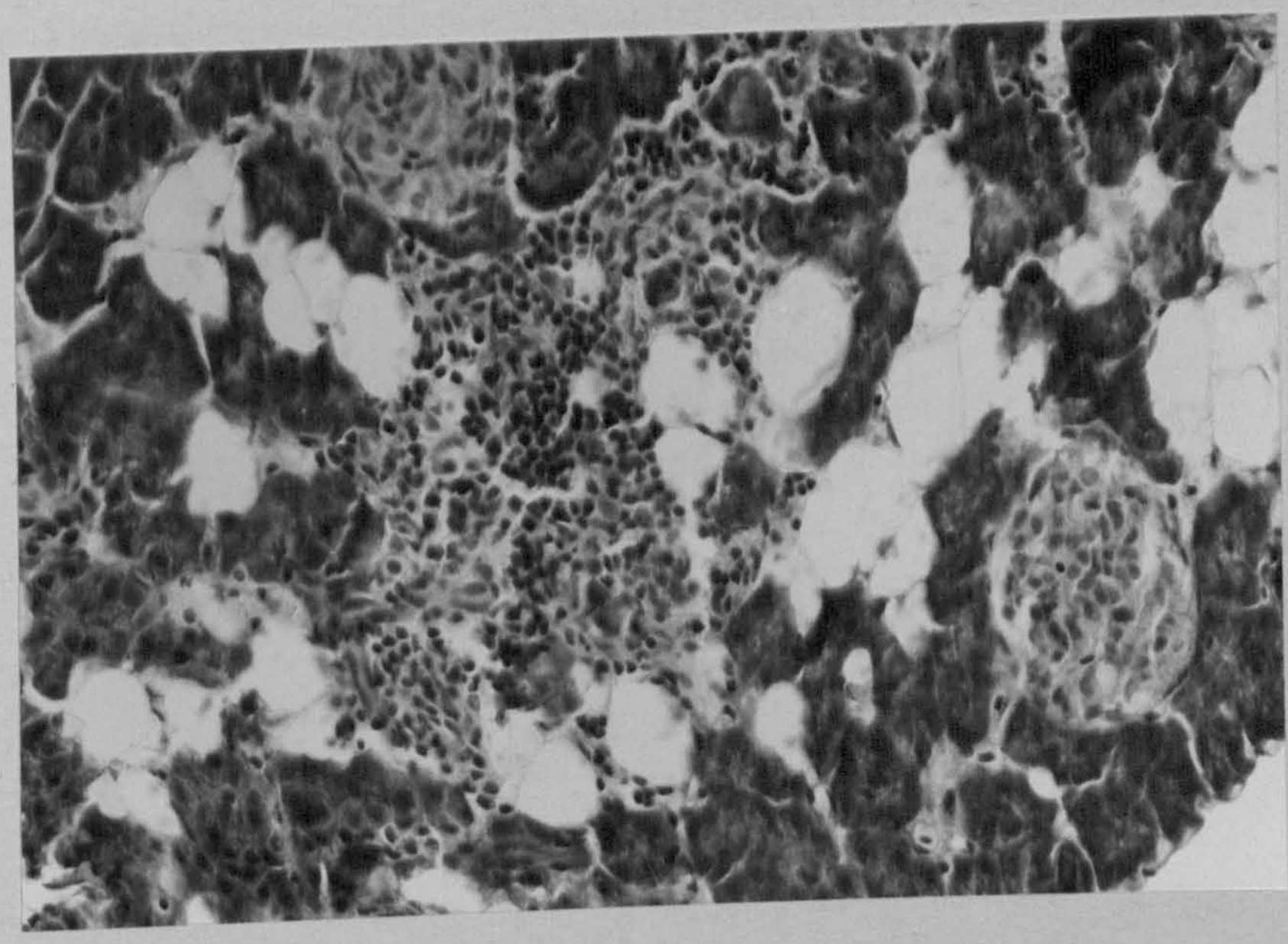

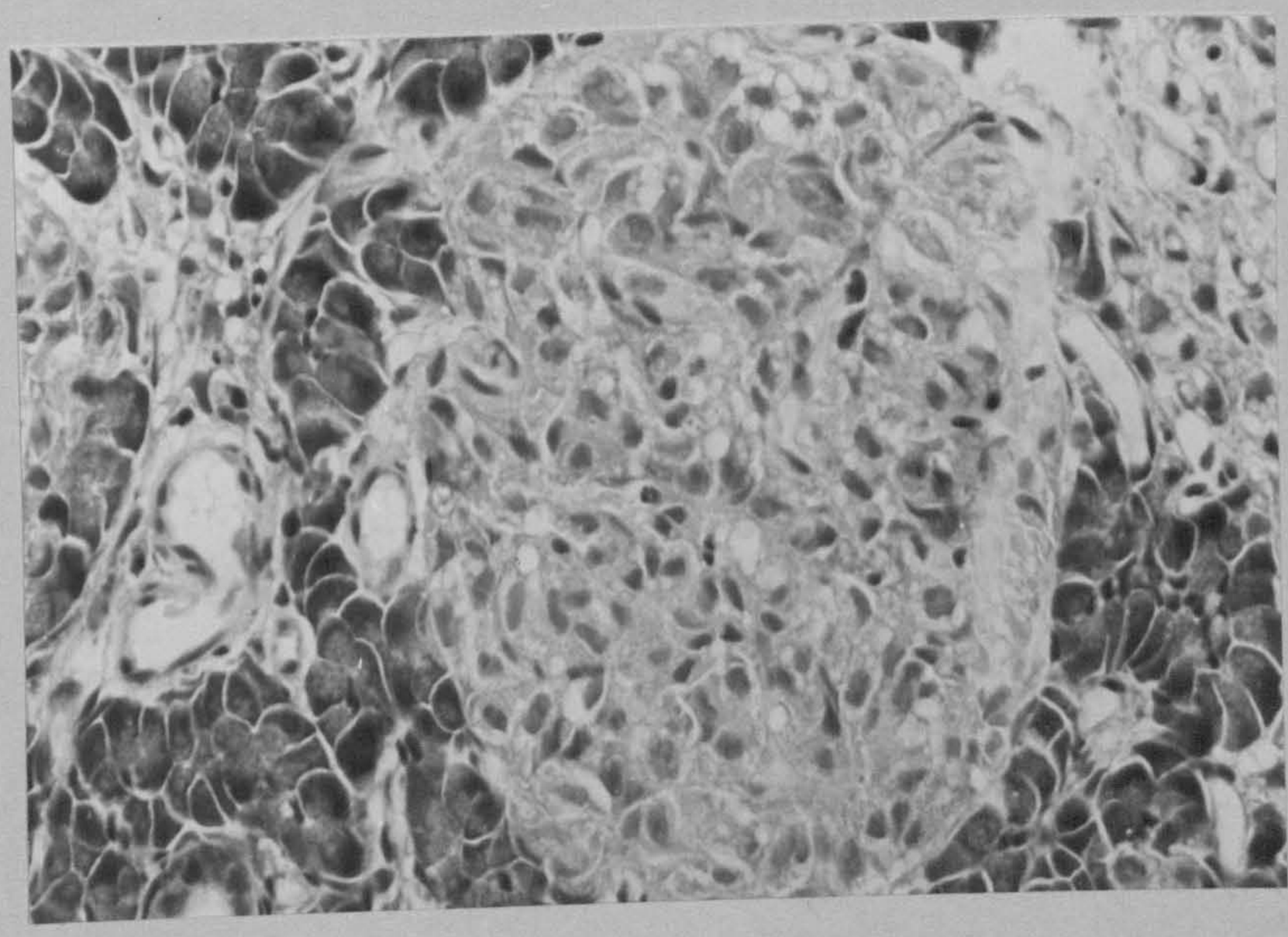

Fig. 121. Early degenerative change in testis of androgen-injected fish. Note nuclear pyknosis and cytoplasmic breakdown in primordial germ cells.

H & E x 500

Fig. 122. Degenerative change in testis following androgen administration. Note cyst formation.

H & E x 320

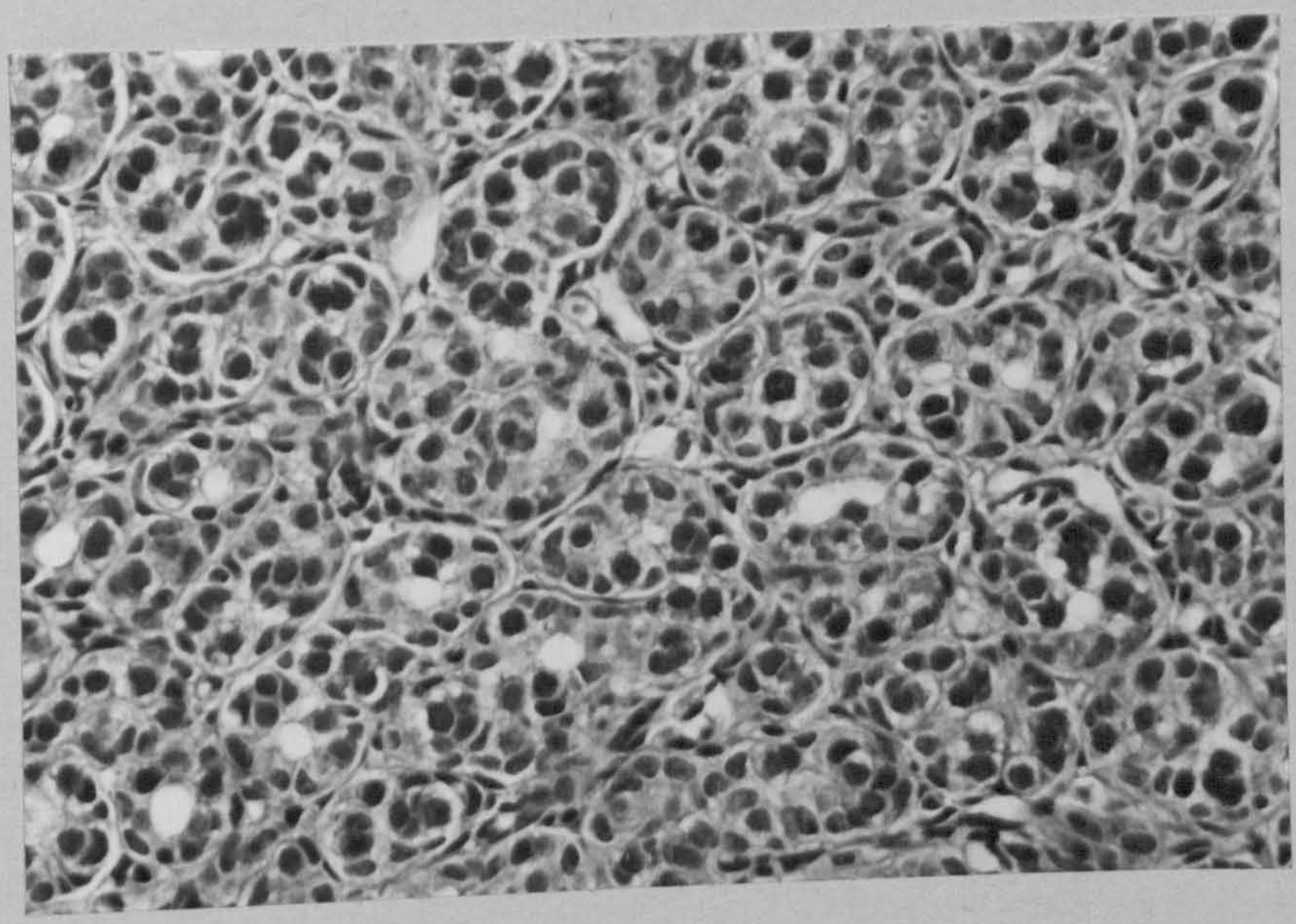

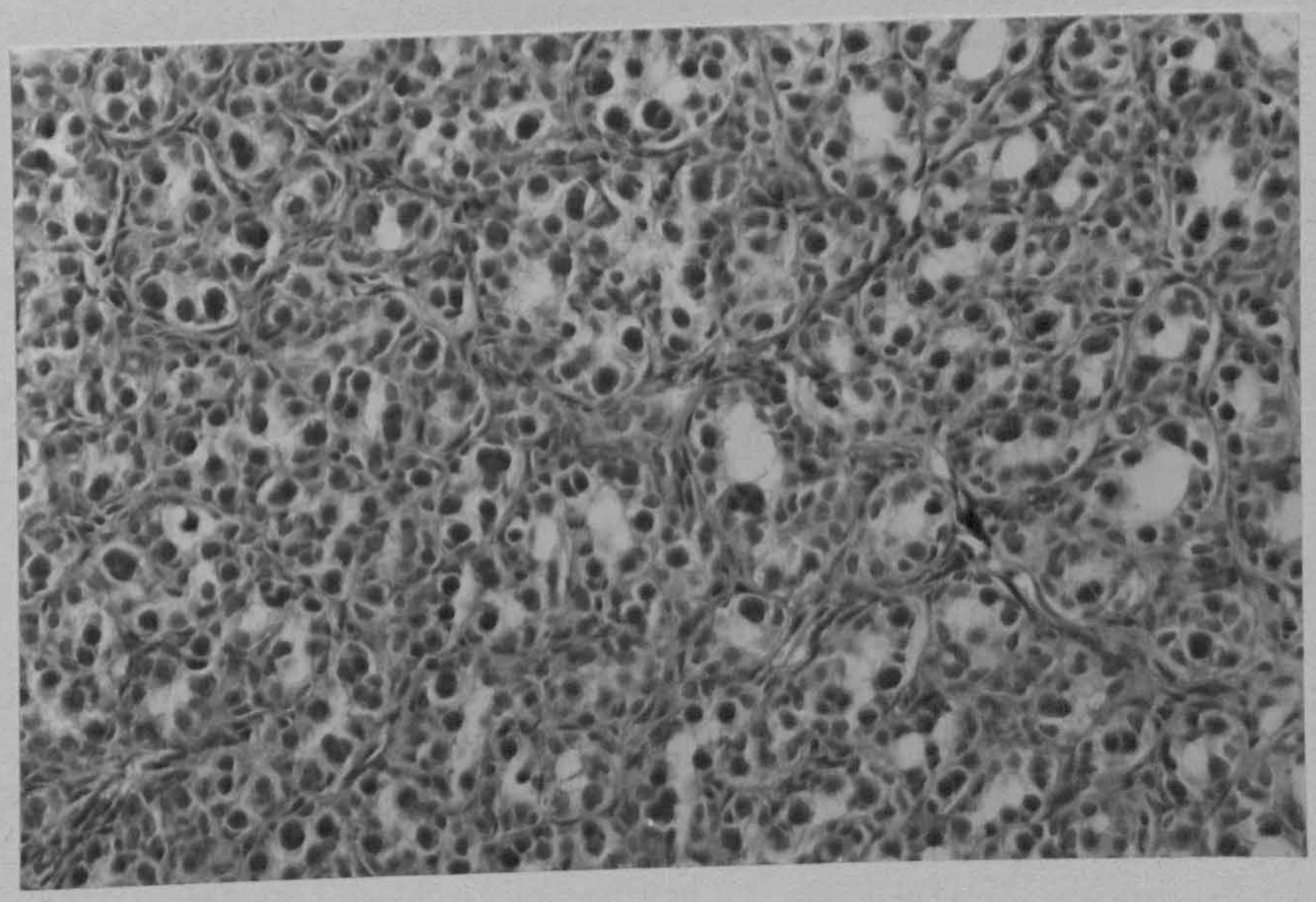

Fig. 123. Marked degenerative change in testis after 7 weeks' androgen administration. Cyst formation is well-developed, with cells sloughing into lumina and there is an increase in interstitial tissue.

H & E x 320

Fig. 124. Control fish. Ovary in vitellogenic phase.

H & E x 125

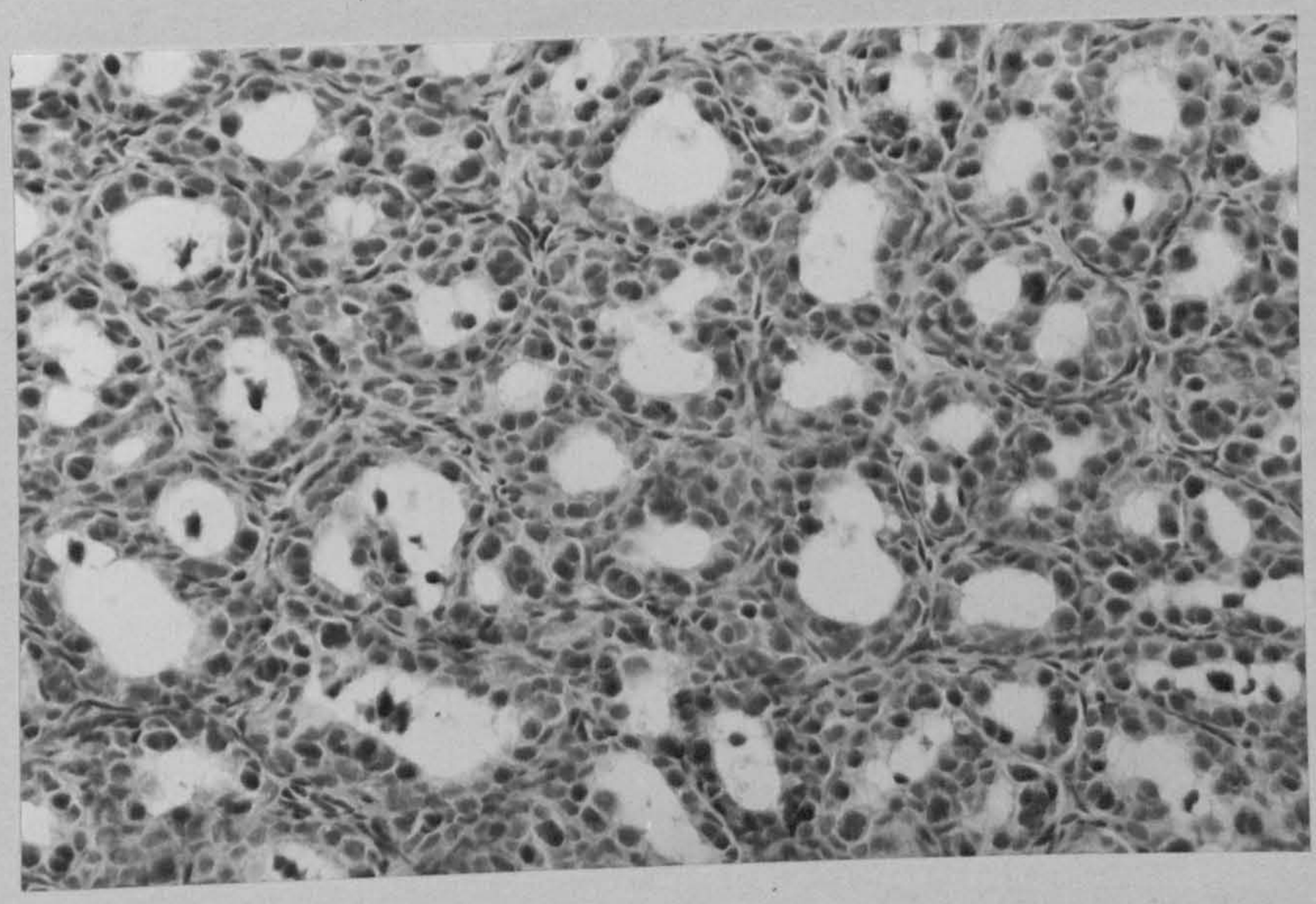

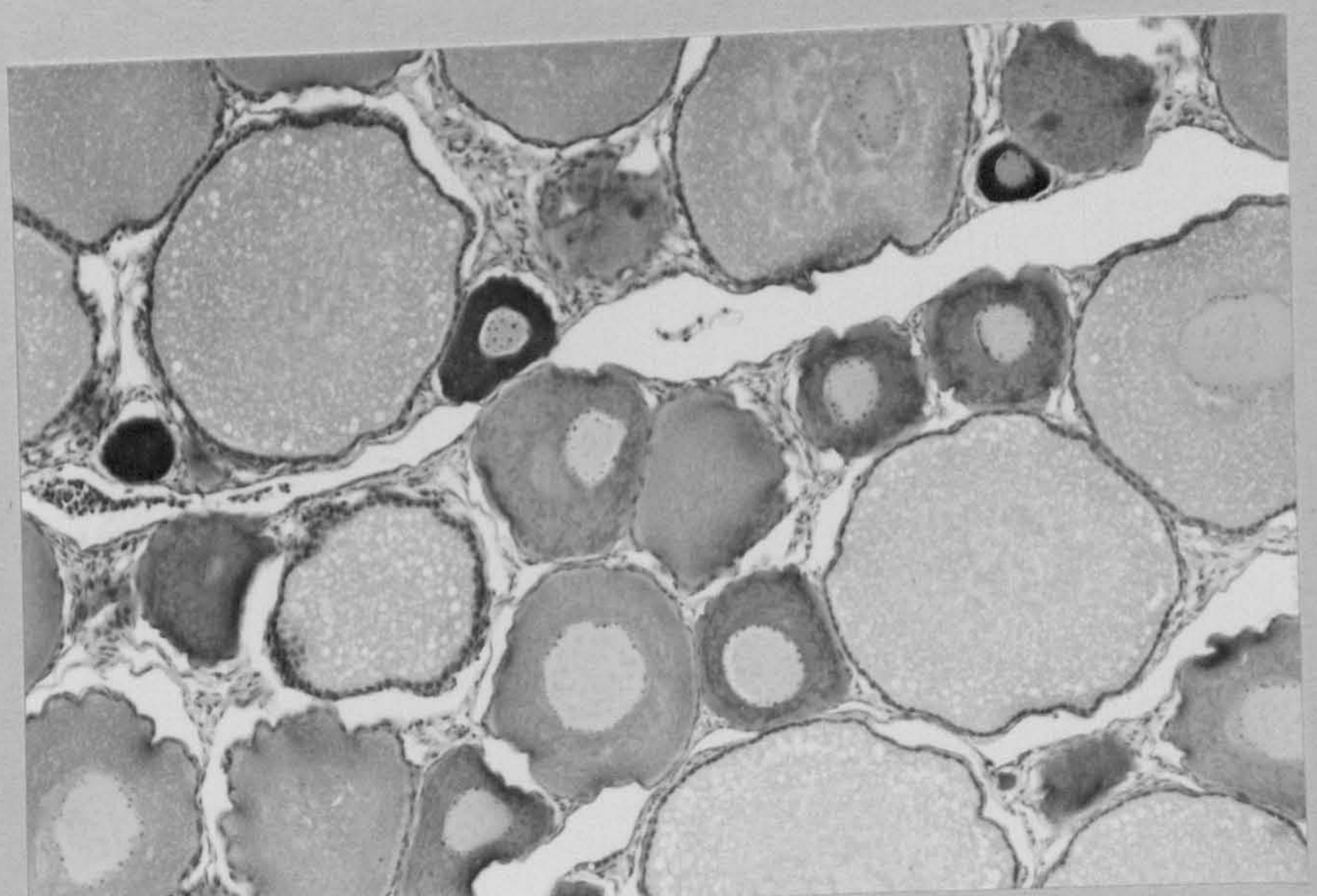

Fig. 125. Ovary after 1 week's androgen administration. Note increase in follicle cells (arrowed) lining oocyte.

H & E x 320

Fig. 126. Ovary 2 weeks after androgen administration. Note atresia of certain yolk-laden oocytes (A).

H & E x 125

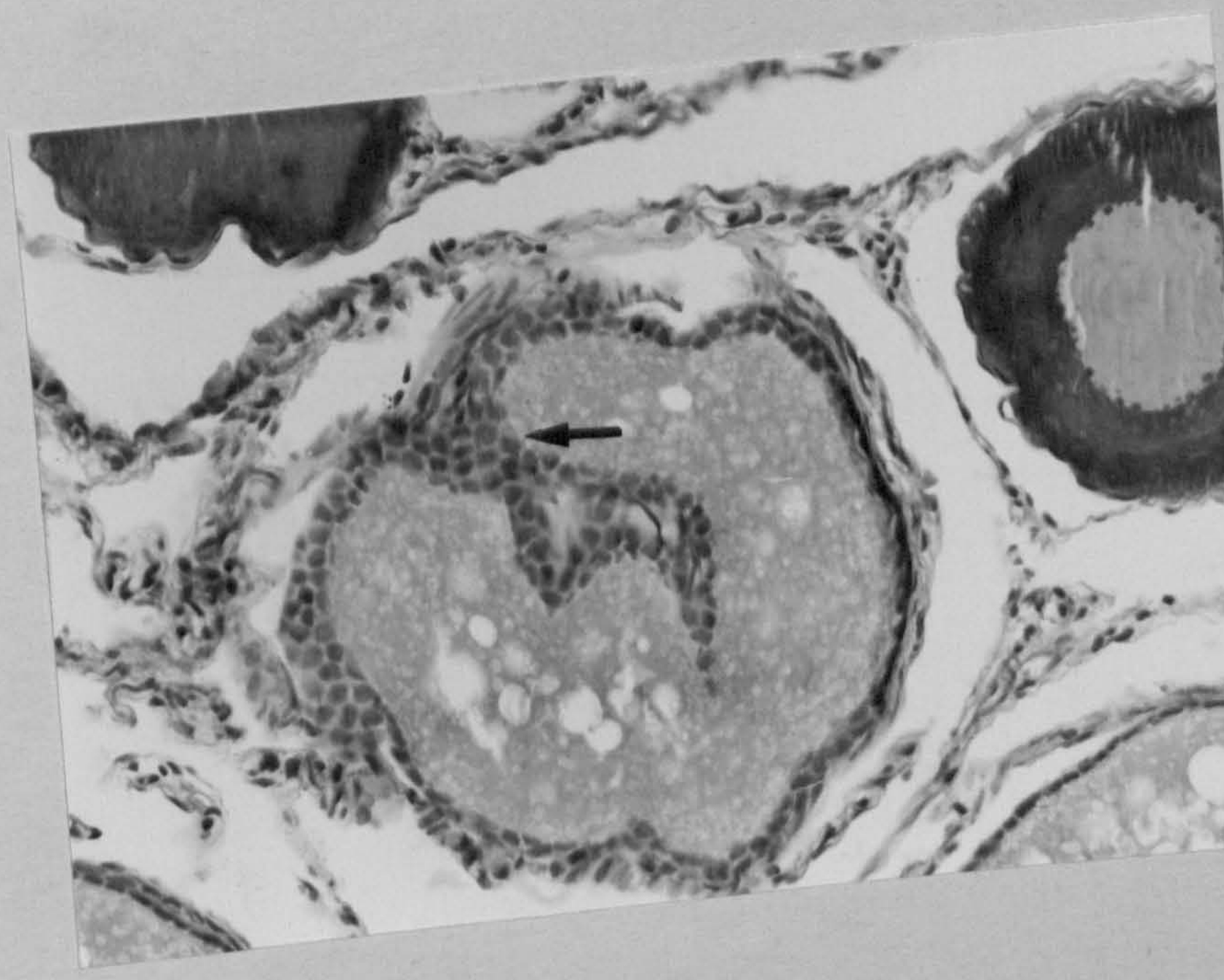

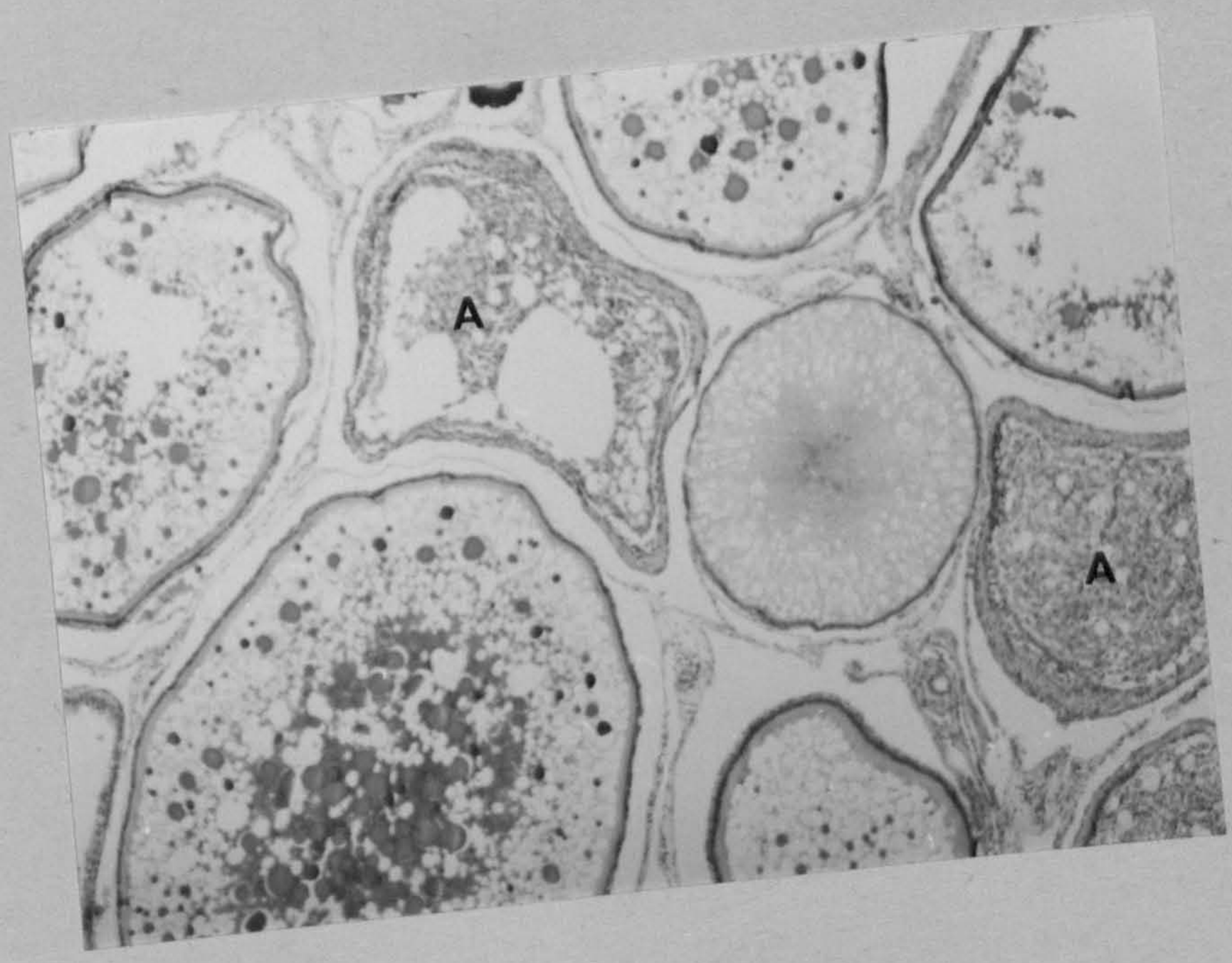
A
A
A

Fig. 127. Ovary 7 weeks after androgen administration. Note normal preyolk oocytes and occasional corpora atretica (C).

H & E x 125

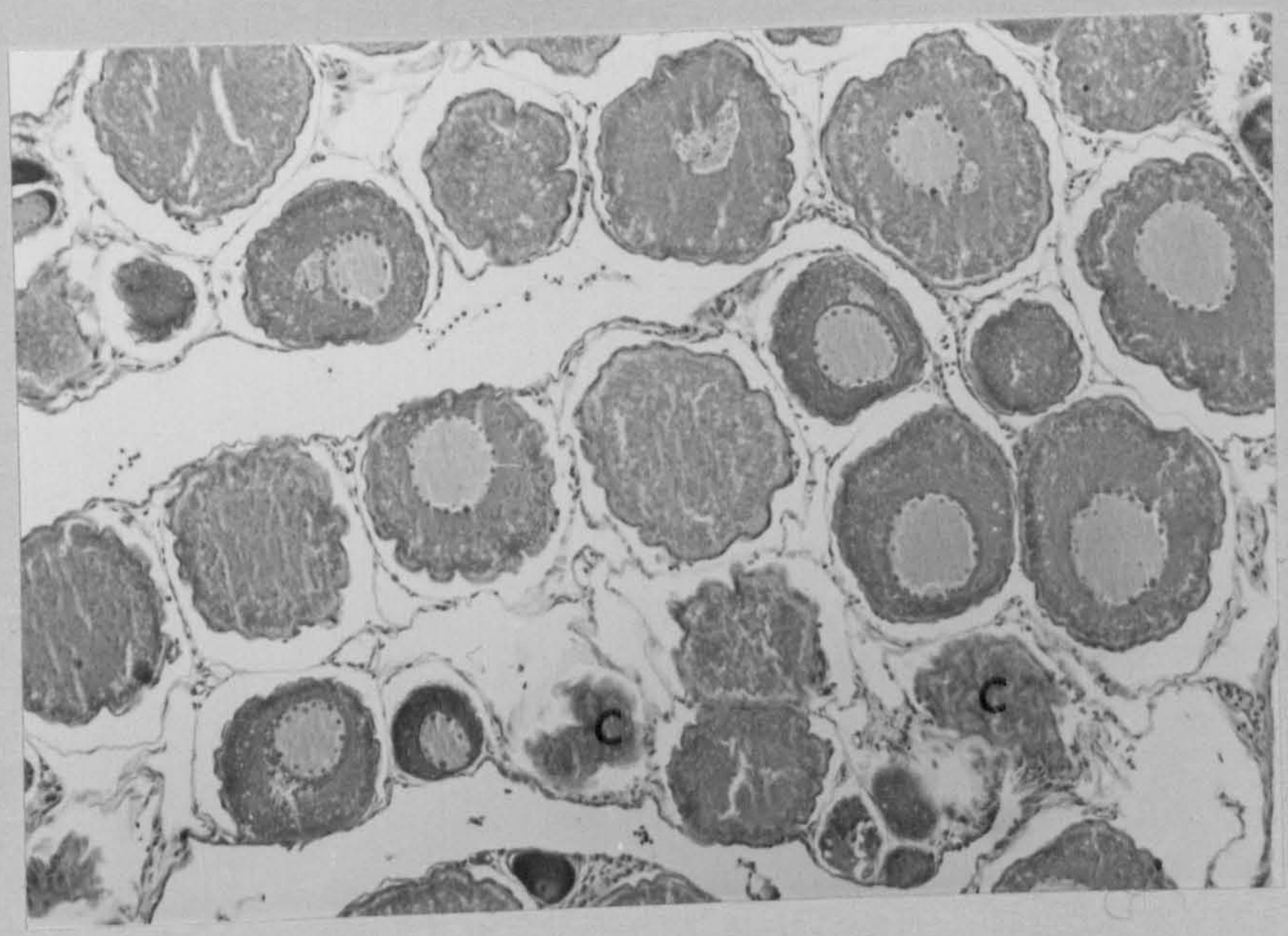
C
C

Fig. 128. Possible pathways of androgen metabolism in human foetal skin (from Sharp, Hay and Hodgins, 1976).

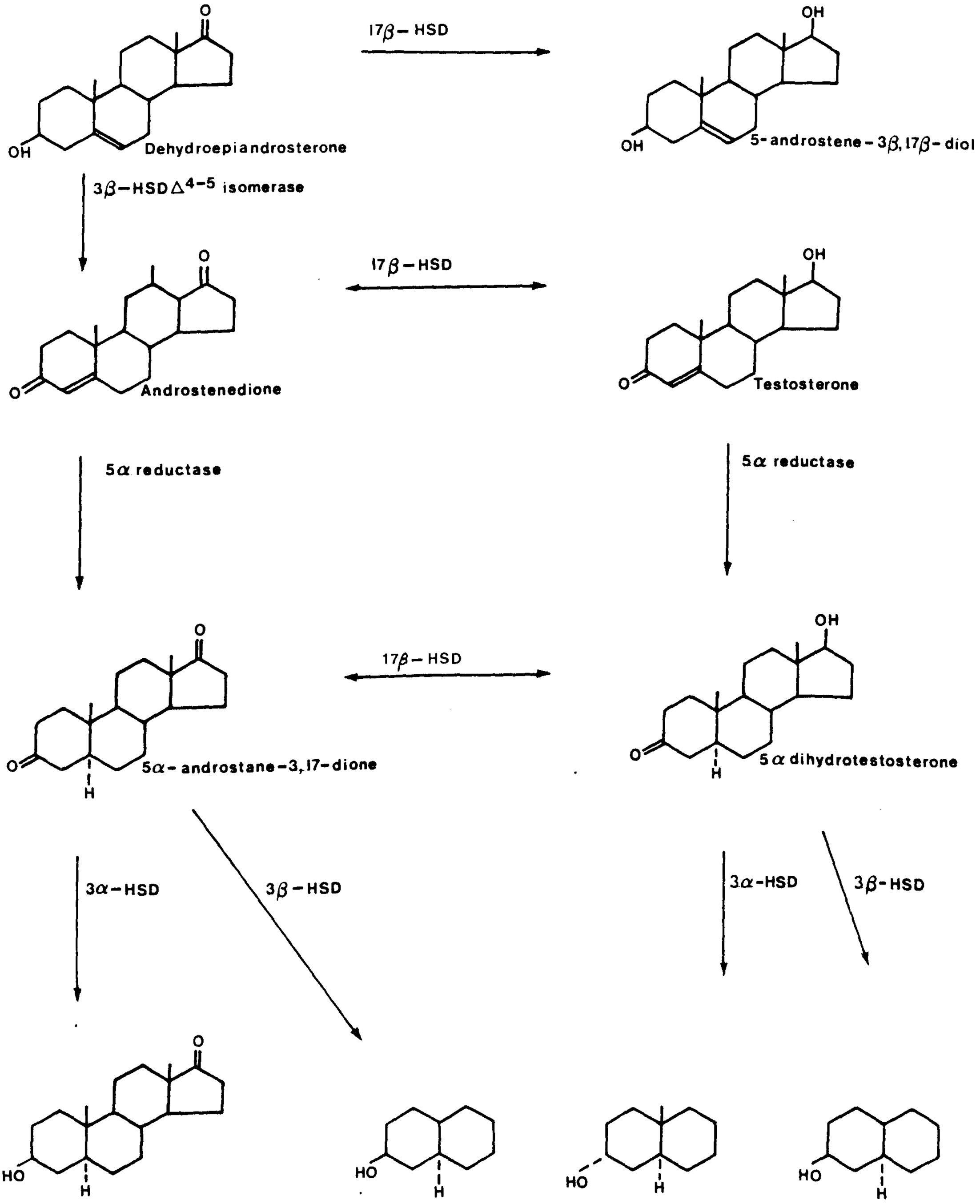
17β – HSD
Dehydroepiandrosterone
5- androstene – 3β, 17β – diol
3β–HSD Δ4–5 isomerase
17β – HSD
Androstenedione
Testosterone
5α reductase
5α reductase
17β – HSD
5α – androstane – 3, 17 – dione
5α dihydrotestosterone
3α–HSD
3β – HSD
3α-HSD
3β-HSD
Androsterone
3- epi Androsterone
3α diol
3β diol

Fig. 129. Possible routes of 11 ketotestosterone metabolism in sockeye salmon (from Idler and Truscott, 1963).

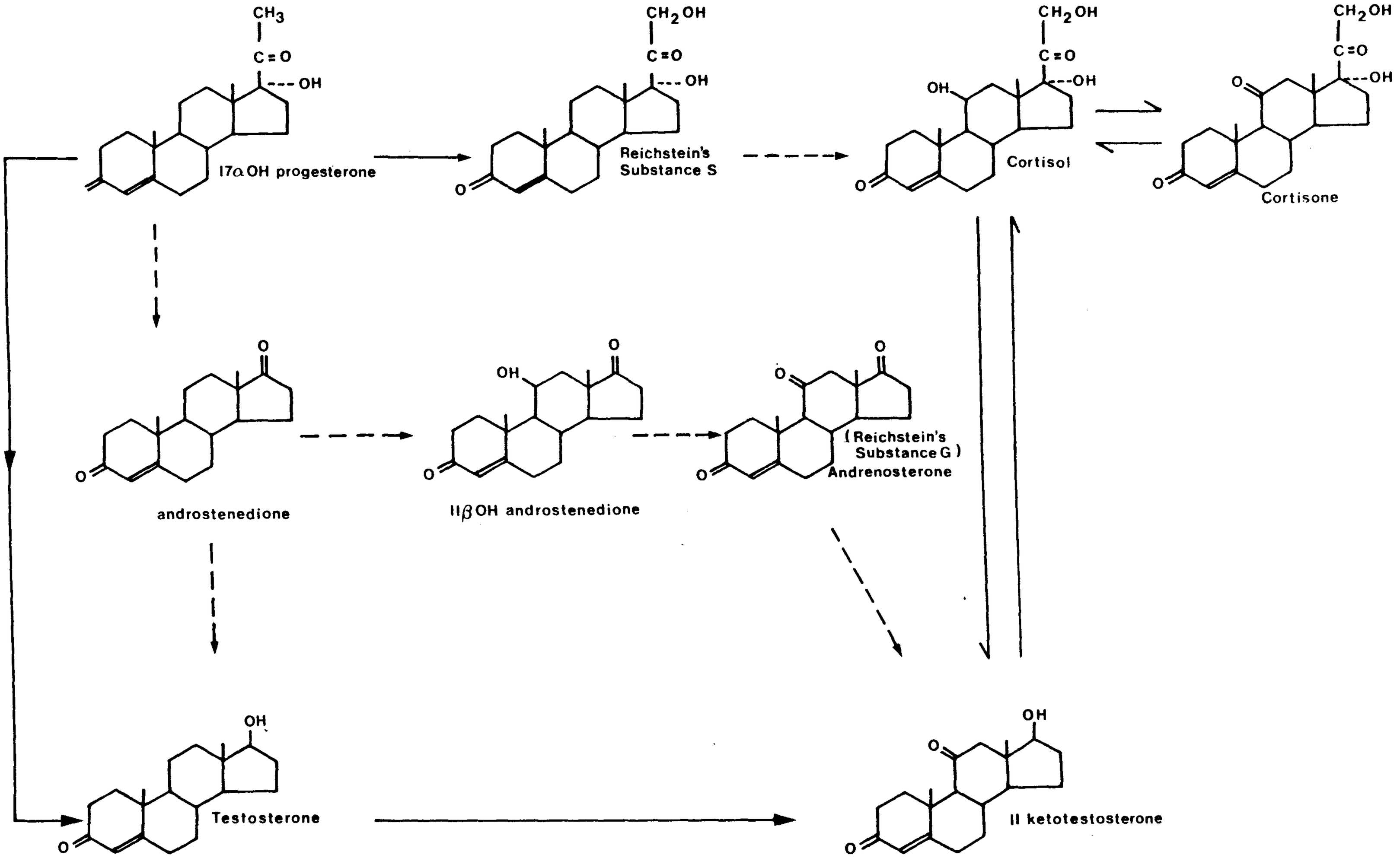
CH3
C=O
OH
17α OH progesterone
CH2OH
C=O
OH
Reichstein's
Substance S
CH2OH
C=O
OH
OH
Cortisol
CH2OH
C=O
OH
Cortisone
androstenedione
OH
IIβOH androstenedione
(Reichstein's
Substance G)
Andrenosterone
OH
Testosterone
OH
II ketotestosterone